THE UNIVERSITY OF HULL

Novel Liquid Crystals with Bulky Terminal Groups for Ferroelectric Displays in Nanotechnology

Being a Thesis Submitted for Degree of Doctor of Philosophy
In the University of Hull

By

Rami Adel Pashameah, BSc MSc

July 2015

Summary of Thesis Submitted for the Degree of PhD

on

Novel Liquid Crystals with Bulky Terminal Groups for

Ferroelectric Displays in Nanotechnology

The field of liquid crystals has become the focus of extensive research over the last century in terms of the design, synthesis and evaluation of novel materials, and the development of high technology applications, particularly displays. Virtually all current liquid crystal displays are based on the nematic phase, however, ferroelectric liquid crystal displays based on the chiral smectic C phase offers many advantages such as faster switching, higher resolution and contrast, bistability and wider angles of view. Although ferroelectric microdisplays are a commercial success, the technology is currently severely limited in their applicability because of problems in aligning the molecules in the ideal so-called bookshelf configuration. A wide range of novel materials has been designed, synthesized and evaluated. The main feature of the molecular design is the inclusion of a bulky group as part of a terminal chain, designed to cause a phase separation and preclude layer shrinkage on formation of the smectic C phase, and hence generate the desired bookshelf alignment. The synthesis was affected most efficiently using a range of synthetic methods, in particular low temperature lithiations and Suzuki coupling reactions. The materials were evaluated for structure and purity, and for mesomorphic and physical properties. The majority of the novel materials exhibit the smectic C phase over a wide temperature range, some compounds generate solely the smectic C phase whereas other additionally show the smectic A and nematic phases, and these results helps to establish patterns of how the mesomorphism relates to the structure of the bulky terminal group. Selected novel compounds were mixed with an established ferroelectric host mixture (KCHM211) to generate a range of novel ferroelectric host mixtures, which were doped with an established chiral dopant (BE8OF2N) to generate a range of novel ferroelectric mixtures, which were evaluated for their ferroelectric properties, namely tilt angle and spontaneous polarization. The results in terms of synthesis, mesomorphism and ferroelectric properties are discussed comparatively between novel compounds and known compounds.

Conferences and Presentations

In below, there is a list of conference presentations and workshops which have attended and participated through the PhD.

- Novel Liquid crystals with bulky groups designed for bookshelf geometry ferroelectric mixtures, R. Pashameah, M. Hird, at the 15th International Conference on Ferroelectric Liquid Crystals, Prague, Czech, June 2015.
- Nanoenergy Conference, Manchester, UK, 2015.
- The PhD Colloquia, Hull University, UK, 2015.
- SID for display conference, Oxford, UK.
- Liquid crystals with bulky terminal groups, R. Pashameah, M. Hird, participation and **organizer** at the 6th PhD Experience Conference, Hull, UK, April 2015.
- Synthesis and properties of novel liquid crystal materials with bulky groups designed for bookshelf geometry ferroelectric mixtures, R. Pashameah, M. Hird, British Liquid Crystals Society Annual Conference, Sheffield, UK, 2015.
- Liquid crystals in nanotechnology, R. Pashameah, M. Hird, participation and **organizer** at the 8th Saudi International Conference, Imperial College, London, UK, 2015.
- Joliot-Curie Conference, Edinburgh, Scotland, 2014.
- Synthesis of liquid crystal materials for bookshelf geometry ferroelectric mixtures, R. Pashameah, M. Hird, at the NUPS Conference, Sheffield, UK 2014.
- Nanosmat Conference, Dublin, Ireland, 2014.
- Nano flows Conference, London, UK, 2014.
- Challenges in Nanoscience Conference, Sandiego, USA, 2014.
- Carbon Nanomaterials Conference, London, UK.
- Synthesis of liquid crystal materials for bookshelf geometry ferroelectric mixtures, R. Pashameah, M. Hird, at the LMC Liquid Material Conference, Lisbon, Portugal, July 2014.

- Liquid crystal materials with bulky groups designed for bookshelf geometry ferroelectric mixtures, R. Pashameah, M. Hird, at the 25th International Liquid Crystal Conference, Dublin, Ireland, June 2014.
- Synthesis liquid crystal materials with bulky groups designed for bookshelf geometry ferroelectric mixtures, R. Pashameah, M. Hird, participation and **organizer** at the 1st Postgraduate Research Conference, Hull, UK, June 2014.
- Synthesis and properties of novel liquid crystal materials with bulky groups designed for bookshelf geometry ferroelectric mixtures, R. Pashameah, M. Hird, at the British Liquid Crystals Society Annual Conference, Durham, UK, April 2014.
- Liquid crystals with bulky terminal groups, R. Pashameah, M. Hird, participation and **organizer** at the 5th PhD Experience Conference, Hull, UK, April 2014.
- Liquid crystals for bookshelf geometry ferroelectric mixtures, R. Pashameah, M. Hird, participation and **organizer** at the Chemistry Organic Division, Hull, UK, 2014.
- Liquid crystals with bulky groups designed for bookshelf geometry ferroelectric mixtures, R. Pashameah, M. Hird, at the German Liquid Crystal Conference, Magdeburg, Germany, March 2014.
- British Liquid Crystal Winter Workshop, Hull University, UK, 2014.
- Novel liquid crystals materials, R. Pashameah, M. Hird, at the 12th European Conference on Liquid Crystals, Rhodes, Greece, September 2013.
- Liquid crystals with bulky groups designed for bookshelf geometry ferroelectric mixtures, R. Pashameah, M. Hird, at the 14th International Conference on Ferroelectric Liquid Crystals, Magdeburg, Germany, September 2013.
- Synthesis and properties of novel liquid crystal materials with bulky groups designed for bookshelf geometry ferroelectric mixtures, R. Pashameah, M. Hird, at the PhD Colloquia, Hull University, UK, 2013.
- The 4th PhD Experience Conference, University of Hull, UK, 2013.

- Synthesis and properties of novel liquid crystal materials with bulky groups designed for bookshelf geometry ferroelectric mixtures, R. Pashameah, M. Hird, British Liquid Crystals Society Annual Conference, Cambridge, UK, 2013.
- Novel liquid crystal materials with bulky groups designed for bookshelf geometry ferroelectric mixtures, R. Pashameah, M. Hird, the 6th Saudi International Conference, Brunel University, London, UK, 2012.
- Synthesis and properties of novel liquid crystal materials with bulky groups designed for bookshelf geometry ferroelectric mixtures, R. Pashameah, M. Hird, PhD Colloquia, Hull University, UK, 2012.
- British Liquid Crystal Winter Workshop, Hull University, UK, 2011.
- The 5th Saudi International Conference, Wrick University, UK, July 2011.

Acknowledgements

I cannot express enough thanks to our God for his continued help. Then, I would like to thank my supervisor of this project, Dr Mike Hird for the valuable guidance and advice. He inspired me greatly to work in this project. I am very grateful for his support.

I also need to thank Dr Rob Lewis, Dr Rob McDonald and Dr L. Saad for their help and continued support. I offer my sincere appreciation for the learning opportunities provided by the Liquid Crystal Group. My completion of this project could not have been accomplished without the support of my classmates, Viswanath, Ibrahim, Srinivas, Qiang, David and Aemose – thank you for allowing me time away from you to research and write.

My thanks and appreciations also go to the King of Saudi Arabia, King Abdullah bin Abdulaziz, the Saudi government, the ministry of higher education and Umm Al-Qura University for their financial support. Also I would like to thank Dr B. Hussain to support me.

I would like to show my greatest appreciation to my lovely mum and dad for their support, pray and efforts to complete my studies abroad. I also wish to express my deep sense of gratitude to my children Yamen, Yman and Kayan.

Finally, to my caring, loving, and supportive wife, Suhailah: my deepest gratitude. Your encouragement when the times got rough are much appreciated and duly noted. It was a great comfort and relief to know that you were willing to provide management of our household activities while I completed my work. My heartfelt thanks.

Contents

1- Introduction

1.1 Historical Aspects of Liquid Crystals

1.1.1 Early Discoveries

In 1888, Reinitzer[1] and Lehmann[2] discovered liquid crystalline phase for the first time. Irregular melting behaviour of cholesteryl benzoate (compound **1.1**) was observed by Reinitzer when this compound melted at 145.5 °C which was cloudy.

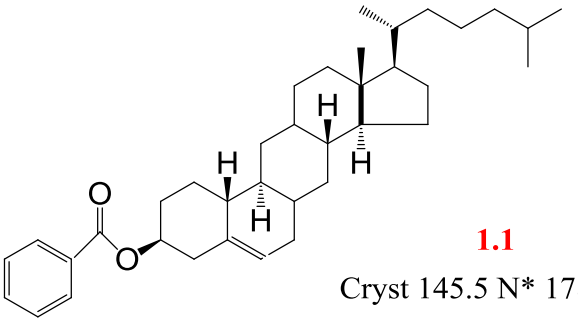

1.1

Cryst 145.5 N* 178.5 Iso ^{o}C

When the temperature rises to 178.5 °C only then this melt became clear, at this point the isotropic liquid was attained. Similar melting behaviour was also observed by Lehmann in 1890[2, 3] for 4-azoxy-phenetole (compound **1.2**). Both cholesteryl benzoate and 4-azoxy-phenetole have a geometrically elongated shape although these molecules are different in their structures.

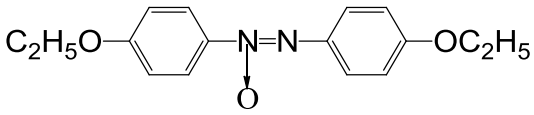

1.2

Cryst 43 N 76 Iso ^{o}C

A recognition that a rod-like shape was the key to generating liquid crystal phases (mesophases) paved the way for further studies in the area. Some other compounds with elongated, rod-like molecular structures were prepared[2], all of which show mesophases. However the complete explanation for this behaviour was not explained at this period. Rather few arguments were given that this turbidity is either due to the colloidal effects of suspended isotropic liquid or some impurities may be the cause for this emulsion.

1.1.2 Early Classification

In 1922 Friedel[4] studied the intermediate state using optical microscopy, and he concluded that there were three different types of mesophases as follows.

(a) The nematic mesophase – this is a mobile cloudy phase. Its name is derived from the Greek word "nematos" which means thread-like.
(b) The cholesteric mesophase – the cloudy, often iridescent phase obtained from cholesterol compounds, so hence the name.
(c) The smectic mesophase – this is a turbid viscous phase which has properties just like a soap. It name has been derived from the Greek word "smectos" meaning soap-like.

The credit for the classification of liquid crystals goes to Friedel which is still today broadly accepted. However, several types of smectic mesophases are now known.

1.1.3 Theories and Early Applications

For the mesomorphic states many theories were established commonly the Swarm Theory and Continuum Theory. Bose[5] established the Swarm Theory in 1909 which was accepted worldwide. As an alternative to Swarm Theory, Zocher[6] (1927) proposed the Continuum Theory which later became established as the main theory of liquid crystals. Many theories were also proposed by Zocher[7] himself in 1933, Oseen[8] (1933) and Frank[9] (1958). It was realized in early fifties that liquid crystals have the potential for various technological applications.

In 1968 Fergason[10] presented the first report on applications of liquid crystals. In this report he described the use of cholesteric materials for the detection of atmospheric pollutants and for surface thermography. Liquid crystal materials generated more interest for their commercial applications when nematic dynamic scattering was discovered which showed realistic electro-optic effects[11]. As the more device application for liquid crystals turned the scientist's interest toward the material design to fulfil the requirements for display device technology, due to which research in area of novel liquid crystals is still going on today. The study of liquid crystals

truly multidisciplinary environment and has attracted the attention of physics, chemistry, biology and engineering[12]. Research and development of liquid crystals have experienced an explosive growth in this era. This has arisen primarily due to the successful high technology applications of liquid crystals, especially in the electro optical displays area[13]. There are a vast number of applications and uses in everyday life such as laptops, TV screens, phones, clocks, electronic instruments, radios, and watches[14].

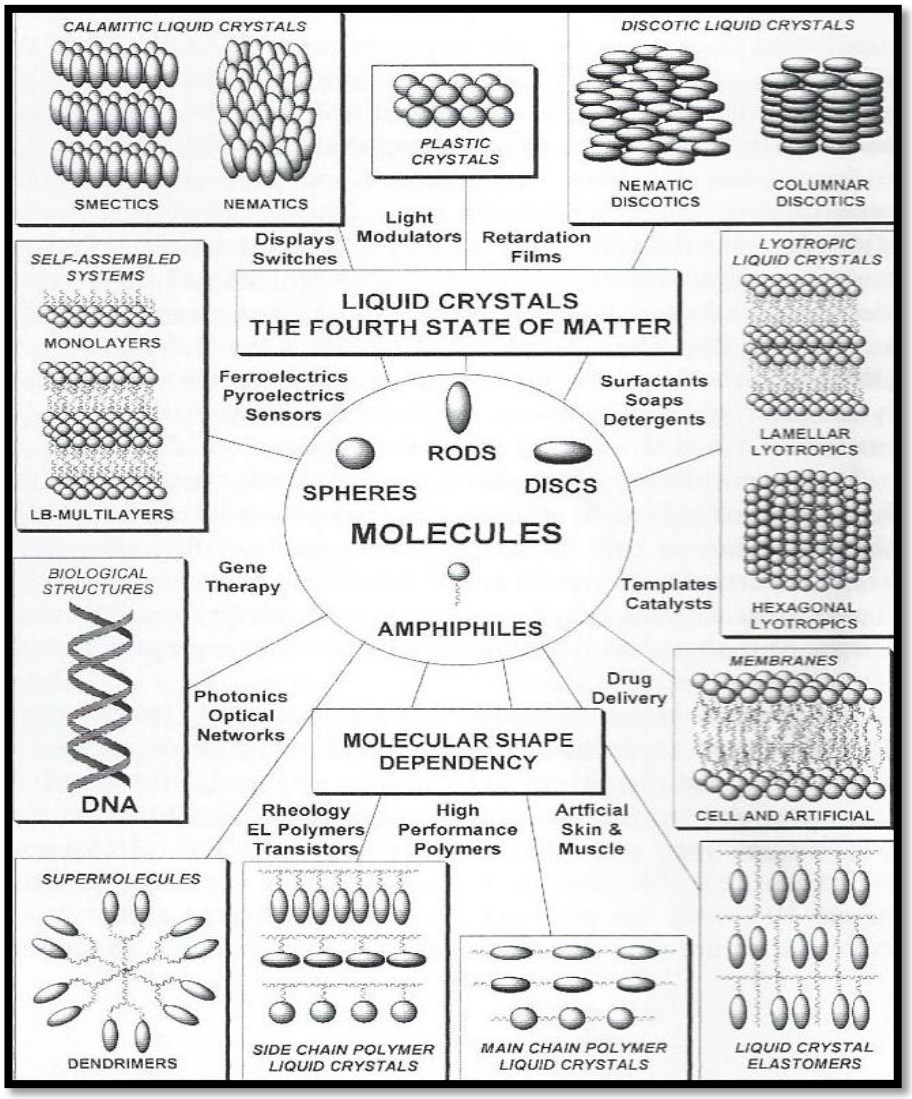

Figure 1.1. The general shapes of the constituent molecules in mesogenic materials, the phases that they form and their applications[12].

1.2 Types of Liquid Crystals

1.2.1 Thermotropic and Lyotropic Liquid Crystals

Liquid crystals appear for more than one reason such as thermotropic crystalline liquids and lyotropic crystalline liquids. If a liquid crystal appears the definite temperature intervals, this is a thermotropic liquid crystal (formed by melting a crystal). However, materials in which liquid crystal properties are induced by the presence of a solvent are called lyotropic liquid crystal (formed by dissolution in solvent which is usually water), see figure **1.2** [15].

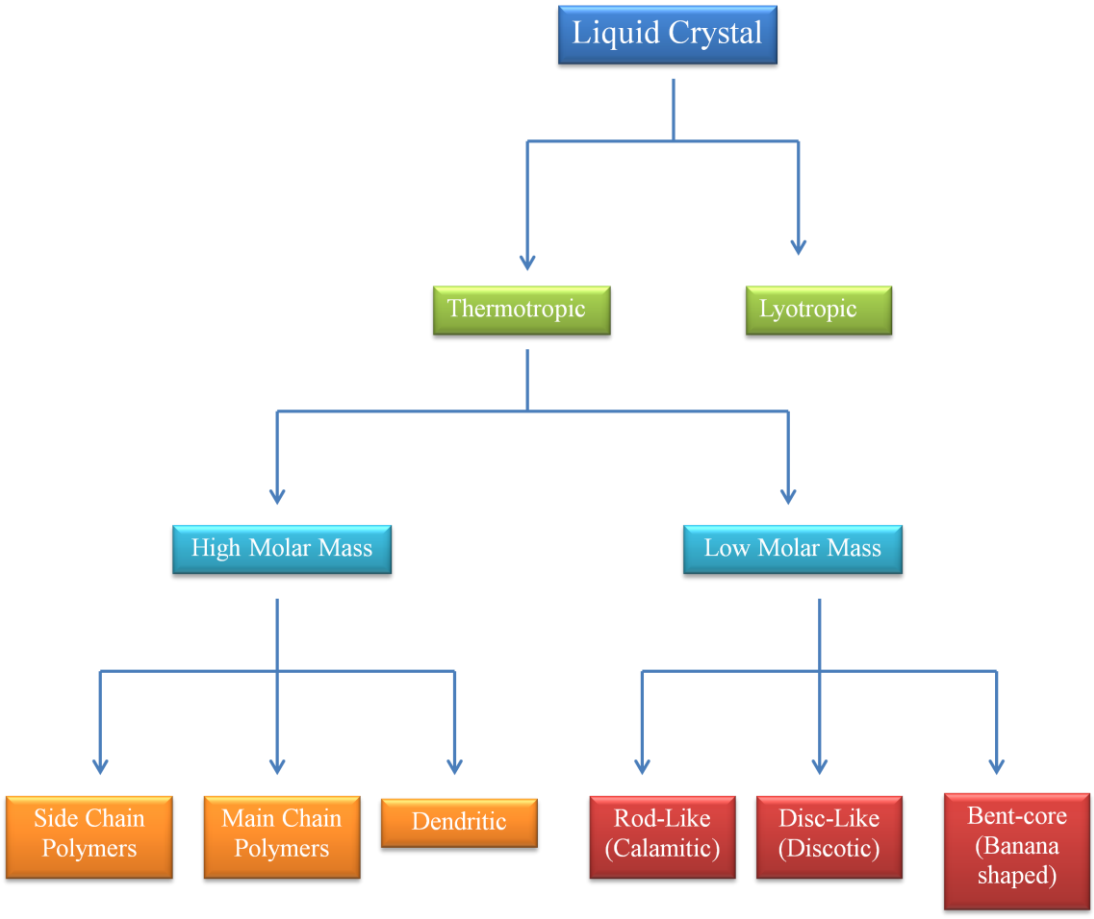

Figure 1.2. The different types of liquid crystals.

1.2.1.1 Lyotropic Liquid Crystals

In nature, the most common liquid crystals are lyotropic liquid crystals. Their phase of matter is changed by changing concentration in addition to temperature. There are several examples of these materials in everyday life, including soaps and surfactants. Similarly cell membranes in our bodies are the most common lyotropic liquid crystal materials, where the lyotropic phase forms from the dissolution of phospholipids in water. Thus life censoriously depends on this universal phase[16]. The product from soaps and other detergent systems and water are a common example of lyotropic liquid crystals[13].

Lyotropic liquid crystals consist of amphiphilic molecules; a single molecule exhibits two different sections. One is hydrophilic and other one is hydrophobic, such as compound **1.3**. At a specific concentration when a compound and suitable solvent interact with each other they form micelles in which the molecules are arranged into spherical shapes, disc or rod shapes[17, 18].

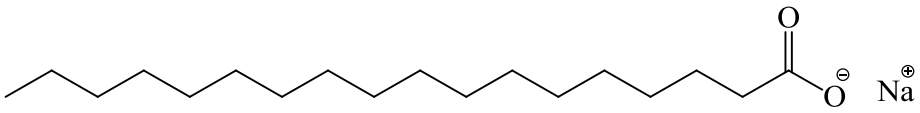

1.3

1.2.1.2 Thermotropic Liquid Crystals

Thermotropic liquid crystals are used in display devices and formed by melting a crystal. The occurrence of thermotropic transitions in a structured way is defined in the following ways. The transition of the liquid crystal to the isotropic liquid is called isotropization, or clearing, point and this transition is reversible and occurs with little hysteresis in temperature like those between liquid crystal phases. Enantiotropic phases occur on the first heating cycle of a material above the melting point. On the other hand, the mesophases formed below the melting point on cooling cycles are metastable and known as monotropic phases. Furthermore, both phases such as monotropic and enantiotropic phases can be investigated by microscopy[17, 19]. Thermotropic mesophases are classified into three major groups of compounds that can form them namely calamitic liquid crystals, discotic liquid crystals and banana liquid crystals. The calamitic liquid crystals consist of rod-like shaped molecules, the

latter consists of disc-like shaped molecules and consists banana shaped liquid crystals[20]. These three main categories can be further sub-divided.

1.2.2 Types of Thermotropic Liquid Crystals

1.2.2.1 Discotic Shaped

Disc-like or disc-shaped molecules consisting of a core of fused aromatic rings and it is flat[21]. It is usually disc shaped[22, 23]. In 1977, the first discotic liquid crystal was identified, synthesized[13] and discovered by researchers in India[24] such as compound **1.4**[25]. Discotic molecules incorporate a rigid central core, usually based on truxene, triphenylene or benzene with six or eight side chains (*e.g.*, compounds **1.5**, **1.6** and **1.7**) [17]. There are two types of discotic liquid crystal, columnar phase and discotic nematic (N_D), see figure **1.3** [13]. The simplest configuration phase between the columnar phase and discotic nematic phase is the columnar phase[26].

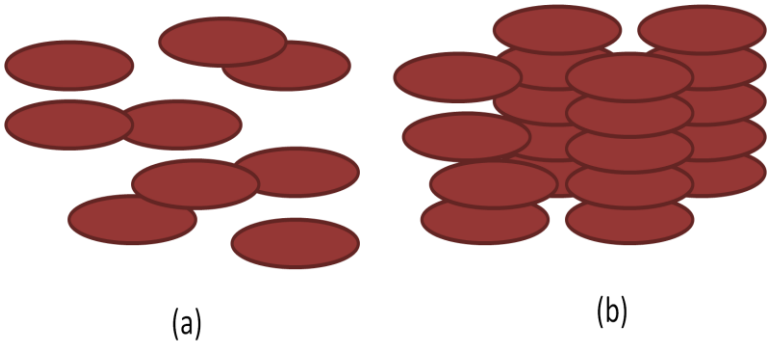

Figure 1.3. (a) A discotic nematic LC phase and (b) a discotic columnar LC phase.

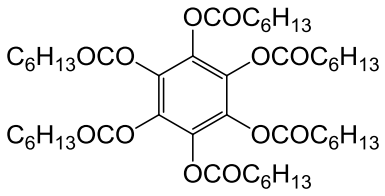

1.4

Cryst 68 Col_h 86 Iso ^oC

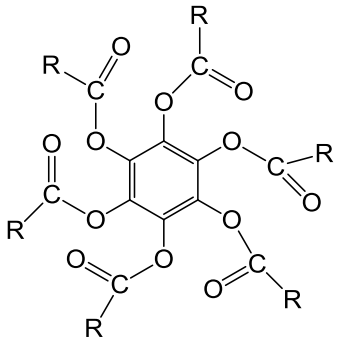

1.5

Hexa-substituted benzene

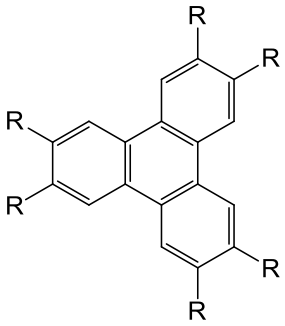

1.6

Triphenylenes

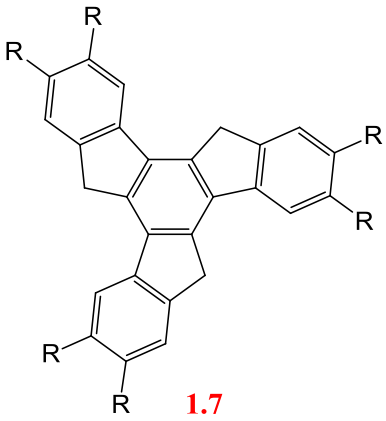

1.7

Truxenes

1.2.2.2 Banana Shaped Molecular Structures

The LC behaviour in bent-core compounds was noticed by Vorlander in the early 1900s. Vorlander's compounds generated an unknown mesophase[27, 28]. Almost one hundred years later, Pelzl re-investigated Vorlander's compounds and confirmed that they exhibited a so-called banana mesophase[28]. In the early 1990s, many banana shaped structures were synthesised by Matsunaga. These banana shaped structures seemed to exhibit smectic and nematic phases, but he was unable to characterise the mesophases thoroughly[27, 29]. However, in 1996, Niori clarified this earlier work through the study of compound **1.8**[27, 30, 31] which generates a completely novel types of mesophase[30, 32]. These novel types of mesophase proved to be immiscible with conventional calamitic mesophases, and they were classed as banana liquid crystals[31]. The mesophases of compound **1.8** were originally designated as S_1 and S_2 but later changed to B_2 and B_3 respectively to reflect the new classification.

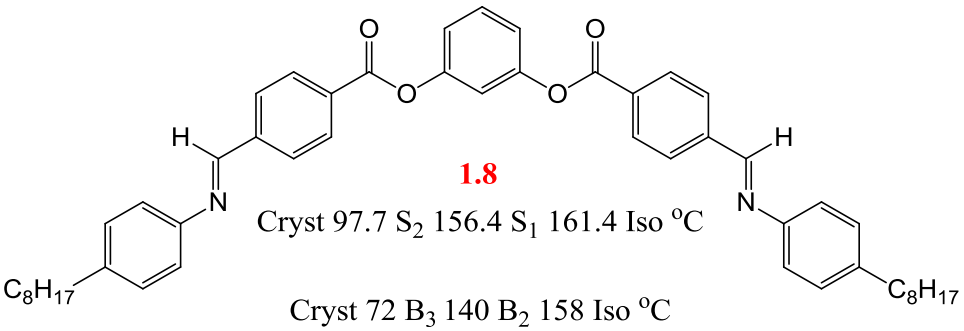

1.8

Cryst 97.7 S_2 156.4 S_1 161.4 Iso ^oC

Cryst 72 B_3 140 B_2 158 Iso ^oC

The most important aspect of the banana-shaped molecules is that the achiral molecular structures generate chiral liquid crystal phases that often produce

ferroelectric or antiferroelectric switching as a result of the decreased symmetry[30]. An equal amount of oppositely-handed domains exist within the bulk phase. There are many volumes of work reporting banana mesomorphism, including reviews by Hird[27], Takezoe[33], Reddy[34], Ros[35] and Pelzl[31]. In Germany (1997), at a (Chirality by Achiral Molecules) workshop, it was recommended that these phases should be described *via* the nomenclature from (B_1) to (B_8)[27, 31, 32, 36-38] according to the order in which they were discovered such as B_1 phase, B_2 phase, B_3 phase, B_4 phase, B_5 phase, B_6 phase B_7 phase and B_8 phase.

1.2.2.3 Thermotropic Calamitic Liquid Crystals

1.2.2.3.1 General Melting Phenomenon

The liquid crystals are the fourth state of matter[39], but many children learn in school, there are just three states of matter[40] such as steam (gas), water (liquid) and solid (ice) as exhibited by water. On the other hand, a mesomorphic material may exhibit four states of matter; gas, liquid, liquid crystal and crystal[41].

The liquid crystal mesophase is the intermediate state in between an ordered solid and an amorphous liquid. The mesomorphic or liquid crystalline state is made up of a number of orientationally ordered phases that occur between the formation of the amorphous liquid and the breakdown of translation positional ordering of the molecules in a solid (crystal)[42]. Liquid crystals have the property of fluidity like ordinary isotropic liquid state and certain molecular ordering[43].

Normally liquids have isotropic properties that are same in all directions. Liquid crystals are not isotropic and the properties are dependent upon orientation of the molecules[1, 44, 45]. Liquid crystals are also called mesophases or mesomorphic phases. Compounds with mesomorphic properties may be called mesogenic[46]. The word ‘mesophase’ is taken from the Greek word ‘mesos’, meaning intermediate, or between[47].

There are two common types of liquid crystal phase coming from calamitic molecules (smectic and nematic phases), see figure **1.4**. The nematic phase is the simplest liquid crystal phase, being much more fluid than the smectic phse. The chiral nematic phase is often called the cholestric phase[48].

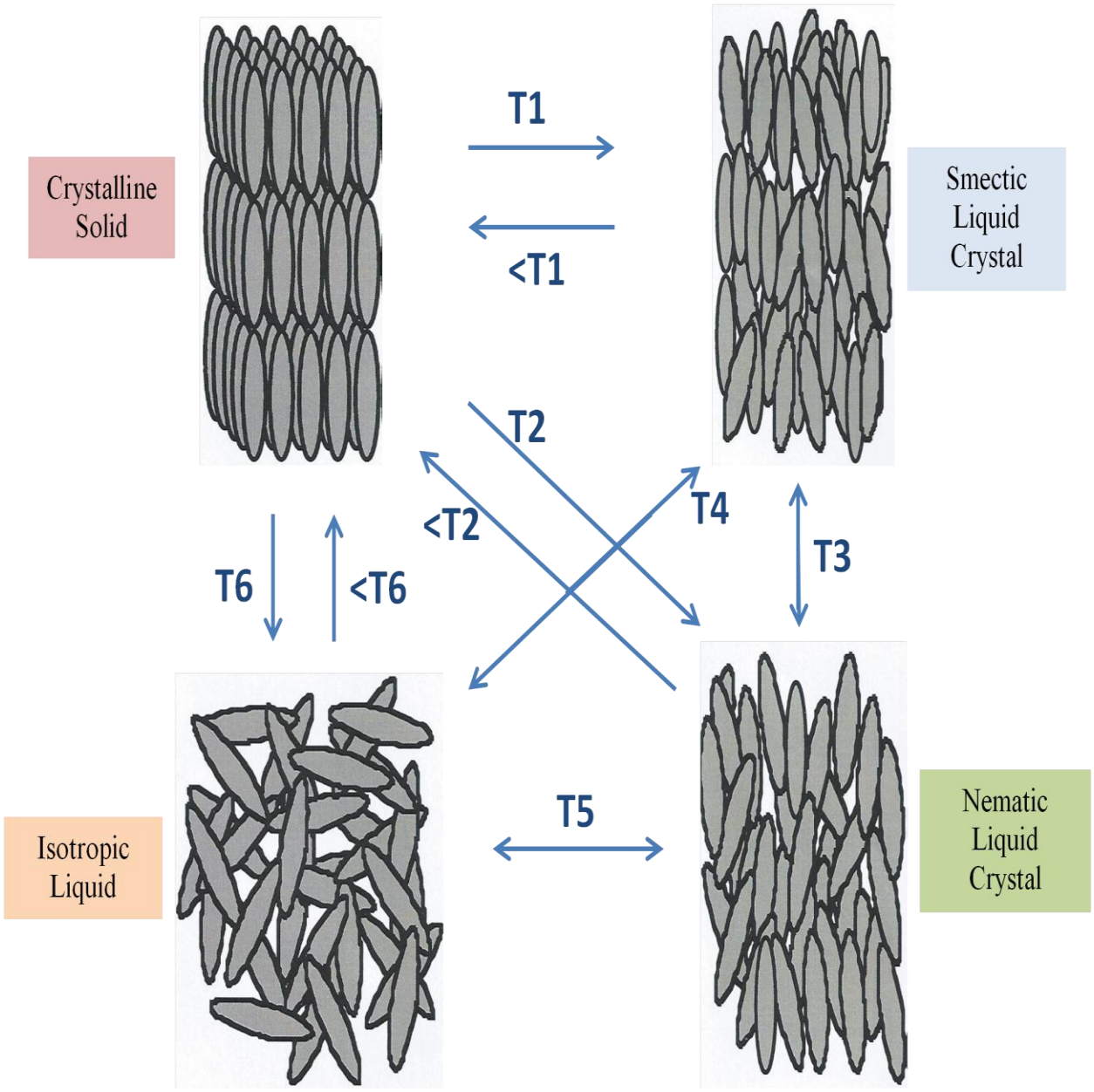

Figure 1.4. Melting sequences for a thermotropic liquid crystal, T is temperature.

Figure **1.4** shows the possible melting behaviour of calamitic liquid crystals when heating the crystal. The thermal motions of the component molecules will rise in intensity. The molecules at the melting point have enough energy to overcome the lattice energy and so the lattice breaks apart.

The strong intermolecular forces such as induced dipole-induced dipole, dipole-dipole and dipole-induced dipole forces hold together the molecules of the crystal lattice. In most molecular systems these forces of attraction are isotropic, and so as they break down an isotropic liquid phase is generated in one destructive step (T6). These forces are dependent on direction and the properties depend on the orientation of the molecules. As these forces are anisotropic so their magnitudes change according to direction. In the crystal phase, the lateral intermolecular forces must be stronger than terminal forces because when it is heated, T1, the terminal forces must breakdown first to give a lamellar arrangement of the molecules, which constitutes the smectic phase, e.g. SmA and SmC.

When a material is further heated, all of the left-over intermolecular forces can break down to result in the formation of an isotropic liquid (T4), or the molecules could be left with just orientational order, which would leave a nematic phase (T3). The nematic phase can be obtained directly from crystalline solid at T2, where both lateral and terminal forces of attraction are lost. In the final stage, at higher temperature, the long range orientational molecular ordering of the nematic phase is broken down, which results in formation of the isotropic liquid, T5[3, 17, 49].

The mesophases are observed for certain compounds on both cooling and heating, whereas for some materials the mesophases are observed only on cooling. Mesophases can be described as enantiotropic in the former core and in latter case monotropic, as illustrated in figure **1.5**[3].

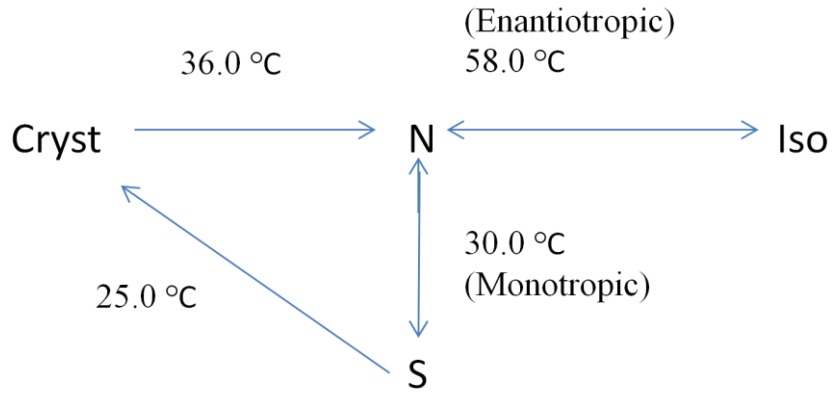

Figure 1.5. An example of an enantiotropic nematic phase and a monotropic smectic phase.

1.2.2.3.2 Nematic Phase

The nematic phase often occurs with a calamitic liquid crystal. The nematic phase is much more fluid than smectic phases[48]. The word 'nematic' comes from the Greek word for thread. In the liquid crystal phases, the nematic phase is the least ordered liquid crystal phase. A long range orientational ordering of the molecular long axes in the nematic phases is called the *Director* (n), see figure **1.6**. The degree of alignment of the molecules along the director is known as the nematic order parameter, S, defined in equation **1**[45, 50, 51].

$$|S| = <1/2\ (3\cos^2\theta - 1)> \qquad \mathbf{1}$$

Where θ is the average angle between the director (n) and the molecular axis. The nematic order parameter (S) equals zero when molecules are isotropically distributed. However, the order parameter (S) = 1 if the molecules are perfectly oriented. In a typical liquid crystal, the order parameter (S) decreases as the temperature is increased, taking on values from 0.3 to 0.7. In the nematic phase, the molecules are orientationally and rotationally disordered with respect to their short axes. The nematic phase is uniaxial. When their breadth is raised, their rotation about their long molecular axis is restricted and therefore the phase is biaxial[49, 50].

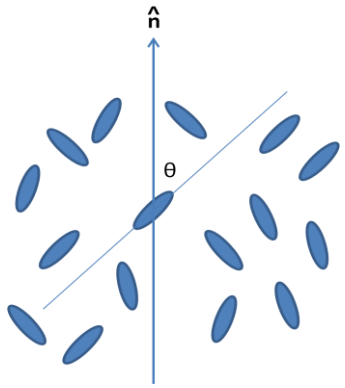

Figure 1.6. Molecular order in a nematic liquid crystal.

1.2.2.3.3 Smectic Phases

This word 'smectic' is taken from the Greek word for soap-like. The smectic phase is more ordered than the nematic mesophase. There are many different types of smectic phase, and these can be identified by optical microscopy and are designated as

smectic A, smectic B, smectic C....etc[17]. The SmA, SmB, SmC, SmF and SmI are five different smectic liquid crystal phases[52]. Every smectic liquid crystal phase possesses a sinusoidal density wave which approximates to a layered structure. The crystal E, crystal G, crystal H, crystal J, crystal K and crystal B all have molecular ordering in three dimensions and so are not liquid crystals, but they are mesophases and are often termed disordered crystals (molecules rotationally disordered). A 'D' phase has in the past been designated as smectic D, but this phase has a cubic structure and is not a smectic phase.

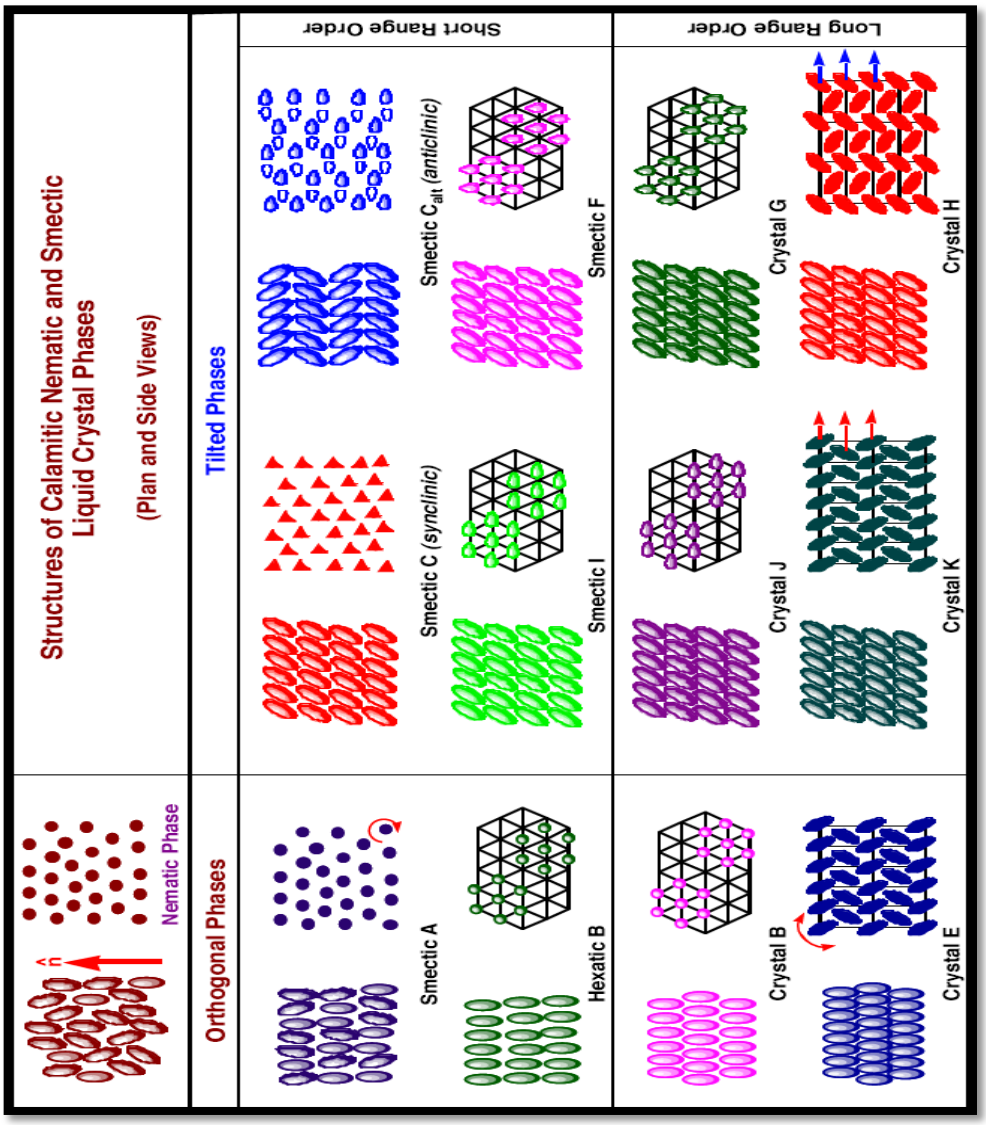

Figure 1.7. Structures of the smectic and nematic phases[47, 53].

1.2.2.3.3.1 The Crystal E, Crystal H and Crystal K

When the isotropic liquid is cooled down then we can attain the crystal E phase. Commonly we obtain crystal E phase by cooling the hexatic smectic B phase or A phase. As defined by the molecular rectangular cross sections, the each layer of crystal E has a herring-bone or chevron like arrangement when molecules are tightly packed. The positional order is interlinked through many layers but the arrangement of packing of long axes of molecules is orthorhombic therefore biaxial. The layer normal and molecular long axes are parallel to each other. As compared to frictional forces of smectic A phase, crystal E has strong forces. The layers of crystal E phase experience shearing which is opposed by frictional forces. Amongst six equivalent positions the molecules vibrate along their long axes as these molecules are unable to rotate completely due to close packing. In a harmonized manner the oscillations occur again. The crystal H and crystal K phases are the tilted modified forms of crystal E phase. The tilted direction of constituent molecules of both crystal H and crystal K are different as also occurs in SmI and SmF phases.

1.2.2.3.3.2 The Crystal B, Crystal J and Crystal G

The crystal B phase can be formed directly by cooling the isotropic liquid. The crystal B phase can also form through other preceding phases as mentioned above. The molecules, within each layer have extensive hexagonal arrangement which is parallel to the normal layer with their long axes. The motion of the molecules is hindered by frictional forces which are greater than the forces present in greater thermally stable smectic phases but still these layers can undergo shear. As in the SmB hex phase these molecules also have a rotational arrangement like 6-fold degenerate and these molecules are unable to rotate freely on their long axes.

Like the crystal B phase, the fundamental structures of crystal J and crystal G phases are similar, but with respect to the normal of layers the constituent molecules are tilted from the normal. Molecules of crystal G phase are tilted toward the face of the pseudo hexagonal net. The molecules of crystal J phase are tilted towards an apex. Thus crystal J and crystal G phases are analogues of respectively SmI and SmF phases.

Crystal J and crystal G both are obtained either through one or more described phases including crystal B phase or when isotropic liquid is cooled. The studies on miscibility explained that thermal stability of crystal J phase is higher than the crystal G phase[54].

1.2.2.3.3.3 Hexatic Smectic B, Smectic I and Smectic F Phases

The SmB hex or hexatic smectic B phase is obtained directly by cooling the isotropic liquid and it can also obtained through more than one preceding phases indirectly.

The molecules exist parallel normal of the layer and in each layer molecules are arranged in hexagonal order. Single layer or multiple layers either in pairs slip over one another as in phases of SmA and SmC due to correlation of positional ordering from layer to layer. Due to their mutual proximity, the rotation of molecules is not freely but in a co-operative behaviour. This ordering of the molecular structure results from hexatic nature and this co-ordinated rotational order is called '6-fold degenerate'.

The structure of smectic F (SmF) and smectic I (SmI) phases are similar to SmB hex phase, but the long axes of molecules of SmI and SmF phases are tilted with respect to the layer planes. The molecules of SmI phase are tilted in the direction of apex of the pseudo hexagonal net. However, the molecules of SmF phases are tilted towards a pseudo hexagonal face. This difference of these phases is apparent; however their separate distinctiveness is well defined through x-ray. The SmF and SmI phases can be obtained directly through cooling of isotropic liquid or indirectly through other phases as described earlier. The materials or mixtures which demonstrate both phases, it has been shown that SmI phase has the higher thermal stability[53].

1.2.2.3.3.4 The Smectic A Phase[17, 53, 55, 56]

X-ray diffraction researches showed that the long molecular axes in the SmA are arranged perpendicular to the planes of the layers and give one dimensional density wave for the molecular mass centre. The lateral distribution of the molecules within each layer is almost random. In the SmA phase, the molecules layers rotate freely along their axes.

The SmA phase can show bilayer ordering and semi bilayer and this can either be caused by partial pairing or interdigitation of molecules. The SmA has different kinds of phases as shown below, see figures **1.8** and **1.9**.

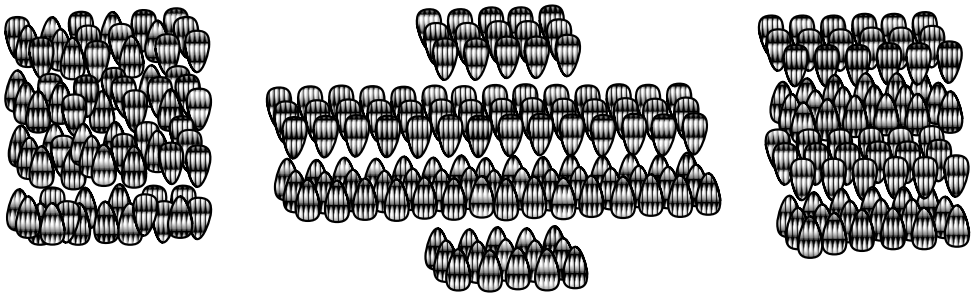

Figure 1.8. Different Structures of smectic A; A_1, A_2 and A antiphase.

In figure **1.8**, the SmA_1 phase is basically a monolayer system where the molecules do not overlap and are disordered. The SmA_2 phase illustrates that the molecules increase to a bilayer and the layer spacing is twice the molecule length. The SmA antiphase is basically the SmA_2 phase, but has a half layer shift end, at the shift points, this brings a SmA_1 kind structure. Every 15 nm or so, these shift points occurs. The figure **1.9** shows the SmA_d phase. Between the molecules, there is some interdigitation. This could be because of polar end groups, *e.g.* cyano group, interacting with the ends of the central core giving the molecules interdigitation. For SmA_d phase, a bilayer of 1.4 times that of the molecular length is observed.

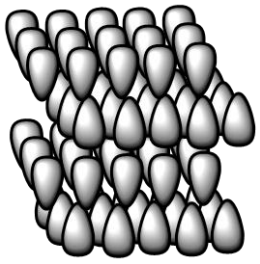

Figure 1.9. A structure of smectic A_d phase.

It has to be known that the diagrams have been simplified as the actual bilayers and pairing of the molecules are constant flux[4, 57, 58].

1.2.2.3.3.5 The Smectic C Phase

When the isotropic liquid is cooled down it can directly form the SmC phase which can also be formed through other phases such as SmA phase. The SmC and SmA phases have similar structures but with the difference that the director of the SmC phase is tilted at an angle Θ with respect to the layer normal. Two different types of behaviour are shown by the tilt angle Θ in SmC and it depends on the nature of the preceding phase[59].

The Θ of the phase will increase rapidly as the temperature falls on cooling the SmC phase. The Θ will increase slightly on decreasing the temperature below the transition temperature or when the temperature reaches the 10 degree or 15 degrees. The value of Θ will be in between 20 and 30 degree if the SmC phase will remain in a specific temperature range.

The temperature independent values of Θ are obtained which are large and this results when the SmC phase is formed by cooling the cholesteric (nematic) phase or the isotropic liquid. The value of Θ ranges in between 35 degrees to 45 degrees.

It is not the case that this only happens when the molecules are tilted they form the SmC phase as it is assumed mostly. Studies on liquid crystalline polyacrylates[60] revealed that, in field-orientated samples, at the SmA to SmC transition, the side chains of polymers are aligned toward the direction of electric field. The backbone polymer achieves the structure of the SmC which becomes inclined when compared with translational experienced mesogenic groups and the arrangement more densely packed due to this reason.

In 1973, many of SmC materials made[61] from symmetrical molecules, which include polar groups linking the aromatic core to alkyl chains. The rotations of molecules are frozen out when SmA phase transit to SmC phase. An electrical torque is created by these polar functions (outboard ‘dipoles’ or terminal) due to which the molecules are tilted with respect to the layers. There is some doubt on the strength of this theory as the molecules of the SmC phase rotate freely thus not all the SmC phases contain polar groups.

The overall molecular shape of the SmC materials suggested by the Wulf[62] is of zigzag nature as these materials consisted of symmetrical molecules, having 2 alkyl chains linked to a central aromatic core. When these structures are tilted, he proposed that these zig-zag shaped molecules could pack more efficiently.

Goodby[63] provided a steric model with variations. He presented the rotational volumes which were swept out by their computer simulation of SmC molecules. He concluded based on the shapes that in the tilted structure the well-organized packing can be attained. The relation between the polar groups of the SmC phase and the thermal stability was also accepted by Goodby.

Laterly a new polar model for SmC phase has also been proposed[64]. In this theory it has been explained that in the neighbouring molecule a dipole is induced in the polarizable core by the permanent dipole of one molecule which is in rotation. A tilted structure is resulted due to the induced attraction between the molecules.

The zigzag properties of individual molecules can be taken for description of the origin of tilt in SmC phase inorder to explain in adequate manner. In SmC phase the tilt in the long axes of molecules is respecting to the normal of the layers planes. According to the director the molecules which are in layers have hexagonal close packing very locally, but only over 1.5 nm, which is a very short distance. The consecutive layers of SmC phase maintain the tilt which make this phase weakly biaxial and gives C_{2h} symmetry. A sub phase of the SmC is also present which is known as the SmC_{alt}, in this phase there is rotation of 180° in the tilt angle of molecules when these molecules passes from one layer to the other.

The director of this sub phase is normal to the layers planes and the layers of this SmC_{alt} alternate. There are sub phases present for the polar materials including the alternative phase which are similar to SmA phase instead of the fact that there is tilt in versions of SmC which can be represented as SmC_1=SmA_1 , SmC_d=SmA_d and so on. When the SmC phase is tilted it gives the version of the SmA and this happens when there is tilt with respect to plane and normal of layers in the axes of molecules. This is the foremost difference between the SmC and SmA phase[17, 53, 65].

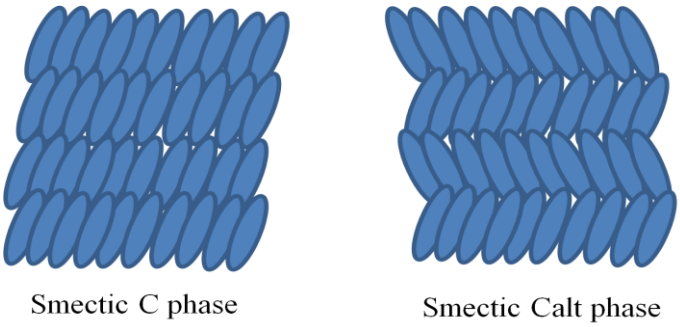

Figure 1.10. Structures of the SmC phase and SmCalt phase.

1.3 Chirality in Liquid Crystal Phases

1.3.1 Chiral Nematic Phase (N*)

The chiral nematic phase (N*) phase is often called the cholesteric phase (the more common name) because, the first materials to illustrate this phase were natural cholesterol derivatives. Today, there are many different kinds of chiral materials that display the chiral nematic phase (cholesteric phase) and these are not similar to cholesterol. The chiral nematic phase can be produced by adding a small amount of a chiral material to a nematic material. The chiral material is not necessarily a liquid crystal[17]. The cholesteric phase is not lamellar. In the cholesteric phase, the important characterising feature is the pitch length (p). The pitch length (p) is known as the physical distance over which the director (n) rotates a full turn 360° in the helix structure of the nematic sheets, see figure **1.11**[66, 67]. The pitch length increases as the temperature decreases[17]. The chiral nematic liquid crystals have found important applications in fields such as thermometers, colour filters, laser cavity mirrors and polymer dispersed chiral nematic liquid crystal display[56].

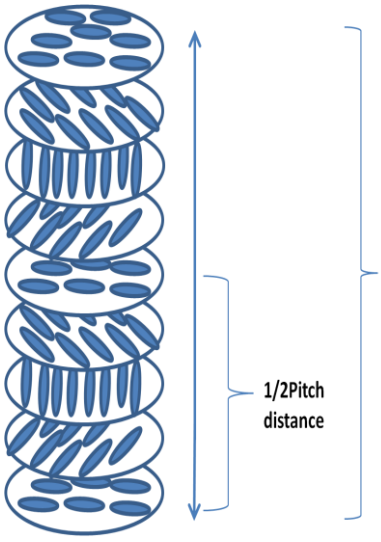

Figure 1.11. The N* phase structure.

1.3.2 Chiral Smectic C Phase (SmC*)

Meyer et al[68] used symmetry arguments in 1975 and explained that chiral smectic phases shows spontaneous polarisation (Ps). The environmental symmetry of the SmC phase when its molecules are achiral consists of a twofold axis, a centre of symmetry and a mirror plane containing molecular tilt and perpendicular to layers giving a C_{2h} symmetry, see figure **1.12**.

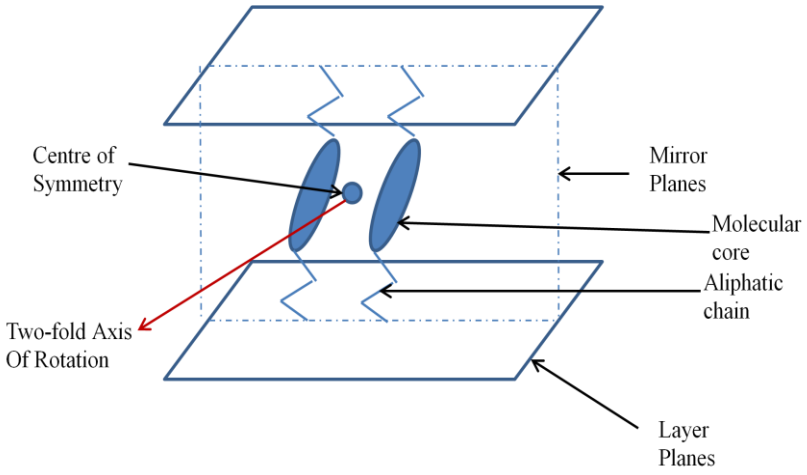

Figure 1.12. The achiral SmC phase C_{2h} symmetry.

The symmetry is decreased to a two-fold axis[69] of rotation when the smectic phase has the chiral molecules and the group symmetry is now C_2. Due to molecular interactions the dipoles which are associated with environment at the chiral centres align, which results in a Ps that develops along the C_2 axis of phase, see figure **1.13**.

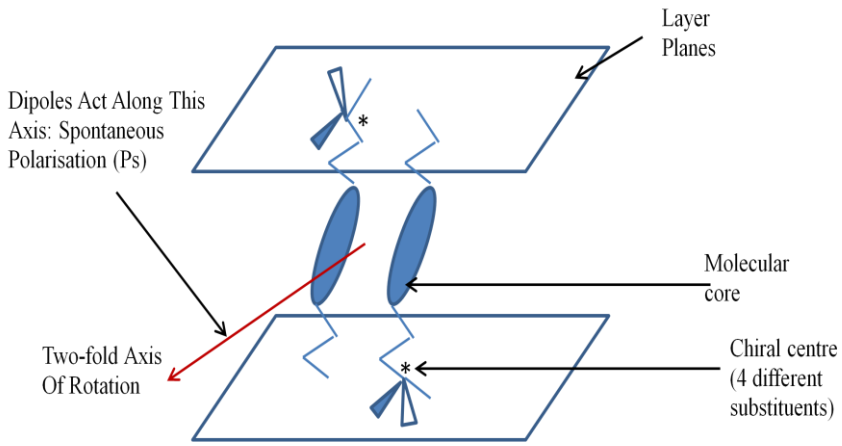

Figure 1.13. The chiral SmC* phase C_2 symmetry.

Upon a single layer of SmC* phase the consequences of reduced symmetry is shown in figure **1.13** also due to chiral units the preferred orientation of molecules is also shown in this figure. A helical structural arrangement can be seen when this concept is applied onto bulk phase and this is similar to chiral nematic. Inherently the structure of SmC* phase is more complex[70] due to layered and tilted nature of molecules within smectic layers. The direction of polarization (**P**) is also caused to rotate from layer to layer due to rotation of direction of tilt, as can be seen in figure **1.14**. Due to rotation throughout the helix, the polarisation direction with each layer within the phase is cancelled out throughout the bulk of phase. It is shown in figure **1.14** that the pitch length of the material is one complete rotation of the director and the polarization is zero, and so the phase is termed "helielectric" rather than "ferroelectric"[17]. At lower temperatures the largest tilt angles are produced and the tilt angle of SmC* phase is dependent on temperature.The optical properties of the SmC* phase in terms of selective reflection of colour are similar to chiral nematic phase in that temperature affects the pitch length in both phases. The tilt angle of the SmC* phase is increased when the temperature is reduced which result in tightening of pitch of the helix which decreases the pitch length. Enlarged pitch length can be observed which is opposite effect when we increase the temperature[17, 65].

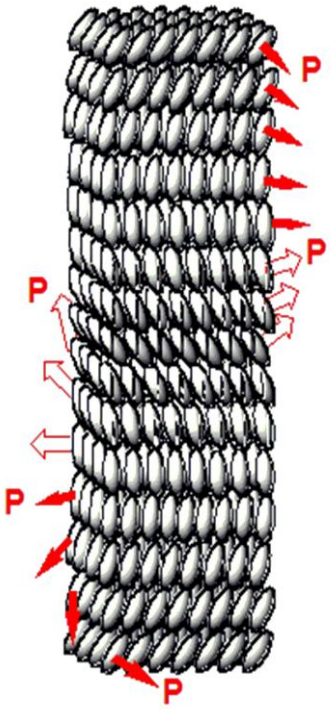

Figure 1.14. The SmC* phase structure.

1.4 Basic Structural Features of Calamitic Thermotropic LCs

When the molecules are rod shaped and have high length to breadth ratio then they are known as “calamitic liquid crystals”. The most renowned type of thermotropic liquid crystals is calamitic liquid crystals[71]. Structurally the molecule possesses a core unit. Some liquid crystals may have lateral substituent also, see figure **1.15**. The rod like shape of molecules is preserved by the material which fit in rigid central core system. This incorporation increases the ordering and arrangement of molecules

which are essential in forming mesophases. Variety of rings of type A or type B can be incorporated into the core system. The core may consist of aromatic rings (commonly 1-4 disubstituted-phenyl rings) (*e.g.*, compound **1.9**) heteroatoms may be present or not, to cyclohexyl rings, bicyclo[2.2.2]- octanes and cyclobutyl rings.

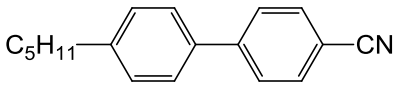

1.9

Cryst 24.0 N 35.0 Iso ^{o}C

In 1970s when Gray and his team were working in the University of Hull synthesised "cyanobiphenyls"[72] which is now basic part of nomenclature of liquid crystals. 4-cyano-4'- pentylbiphenyl (**1.9**) or (5CB as it is known) is the most famous compound synthesised by Gray and his team.

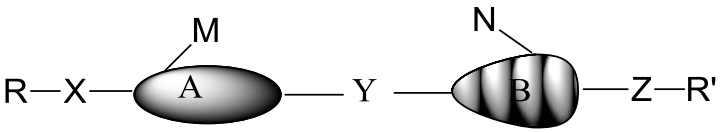

Figure 1.15. A general structural template for calamitic liquid crystals.

Figure **1.15** illustrates a general template that can be used to represent the structure calamitic liquid crystals, counting those that display the smectic phases and nematic phase.

- A and B in figure **1.15** are the core units. A and B are sometimes linked by a linking group (Y) but often a direct link is used.
- R and R' are the terminal chains which can be linked to the core with groups (X) and (Z) but the terminal chains are usually straight linked to the core.
- M and N are the lateral substituents which are often used to modify the physical properties and the mesophase morphology of liquid crystals to produce enhanced properties for applications[17].

1,4-phenyl, *trans*-1,4-cyclohexyl and 2,5-pyrimidyl are an examples for the linked cyclic units which provide the rigidity to structures which is the most important need for mesogenic behaviour. Ethynyl, carboxylate and dimethylene are the typical

groups used for linking. Usually, the rigid core alone is not enough to get liquid crystal phases and sure flexibility is wanted to get low melting points and for stability of molecular alignment within the mesophase structure. The terminal substituents R and R' provide flexibility, R and R' are usually straight alkoxy or alkyl chains. Isothiocyanate and cyano are an example for small polar species which are also used. When the lateral substituents M and N are incorporated then the core unit is modified which change the physical properties and morphology of mesophase. F, Cl, CH_3, CN etc are various examples of lateral substituents that are used. As fluorine has high electronegativity and small size it is a widely used unit due to this combination of properties. To produce the mesophase lateral units which are larger in size are less successful[17].

1.4.1 Core Units

1,4-disubstituted benzene ring is used in production of liquid crystals as it is a standard building block. 2,6-naphthalene and 2,5-pyrimidine are also commonly used but 1,4-disubstituted benzene ring is highly polarisable and basic rod structure is also defined by it, see figure **1.16**.

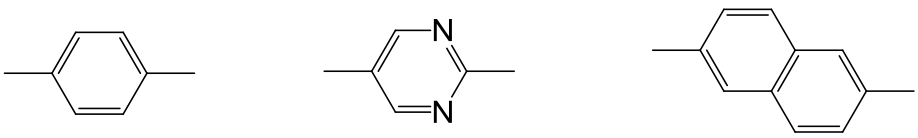

1,4-phenyl 2,5-pyrimidinyl 2,6-naphthyl

Figure 1.16. Selected different aromatic core units.

Next to benzene, the most widely used unit is biphenyl as it provide the necessary rod like shape in the crystalline state due to its linearity[73]. Commercially feasible compound used first time in display devices is the compound **1.9** or 5CB. The *para*-terphenyl is an example of three ring systems and has similar linearity. Due to strong lateral forces of attraction in terphenyl materials the three rings are compatible in structure which gives high stability to liquid crystal phase (smectic phase). To extend the thermal stability of the nematic phase a small amount of 4-alkyl 1,4''-cyanoterphenyl **1.10** is used in commercial nematic mixtures of biphenyls[17].

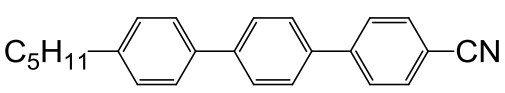

1.10

Cryst 130.0 N 239.0 Iso ^{o}C

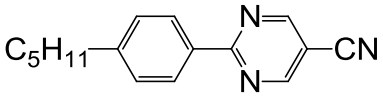

1.11

Cryst 71.0 (N 52.0) Iso ^{o}C

Heteroaromatic rings have been investigated as possible core unit *e.g.*, compound **1.11**[74, 75]. The properties of mesogenic bi- and ter-phenyls have been compared with their heterocyclic analogues. A higher melting point and clearing point is observed if nitrogen is the heteroatom as in the most of investigations. The heterocyclic pyrimidine ring such as in compound **1.11** gives a reasonable increase in T_{N-I} because the steric hindrance in the inter ring, bay region from the protons of compound **1.9** has been removed and the two aromatic rings can now adopt a more planar arrangement with less interannular twisting of the parent system which gives a high T_{N-I} value because of the increased longitudinal polarisability. Due to increased polarity from the nitrogens, compound **1.10** has a high melting point which is a disadvantage[17].

1.4.2 Terminal Groups[17, 45, 76]

Liquid crystal systems usually include the terminal groups which are shown by R and R' in figure **1.15**. The selection of terminal units determines the physical properties and the type of liquid crystal phase. The most successful terminal units are a small polar substituent as cyano group or straight chain fairly long hydrocarbon which is usually alkoxy or alkyl. It is still not fully understood the function of terminal units performed in liquid crystal phases. The molecular orientation could be established by alkyl/alkoxy chains which is important for generation of liquid crystal phase. The flexibility is added to the rigid core by the long alkoxy/alkyl chains to reduce melting point and allow the phases of liquid crystal to be displayed[17].

When the length of the chain is increased it reduces the melting points because of increased flexibility. On the other hand, when very long, the melting points are increased by the excessive van der Waals intermolecular forces of attraction. The chain in the T_{N-1}, clearing points, values could be similar to that explained above about melting points, the T_{N-1} fall with rising chain length, and raise with very long chains. On the other hand, there is odd-even effect shown by the chains which is that

those chains which are odd-membered produce high T_{N-1} value and even-membered chains give reduced value of the T_{N-1}. When the compounds **1.12** and **1.13** are compared they exemplify this odd-even effect. The compound **1.13** is deviated from linear structure of the more favourable all-trans conformation of the chain due to extra carbon which makes the chain of the compound even in number and this decrease the T_{N-1} value. The smectic tendency rises with the increase in length of terminal chains. The lamellar packing is facilitated by the long chain and required for smectic phase generation.

The molecular packing is disturbed when the alkyl chains are branched due to which the melting point and the liquid crystal phase stability are reduced. This disturbance is more when branch is close to the core of structure thus a low melting point results. The effect of branching can be reduced by moving the branch away from the core and extending the chain[17].

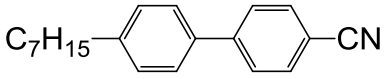

1.12

Cryst 30.0 N 43.0 Iso ^{o}C

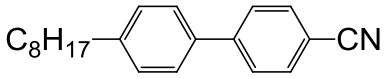

1.13

Cryst 21.5 SmA 33.5 N 40.5 Iso ^{o}C

1.4.3 Lateral Substituents

The physical properties and morphology of mesophase have been modified by the substituents which are attached off of the molecular axis and they are known as the lateral substituents. There are many different lateral substituents, such as F, Cl, CN, NO_2, CH_3 and CF_3 that have interpolated into liquid crystal systems.

Lateral substituents disturb the molecular packing mostly lamellar packing which decreases the stability of liquid crystal phase in smectic phase mostly. On the other hand, lateral substituents reduce the melting points and are necessary to produce the desired liquid crystal phases. For instance, a fluoro substituent in some systems is used to eliminate all smectic phases and produce nematogens of the low melting points. For a certain device application lateral substituents are also used to modify physical properties like elastic constants, dielectric anisotropy etc, of liquid crystals. Relevant steric reasons, the effect on polarity and the resultant polarisability

anisotropy are all necessary reasons to consider when a lateral substituent in fitted into a system of mesogenic[77, 78].

Fluorine is the most useful lateral substituent type widely used. It exerts significant effect on breadth of molecules to modify melting point and liquid crystal phase morphology due to small size (the smallest van der Waals radius except for H, 1.47 Å) and high electronegativity (the highest of the elements, 4.0). Moreover, the polarity of the fluoro substituent is helpful in formation of the tilted SmC phase. The fluoro substituent is also necessary in modifying physical properties as the viscosity is decreased due to small size of fluorine and also gives zero or negative value of dielectric anisotropy. This fluorine substituent also modifies the physical properties of system, without too much disruption to the stability of liquid crystal phase.

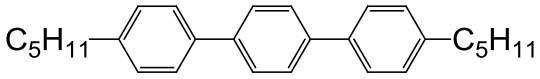

1.14

Cryst 92.0 SmA 213.0 Iso ^{o}C

For formation of liquid crystal phases, the terphenyl core is very good choice, as in compound **1.14**. Due to it possesses very high polarisability anisotropy and very high length to breadth ratio. A lateral substituent of fluorine is supported by such a core unit and this core can also produce high transition temperatures of liquid crystals[79].

A fluoro-substituent can be located in 6 different positions out of 12 positions in unsymmetrical 4,4''-disubstituted terphenyl. There are two types of locations in terphenyl for lateral fluoro substituent which are 'outer edge' and 'inner core'. The lateral fluoro-substituent causes much disruption in the side-to-side intermolecular packing at inner core location (*e.g.*, compound **1.15**). This results in a decrease stability of smectic phase and allows the generation of a nematic phase. An interannular twisting is caused by fluoro-substituent at inner core and this twisting is greater than twists produce by hydrogen which decreases the polarisability anisotropy. This will further depress the thermal stability in liquid crystal phase[79]. At the 'outer edge' position (*e.g.*, compound **1.16**) the fluoro-substituent tends to fill space in polar unit which facilitates the side-to-side intermolecular forces of attraction and which upholding the stability of smectic phase, despite of steric effect

and the nematic phase is not displayed. The fluoro-substituent does not produce additional interannular twisting and this result in high polarisability anisotropy. Thus supports the high transition temperatures[79].

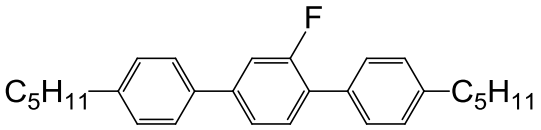

1.15

Cryst 51.5 B 62.0 SmA 109.5 N 136.5 Iso °C

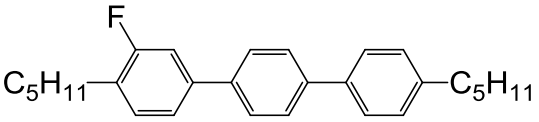

1.16

G 156.5 SmA 185.5 Iso °C

The positions which are next to each other are the best positions for two fluoro-substituents, for example ortho-difluoroterphenyls. The molecular breadth is minimized due to both fluoro substituents are inherently fixed on one side of the molecule which results in LC phase transition temperatures being upheld. When terminal chains both are alkyl, short and the fluoro-substituent are at the inner core position then the materials possess high temperatures and are nematogens as melting points are more than ideal (*e.g.*, compound **1.17**)[76, 79]. Smectic phases are prevalent when the fluoro-substituents are at the outer edge due to their space filling influence of the polar substituent (*e.g.*, compound **1.18**).

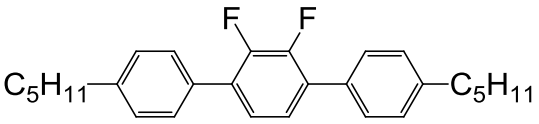

1.17

Cryst 60.0 N 120.0 Iso °C

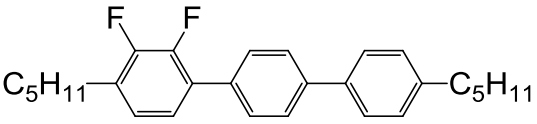

1.18

Cryst 81.0 SmC 115.5 SmA 131.0 N 142.0 Iso °C

1.5 Physical Properties of Liquid Crystals[17, 45, 80, 81]

The physical properties are very important for using that liquid crystal in distinctive applications. These properties will be discussed relevant to the smectic and nematic liquid crystals.

1.5.1 Viscosity

Liquid crystalline materials are fluids and they exhibit anisotropy in their flow behaviour. This can be easily understood by measuring the viscosity of the liquid

crystal (LC) by placing it between two flat surfaces and measuring the force needed to move one plate past the other at a constant velocity. In figure **1.17**, the plates lie in the xy plane and are separated by a uniform distance (d). The underneath plate is fixed and the force (Fx) acting on the top plate is in the x direction. The top plate velocity is also in the x direction, v_x [17].

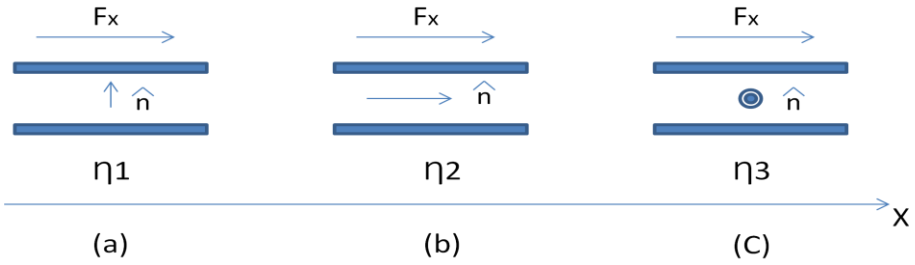

Figure 1.17. Measuring the three viscosities of a nematic liquid crystal. (a) is η1 the director perpendicular to the flow and parallel to the velocity gradient), (b) is η2 the director parallel to the flow, (c) is η3 the director perpendicular to the flow and perpendicular to the velocity gradient.

The velocity of the fluid next to every plate moves with the similar velocity as the plate[17]. Sometimes the three viscosities are called the Miesowicz coefficients. In addition, the three viscosities are known as η1 (the first viscosity is the director perpendicular to the flow and parallel to the velocity gradient), (b) is η2 (the second viscosity is the director parallel to the flow), (c) is η3 (the third viscosity is the director perpendicular to the flow and perpendicular to the velocity gradient)[17].

1.5.2 Optical Anisotropy (Birefringence)[48, 72, 82]

Through a solid when the light propagates, there is interaction between the atoms of solid using electronic clouds and electric field components of the light beam. This is because of the reason that the separation between atoms of solids is smaller than the wavelength of the incident light beam or in other words that atomic spacings are small then the electric field minima and maxima which are widely spaced. The interaction between the constituent atom of the material and electric field components of the light when light propagates through liquid crystals or anisotropic media, is affected by certain factors described below:

- The direction toward which the light rays propagate and,

- The orientation of the vector of the electric field with respect to structure of the liquid crystal.

The light rays which enter into the anisotropic media with the direction toward propagation are divided into two different rays which have different refractive indices due to different velocities. This is known as birefringence or double refraction. The two rays arising from light ray are known as the ordinary ray and extraordinary ray. The ordinary ray (n_o) is coupled to the optic axis of molecules and has refractive index n_o whereas the extraordinary ray (n_e) is perpendicular to optic axis with the refractive index n_e. There is a relation between the refractive index (n) velocity of light (v) and velocity of light in vacuum (c).

$$n = c / v \qquad \mathbf{2}$$

Double refraction does not take place when the difference between the velocities of extraordinary ray and ordinary ray is zero, i.e along the optic axis. Positive or negative values for the difference in refractive indices 'Δn' can be found.

$$\Delta n = n_e - n_o \qquad \mathbf{3}$$

When the isotropic liquid is formed from the nematic mesophase there is a decrease in the two refractive indices and these will depend upon temperature. For applications of displays property of birefringence is very important. Through molecular engineering the suitable value of Δn can be designed. There are high Δn values for the materials which have terminal chains and mesogenic cores which are electron rich. For example compound **1.9** has a high Δn value, whereas there is a low birefringence value for the compound with a terminal alkyl chain and saturated alicyclic rings like compound **1.19** whose value is near to zero.

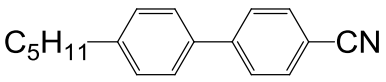

1.9

Δn = 0.20

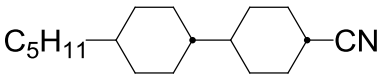

1.19

Δn = 0.05

1.5.3 Dielectric Anisotropy[48, 83]

Dielectric is that material which is non-conducting and polarisable. It creates induced dipole moment in non-polar molecules. Due to differences in electronegativity of atoms there is permanent dipole moment because atoms of the molecules have partial charges on them.

There are two dielectric permittivities as uniaxial liquid crystals are anisotropic in nature. The dielectric anisotropy of liquid crystals is described by the equation below, where ($\varepsilon_{\parallel}$) is parallel permittivity, the permittivity along the long molecular axis, and ($\varepsilon_{\perp}$) is perpendicular permittivity the permittivity which is perpendicular to the director and to the long molecular axis.

$$\Delta\varepsilon = \varepsilon_{\parallel} - \varepsilon_{\perp} \qquad 4$$

The magnitudes of $\varepsilon_{\parallel}$ and $\varepsilon_{\perp}$ are dependent upon many factors, namely:

a) Spatial structure of molecules

b) Degree of order within the phase and dependent upon the temperature.

c) Presence of dipole moments, either permanent or induced, in nature which are acting along different directions like parallel or perpendicular to axis.

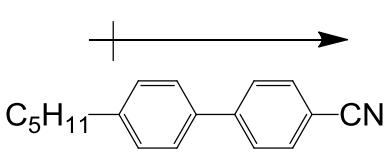

1.9

$\Delta\Sigma = +12$

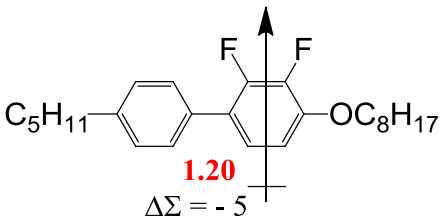

1.20

$\Delta\Sigma = -5$

1.5.4 Elastic Constants

Elastic forces in a solid subjected to pressure or tension act to reinstate it to the initial shape if the elastic limit is not exceeded. However, there are likely deformations for a mesophase of a liquid crystal especially the nematic mesophase where three deformations would result. Here, the elastic forces are weaker compared to the solid case but they play crucial part for display purposes. The elastic constants compel the relaxation for instance, the movement of molecules from homeotropic alignment

back to their planar configuration in a twisted nematic display. The three likely deformations are: bend (K_{33}), twist (K_{22}) and splay (K_{11}**)** as shown in figure **1.18**. The ratio of bend/splay (k33/k11) is more useful than the specific values and is required to be low for optimum electro-optical characteristics with typical values in the range 0.6 and 0.8. However, it is harder to determine values and ratios for elastic constants by use of molecular engineering compared to determination for viscosities as well as anisotropies for optic and dielectrics [48, 49].

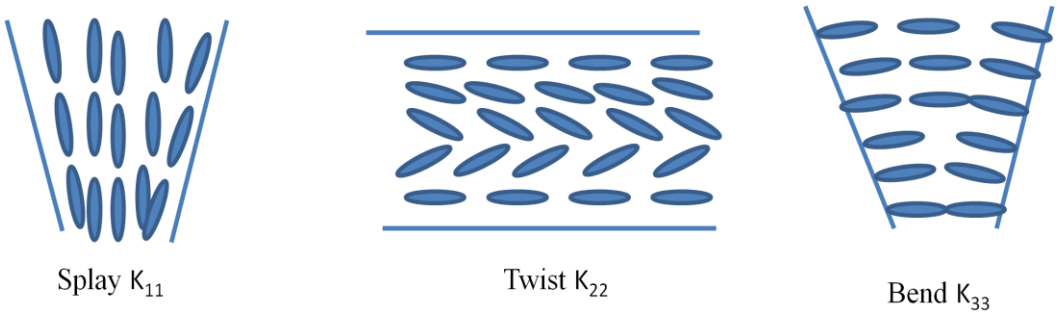

Figure 1.18. Three possible deformations: splay(K_{11}), twist (K_{22}) and bend (K_{33}).

1.6 Identification and Characterization of Liquid Crystals

A large number of liquid crystal phases have been discovered. These phases have to be identified. The different structures between these phases are quite narrow and so the precise characterization of liquid crystal phases needs the use of different techniques. The most common these days to use a combination of these techniques as shown below:

- Polarizing Optical Microscope (POM).
- Differential Scanning Calorimetry (DSC).
- X-ray Diffraction (XRD).

1.6.1 Polarizing Optical Microscopy (POM)[53, 78, 84-86]

The polarizing optical microscope (POM) is one of the most commonly used devices to identify the liquid crystal phases. It reveals the characteristic optical texture of the liquid crystal phases. A sample of material is sandwiched between two glass plates (microscope slide and cover-slip) and placed into a hot-stage (temperature can be controlled accurately) in an optical polarizing microscope. In the nematic phase two

molecular orientations are possible, homeotropic and homogeneous (figure **1.19**). The polariser and analyser set at 90° when viewed through a polarizing microscope, and so with homeotropic molecular alignment an optically extinct texture results. However, with homogeneous molecular alignment a birefringent texture is generated with colours and black lines or brushes where the molecular direction coincides with the polarization direction (figures 1.20 and 1.21). Some examples of optical textures generated by common liquid crystal phases are shown in figures **1.20** to **1.25**.

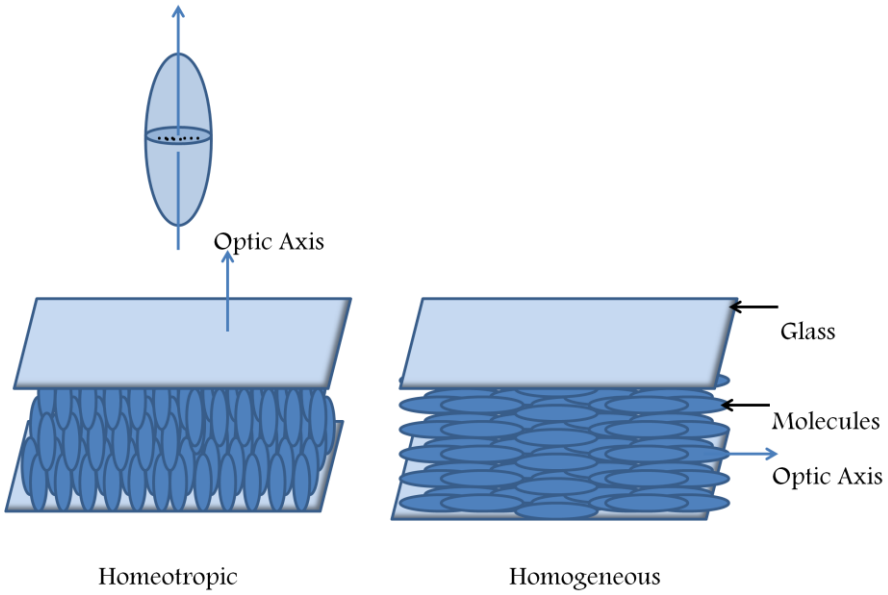

Figure 1.19. The homeotropic and homogeneous alignment.

Figure 1.20. Nematic droplets obtained on cooling an isotropic liquid[3].

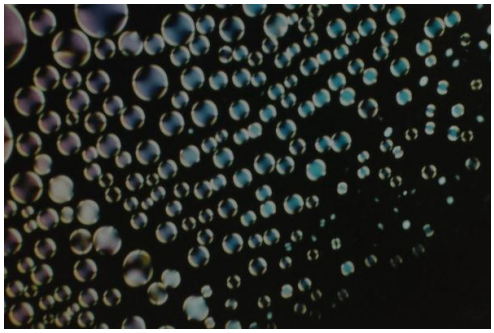

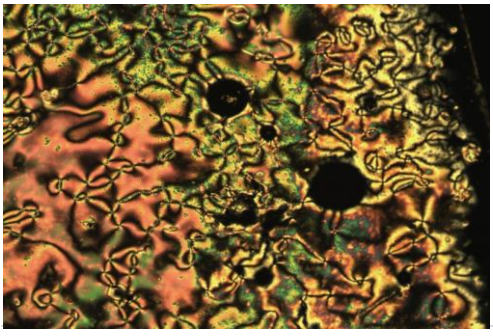

Figure 1.21. The Schlieren texture of a nematic phase.

Figure 1.22. Cholesteric phase (Grandjean planar texture)[87].

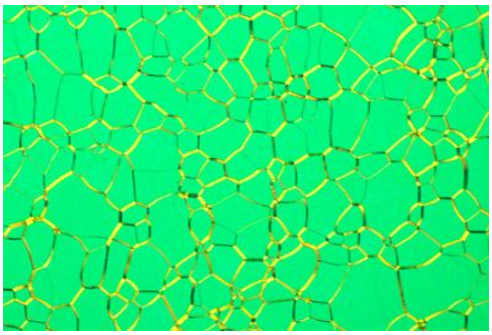

Figure 1.23. Cholesteric phase (Pseudo focal conic texture)[3].

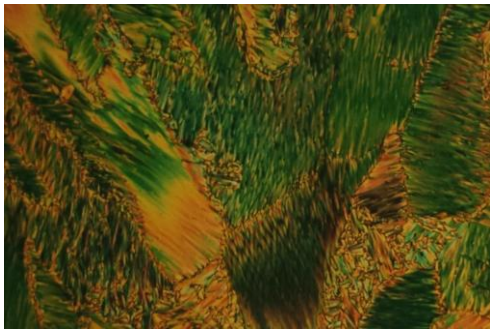

Figure 1.24. The Schlieren texture of a smectic C phase

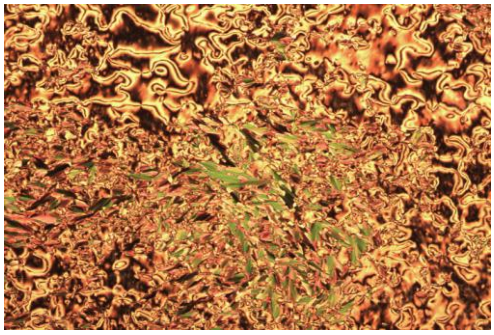

Figure 1.25. The focal conic texture of a smectic A phase

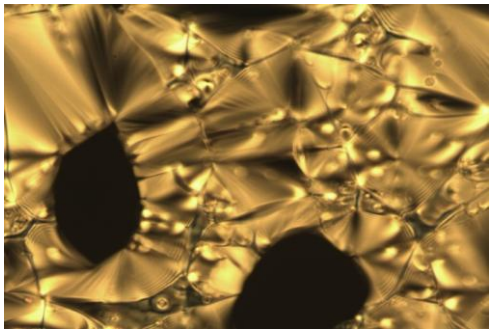

1.6.2 Differential Scanning Calorimetry (DSC)[88]

After the polarizing optical microscope (POM), differential scanning calorimetry (DSC) is one of the most commonly used devices and useful technique to identify the liquid crystal phases. Polarizing optical microscope (POM) and differential scanning calorimetry (DSC) are complimentary techniques to know the precise liquid crystal transition temperature and the enthalpy change associated with the transition. DSC cannot distinguish the actual phase type, whereas POM can. On the other hand, there are limitations in liquid crystals phase characterization by either of these techniques as the optical textures of diverse smectic or columnar liquid crystal phase are

difficult to distinguish and the values of enthalpy cannot be so characteristic for diverse liquid crystal phase transitions.

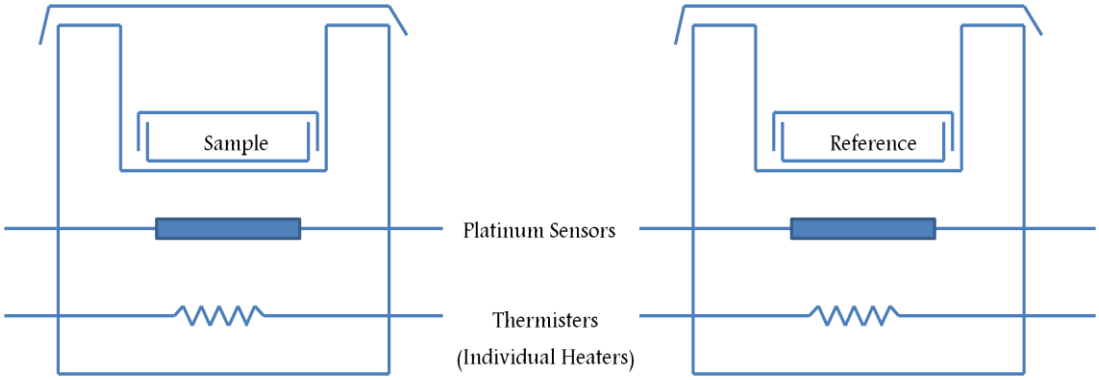

Figure 1.26. The operation of the differential scanning calorimetry (DSC).

In figure **1.26**, the operation of the differential scanning calorimetry (DSC) is shown. There is a gold pan on the right-hand side. The gold pan acts as the reference, and on the left-hand side there is the sample (Aluminium pan). The form of the method separates micro furnace for both reference and sample, and therefore needs separate temperature sensors and heaters.

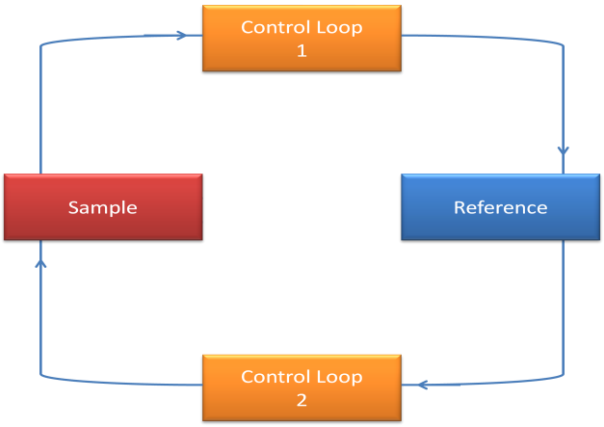

Figure 1.27. The two control loops of the differential scanning calorimetry (DSC) system.

The differential scanning calorimetry (DSC) system has two control loops, see figure **1.27**. The first control loop (control loop 1) provides the temperature change (decrease/increase) at the operator for both sample and reference. The second control loop (control loop 2), the differential control loop, ensures that the temperature of the two pan holders is always identical and the same. If a transition occurs in the material under investigation, an increase in temperature has to be provided to balance

the sample and reference. Then the control loop 2 will feed energy to either the sample or the reference to correct this imbalance. This extra energy can be measured by the instrument and is directly proportional to the energy change (enthalpy of transition, ΔH) of the system. The differential scanning calorimetry (DSC) instruments calibrated for enthalpy and temperature using pure indium (as the standard). The ΔH for pure indium is 28.45 J/g and the melting point is 156.6 °C.

1.6.3 X-ray Diffraction[89]

Since 1920, X-ray diffraction has been used in the determination of LC structures, especially those of the more ordered smectic phases. X-ray diffraction and neutron scattering techniques are the only ones that examine the actual structure of the liquid crystal phase[90].

The only bright reflections are observed when X-rays are passed through material and constructive interference of the beam occurs. The important conditions for this interference are provided by the Bragg Law as shown below:

$$n\lambda = 2d.\sin\theta \qquad 5$$

Where $n =$ denotes the order, i. e. $n = 1$ is first order, $n = 2$ is second order.

λ = Wavelength of incident X-ray radiation.

d = Layer thickness.

θ = Angle of Incidence.

The primary use of the Bragg Law is the determination of the spacing between planers molecules in the liquid crystal material.

There are 4 points to remember:

1- Small scattering angle means large distances – large scattering angle means small distances.
2- Diffuse peaks denote only short-range order (liquid) – sharp peaks denote long range order (crystal).

3- Inner arc gives details about layer spacings (d) – outer arc gives details about spacing (D) of the molecules within the layer plane.
4- If the spacing d is temperature dependent, then the molecules are tilted within the layer plane.

In figure **1.28**, there is the diffraction pattern for a selective number of LC phases.

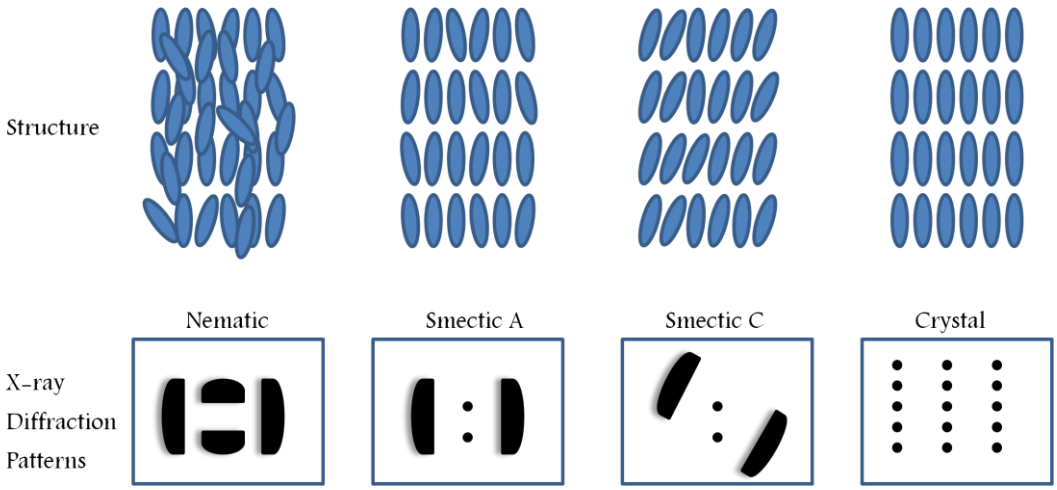

Figure 1.28. Diffraction pattern for a selective number of LC phases.

1.7 Display Applications of Liquid Crystals

1.7.1 Display using the Nematic Phase

1.7.1.1 Twisted Nematic (TN) Device[17, 91]

In the late 1970s, twisted nematic became popular and represented the first successful application of liquid crystals. Also, the twisted nematic became a fixture in the market for displays with low information required such as calculators and watches, due to the low power consumption of the LC devices[92]. The majority of liquid crystal displays are based on twisted nematic (TN) devices.

The figure **1.29** gives the basic operation of a conventional twisted nematic display device. A thin film (6 – 10 μm) of a nematic LC is sandwiched between two glass plates, held between crossed polarizers. The (electrodes) inner surfaces carry a patterned, transparent conductive coating of indium-tin oxide (ITO).

In the ‘off’ state of the twisted nematic device (Bright- Light state), the surface alignment makes the nematic molecules form a twisted structure (90° twist through the cell). This leads the polarized light so that it can pass through the crossed polariser (bottom polariser), see figure **1.29 (a)**.

In the ‘on’ state of the twisted nematic device (Dark state), the device has transparent electrodes so a voltage can be applied. In an electric field, the nematic molecules switch orientation and the twist is destroyed, and so light cannot pass through the crossed polariser (bottom polariser), see figure **1.29 (b)**.

Drawback of the twisted nematic (TN) devices:

- Slow (around 10 ms).
- Poor viewing angle.

Advantages of the twisted nematic

- Well understood.
- Cheap to manufacture and very successful.

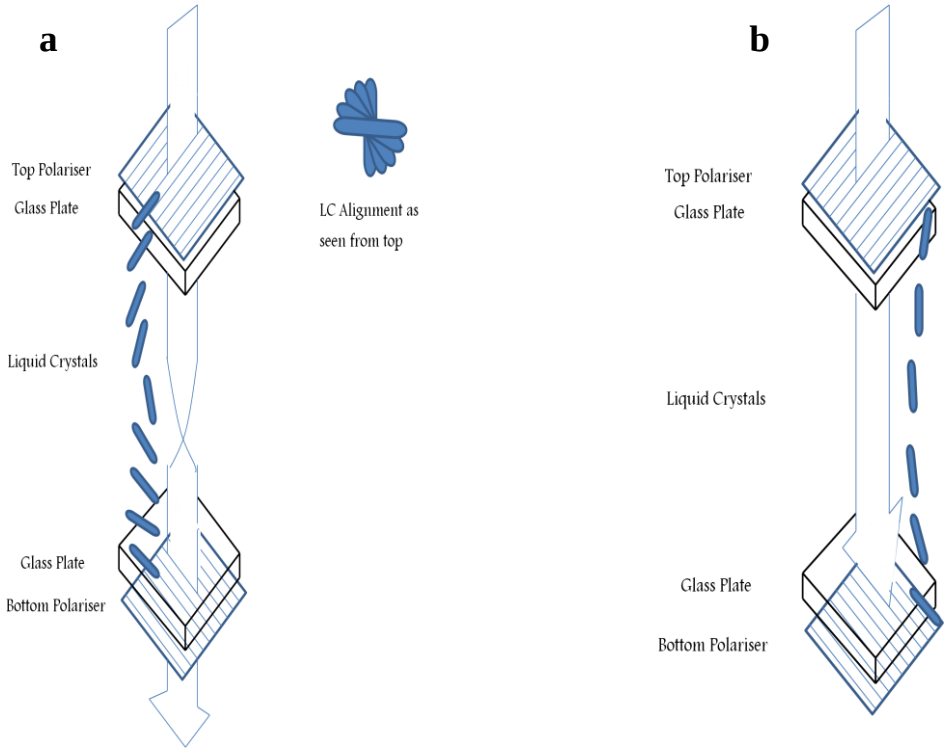

Figure 1.29. Operation of the twisted nematic display device. (a) left side shows bright state and right side shows dark state.

1.7.1.2 In-plane switching (IPS)

In 1996, in-plane switching (IPS) technology was introduced by Hitachi Displays Ltd as a solution to solve these two drawbacks of the twisted nematic (TN) display: low contrast and limited viewing angle. The long axis of the crystals in the in-plane switching (IPS) display is always oriented parallel to the glass panels. The crystals turn around horizontally (in the same plane) when an electrical field is applied, see figure **1.30**.

There are advantages of the in-plane switching (IPS) display. A main feature of the in-plane switching (IPS) display is that it passes the light only in its 'on' state (voltage) and blocks the light it in the 'off' state (no voltage). So, the pixel will be dark (less disturbing than a bright state) when a transistor becomes defective.

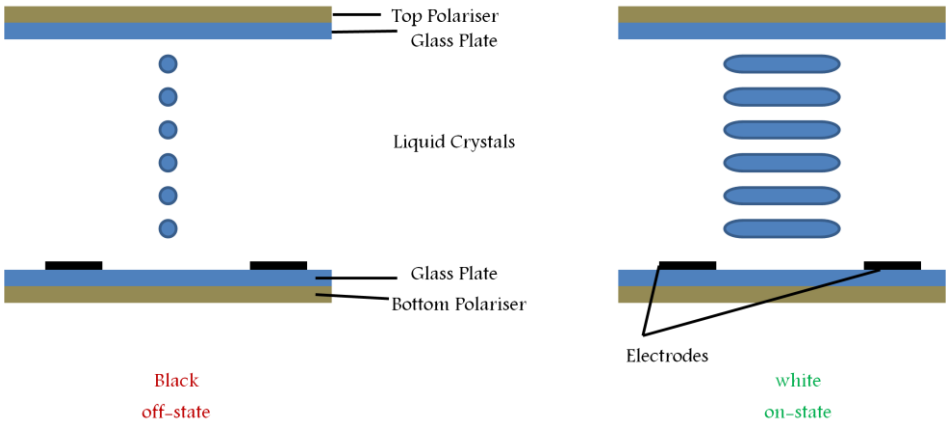

Figure 1.30. Operation of the IPS display device.

Advantages of the in-plane switching (IPS) display:

- Viewing angles are excellent up to 170 degrees.

Drawback of the in-plane switching (IPS) display:

- The electrodes may not be located on both glass surfaces (as with TN displays) because of the parallel alignment of the LCs.
- When using the some backlight, the in-plane switching (IPS) panel has a lower brightness than the twisted nematic (TN) panel.
- Somewhat, the contrast ratio of the in-plane switching (IPS) panel will be lower.

1.7.1.3 Multidomain Vertical Alignment (MVA)

Vertical alignment (VA) technology is very important for display[93]. In 1998, the multidomain vertical alignment (MVA) was introduced by Fujitsu. The multidomain vertical alignment (MVA) technology is as a compromise between the in-plane switching (IPS) and the twisted nematic (TN). There are advantages of the multidomain vertical alignment (MVA) such as a good contrast ratio, a wider viewing angle, fast response times and a good image better than the twisted nematic (TN) displays.

In figure **1.31 (a)**, (dark state, voltage 'off') the LCs remain perpendicular to the substrate, making a dark display between crossed polarisers. On the other hand, in figure **1.31 (b)**, (voltage - 'on') the LCs shift to a tilted position which allows light to pass through and the cell will look grey depending on the amount of tilt produced by the voltage.

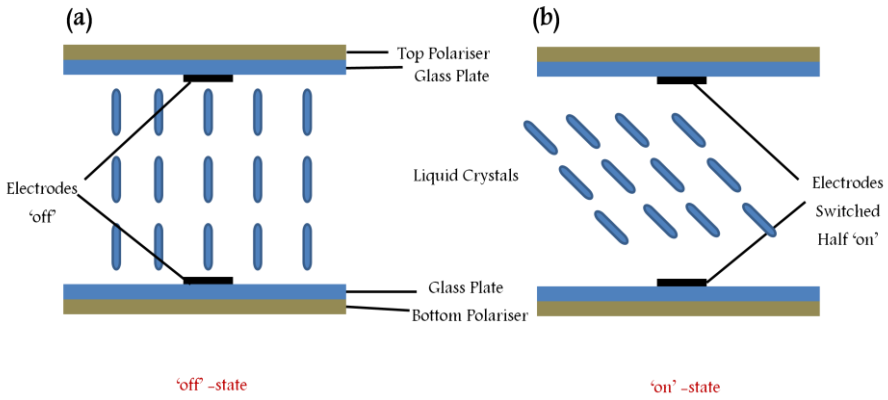

Figure 1.31. Operation of the VA display device.

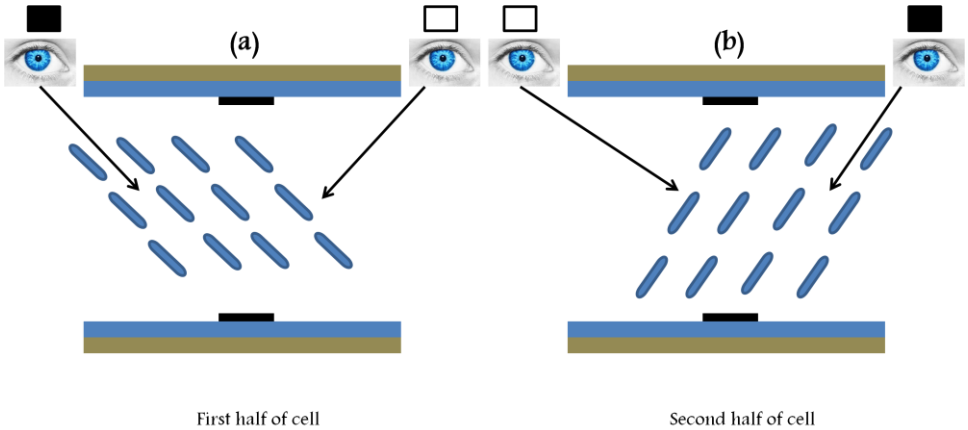

Figure 1.32. Improved viewing angle with VA display device.

In figure **1.32 (a)**, (first half of cell) from left side, the viewing angle is parallel to the LCs (cell will be dark). However, from the right side, the LCs will be seen under a straight angle (cell will be bright).

In figure **1.32 (b)**, (second half of cell) from right side, the viewing angle is parallel to the LCs (cell will be dark). However, from the left side, the LCs will be seen under a straight angle (cell will be bright).

1.7.2 Ferroelectric Displays

1.7.2.1 Surface Stabilized Ferroelectric Liquid Crystal Display[94]

Clark and Lagerwall in 1980 introduced a fast-switching, symmetrically bi-stable electro-optical device which is known as surface-stabilized ferroelectric liquid crystal (SSFLC) display device[95]. In geometry of SSFLC due to elastic interactions the helix of SmC* phase unwinds with two polyimide-coated glass sides which are separated to each other by a gap. It has been recommended that pitch should be four times greater than cell gap (gap has to be 1-2 μm). Two degenerate director orientations came into existence when the tilt plane of each phase is forced to orient in plane of glass plates (bookshelf geometry) which are + θ and - θ. This result in two opposite Ps orientations along polar axis as described in figure **1.33**.

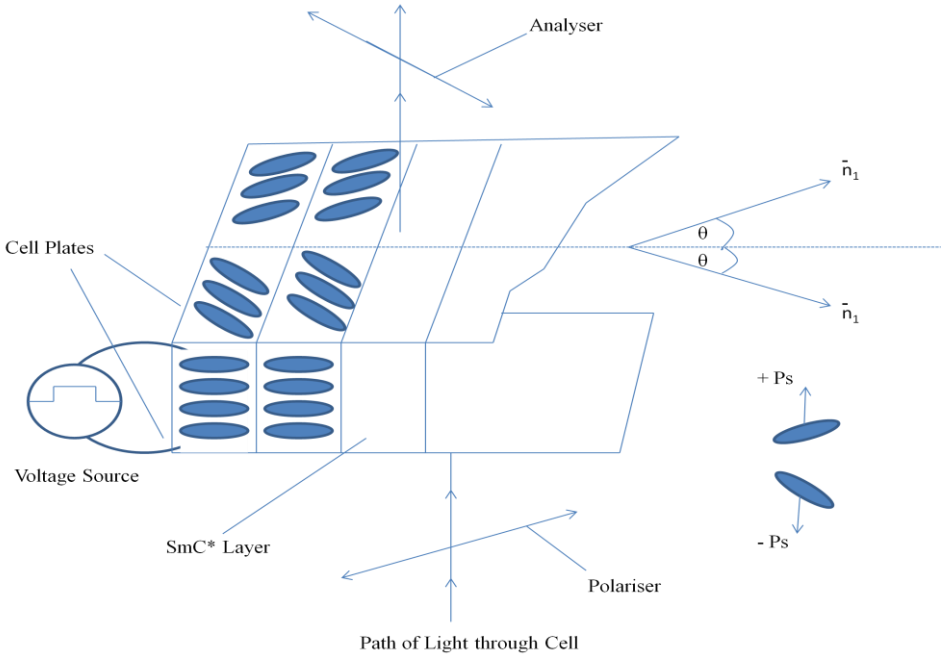

Figure 1.33. The SSFLC display device structure.

The cell consist of material which is liquid crystalline present between the glass plates which are parallel to each other and an electrode layer (ITO) is coated on them and then an alignment material like nylon, polyimide (rubbed in a single direction)[96] is coated which ensures the unidirectional orientation of molecules of liquid crystal because of liquid crystal-surface interactions. For a material which exhibit SmA^*-SmC^* transition when it is cooled from isotropic to SmC* mesophase those molecules which are in contact with orientation layer are forced to lie in glass plates plane. In SmC^* phase only two possible orientations are the switching cone and tilt direction related to cross section between plane of the plates, see figure **1.34**[96, 97].

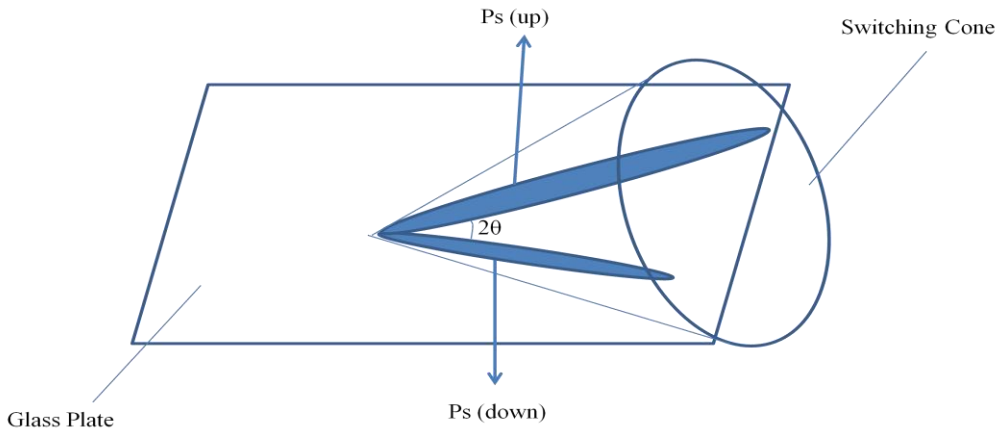

Figure 1.34. Two molecular orientation in the SSFLC display device.

In the bookshelf configuration (ideally), the SmC layers are perpendicular to the plane of the cell. One of the crossed polarisers is parallel to one optic axis of one bistable state, see figure **1.35**. The light is absorbed by the analyser when the plane of polarization and molecular optic axis are aligned parallel to each other thus light passes through liquid crystal material and the cell appears dark. Alternatively, the inversion of the direction of the spontaneous polarization happens to be affected by an external DC field. Also, the external DC field forces the long molecular axis to rotate around the SmC cone (45°, ideally) with respect to the polarisers and the plane of incident light is rotated through 90° degree by half wave plate material, so the cell is bright. The light passed through the SSFLC can be switched OFF and ON through reversed polarity of the applied field.

The SSFLC display have multiple advantages as compared to the conventional twisted nematic liquid crystal displays. Also, the SSFLC cell affords wide viewing angles, low power consumption, higher viewing contrast and bistability[96, 98, 99].

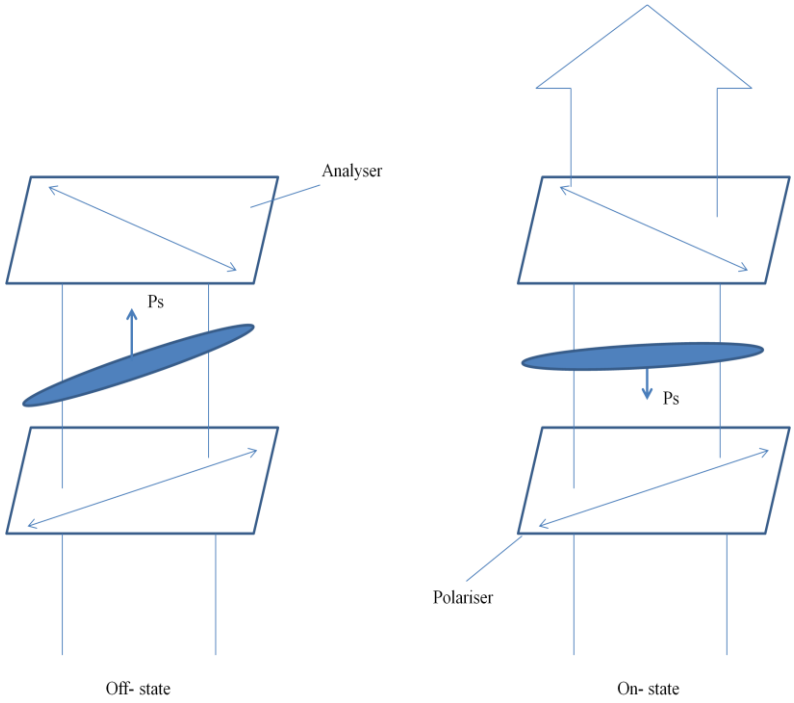

Figure 1.35. Off state and On state in the SSFLC display device.

The SSFLC geometry has the simplest form of originally described bistable "bookshelf" structure. However, the bookshelf geometry is sensitive to external perturbations such as mechanical shock[96], so resulting in the defect formation within the cell. According to the X-ray scattering studies performed by Ricker et al[100, 101], the layers are somewhat bent and tilted within the cell which results in a "chevron" structure being present due to bent smectic layer, see figure **1.36**.

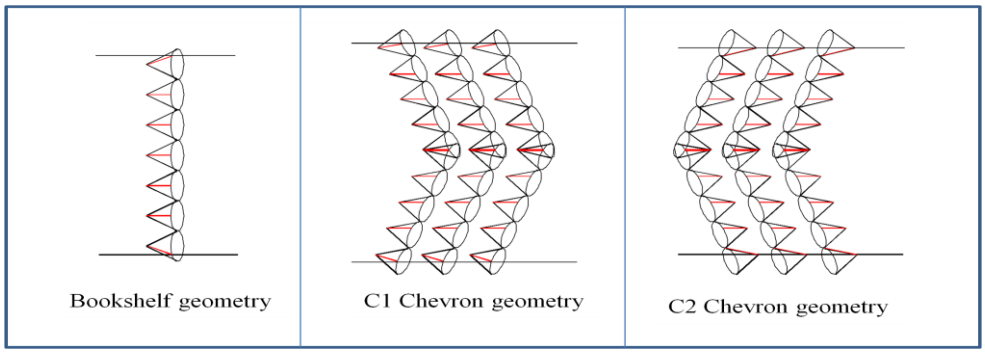

Figure 1.36. Different layer geometries in the SSFLC.

It is generally accepted that the thermodynamically most stable configuration within the ferroelectric liquid crystal (FLC) cell is the chevron structure. The chevron structure is a planar defect in the local layer. It causes consequences for the electro-optical properties of the surface-stabilized ferroelectric liquid crystal (SSFLC) cells. The zig-zag disclination[96] is one undesired appearance of chevrons. It comes when structures of chevron (C1 and C2) co-exist regions within a cell where chevrons with opposite way are in contact, see figure **1.36**. Near the middle, the cone angle of switching is virtually zero. This means very poor contrast.

1.8 Physical properties of ferroelectric liquid crystalline material[17, 52]

Performance of SSFLC cell is dependent upon a number of factors such as birefringence, spontaneous polarization, tilt angle and rational viscosity. Intensity of light transmitted through cell can be explained by expression.

$$I = I_{\circ} \sin^2 4\theta \sin^2 (\pi \Delta nd/\lambda)$$

Where d is cell thickness, $I_{\circ}$ is intensity of incident light, λ is wavelength and Δn is the effective material birefringence.

Intensity of transmitted light will be considered as maximum it will be equal to intensity of incidental light i.e. $I = I_{\circ}$

This condition can be achieved if: $\sin^2 4\theta \sin^2 \left(\pi \Delta nd/\lambda\right) = 1$

The above condition can only be fulfilled if switching angle $4\theta = 90^{\circ}$

And material birefringence and cell thickness are such as $\Delta nd = \frac{\lambda}{2}$

Second major factor which effects device performance is spontaneous polarization expression[65] of which is given below:

$$P_s = P_o (T_c - T)^{\beta}$$

Where

P_s = Magnitude of polarization at a given temperature T

Po = Constant

P_o = Transition temperature from smectic A phase to smectic C*

T = actual temperature

β = an exponent which has a value theoretically equal to 0.5.

The spontaneous polarization (Ps) value increases to an almost constant value when the temperature decreases.

Another cell performance indicator is the switching time (time is required to get change in optical transmission from 10 % to 90 %) which is approximated by expression below[96]:

$$\tau_s = \eta / P_s.E$$

Where τ_s = switching time

η = Rational viscosity

Ps = Spontaneous Polarization

E = Applied electric field

The synthesis of novel ferroelectric materials has focused on the development of compounds having a low viscosity and a spontaneous polarization to get a fast switching. So, short switching times can be achieved with applying a high electrical field, a low rotational viscosity and using a material with a high spontaneous polarization. On the other hand, applying a high electric field is not a good solution for many reasons, shorting the cell, including the possibility of conductivity problems and the drawback of using high power supplies. A high spontaneous polarization can cause build of charges in cell so low viscosity is what is desired.

1.9 Ferroelectric Liquid Crystal Materials[17, 102]

The material properties in addition to mesomorphic behaviour have greater impact on the appearance and performance of surface established ferroelectric liquid crystal display device (SSFLC). The material optimization based on the material's requirements is essential due to the complex relationship between material parameters and device performance. So, it is mandatory to have a basic understanding of the dependency of physical properties of a liquid crystal on the chemical composition of the material. Moreover, the suitability of physical criteria for a ferroelectric smectic C (SmC) material for display applications are harder to satisfy as compared to nematic materials used in supertwisted or twisted devices. The physical requirement listed below are mentioned

1- In order to attain optimum alignment, a cooling phase sequence
chiral nematic (N*) → chiral smectic A (SmA*) → chiral smectic C (SmC*) is essential.

2- The magnitude of the spontaneous polarisation (Ps) of a material determines the response time which is called high spontaneous polarisation.

3-The usage of the device over the normal ambient temperature range (good below room temperature – 20 °C to over 80 °C) is to be allowed by a wide SmC* temperature range with no fundamental ordered smectic phases.

4- To prevent the tendency to formulate a helical chiral smectic C phase and to permit good alignment, the pitch of the helix of the chiral nematic phase should be greater than the cell gap (1-2 μm).

5- A spontaneous polarisation can be obtained through the suppression of greater the pitch of the helix of the chiral smectic C phase than the cell gap.

6- A suitable optical anisotropy (Δn) depending upon the cell thickness, the dispersion of which should be as small as possible.

7- Need a low rotational viscosity to achieve fast switching times.

8- A high dielectric positive biaxiality preserves good alignment due to its coupling nature to an AC external field in the Ps direction.

9- Optimum transition due to tilt angle of 22.5 degree.

10- For optimal colour operation, there is no absorption of visible light.

11- The material has to be photo-chemically and chemically stable**.**

1.9.1 The "All-Chiral" Approach

It is unlikely that a single compound have all such properties so many compounds are used in a mixture to give good materials for use in surface stabilized ferroelectric liquid crystal (SSFLC) display devices.

There are two methods of which we can achieve this mixture and realize broad temperature range ferroelectric liquid crystal (FLC) mixtures.

- First approach is All-Chiral approach in which all compounds used are chiral SmC compounds and these give mixture collective chirality.
- Second approach is 'Host Dopant'[103] in which chiral compounds are added to achiral SmC host material to achieve ferroelectric chiral SmC phase.

Both approaches can be used to achieve chirality in a mixture which is a key to have ferroelectric properties in mixture. But the first approach i.e. all chiral have certain disadvantages as in all-chiral mixture chiral chains have branched structure which give mixture a high level of viscosity. In addition this mixture develops low polarity and problems with adjusting pitch and Ps parameters. To get better switching time low viscosity and high polarity are required. But All –chiral approach lacks these properties. At the same time the synthesis of chiral material is difficult and they are hard to purify. These entire difficulties make All-chiral approach less attractive.
But in Host-Dopant approach material exhibits all such desirable properties as low viscosity and high polarity. In Host-Dopant approach achiral SmC host mixture is doped with chiral material 10 % or less to achieve chirality in overall structure. But chiral structure must be that of host material.

1.9.2 Host Materials

In a host system several compounds are mixed up to optimize the physical properties as a result an appropriate achiral SmC host mixture is developed. The composition of mixture is changed and fine tuning of physical properties is done like dielectric anisotropy or birefringence and all this is according to the requirement of device. Broad research is done on the synthesis and design of novel ferroelectric host materials[104-106] and there is certain criterion on which the quality of host material depends, as described below:

- Low viscosity
- High photochemical and chemical stability
- Low (mp) melting point
- Wide temperature range of SmC

Careful deliberation is required during designing of ferroelectric host materials mostly extensive consideration is required toward generation of low melting point (under room temperature) and low viscosity of materials which should possess strong smectic C tendency.

More attention is paid to the type of molecular structure that will produce SmC phase, during designing of ferroelectric host materials which has a strong smectic C tendency. The first requirement is that molecules should possess sufficient lateral attractions to adopt lamellar such as ordering. Secondly, molecules have to contain a lateral dipole to give the torque enable tilting. The mechanism of tilting includes relative positioning of lateral dipoles and its correct magnitude with correct combination of terminal chain length. The relative positioning of lateral dipoles, the correct magnitude and the correct combination of terminal chain length (in some systems) are required by the tilting mechanism.

Also a wide smectic C temperature range is required to support the display performance and ensure minimization of physical property fluctuation with changing temperature. Also due to allowance must be made for the probable depression of the smectic C phase stability (caused by adding of the chiral dopant).

The majority of ferroelectric materials have two ring and three ring compounds such as phenyl benzoates[107], phenylpyrimidines, phenylpyridines and difluorophenylpyrimidines[97] have two rings whereas mono-fluoroterphenyls, di-fluoroterphenyls[76, 108], 2,5-di-phenyl, 1,3,4- thiadiazoles[109, 110], phenyl biphenylcarboxylates, cyclohexanecarbonitrile derivatives (NCB) and monofluorophenyl biphenylcarboxylates (MBF esters)[97] have three rings.

Negative dielectric anisotropy, broad temperature range and optical anisotropy is ensured by all the above mentioned compounds.

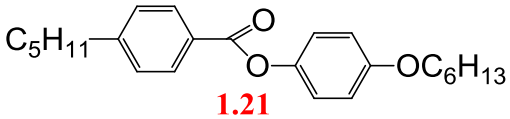

1.21

Cryst 63.0 SmC 77.5 SmA 83.5 N 89.5 Iso

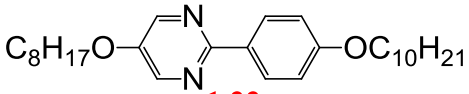

1.22

Cryst 32.0 SmC 59.5 SmA 65.5 N 69.5 Iso

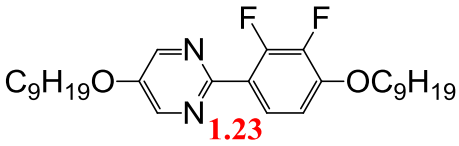

1.23

Cryst 48.0 SmC 78.0 Iso

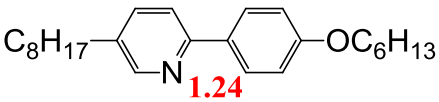

1.24

Cryst 28.0 SmI 55.0 SmC 77.0 Iso

Figure 1.37. Different kinds of two ring smectogens.

The example of simple esters is compound **1.21** which is used as host materials in FLC mixtures and they possess smectic phases.

Ester linking group is present which imparts a stepped structure to the core due to sp^2-hybridization of the carbonyl carbon and due this structure they possess smectic phases. This structure leads to tilting of molecules with respect to layer normal due to the terminal chains which are long and alkoxy. However to generate SmC phase with the long terminal alkoxy chains means that these simple esters have high melting points, high viscosity and both these properties are not suitable to be used in mixtures.

In figure **1.37**, the compound **1.22** has long terminal chains which formulate excellent host materials for ferroelectric mixtures with having low viscosities, melting point and narrow smectic C temperature range. Two alkoxy terminal chains are to be used to increase the smectic C range which causes an increment in viscosity. Aromaticity is needed in the central rigid core region with dipolar

functionalities near one end and long terminal chains which engender SmC phase with acceptable properties. The compound **1.23** (shown in figure **1.37**) displayed just a SmC phase contrary to phenylpyrimidine. This phenomenon is caused by strong lateral dipole provided by the ortho fluoro substituents which support molecular tilting so all the Sm character is shown as tilted smectic C phase. On the other hand, two (at least one but preferable two) alkoxy terminal chain is required to produce SmC phase as with the phenylpyrimidines.

The compound **1.24** phenylpyridine shown figure **1.37** is purely smectogenic in nature with low melting point (28 $^{\circ}$C). Also, the stability of SmC phase is improved compared to the phenylpyridine (**1.22**). On the other hand, when considering SmI phase use as a ferroelectric host materials the underlying ordered SmI can be disadvantageous.

The three ring systems contain a higher length to breadth ratio such as mono-fluoroterphenyls and di-fluoroterphenyls. The two ring systems have less liquid crystal stabilities than the three rings system. This makes the three ring systems more appropriate for use as ferroelectric host materials. However, the raise of the size of these molecules can cause a raise in viscosity.

Materials with no linking group within the core are the best materials, so that the smectic C is displayed to high temperature and the viscosity is not very great. Because of these points, the achiral host materials for ferroelectric systems were developed by Gray *et al*[111, 112] using a terphenyl core unit with one lateral fluoro substituents or more to change mesophase behaviour and the transition temperatures due to its high electronegativity and its small size. Fluoro substitution usually decreases melting point, introduce the tendency for the molecules to tilt and suppresses underlying Sm phases.

The compound **1.25** (shown in the figure **1.38**) in the form of monofluoroterphenyls have a high smectic tendency. The fluoro substituent generates lateral dipole and it causes a molecular tilting and therefore, the production of tilted Sm phases like the SmC phase. The compound **1.25** (shown in the figure **1.38**), produces a tilted SmC phase, and actually more ordered tilted smectic phases due to the combination of

ether oxygen present in the terminal chain and the polarity of the lateral fluoro substituent[79].

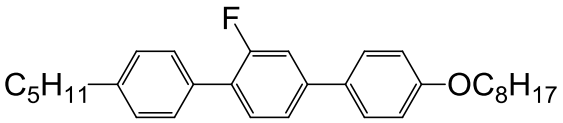

1.25

Cryst 69.0 G 83.0 B 100.5 SmC 124.5 SmA 158.0 N 161.0 Iso

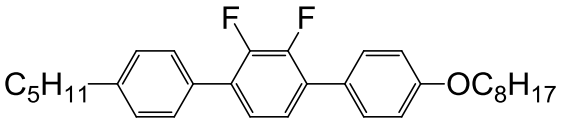

1.26

Cryst 48.5 SmC 95.0 N 141.5 Iso

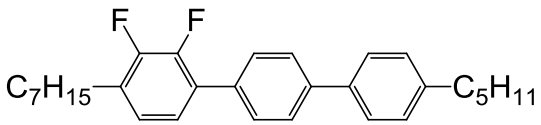

1.27

Cryst 56.0 SmC 115.5 SmA 131.0 N 166.0 Iso

Figure 1.38. *O*-fluoro-substituted terphenyls.

The compound *ortho* difluoroterphenyls **1.26** and **1.27** (shown in the figure **1.38**) formulate excellent ferroelectric host materials. Both fluoro substituents are held naturally fixed on one side of the molecule which promotes the lateral dipole due to both fluoro substituents support each other. Due to this, the difluoroterphenyl materials represent high negative dielectric anisotropy with fairly high stability of smectic C. Figure **1.38** shows that 2, 3-difluoroterphenyls or 2', 3'-difluoroterphenyls are no broader comparative to mono-fluoro substituted terphenyls, the ordered Sm phases are eliminated. Then dielectric anisotropy becomes negative and the melting point as well as viscosity is not affected.

Generation of high SmC phase stability from dialkyl analogues is a major advantage of the ortho-difluoroterphenyls. F, C and H are present, so although the three rings, the viscosity is low. The mesomorphism, melting and clearing points are to be effected by the position of the ortho-difluoro substituent. As compared to 2,3-difluoroterphenyls (compound **1.27**, figure **1.38**), 2',3'-difluoroterphenyls[76, 113, 114] (compound **1.26**, figure **1.38**) have a lower smectic C mesophase stability with lower melting point and greater nematic tendency. The smectic C phase is augmented in the case when the two fluoro substituents are on an outer ring with lateral dipole on end of the molecule. Both cores displayed SmC such as attached long terminal chain and the compounds with high clearing points and high negative dielectric anisotropies have the desired cooling phases sequence of nematic → smectic A→ smectic C.

Mesophases can be observed through the anisotropy provided by the core essential to give mesomorphic behaviour and the terminal chains to minimize melting point and this is the simplistic observation of mesogenicity increase occurs in the molecules. The majority of the liquid crystal research surrounds on the synthesis, design of novel cores and the flexible part of the calamitic liquid crystals (alkyl or alkoxy terminal chains).

The detail study on the effect of changing the nature of the terminal chains on transition temperature and mesomorphism are only studied and linked with respect to their length. Recently, the research study has been started by the researchers on the influence of the chain structures on the transition temperature and mesophase morphology[115]. The effect of the position of a double bond along a chain[116] and an impact of an oxygen atom at varying positions along a chain have been studied by Kelly[116] and (Goulding and co-workers)[117] respectively. Based on these researches it is evident that the mesomorphic properties of the material can be influenced by the nature and the length of the terminal chain. The effect of a methyl-branching at different positions along the chain is studied by Coates[118, 119] and demonstrates that more effectively mesophase stability is depressed as the closer the branching point to the core. Also, the melting points of the materials were reduced. Its effect on the stability of mesophase was less when the branching point was further away from the core but the melting points of the materials were seen reduced.

1.9.3 Chiral Dopants

In order to confer chirality to the whole system through the generation of a chiral environment, chiral dopants are mandatory to be incorporated into the structure of the achiral assembly. Small amount of chiral dopants are required to be added to confer chirality. Moreover, the chiral properties are more interlinked with the added amount and nature of dopant. Easily accessible and chemically stable chiral groups with a reproducible enantiomeric purity are necessary for chiral dopants with practically applicable FLC mixtures in ideal form.

Chiral dopant is a fundamental component which accounts for less than 10% of the total ferroelectric mixture. In order to be useful in imparting ferroelectric properties to the SmC host mixture, chiral dopant need not to be mesogenic. Chiral dopant

should have a mesogenic like structure in maintenance the properties of the host mixture similar to that of the host materials. Structural nature of the chiral dopant needs to be considered to maintain the SmC phase stability. For example, it is important for the chiral dopant to exhibits a chiral smectic C phase for the maintenance of chiral smectic C phase stability in the ferroelectric mixture during the low SmC phase stability of the host mixture. The mesogenic nature of the dopant is less significant in the case of high SmC phase stability in host mixtures and other features of the dopants should be under consideration such as good solubility, high Ps and long chiral nematic pitch length. Most of the chiral dopants used in ferroelectric mixtures provide the necessary high Ps and have a polar group (e.g., F, CN or Cl) at the chiral centre.

There is clear illustration of chemical structure of two chiral dopants in figure **1.39**. In compound **1.28**[17], the cyanohydrin ester consists of a polar cyano substituent at the chiral centre. The high Ps magnitude is to be generated through the large dipole with cyano unit. Compound **1.28**, is non mesogenic, has a mesogenic-like architecture and can be useful for ferroelectric mixtures as a chiral dopant. When use at the chiral centre a cyano group, the problems such as viscosity, solubility problem issues in addition to the major depressions in the SmC phase stability of the host mixture are caused by size of the cyano substituent and the high polarity.

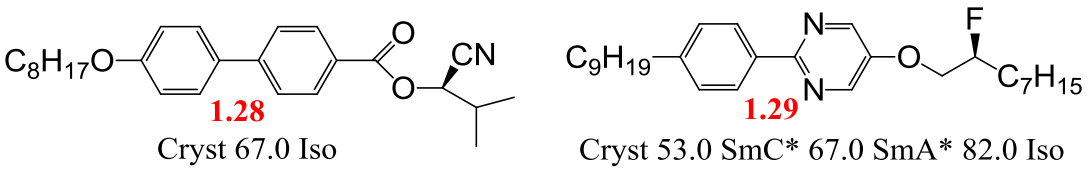

Figure 1.39. The chemical structure of two chiral dopants.

There are a lot of advantages when use a fluoro at the chiral centre and designing chiral dopant materials. The fluoro is high electronegativity and small size ensure the production of high spontaneous polarization (Ps) without adversely affecting solubility or enhancing viscosity. Moreover, the fluoro substituent has a small size which upholds the smectic C phase stability of the original host mixture. This is especially very fundamental for ferroelectric host mixtures based on phenylpyrimidines. The phenylpyrimidines have especially low stabilities of SmC.

There is a fluoro substituent at the chiral centre in compound **1.29**[17]. However, a high stability of SmC phase is displayed by compound **1.29**. This is useful and good for ferroelectric applications. In compound **1.29**, the pyrimidine-based finds use in ferroelectric mixtures based on phenylpyrimidine host materials but the generally stability of SmC phase does not because it shows the SmC* phase to high temperature[79]. 3

1.9.4 The Influence of Terminal Substituents on Mesomorphism

Terminal substituents of some form are always employed in the liquid crystal systems as shown in figure XX. There are many structural moieties that can be classified as terminal substituents, most notably long alkyl chains that may be directly linked to the core or linked through an ether oxygen to constitute an alkoxy chain, or some other linking group such as an ester or an alkynyl group. Such alkyl chains serve to reduce melting point through the disruption of molecular packing caused by the rotational flexibility, and they also provide some degree of assistance to the core in generating orientational ordering in the liquid crystal phase. However, it is also very common to employ one polar substituent or a polar group (e.g., CN, F, NCS, NO_2) in a terminal location, and this serves to generate the longitudinal polarity required for molecular switching in some display device formats (e.g., the twisted nematic display). Occasionally, the terminal chains are more elaborate in nature, such as those that include a branch and the branched unit can be non-polar (e.g., CH_3) or polar (e.g., CN, F, CF_3): normally this design feature is used to confer chirality to the molecules.

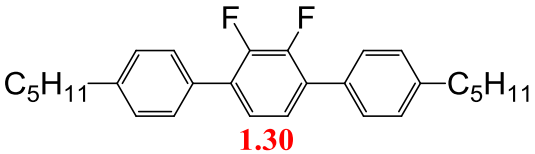

1.30

Cryst 60.0 N 120.0 Iso

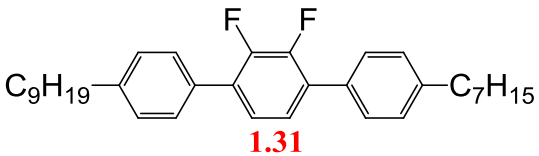

1.31

Cryst 49.0 SmC 77.0 SmA 93.0 N 109.0 Iso

Where the terminal chains are relatively short, and both alkyl (e.g., compound **1.30**), then the materials are commonly seen as nematogens to a high temperature, although

melting points are higher than ideal. Compound **1.31**[76] has longer alkyl chains can intermingle and enhance the smectic character of the material, in this case the smectic C phase is generated because of the lateral dipole of the two fluoro substituents, and the greater conformational flexibility confers a lower melting point, and has reasonably high SmC phase stability, but viscosity also increases with longer chain lengths. Materials such as **1.30** and **1.31** have a relatively low viscosity (around 90 mPa s) and a reasonably high negative dielectric anisotropy (-2.5), and hence find use in nematic mixtures for vertically aligned nematic (VAN) displays. The generation of the smectic C phase and the relatively low viscosity enables compound **1.31** to be employed as achiral host materials for fast-switching, high resolution ferroelectric display devices.

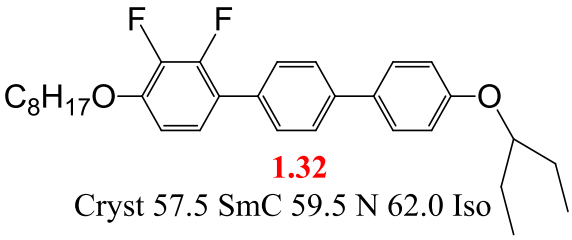

1.32

Cryst 57.5 SmC 59.5 N 62.0 Iso

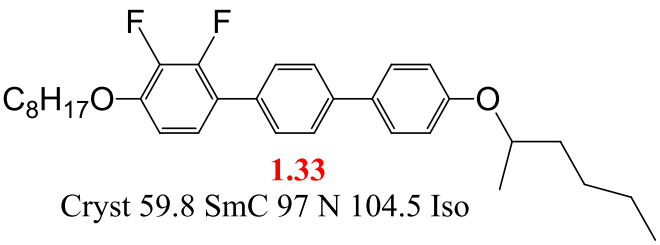

1.33

Cryst 59.8 SmC 97 N 104.5 Iso

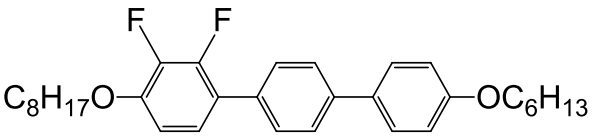

1.34

Cryst 117.0 SmC 181.0 SmA 182.0 N 185.0 Iso

Compounds **1.32**, **1.33**[120] and **1.34**[121] serve to illustrate the influence of a branched chain on mesomorphism. The parent system (**1.34**) has two unbranched chains, and hence the molecules pack together relatively well, and so a high melting point is seen. Further, the liquid crystal phase stability is upheld because the molecular structure can maintain a rod-like shape, hence the very high clearing point of 185 °C. A simple methyl branch in the chain of compound **1.33** causes a massive disruption in molecular packing, so the melting point is much lower, and a massive disruption in the rod-like nature of the molecules, and hence the liquid crystal phase stability is much lower. Making the branch even larger (compound **1.32**) tends not to cause

much further reduction in melting point, and in any case melting points are rather unpredictable, however, the rod-like nature of the molecular structure is severely reduced and so is the liquid crystal phase. Perhaps the most interesting aspect of the branched chain compounds (**1.32** and **1.33**) is the lack of smectic A phase, showing that the smectic phase is reduced by more than the nematic phase is such cases, and the smectic C phase is upheld by the better ability of the chains to be accommodated by a tilted structure (smectic C) rather than in an orthogonal structure (smectic A)[122].

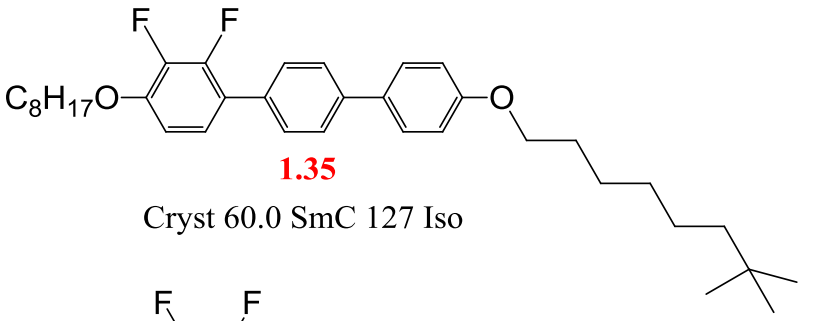

1.35

Cryst 60.0 SmC 127 Iso

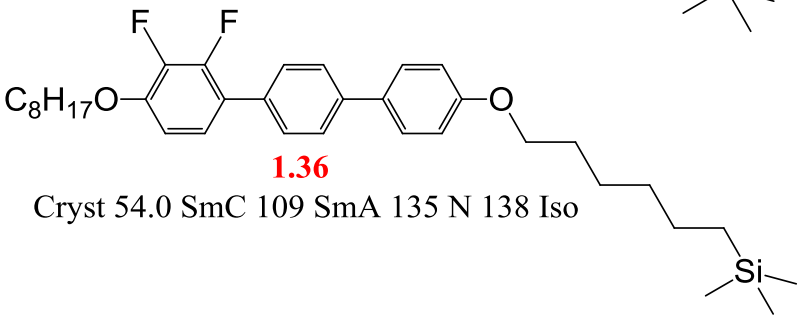

1.36

Cryst 54.0 SmC 109 SmA 135 N 138 Iso

Compounds **1.35** and **1.36**,[122] which have bulky groups from multiple branching at one atom far from the core, can also be compared with the parent system **1.34**, and of course the rather differently branched compounds (**1.32** and **1.33**) just discussed above. Locating the branch much further from the core has the advantage of less disruption to the core-core interactions, and effectively this maintains the rod-like nature of the structure and hence tends to uphold liquid crystal phase stability far more so than when the branch is close to the core. The most odd aspect of compounds **1.35** and **1.36** is that the compound with the larger silicon atom at the branch (**1.36**) confers a higher smectic phase stability and also exhibits a nematic phase above, thus giving a far higher clearing point than compound **1.35**, which possesses a smaller carbon atom at the branch. As will be seen later in the results of

this thesis, invariably the larger silicon atom confers a lower liquid crystal phase stability than the carbon atom, which is what would be expected on the basis of disruption through size. Generally, most of the materials that have terminal groups containing exposed heteroatoms, that is, they are not crowded with aliphatic groups, tend to exhibit nematic phases. This property is important when a nematic phase is required to aid in the alignment of a material, for example, for a display device. Thus controlling the structure of the end group can have benefits in practical applications. Conversely, terminal groups that tend to be sterically crowded, such as those found in compound **1.35**, do not exhibit nematic phases and give a direct isotropic liquid from the SmC phases[122].

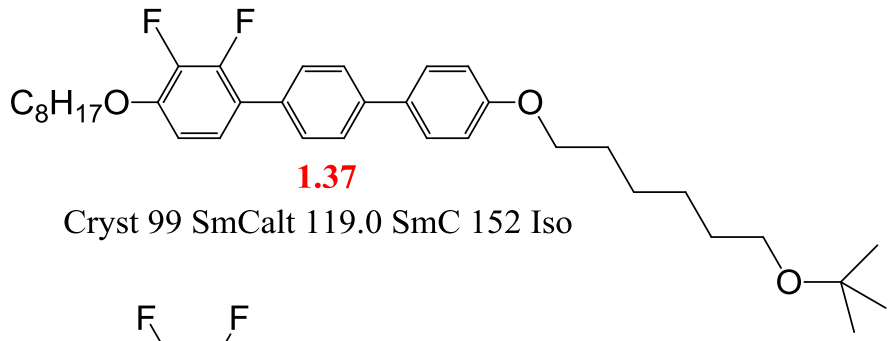

1.37

Cryst 99 SmCalt 119.0 SmC 152 Iso

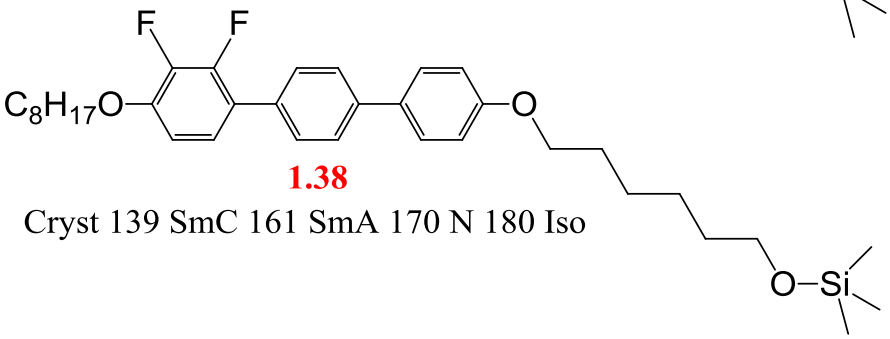

1.38

Cryst 139 SmC 161 SmA 170 N 180 Iso

Compounds **1.37** and **1.38** make good comparisons with compounds **1.35** and **1.36** respectively, and show the influence of the oxygen linkage in the chain. Such influence is rather more significant than expected, particularly in terms of how the oxygen close to the bulky group changes the geometry of conformation of the chain and enables the alternating tilt direction variant (SmCalt) of the conventional smectic C phase to be generated. Moreover, the phase stability of the SmC phase of compound **1.37** is markedly enhanced, perhaps due to the polar nature of the oxygen. The larger silicon atom once again confers higher liquid crystal phase stability

(rather unexpectedly given the larger size of silicon compared with carbon), but the SmCalt phase is not generated[122].

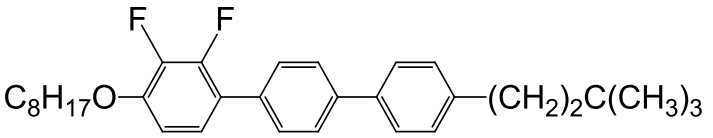

1.39

Cryst 81.3 SmC 131.0 Iso

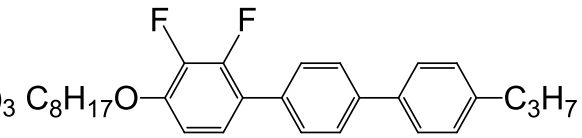

1.40

Cryst 93.5 SmC 144.0 SmA 148.0 N 159.0 Iso

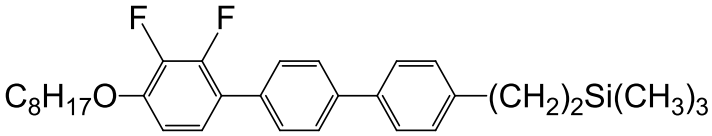

1.41

Cryst 78.8 SmC 118.6 Iso

Compounds **1.39** and **1.41** [49] have bulky groups very close to the core in comparison with those seen in compounds **1.35** and **1.36** respectively, and the overall length of the terminal chain is much shorter. The shortness of the chain means that melting points are not much lower than that of the parent system (compound **1.40**)[76] due to the conformationally more rigid nature of short terminal chains. Further, because the bulky group is closer to the core, the disruption to the core-core interactions is significant and hence liquid crystal phase stability is markedly reduced when compared with the parent system (**1.40**), but the smectic phase stability is rather more upheld than the nematic phase, likely due to a phase separation effect, which confers a layered phase structure because the terminal chains cannot mix easily. The smectic phase is exhibited solely as the tilted SmC phase because of the strong lateral dipole generated by the lateral fluoro substituents and the ether oxygen. Interestingly, here, in contrast to the earlier comparisons, the larger trimethylsilyl group (compound **1.41**) does have a disruptive effect on intermolecular interactions and confers a lower melting point and a lower liquid crystal phase stability than the smaller tertiarybutyl analogue (**1.39**).

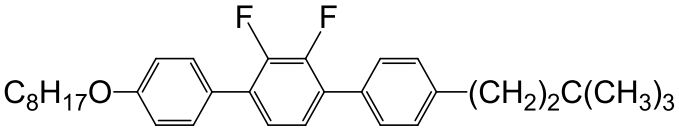

1.42

Cryst 89.0 SmC 106.9 N 114.4 Iso

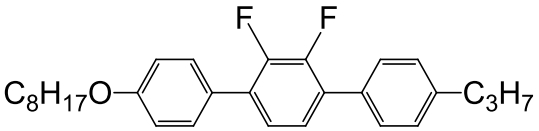

1.43

Cryst 48.5 SmC 95.0 N 141.5 Iso

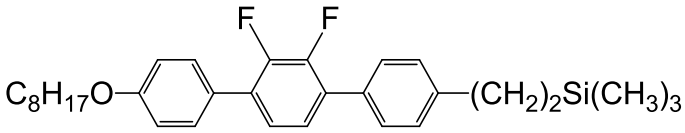

1.44

Cryst 56.1 SmC 101.9 Iso

In contrast to the earlier comparison of compound **1.35** with compound **1.36**, the tertiary butyl compound (**1.42**)[49] exhibits a nematic phase whereas the trimethylsilyl analogue (**1.44**)[49] does not. Such a situation is not unexpected given the phase separation issues would be greater for the larger trimethylsilyl group due to greater incompatibilities with the chains, and hence more smectic tendedncy and less nematic tendency might be expected. However, the smectic phase stability for compound **1.44** is lower than that of compound **1.42**, but not by much. In comparison with the parent system (**1.43**)[76], the melting points of compounds **1.42** and **1.43** are higher due to the greater conformation rigidity of the shorter terminal chain, but as expected the liquid crystal phase stability is lower due to the increased bulk of the terminal chain. However, remarkably in both cases, the bulky group compounds (**1.42** and **1.44**) have higher smectic C phase stability than the parent system, which is due to the strong phase separation overcoming the bulk to support smectic phase stability very strongly.

The two sets of compounds just discussed (**1.39**-**1.41** and **1.42**-**1.44**) are of particular relevance to the aims and objectives of the research of this thesis in terms of examining the influence of relatively short bulky groups, close to the core, on melting point, mesophase morphology and phase transition temperatures. The use of such terminal chains is certainly seen to cause a strong phase separation and this issue is expected to be of relevance in generating ferroelectric mixtures that do not show a layer shrinkage on cooling from the SmA phase into the required SmC phase.

1.10 References

1. F. Reintzer, *Wiener Monatscher Chemie*, 1888, **9**, 421.
2. O. Lehmann, *Verhandl Deutschen Phys Ges*, 1900, **16(3)**, 1.
3. L. K. M. Chan, Hull University, 1987.
4. G. Friedel, *Ann Phys*, 1922, **18**, 273.
5. E. Bose, *Z Phys*, 1909, **10**, 230.
6. H. Zocher, *Z Phys*, 1927, **28**, 790.
7. H. Zocher, *Trans Faraday Soc*, 1933, **29**, 945.
8. C. Oseen, *Trans Faraday Soc*, 1933, **29**, 883.
9. F. Frank, *Discuss Faraday Soc*, 1958, **25**, 19.
10. J. Fergason, *Appl Optics* 1968, **7**, 1729.
11. G. Heilmeier, L. Zanoni and L. Burton, *Proc IEEE*, 1968, **56**, 1162.
12. J. W. Goodby, D. W. Bruce, M. Hird, C. Imrie and M. Neal, *Journal of Materials Chemistry*, 2001, **11**, 2631-2636.
13. G. W. Gray, in *Thermotropic Liquid Crystal,*, John Wiley and Sons, 1987.
14. M. R. Fisch, *Liquid Crystals, Laptops And Life*, World Scientific Publ., 2004.
15. A. A. Collyer, *Liquid crystal polymers: from structures to applications*, Elsevier Applied Science, 1992.
16. S. J. Woltman, G. P. Crawford and G. D. Jay, *Liquid Crystals: Frontiers in Biomedical Applications*, World Scientific, 2007.
17. P. J. 0000 Collings and M. Hird, *Introduction to Liquid Crystals Chemistry and Physics*, Taylor and Francis, London, 1997.
18. C. L. Khetrapal, A. Kunwar, A. S. Tracey and P. Diehl, *Nuclear Magnetic Resonance Studies in Lyotropic Liquid Crystals*, Springer, 2012.
19. J. W. Goodby, in *Encyclopedia of Analytical Science (Second Edition)*, eds. W. Editors-in-Chief: Paul, T. Alan and P. Colin, Elsevier, Oxford, 2005, pp. 74-84.
20. K. Fergusson and M. Hird, *Advanced Materials*, 2007, **19**, 211.
21. D. M. P. Mingos and M. Athanassopoulou, *Liquid Crystals*, Springer, 1999.
22. D. Demus, *Liquid Crystals*, 1989, **5**, 75.

23. S. Laschat, A. Baro, N. Stenke, F. Giesselmann, C. Hagele, G. Scalia, R. Judele, E. Kapatsina, S. Sauer, A. Schreivogel and M. Tosoni, *Angewandte Chemie-International Edition*, 2007, **26**, 4832.
24. P. J. Collings, *Liquid Crystals: Nature's Delicate Phase of Matter*, Princeton University Press, 2002.
25. S. Chandrasekhar, B. Sadashiva and K. Suresh, *Pramana*, 1977, **9**, 471.
26. G. P. Crawford, *Liquid Crystals: Frontiers in Biomedical Applications*, World Scientific Publishing Company, Incorporated, 2007.
27. M. Hird, *Liq. Cryst. Today*, 2005, **14**, 9.
28. G. Pelzl, I. Wirth and W. Weissflog, *Liq. Cryst.* , 2001, **28**, 969.
29. T. Akutagawa, Y. Matsunaga and K. Yasuhara, *Liq. Cryst.*, 1994, **17**, 659.
30. T. Niori, T. Sekine, J. Watanabe, T. Furukawa and H. Takezoe, *J. Mater. Chem.*, 1996, **6**, 1231.
31. G. Pelzl, S. Diele and W. Weissflog, *Adv. Mater.*, 1999, **11**, 707.
32. W. Weissflog, H. Nadasi, U. Dunemann, G. Pelzl, S. Diele, A. Eremin and H. Kresse, *J. Mater. Chem.*, 2001, **11**, 2748.
33. H. Takezoe and Y. Takanishi, *Jpn. J. Appl. Phys.*, 2006, **45**, 597.
34. R. A. Reddy and C. Tschierske, *Mater. Chem.*, 2006, **16**, 907.
35. M. Ros, L. Serrano, M. R. d. l. Fuente and C. L. Folcia, *Mater. Chem.*, 2005, **15**, 5093.
36. J. P. Bedel, J. C. Rouillon, J. P. Marcerou, M. Laguerre, H. T. Nguyen and M. F. Achard, *J. Mater. Chem.*, 2002, **12**, 2214.
37. M. Hird, J. W. Goodby, N. Gough and K. J. Toyne, *J. Mater. Chem.*, 2001, **11**, 2732.
38. J. Svoboda, V. Novotna, V. Kozmik, M. Glogarova, W. Weissflog, S. Diele and G. Pelzl, *J. Mater. Chem.*, 2003, **13**, 2104.
39. F. D. Saeva, *Liquid Crystals: The Fourth State of Matter*, CRC PressINC, 1979.
40. I. Dierking, *Textures of Liquid Crystals*, Wiley-VCH, 2003.
41. G. W. Gray, K. J. Harrison, J. A. Nash and E. P. Raynes, *Electronics Letters*, 1973, **9**, 616-617.
42. J. W. Goodby, *The Encyclopedia of Advanced Materials* 1994, 1325-1334.

43. G. Meier, E. Sackmann and J. G. Grabmaier, *Applications of Liquid Crystals*, Springer London, Limited, 2012.
44. F. Reinitzer, *(English Translation) Liquid Crystals*, 1989, **5**, 7.
45. P. J. Collings, *Liquid Crystals, 1 edn., Princeton Universty Press, Princton, New Jersey, USA* 1990.
46. H. Stegemeyer, *Liquid Crystals*, Steinkopff, 1994.
47. K. M. Fergusson, PhD thesis, The Synthesis and Properties of Achiral and Chiral Bent-core Liquid Crystals, Hull University, 2008.
48. S. Singh and D. A. Dunmur, *Liquid Crystals: Fundamentals*, World Scientific, 2002.
49. I. A. Radini, PhD thesis, The Synthesis and properties of Liquid Crystal with Bulky Terminal Groups for Bookshelf Geometry Ferroelectric Mixtures, Hull University, 2010.
50. A. D. Price, *Surface Anchoring of a Nematic Liquid Crystal at Solid and Fluid Interfaces*, University of Colorado at Boulder, 2007.
51. P. Oswald and P. Pieranski, *Nematic and Cholesteric Liquid Crystals: Concepts and Physical Properties Illustrated by Experiments*, Taylor & Francis, 2006.
52. G. Cosquer, Liquid Crystal with Novel Terminal Chains as Ferroelectric Hosts' PhD Thesis, University of Hull, UK, 2000.
53. G. W. Gray and J. W. Goodby, *Smectic Liquid Crystal, Glasgow*, 1984.
54. P. Gane, A. Leadbetter, P. Wrighton, J. Goodby, G. Gray and A. Tajbakhsh, *Liquid Crystals*, 1983, **67**, 100.
55. J. Goodby, *Journal of materials chemistry*, 1991, **1**.
56. I. C. Khoo and S. T. Wu, *Optics and Nonlinear Optics of Liquid Crystals*, World Scientific, 1993.
57. L. Gattermann and A. Rischke, *Ber Dtech Chem Ges*, 1980, **23**, 1738.
58. G. W. Gray, K. J. Harrison and J. A. Nash, *Electronics Letters*, 1973, **9**, 130-131.
59. R. Bryan, A. Leadbetter, A. Mehta and P. Tucker, *Cryst. Liq. Cryst*, 1984, **104**, 257.

60. S. Kostromin, V. Sinitzyn, R. Talroze, V. Shibeav and N. Plate, *Makromol. Chem. Rapid Commun* 1982, **3**.
61. W. McMillan, *Phs. Rev*, 1973, **A8 (4)**.
62. A. Wulf, *Phs. Rev*, 1975, **A11 (1)**.
63. J. Goodby, PhD. Thesis, University of Hull, 1977.
64. B. V. d. Meer and G. Vertogen, *Phys (Paris)*, 1979, **40**.
65. J. Goodby, *J Mater Chem*, 1991, **1**, 307.
66. B. D. Fahlman, *Materials Chemistry*, Springer Verlag, 2007.
67. C. Tropea, A. L. Yarin and J. F. Foss, *Springer Handbook of Experimental Fluid Mechanics*, Springer, 2007.
68. R. B. Meyer, L. Liebert, L. Strzelecki and P. Keller, *Journal De Physiqu Letters*, 1975, **36**, 1975.
69. R. B. Meyer, *Molecular Crystals and Liquid Crystals*, 1977, **40**.
70. J. Goodby, S. Pikin, R. Blinc, N. Clark, S. Lagerwall, M. Osipov, T. Sakurai, K. Yoshino and B. Zeks, *Ferroelectric liquid crystals: principles, properties and applications*, Gordon and Breach Science Publishers, New York, 1991.
71. N. Boden, R. Borner, R. Bushby, A. Cammidge and M. Jesudason, *Liquid Crystals*, 1993, **15**, 851.
72. G. W. Gray, V. Vill, H. W. Spiess, D. Demus and J. W. Goodby, *Physical Properties of Liquid Crystals*, Wiley, 2009.
73. J. W. Goodby, V. Gortz, S. J. Cowling, G. Mackenzie, P. Martin, D. Plusquellec, T. Benvegnu, P. Boullanger, D. Lafont, Y. Queneau, S. Chambert and J. Fitremann, *Chemical Society Reviews*, 2007, **36**, 1971.
74. C. S. Oh, *Molecular Crystals and Liquid Crystals*, 1972, **19**, 95.
75. D. L. Fishel and P. R. Patel, *Molecular Crystals and Liquid Crystals*, 1972, **17**, 139.
76. G. Gray, M. Hird, D. Lacey and K. Toyne, *Journal of the Chemical Society-Perkin Transactions 2*, 1989, **12**, 2041.
77. G. Gray and P. Winsor, *Liquid crystals and plastic crystals*, Eiilis Harwood, Chichester, 1974.
78. G. Gray, Academic P., London, 1962.
79. M. Hird, *Chemical Society Reviews*, 2007, **36**, 2070.

80. D. Demus, G. W. Gray, J. W. Goodby, H. W. Spiess and V. Vill, *Physical Properties of Liquid Crystals*, Wiley-VCH, New York, 1999.
81. J. W. Goodby, *Liquid Crystals*, 2011, **38**, 1363-1387.
82. R. A. Seeway, *Phsics for scientists and engineers*, International 3ed edition edn, Thomson Learning, Orlando, USA, 1992.
83. , British liquid crystal winter work shop, Microscope equipment and use, Hull University, 2014.
84. D. Demus and H. Sackmann, *Mol Cryst Liq Cryst*, 1966, **2**, 81.
85. D. Coates and G. Gray, *The Microscope*, 1976, **24**, 117.
86. H. Sackmann and D. Demus, *Mol Cryst Liq Cryst*, 1973, **21**, 239.
87. B. Senyuk, 24/12/2013 http://dept.kent.edu/spie/liquidcrystals/textures2.html.
88. D. W. Bruce, British Liquid Crystal Society Winter Workshop, DSC and Liquid crystals, The University of Hull, 2012.
89. R. M. Richardson, British Liquid Crystal Society Winter Workshop, X-ray Diffraction from Liquid crystals, The University of Hull, 2012.
90. M. D. Broglie and E. Friedel, *Compt rend Acad Sci*, 1923, **176**, 475.
91. G. Lester, British Liquid Crystal Society Winter Workshop, Liquid crystal Devices, The University of Hull, 2012.
92. D. Pauluth and K. Tarumi, *J Mater Chem*, 2004, **14**, 1219.
93. G. W. Gray, *Liquid Crystals*, 2011, **38**, 1361-1362.
94. M. Hird, *Liquid Crystals*, 2011, **38**, 1467-1493.
95. N. A. Clark and S. T. Lagerwall, *Applied Physics Letters*, 1980, **36**, 899.
96. U. Finkenzeller, A. E. Pausch, E. Poetsch and J. Suermann, *Kontakte (Darmstadt)*, 1993, **2**, 3.
97. M. Glendenning, 'Liquid Crystalline Materials for Ferroelectric Mixture of High Dielectric Biaxiality' University of Hull, Englend 1998.
98. S. Elston, *Journal of Modern Optics*, 1995, **42**.
99. D. Vizitiu, 'The Influence of Molecular Structure on The Polarization Power of Atropisomeric Dopants for Ferroelectric Liquid Crystals', PhD Thesis, Queen's University, 1999.
100. T. Rieker, N. Clark, G. Smith, D. Parmar, E. Sirota and C. Safinya, *Physical Review Letters*, 1987, **59**.

101. N. Clark and T. Rieker, *Physical review* 1988, **37**.
102. J. W. G. Goodby, *Ferroelectric Liquid Crystals: Principles, Properties, and Applications*, Gordon & Breach Publishing Group, 1991.
103. P. deGennes, The Physics of Liquid Crystals, Clarendn press, Oxford, 1974.
104. D. Demus and h. Zaschke, *Molecular Crystals and Liquid Crystals*, 1981, **63**, 129.
105. D. Demus, B. Krucke, F. Kuschel, H. Nothnick, G. Pelzl and H. Zaschke, *Molecular Crystals and Liquid Crystals*, 1979, **56**, 115.
106. M. Neubert, L. Carlino, D. Fishel and R. Dsidocky, *Molecular Crystals and Liquid Crystals*, 1980, **59**, 253.
107. L. Beresnev, L. Blinov, V. Baikalov, E. Pozhidayev, G. Purvanetskas and A. Pavluchenko, *Molecular Crystals and Liquid Crystals*, 1982, **89**, 327.
108. L. Chan, G. Gray and D. Lacey, *Molecular Crystals and Liquid Crystals*, 1985, **123**, 185.
109. T. Geelhaar, *Ferroelectrics*, 1988, **85**, 717.
110. G. Pelzl, S. Diele, I. Latif, D. Demus, W. Schafer and H. Zaschke, *Molecular Crystals and Liquid Crystals*, 1985, **1**, 39.
111. L. Chan, G. Gray, D. Lacey and K. Toyne, *Molecular Crystals and Liquid Crystals*, 1988, **158**, 209.
112. G. Gray, M. Hird, D. Lacey and K. Toyne, *Molecular Crystals and Liquid Crystals*, 1989, **172**, 165.
113. G. Gray, M. Hird and K. Toyne, *Molecular Crystals and Liquid Crystals*, 1991, **204**, 43.
114. M. Hird, K. Toyne and G. Gray, *Liquid Crystals*, 1994, **16**, 625.
115. M. Hird, K. Toyne, G. Gray, D. McDonnell and I. Sage, *Liquid Crystals*, 1995, **18**, 1.
116. S. Kelly, *Liquid Crystals*, 1996, **20**, 493.
117. M. Goulding and S. Greenfield, *Liquid Crystals*, 1993, **13**, 345.
118. D. Coates, *Liquid Crystals*, 1987, **2**, 63.
119. D. Coates, *Liquid Crystals*, 1987, **2**, 423.
120. R. Bartolino, J. Doucet and G. Durand, *ann Phys (paris)*, 1978, **3**, 389-395.

121. C. C. Doug, M. Hird, J. W. Goodby, P. Styring and K. J. Toyne, *Ferroelectrics*, 1996, **180**, 245-257.

122. J. W. Goodby, I. M. Saez, S. J. Cowling, V. Gortz, M. Draper, A. W. Hall, S. Sia, G. Cosquer, S. Lee and E. P. Raynes, *Angewandte Chemie-International Edition*, 2008, **47**, 2754-2787.

2- Aims and objectives

2.1 Aims of this Research

In 1975, Meyer demonstrated that the chiral SmC phase behaved as a ferroelectric material when confined in a thin cell[1]. This realization enabled Clark and Lagerwall to report the concept of a surface-stabilized ferroelectric liquid crystal display in 1980[2]. Despite displays based on ferroelectric liquid crystals offering many advantages over displays based on the nematic phase,[3-7] such as very fast switching, high resolution, bistability and wide angles of view, and intense research in terms of the design, synthesis and evaluation of many novel materials, virtually all current liquid crystal displays are based on the nematic phase. Nevertheless, ferroelectric liquid crystal displays are commercially successful in microdisplays.

However, ferroelectric liquid crystal displays are currently severely limited in their applicability because of problems in aligning the molecules in the ideal so-called bookshelf configuration. During the alignment process the material is cooled from the isotropic liquid phase through the very fluid nematic phase, where the molecules are aligned homogeneously, into a smectic A phase, where the planar aligned molecules are in layers that are perpendicular to the alignment surface, this is a so-called bookshelf alignment. Ideally, on further cooling, the bookshelf geometry would be retained when the molecules tilt within the layers, however, the tilting of the molecules causes a shrinkage of the layer spacing, which causes a buckling of the bookshelf alignment to generate a so-called chevron alignment to efficiently fill free space. The chevron alignment arises in two ways (C1 and C2), and having both present in a cell generates serious zig-zag defects. These defects can be eliminated by using a pretilt in the alignment layer, which ensures that only one type of chevron alignment is conferred. However, the chevron alignment is still far from ideal as it causes a loss of contrast in displays, and although the problem can be minimized by switching electronics, the full scope and applicability of the display is severely limited. Hence the need for materials that do not cause a layer shrinkage when the molecules tilt in the required SmC phase.

The research of this thesis is aimed at the design, synthesis and evaluation of novel liquid crystal materials that have all the usual attributes of ideal ferroelectric host materials, as discussed in the Introduction, yet also have attributes that maintains the

layer thickness on the tilting of the molecules when the smectic C phase is generated from cooling of the smectic A phase. The approach taken was to employ bulky terminal groups as part of a terminal chain.

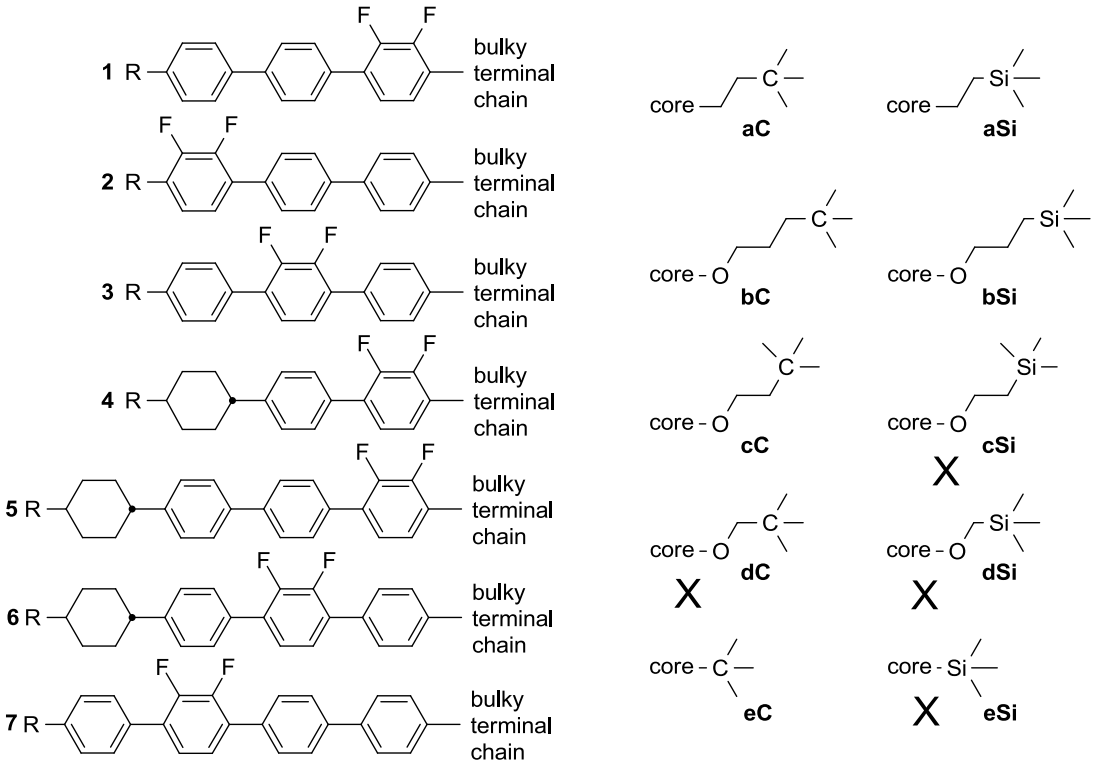

Figure 2.1. The general molecular architectures of the targeted novel materials

A previous programme focussed on tertiary butyl and trimethylsilyl bulky terminal groups linked to difluoroterphenyl cores (**1** to **3**) through a dimethylene unit so as to place the bulky unit fairly close to the core (**aC** and **aSi**). Such materials brought some excellent results in terms of mesomorphism, and through collaborators at Miyota in Boulder, Colorado, USA (formerly Micron and Displaytech) the compounds showed promise in conferring bookshelf alignment in ferroelectric mixtures. Hence the decision to extend this research theme along similar lines, and the scope can be seen in Figure 2.1, which shows the range of core units and bulky terminal groups. Ideally, the priority would have been through the use of bulky groups **dC** and **dSi**, however, the bulky nature of these groups, as expected caused problems in the synthesis. Hence, bulky units **bC** and **bSi** were targeted where the spacer between the core and bulky group was rather larger than desirable, but at least had the bulky group extending in line with the long axis of the core in the favoured

molecular conformer, and so would be expected to be advantageous for mesomorphism. The next targeted bulky terminal units (**cC** and **cSi**) were closer to the core, but radiated off of the long molecular axis, and so would be more challenged in terms of mesomorphic behaviour, but perhaps would be more conducive to maintaining layer thickness on cooling into the SmC phase. In the event, the materials with the larger silicon terminal group (**cSi**) proved elusive due to synthetic issues. The ultimate of bulky terminal group close to the core would be to use **eC** and **eSi**, however, time constraints and ease of synthesis, led only to the synthesis of compounds containing **eC** as the terminal group.

The novel materials, which were synthesised in this research, are difluoroterphenyl, difluoroquarterphenyl, cyclohexylbiphenyl and cyclohexylterphenyl compounds, with bulky terminal units.

All the intermediate compounds were confirmed by Mass Spectrometry (MS) and Proton Nuclear Magnetic Resonance Spectroscopy (^{1}H NMR). However, final compounds and products were confirmed by (MS), (^{1}H NMR), Carbon Nuclear Magnetic Resonance Spectroscopy (^{13}C NMR), Elemental Analysis (EA) and High Performance liquid Chromatography (HPLC), as appropriate. The Polarising Optical Microscopy (POM) and Differential Scanning Calorimetry (DSC) were used for the liquid crystal properties of all final compounds and products to see the transition temperature and liquid crystal phases.

Some of final compounds mixed with **KCHM211** mixtures and doped with chiral dopant (**BE8OF2N** dopant) to be chiral compound and measure the tilt angle and spontaneous polarisation (Ps).

2.2 References

1. R. B. Meyer, L. Liebert, L. Strzelecki and P. Keller, *Journal De Physiqu Letters*, 1975, **36**, 1975.
2. N. A. Clark and S. T. Lagerwall, *Applied Physics Letters*, 1980, **36**, 899.
3. M. D. Wand, W. N. Thurmes and R. T. Vohra, *Ferroelectrics*, 2000, **246**, 1061.
4. T. D. Wilkinson, W. A. Crossland and A. B. Davey, 2002, **278**, 799.
5. U. Finkenzeller, A. E. Pausch, E. Poetsch and J. Suermann, *Kontakte (Darmstadt)*, 1993, **2**, 3.
6. I. Radini and M. Hird, *Liquid Crystals*, 2009, **36**, 1417.
7. S. T. Lagerwall, *Ferroelectrics*, 2004, **301**, 15.

3- Experimental

3.1 Techniques and Methods of Analyses

Many different procedures and techniques[1-4] have been used for the synthesis and characterization of the materials generated and discussed in this thesis, and these procedures and techniques are described below.

3.1.1 Purification of Materials

The mesomorphic and physical properties of liquid crystal materials are highly affected by impurities, hence great care was taken. The starting materials and solvents which are commercially available are used to synthesise compounds without further purification. From Aldrich anhydrous tetrahydrofuran was used which was free from inhibitors and this is used in case of low temperature lithiation reactions. Also, the *n*-butyllithium is acquired from Aldrich in a 2.5 M solution in hexanes. Tetrakis(triphenylphosphine)palladium was synthesised according to well-established literature[5] procedures. Thin layer chromatography was used to monitor the progress of reactions. The purification of compounds was effected through distillation, recrystallisation and by using silica gel in column chromatography or through a combination of these techniques.

BDH silica gel was used in gravity column chromatography, which has pore size of 33-70 ųm and eluted using the solvents specified in the experimental procedures. Schleicher and Schuell filter papers were used to filter the final products to remove particulates. Standard distillation processes were carried out and the temperature and pressure was maintained according to experimental procedures.

3.1.2 Structural Analysis and Purity

Confirmation of the purity and structures of all the intermediate compounds was obtained by Mass Spectrometry (MS) and Proton Nuclear Magnetic Resonance Spectroscopy (^{1}H NMR). Moreover to MS and ^{1}H NMR, final compounds and products were subjected to additional Carbon Nuclear Magnetic Resonance Spectroscopy (^{13}C NMR), Elemental Analysis (EA) and High Performance liquid Chromatography (HPLC), as appropriate. The Polarising Optical Microscopy (POM) and Differential Scanning Calorimetry (DSC) were used for the liquid crystal properties of all final compounds and products to see the transition temperature and liquid crystal phases.

3.1.3 ^{1}H and ^{13}C Nuclear Magnetic Resonance Spectroscopy (NMR)

NMR is used in many areas of scientific research especially in the identification and analysis of organic compounds also. It is a physical phenomenon and depends on magnetic properties of nuclei. The nucleus of ^{1}H and ^{13}C are the most commonly studied.

^{13}C NMR and ^{1}H NMR spectra were obtained on a Jeol JNM-ECP 400 MHz with TMS $\delta_H = 0$ as the internal standard or residual protic solvent ($CDCl_3$, $\delta_H = 7.26$; $(CD_3)_2SO$, $\delta_H = 2.50$) at Hull University. [ppm = part per million, $CDCl_3$ = chloroform-D1], Coupling constants (*J*) are given in Hertz (Hz) and chemical shifts are given in ppm (δ). As the internal reference, ^{13}C NMR were recorded at 100.5 MHz ($CDCl_3$, $\delta_C = 77.0$ ppm; $(CD_3)_2SO$, $\delta_C = 30.8$) and ^{1}H NMR were recorded at 400 MHz[6, 7]

3.1.4 Mass Spectrometry (MS)

Mass spectrometry (MS) is one of the best ways to identify and analyse organic compounds. It was used to confirm the molecular weight for the compounds. (MS) were obtained on two instruments[8]:

Firstly, Solid Probe EI MS spectra were reported using a Shimadzu QP5050A quadruple GC/MS instrument at 70 eV, with the probe heated to 350 °C to vaporise the sample. Information was processed on a PC running Shimadzu class-5000 processing software.

Secondly, MALDI MS spectra were reported on a Bruker Reflex IV MALDI-TOF MS operating in reflecting mode with accelerating voltage in the range 20-25 kV. The laser is known as a nitrogen laser providing photons at 337 nm, with 100-150 laser shots averaged and accumulated. Information was processed on a PC running Bruker Compass software compriding FlexAnalysis and FlexControl packages. 2-(4-hydroxyphenylazo)benzoic acid was used as the matrix.

3.1.5 Thin Layer Chromatography (TLC)

Thin Layer chromatography was run on silica coated thin aluminium plate. It was used as slides (its size is almost 2.0 x 7.0 cm) for testing the purity of the products.

3.1.6 Rotary Evaporator

A BUCHI Rotavapor R-200 was used to remove the solvent from the compound.

3.1.7 Elemental Analysis (EA)

Elemental analysis was carried out to get an indication of purity for all final products. This analysis carried out using a Fissons EA1108 CHN analyser.

3.1.8 High Performance Liquid Chromatography (HPLC)

HPLC was used for the purity of all the final products. HPLC was carried out on a Gilson High Performance Liquid Chromatography system comprising of 151 UV/VIS detector, Valvemate column changer, Unipoint ver 3.3 software, 233XL autosampler/fraction collector, 321 binary solvent pump, Phenomenex Luna 5 µm

C18 250 x 4.6 mm analytical column using acetonitrile 70% and dichloromethane 30% (DCM) as eluent[6].

3.1.9 Polarising Optical Microscopy (POM)

Optical Microscopy was used to identify the types of mesophase and transition temperatures for the final compounds. The final compounds were observed and measured using an Olympus BH2 polarising microscope, in conjunction with a Mettler FP5 controller and FP52 hot hostage[7].

3.1.10 Differential Scanning Calorimetry (DSC)

Transition temperature for the final product were observed and measured utilising polarising optical microscopy and then were confirmed by differential scanning calorimetry on one of two instruments: (a), Mettler DSC822e, calibrated with indium (mp = 156.6 $^{\circ}$C, 28.45 J/g) and zinc (419.47 $^{\circ}$C), aluminium reference. Information was collected by a PC running Star software, or (b), Perkin Elmer DSC7, calibrated with indium (mp = 156.6 $^{\circ}$C, 28.45 J/g) and lead (327.47 $^{\circ}$C), gold reference. Information was collected by a PC running Pyris software[6].

3.2 Experiment abbreviation

In this thesis the IUPAC system of nomenclature has been used as a reference and guide. The abbreviations used are shown below in Table **3.1**:

Table (3.1). Abbreviations and nomenclatures.

Abbreviation	Meaning	Abbreviation	Meaning
Cr	Crystal	I	Isotropic
LC	Liquid Crystal	mp	Melting Point
bp	Boiling Point	N	Nematic
SmA	Smectic A	SmA*	Chiral Smectic A
SmC	Smectic C	SmC*	Chiral Smectic C
	^{1}H NMR nomenclature		
s	singlet	d	doublet
t	triplet	q	quartet
m	multiplet	quint	quintet
dd	double doublet	ddd	double double doublet
dt	double triplet	dddd	double double double doublet
	Solvent and Reagents		
$CDCl_3$	deuterated chloroform	DCM	dichloromethane
DMSO	dimethylsulphoxide	DME	1,2-dimethoxyethane
THF	tetrahydrofuran	*n*-BuLi	*n*-butyllithium
EtOH	ethanol	Et_2O	Diethyl ether
EtOAc	ethyl acetate		

3.3 Synthetic Schemes

Scheme 1

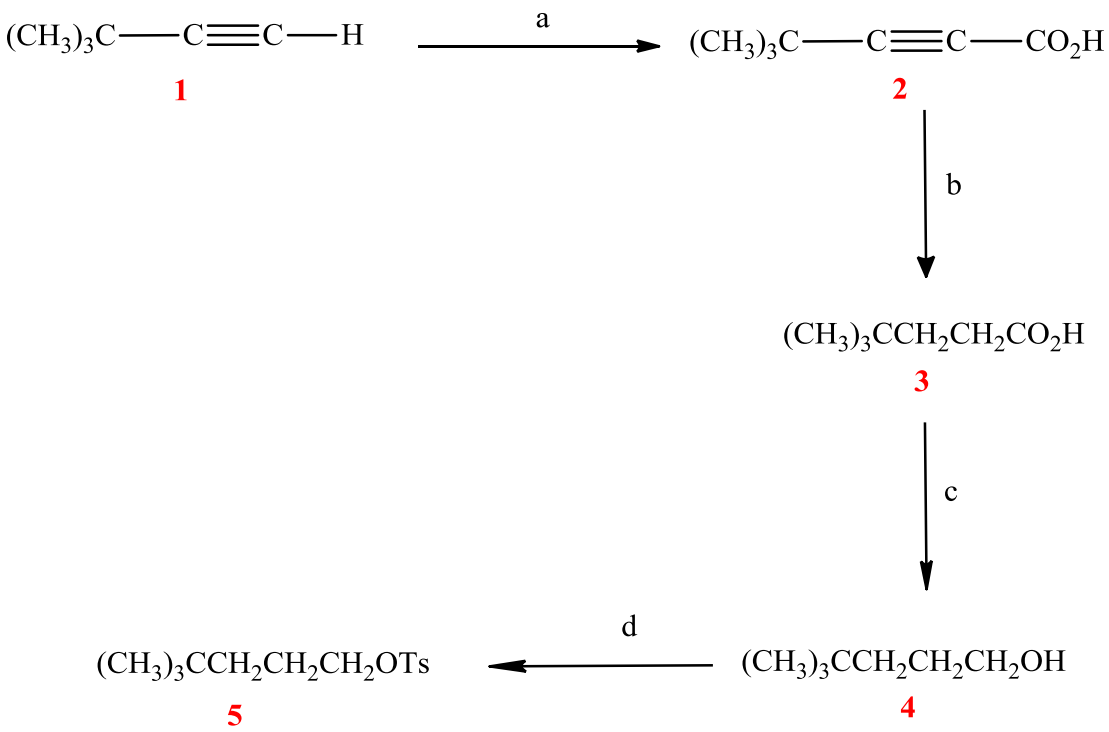

1 **2** **3** **4** **5**

a...(i) n-BuLi; (ii) CO_2: (iii) 36 % HCl.
b... H_2, Pd/C.
c... $LiAlH_4$.
d...TsCl, pyridine, chloroform.

Ts = 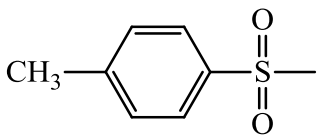

Scheme 2

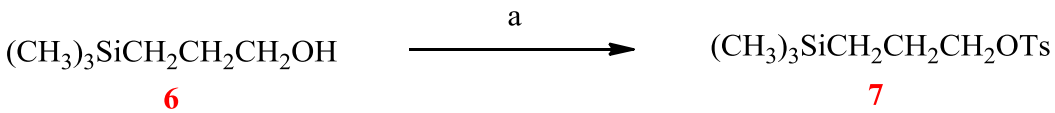

6 **7**

a...TsCl, pyridine, chloroform.

Scheme 3

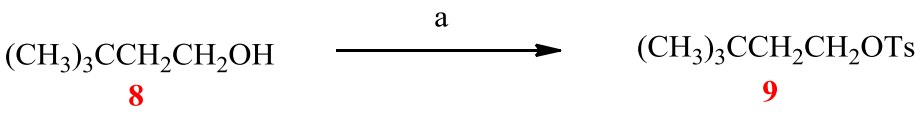

a...TsCl, Et_3N, DMAP, DCM.

Scheme 4

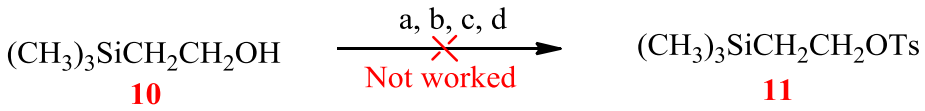

a...TsCl, pyridine, chloroform.
b...TsCl, pyridine.
c...TsCl, DMAP, triethylamine.
d...TsCl, DMAP, *N*,*N*-Diisopropylethylamine.

Scheme 5

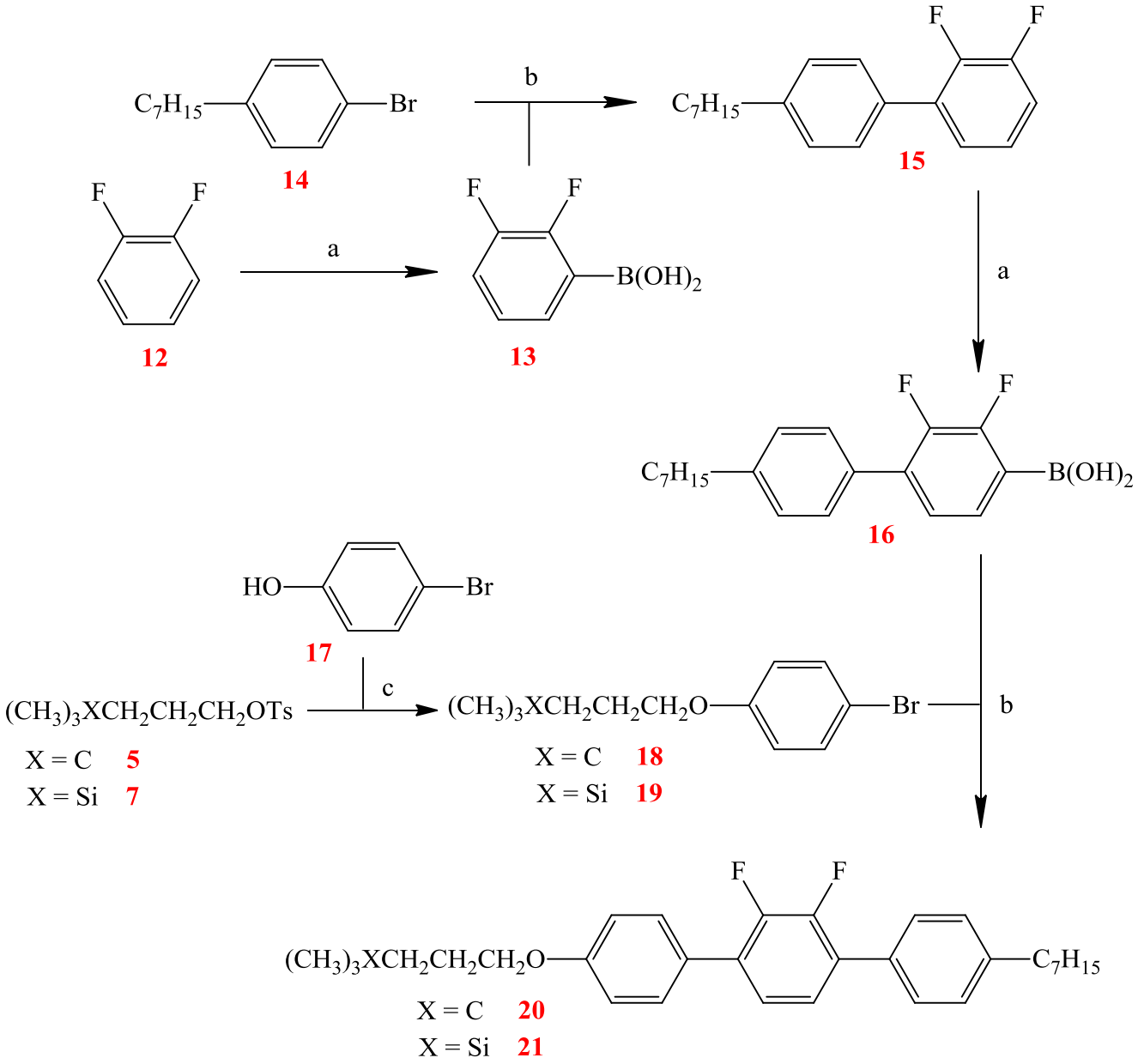

a...(i) *n*-BuLi -78 C; (ii) $(MeO)_3B$; (iii) 10% HCl.
b...$Pd(PPh_3)_4$, Na_2CO_3, DME, H_2O.
c...K_2CO_3, butanone.

Scheme 6

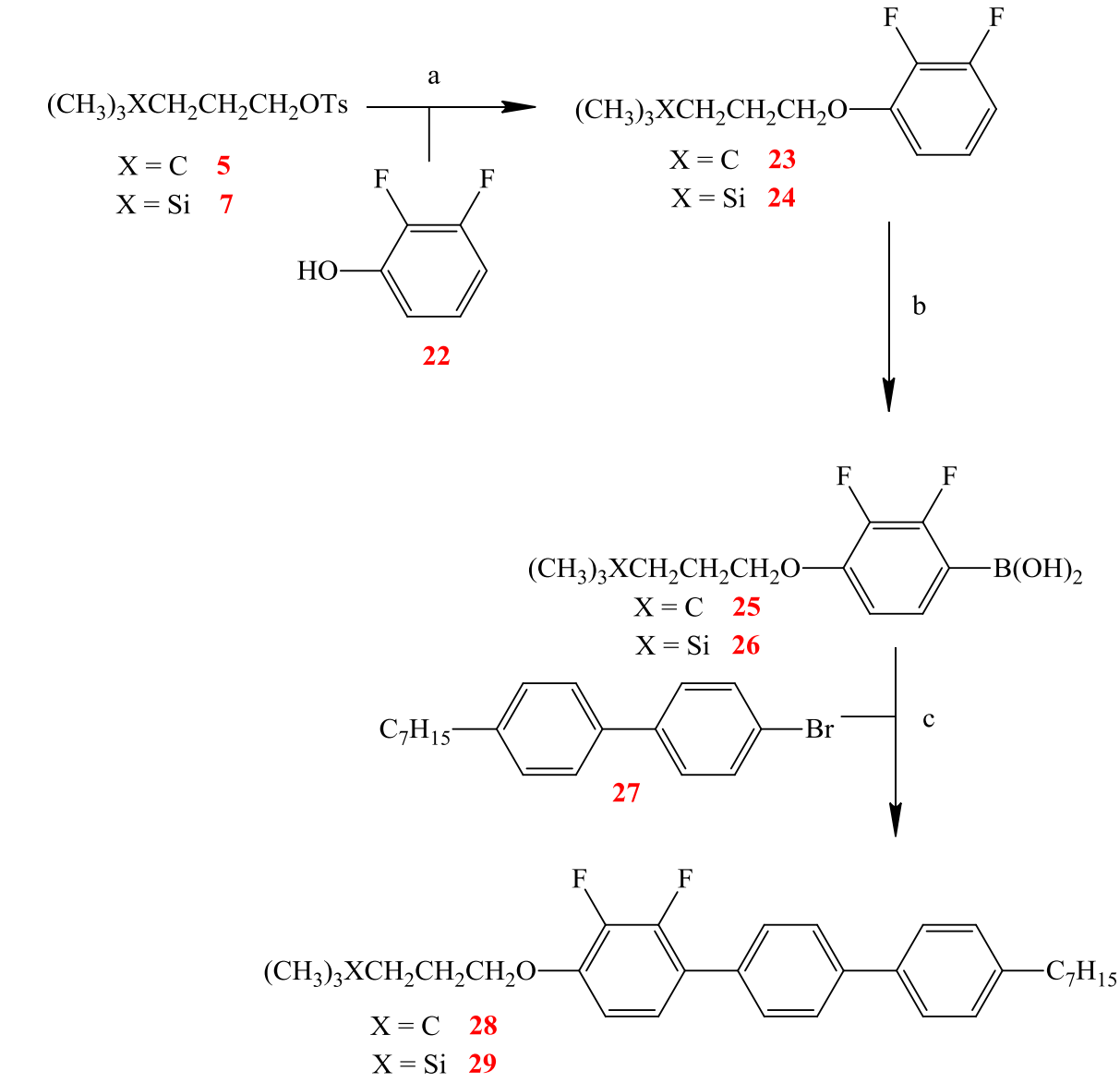

a...K_2CO_3, butanone.
b...(i) *n*-BuLi -78 C; (ii) $(MeO)_3B$; (iii) 10% HCl.
c...$Pd(PPh_3)_4$, Na_2CO_3, DME, H_2O.

Scheme 7

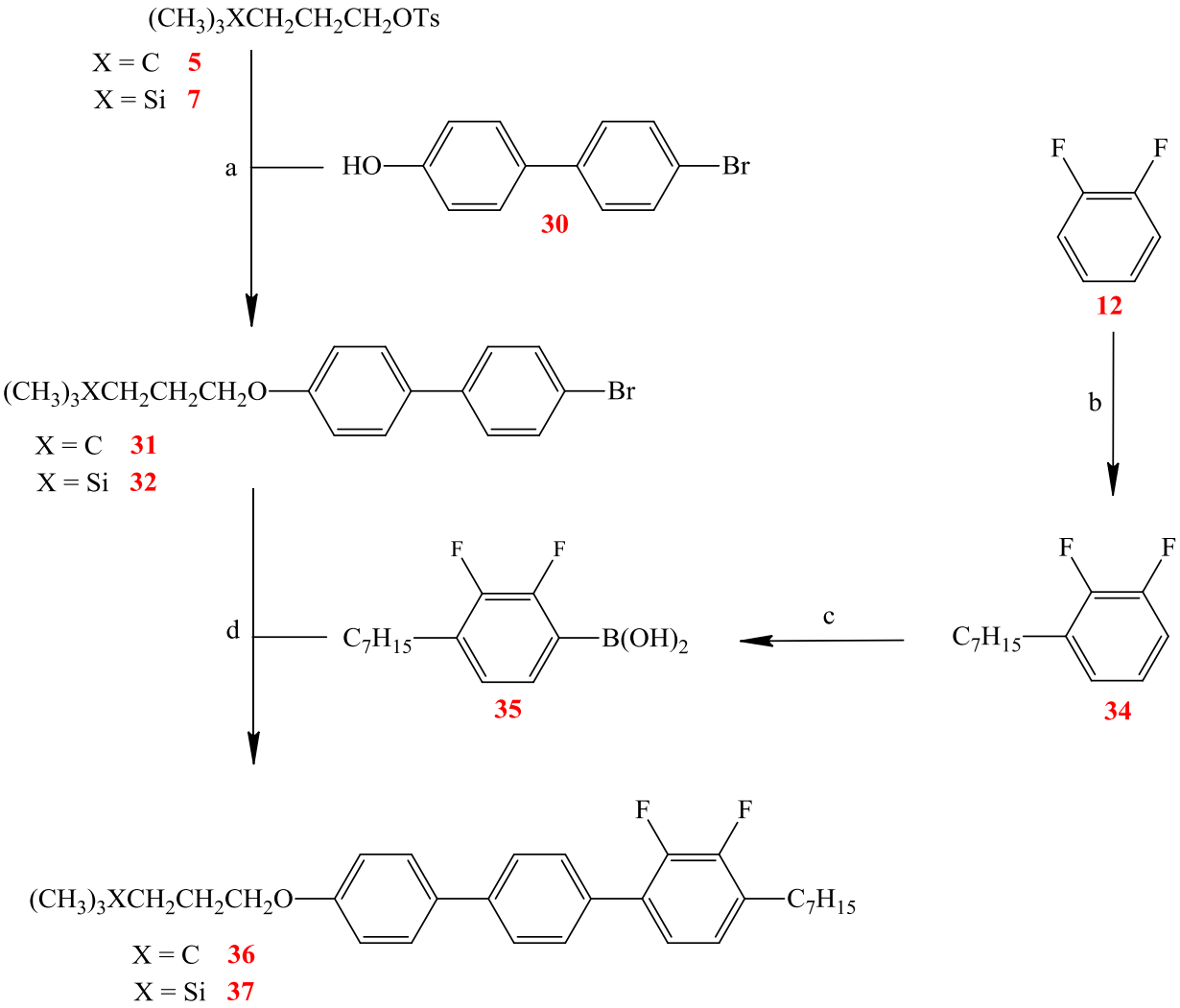

a...K_2CO_3, butanone.
b...(i) *n*-BuLi -78 C; (ii) $C_6H_{13}CHO$ (**33**); (iii) NH_4Cl; (iv) PTSA, toluene; (v) H_2, Pd/C.
c...(i) *n*-BuLi -78 C; (ii) $(MeO)_3B$; (iii) 10% HCl.
d...$Pd(PPh_3)_4$, Na_2CO_3, DME, H_2O.

Scheme 8

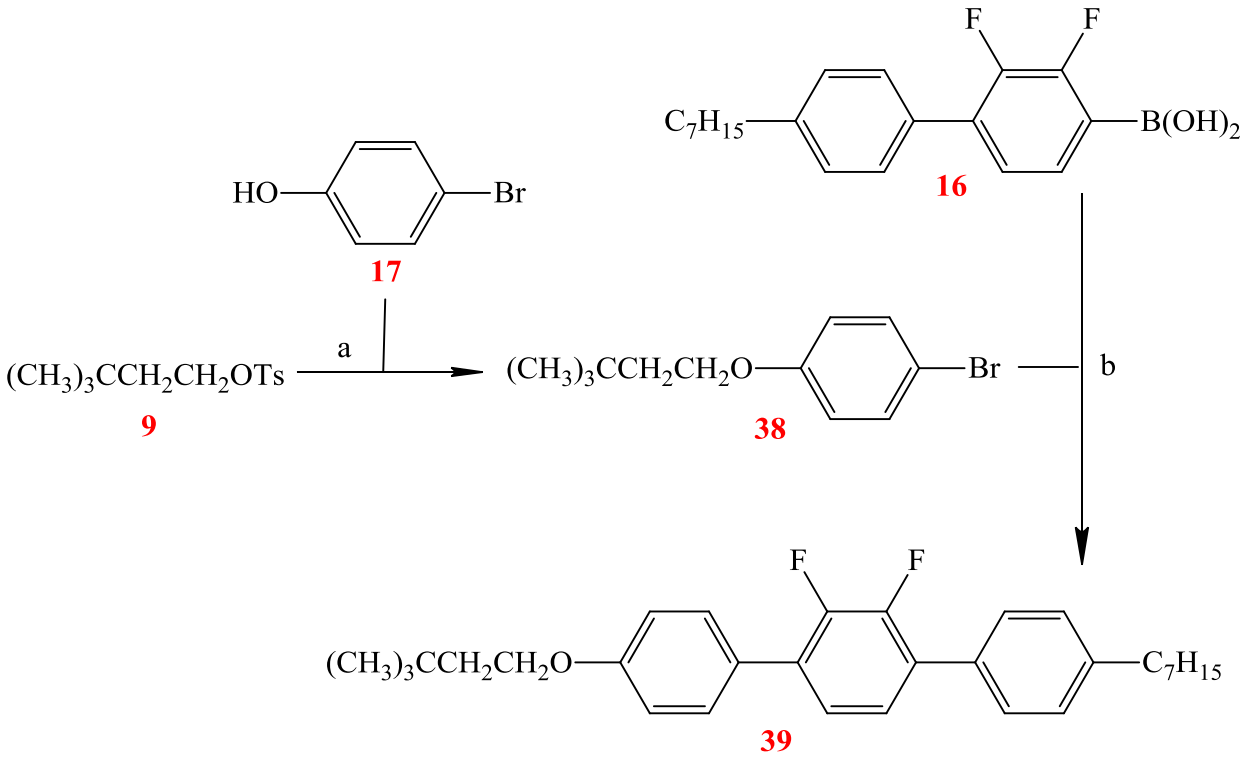

a...K_2CO_3, butanone.
b...$Pd(PPh_3)_4$, Na_2CO_3, DME, H_2O.

Scheme 9

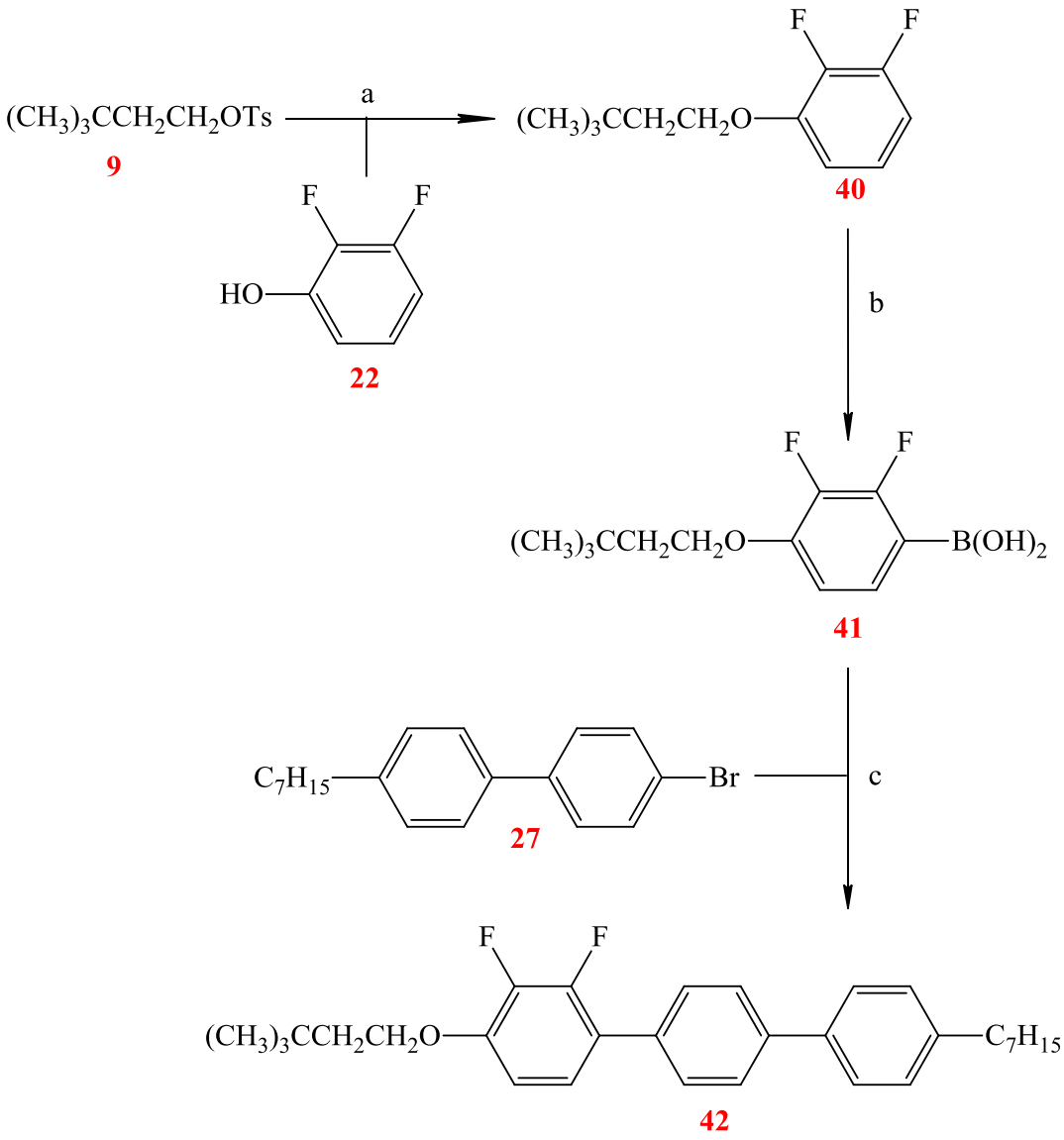

a...K_2CO_3, butanone.
b...(i) *n*-BuLi -78 C; (ii) $(MeO)_3B$; (iii) 10% HCl.
c...$Pd(PPh_3)_4$, Na_2CO_3, DME, H_2O.

Scheme 10

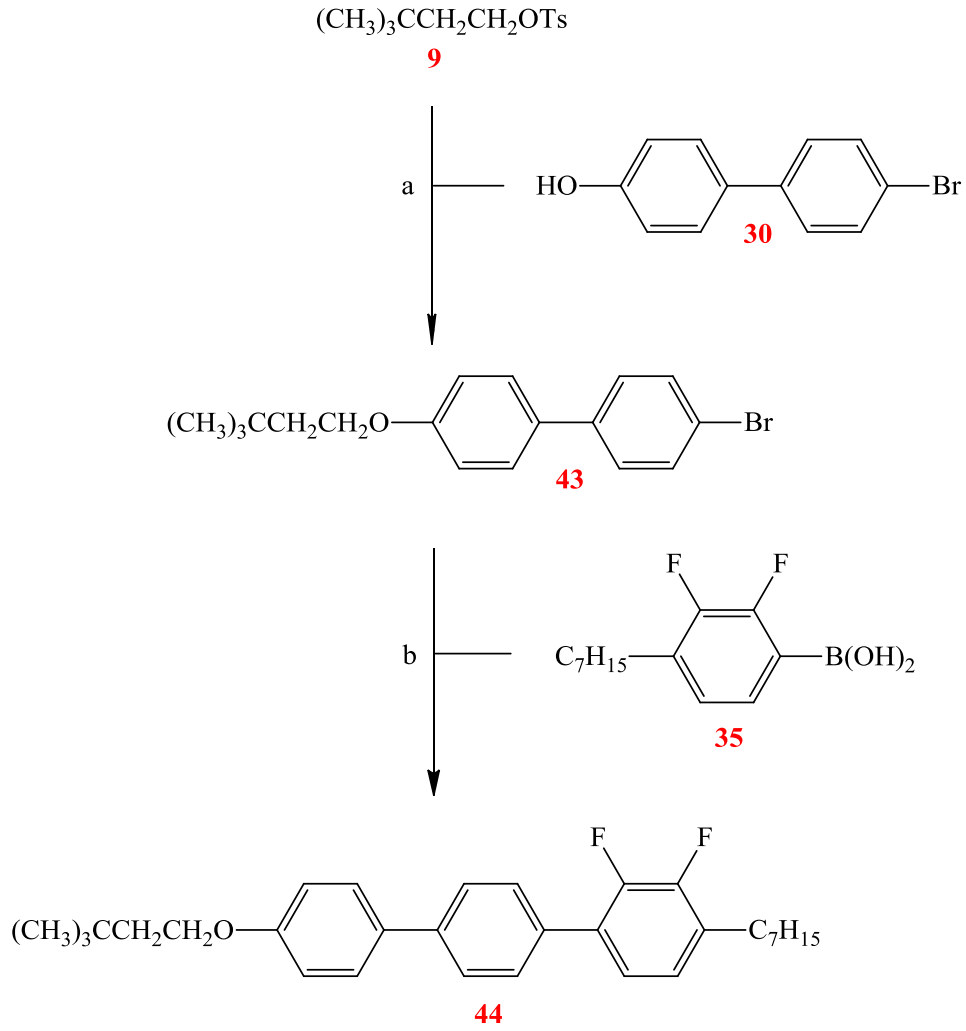

a...K_2CO_3, butanone.
b...$Pd(PPh_3)_4$, Na_2CO_3, DME, H_2O.

Scheme 11

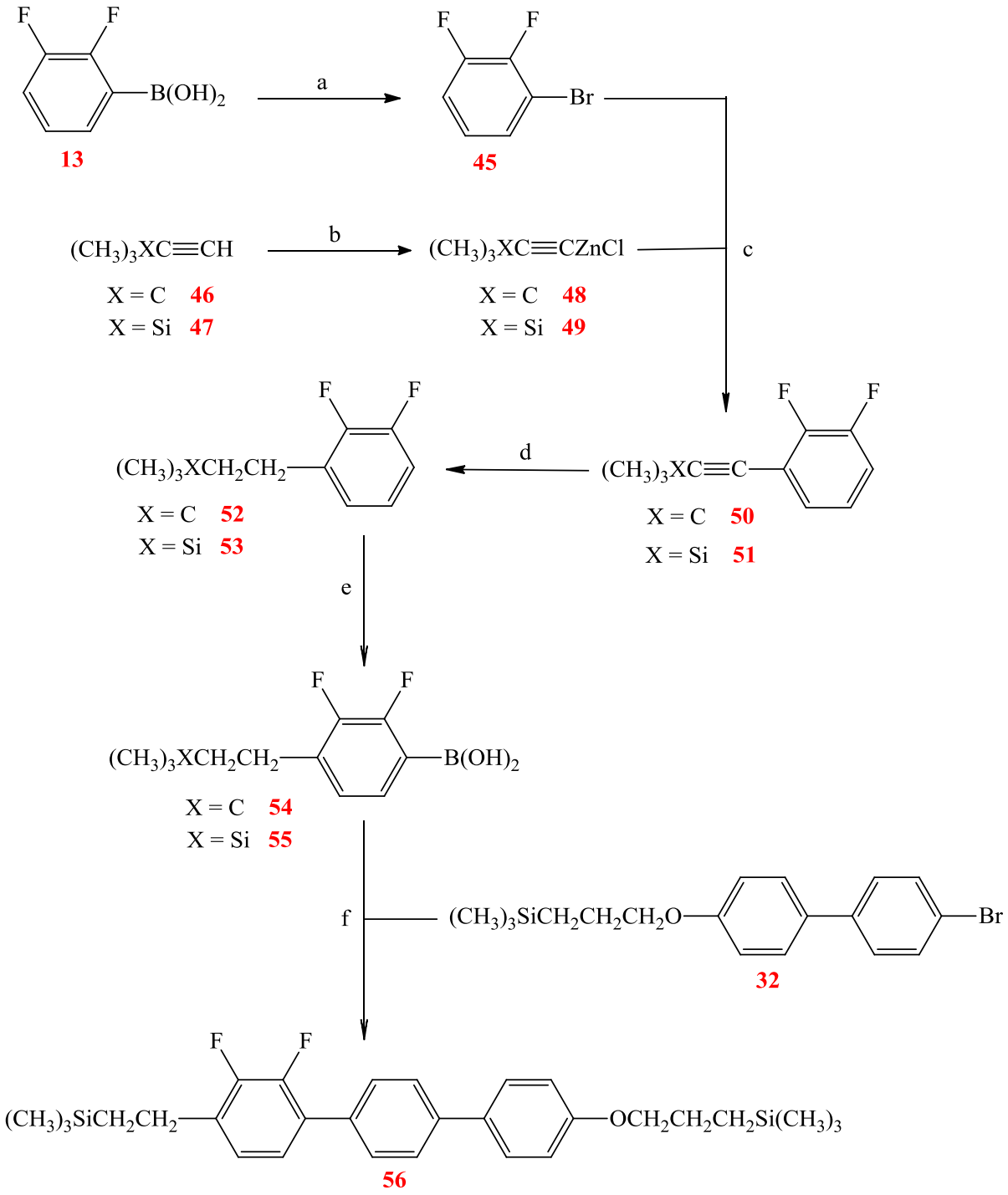

a...NBS.
b...(i) *n*-BuLi, THF, (ii) $ZnCl_2$.
c...$Pd(PPh_3)_4$.
d...H_2, Pd/C.
e...(i) *n*-BuLi -78 C; (ii) $(MeO)_3B$; (iii) 10% HCl.
f...$Pd(PPH_3)_4$, Na_2CO_3, DME, H_2O.

Scheme 12

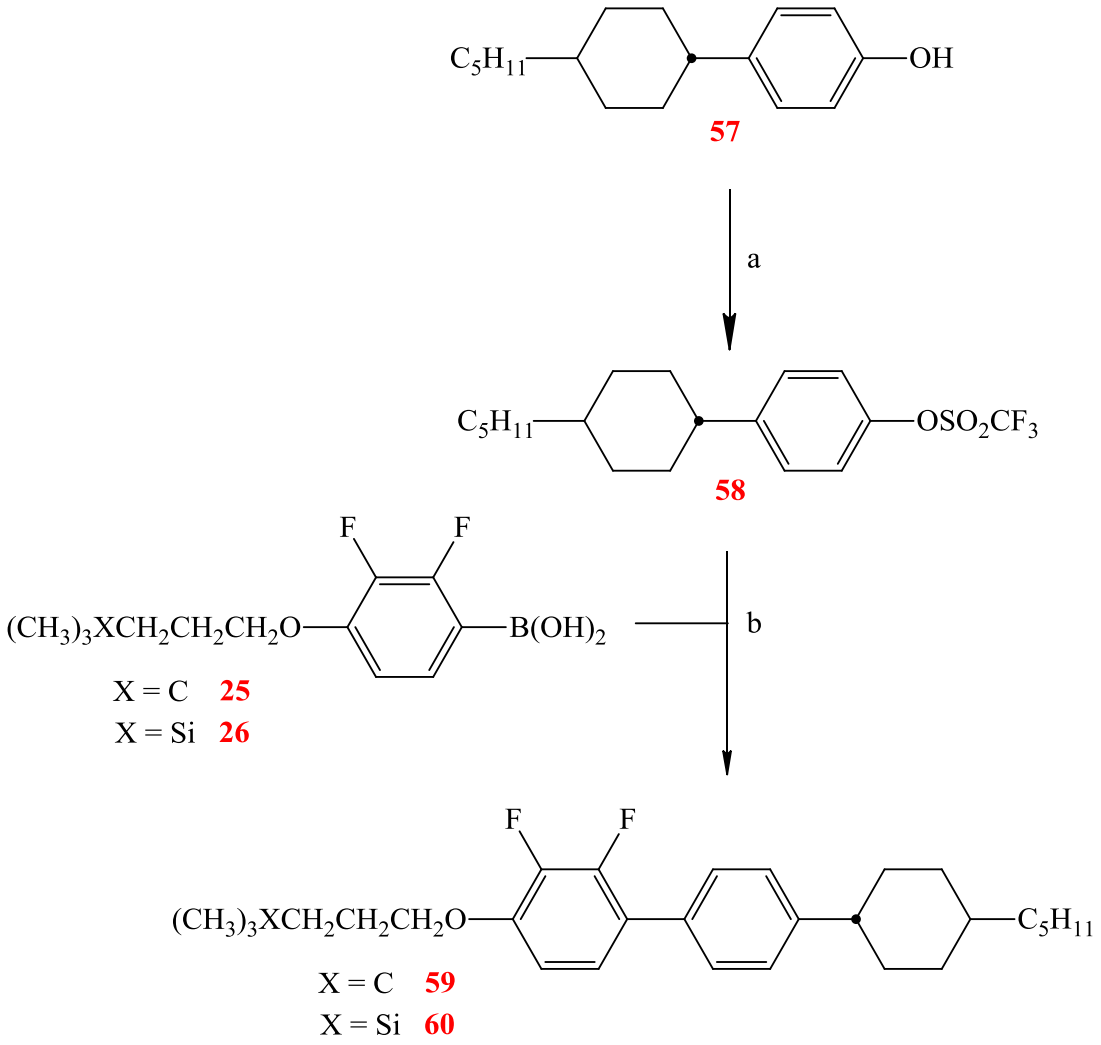

a...$(CF_3SO_2)_2O$, pyridine.
b...$Pd(PPh_3)_4$, Na_2CO_3, LiCl, DME, H_2O.

Scheme 13

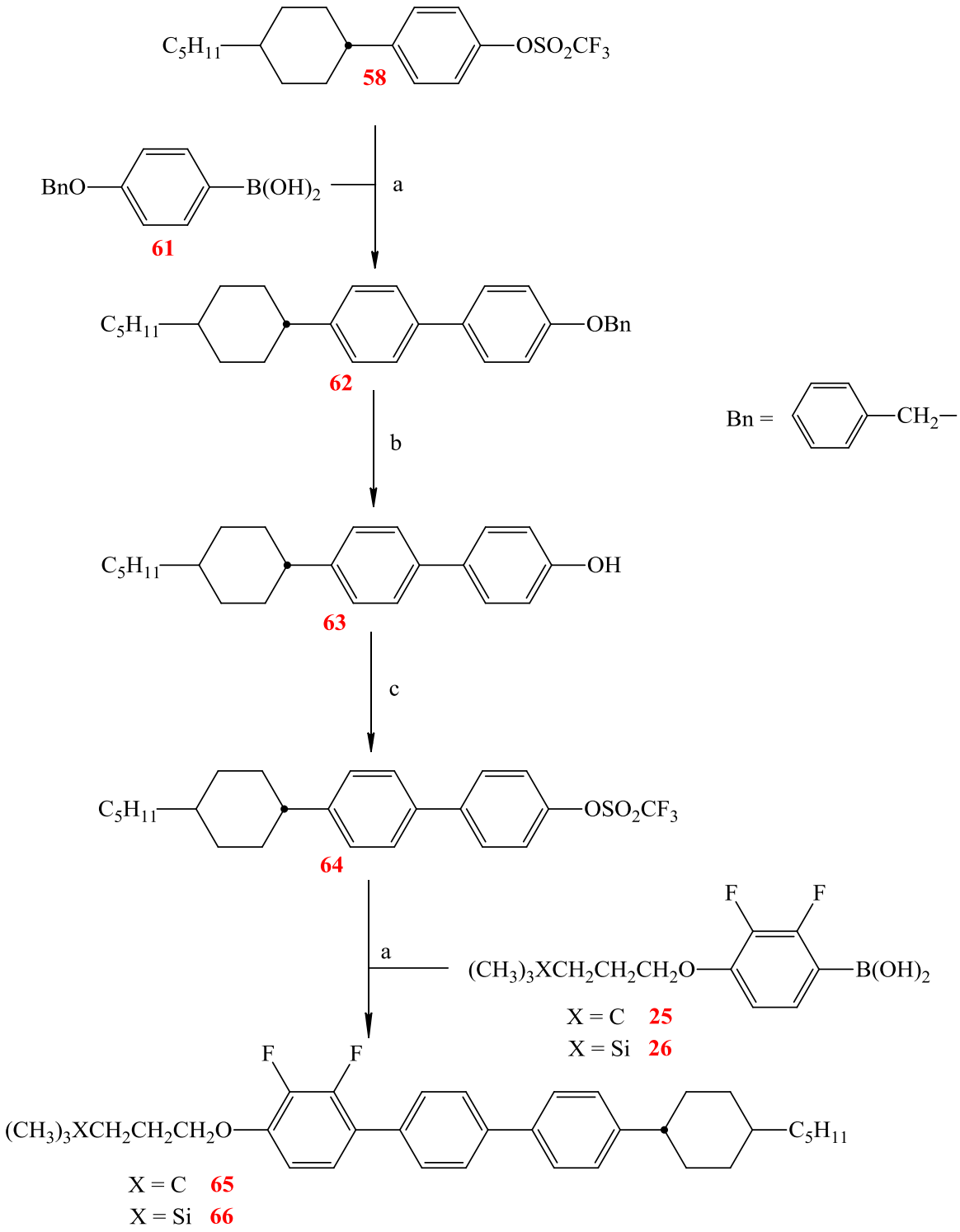

a...$Pd(PPh_3)_4$, Na_2CO_3, LiCl, DME, H_2O.
b...H_2, Pd/C, THF.
c..$(CF_3SO_2)_2O$, pyridine.

Scheme 14

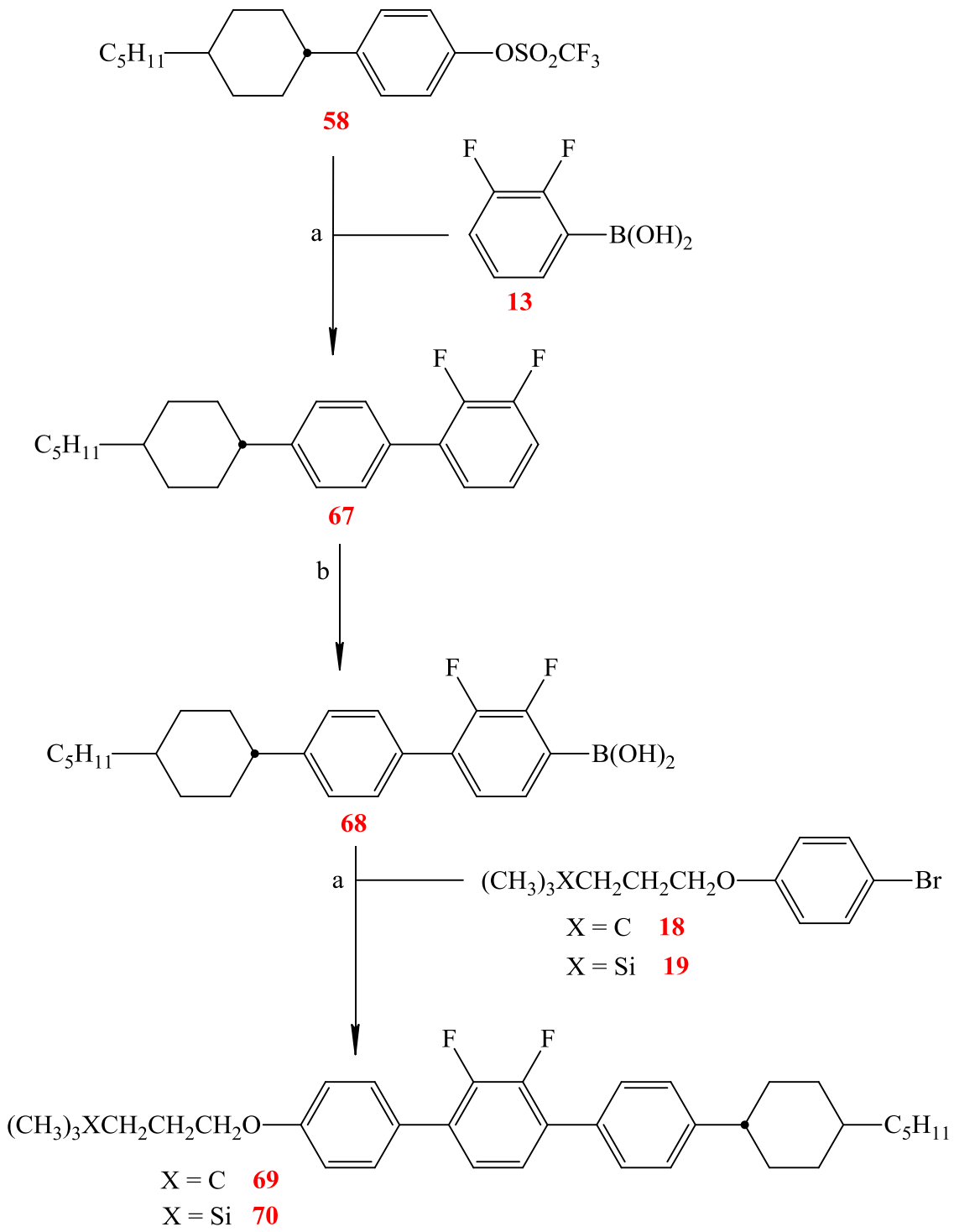

a...$Pd(PPh_3)_4$, Na_2CO_3, LiCl, DME, H_2O.
b...(i) *n*-BuLi -78 C; (ii) $(MeO)_3B$; (iii) 10% HCl.

Scheme 15

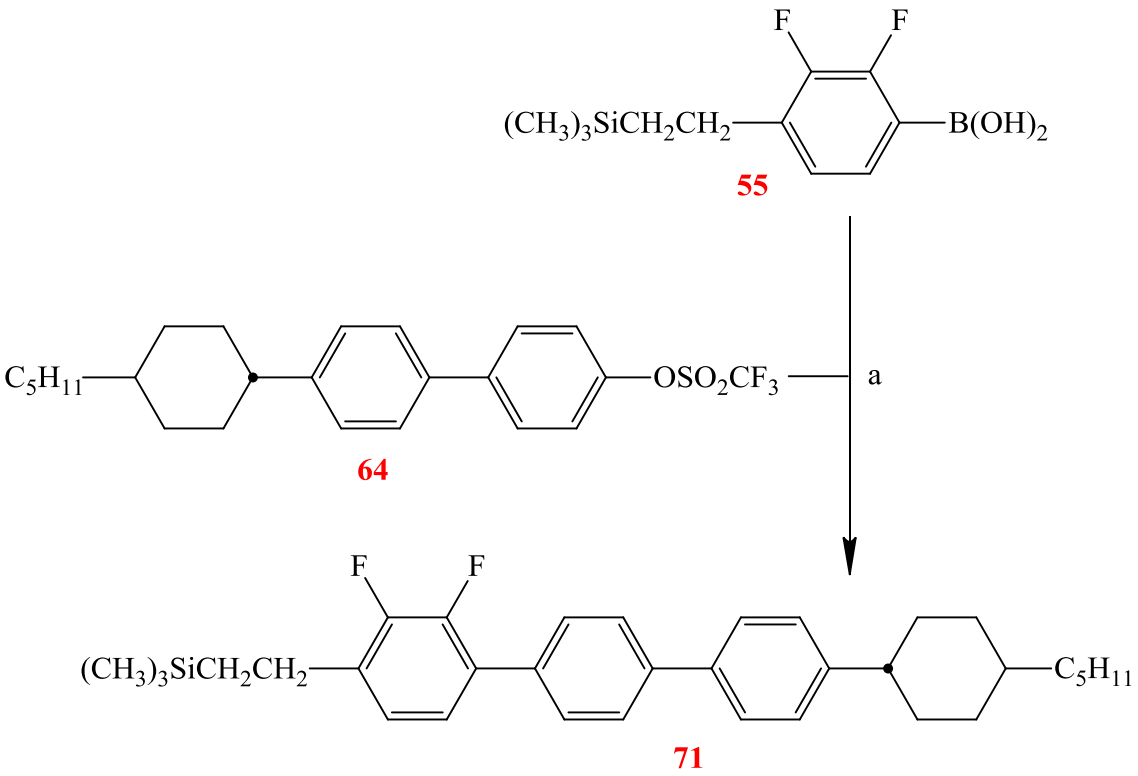

a...$Pd(PPh_3)_4$, Na_2CO_3, LiCl, DME, H_2O.

Scheme 16

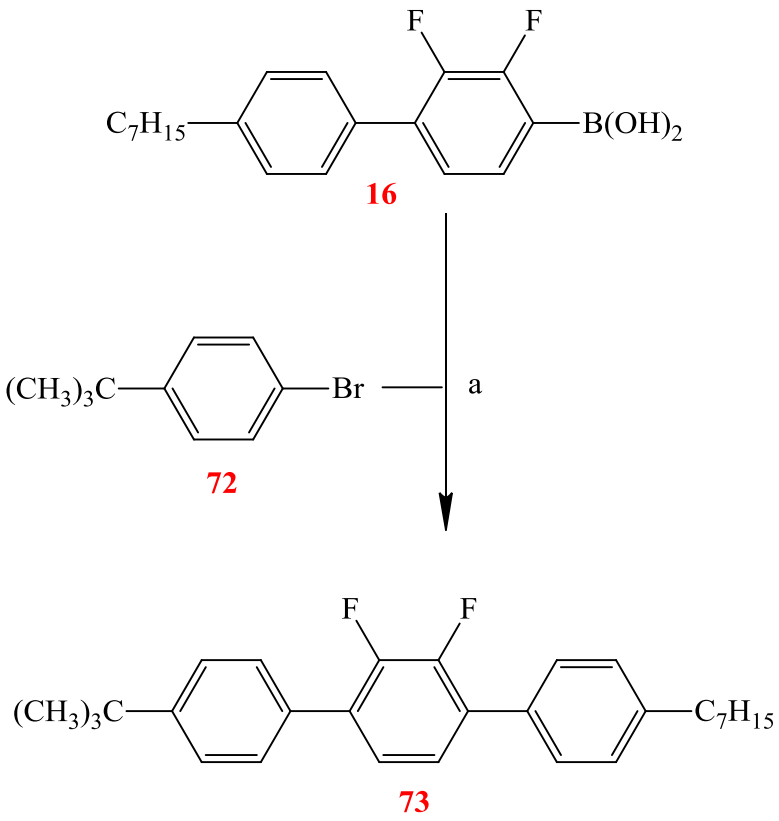

a...$Pd(PPh_3)_4$, Na_2CO_3, DME, H_2O.

Scheme 17

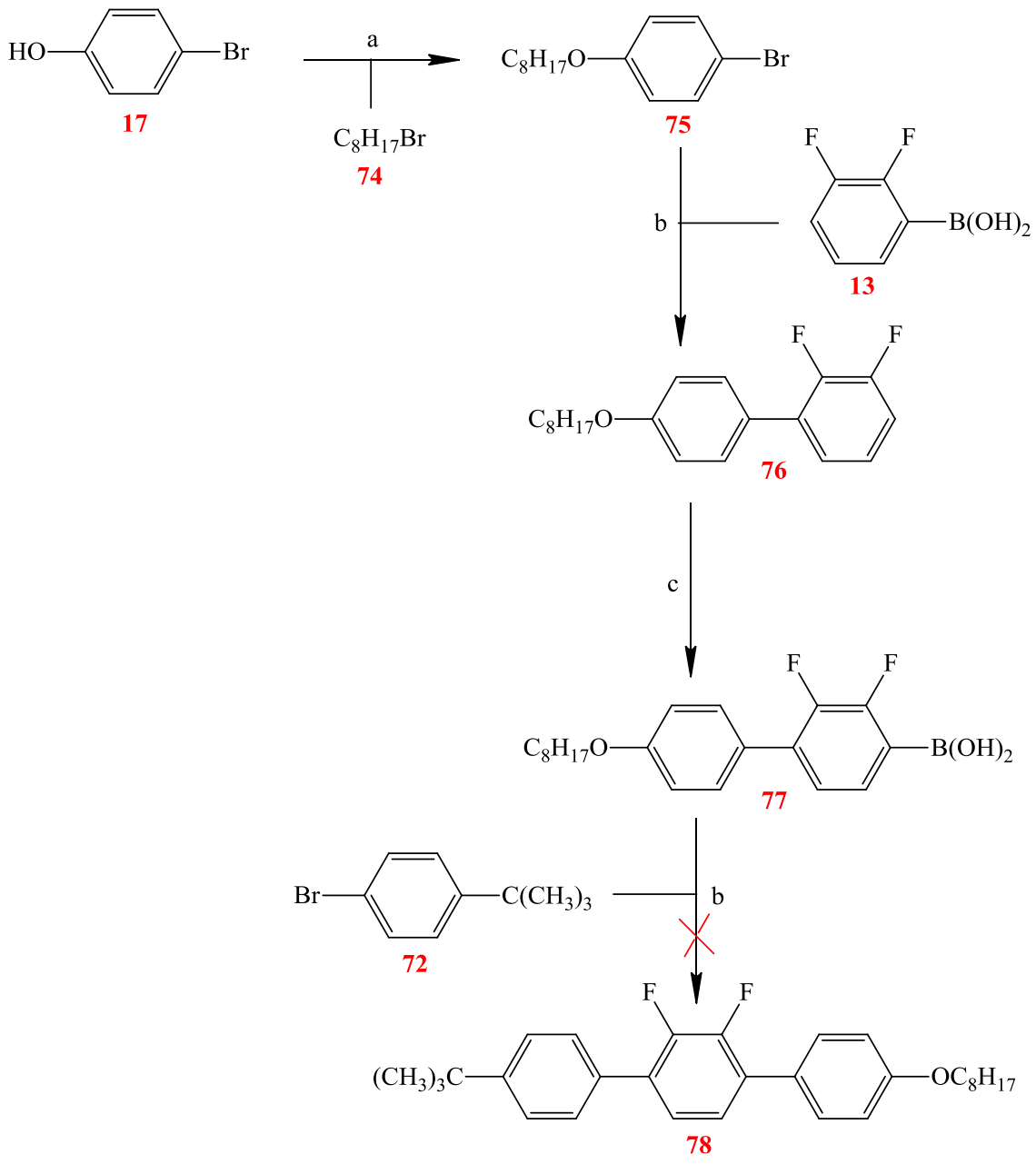

a...K_2CO_3, butanone.
b...$Pd(PPh_3)_4$, Na_2CO_3, DME, H_2O.
c...(i) *n*-BuLi -78 C; (ii) $(MeO)_3B$; (iii) 10% HCl.

Scheme 18

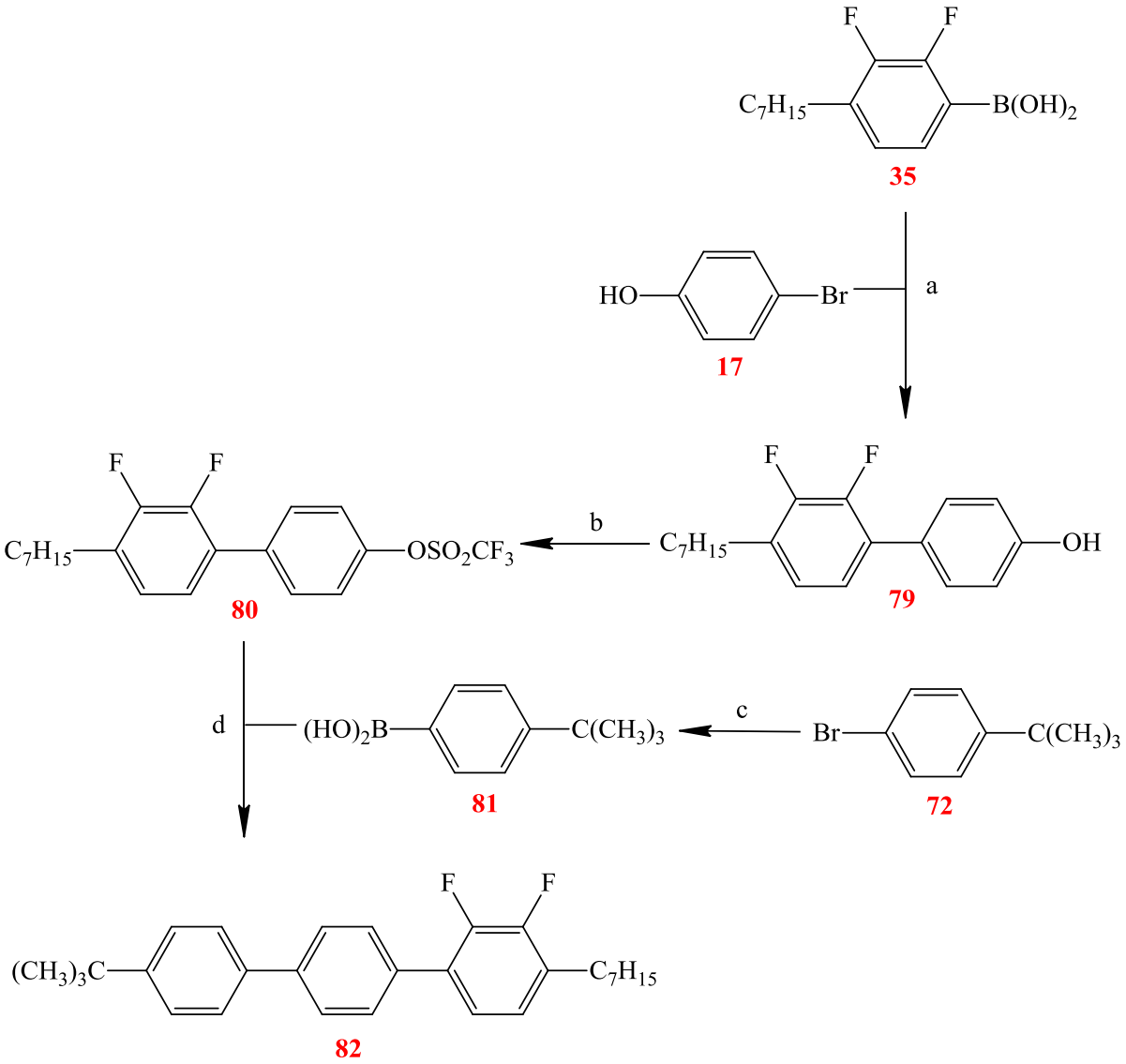

a...$Pd(PPh_3)_4$, KF, DME.
b...Pyridine, $(CF_3SO_2)_2O$.
c...(i) Mg, THF; (ii) $(MeO)_3B$; (iii) 10% HCl.
d...$Pd(PPh_3)_4$, Na_2CO_3, LiCl, DME, H_2O.

Scheme 19

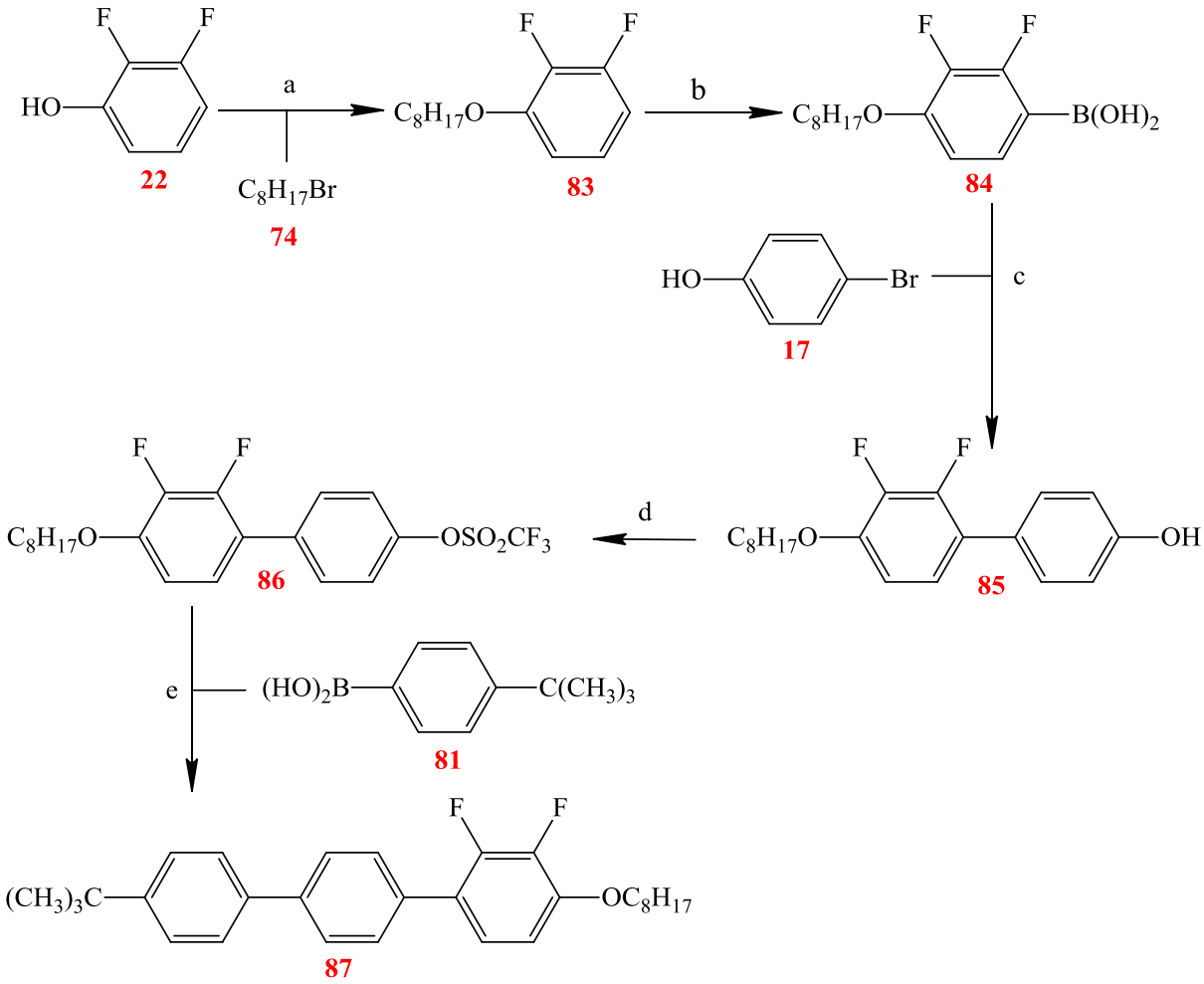

a...K_2CO_3, butanone
b...(i) *n*-BuLi -78 C; (ii) $(MeO)_3B$; (iii) 10% HCl
c...$Pd(PPh_3)_4$, KF, DME
d...Pyridine, $(CF_3SO_2)_2O$
e...$Pd(PPh_3)_4$, Na_2CO_3, LiCl, DME, H_2O

Scheme 20

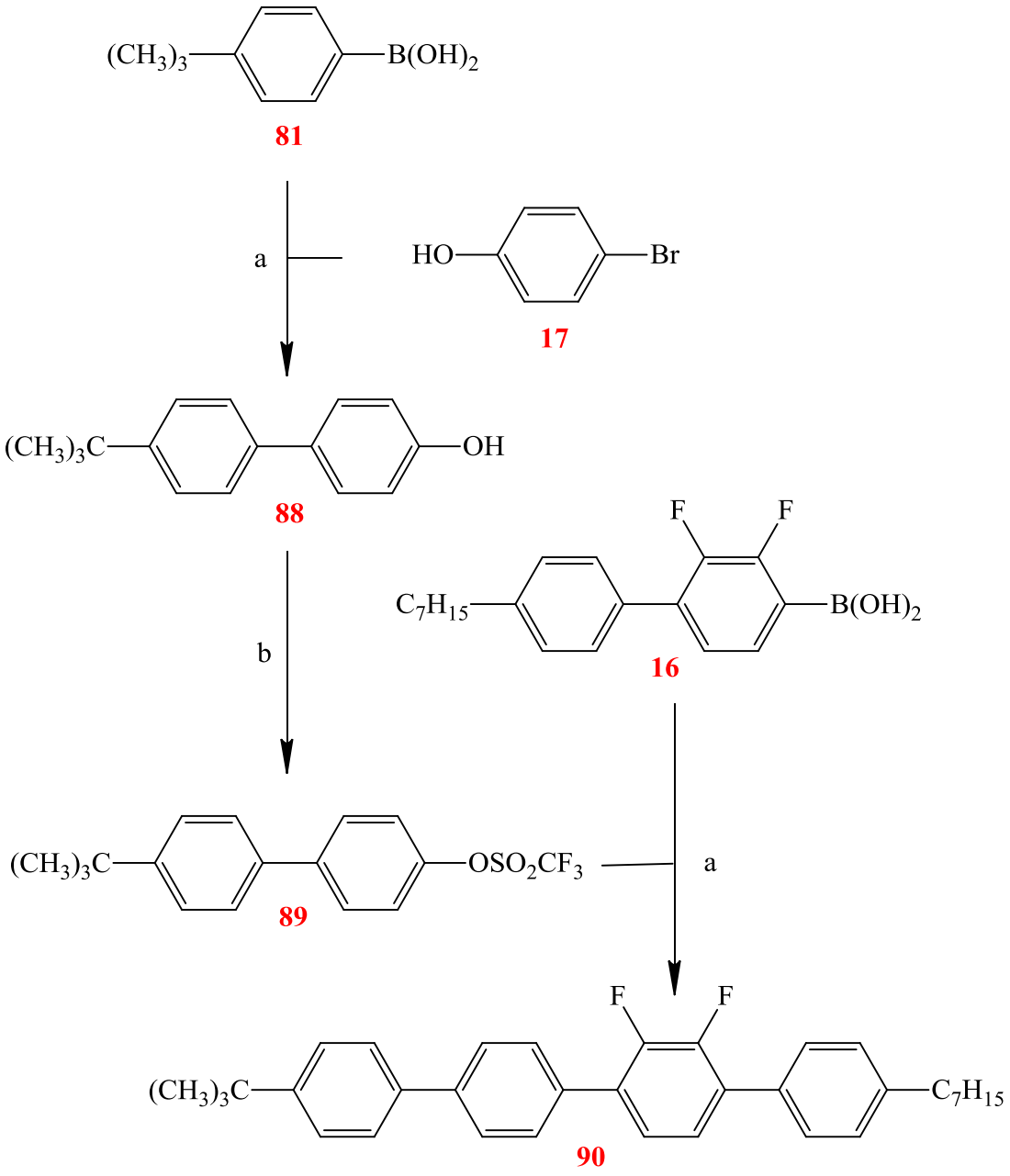

a...$Pd(PPh_3)_4$, KF, DME.
b...$(CF_3SO_2)_2O$, pyridine.

Scheme 21

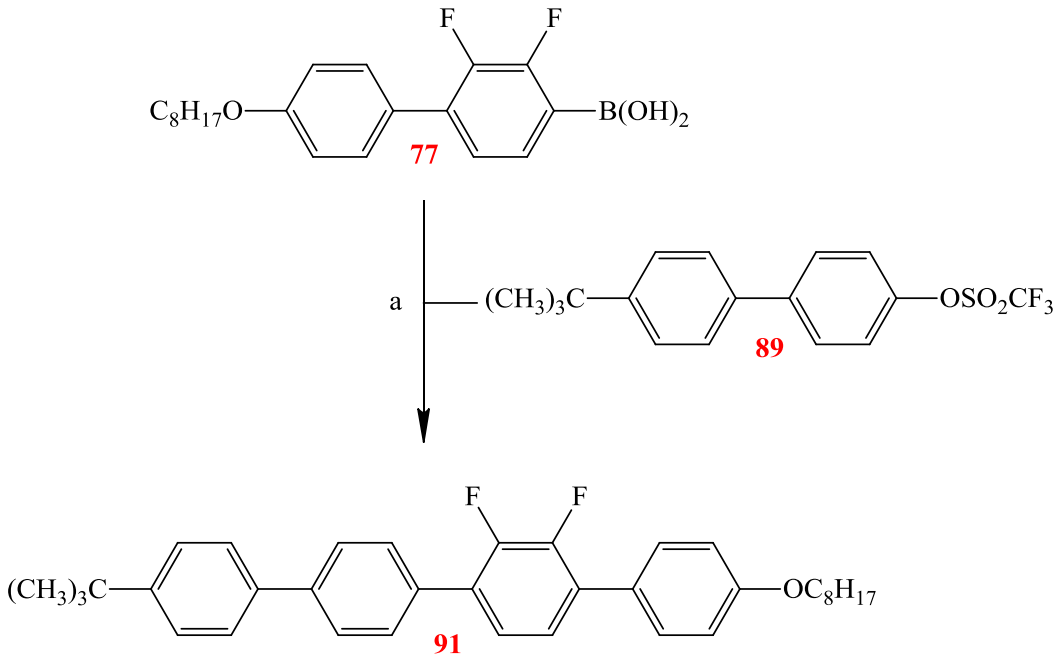

a...$Pd(PPh_3)_4$, Na_2CO_3, DME, H_2O

3.4 Experimental Procedures

Scheme 1

4,4-Dimethylpent-2-ynoic acid (2)

n-Butyllithium solution (250 ml, 2.5 M, 0.54 mols) was added dropwise to a stirred, cooled (-78 °C) solution of compound **1** (50 g, 0.61 mol) in dry THF (500 ml) under dry nitrogen. The reaction mixture was stirred at -78 °C for 30 min and poured into carbon dioxide. The mixture was left overnight at room temperature, ice was added, and 36 % HCl was added carefully. The product was extracted into ether (x2), and the combined ethereal extracts were washed with brine and dried ($MgSO_4$). The solvent was removed *in vacuo* to leave a colourless oil.

Yield = 65.49 g, (90 %).

^{1}H-NMR ($CDCl_3$), δ: 1.30 (9H, s), 11.10 (1H, s).

MS *m/z* 125 (M^+).

4,4-Dimethylpentanoic acid (3)

A mixture of compound **2** (65 g, 0.561 mol) and 10% Pd on carbon (3.3 g) in ethyl acetate was hydrogenated at 40 psi for one day. Following evacuation of the hydrogen, 10 % Pd/C was filtered off through hyflosupercell and washed with ether. The solvent was removed *in vacuo* and the crude product was distilled under vacuum to yield colourless oil.

[bp 80 °C at 15 mm Hg].

Yield = 28.13 g, (66 %).

^{1}H-NMR ($CDCl_3$), δ: 0.90 (9H, s), 1.57 (2H, t), 2.32 (2H, t), 11.97 (1H, s).

MS *m/z* 130 (M^+).

4,4-Dimethylpentan-1-ol (4)

Lithium aluminium hydride (20 g, 0.52 mol in a THF soluble bag) was added to a 2000 ml 3-necked (straight) flask equipped with a double surface reflux condenser with nitrogen bubbler on top. Dry THF (250 ml) was added quickly (this helps to absorb the heat generated). Then a solution of compound **3** (50 g, 0.38 mol) in dry THF (150 ml) was added slowly dropwise with stirring. The stirred mixture was heated under reflux for 4 h, left to cool, cooled in a salt-ice bath, and aqueous THF (10 % water) was added slowly dropwise (careful). When the reaction ceased, 36% HCl was added and the product was extracted into ether (x2), and the combined ethereal extracts were washed with brine and dried ($MgSO_4$). The solvent was removed *in vacuo* and the crude product was distilled at atmospheric pressure to yield a colourless oil.

[bp 160 $^{\circ}$C at 760 mm Hg].

Yield = 26.68 g, (79 %).

^{1}H-NMR ($CDCl_3$), δ: 0.70 (9H, s), 1.00 (2H, t), 1.32 (2H, quint), 3.35 (2H, t), 3.61 (1H, s).

MS *m/z* 116 (M^+).

4,4-Dimethylpentyl 4-methylbenzenesulfonate (5)

Tosyl chloride (40 g, 0.21 mol) was added in small portions to a stirred, cooled (-5 $^{\circ}$C) solution of compound **4** (17.89 g, 0.154 mol) and pyridine (22 g, 0.28 mol) in chloroform (180 ml). The mixture was stirred at 30 $^{\circ}$C overnight. Lots of water was added, and the product was extracted into ether (x2). The combined ethereal extracts were washed successively with 10 % HCl (x2), water, saturated sodium hydrogen carbonate solution and water then dried ($MgSO_4$). The solvent was removed *in vacuo* to yield a colourless oil.

Yield = 34.34 g, (83 %).

^{1}H-NMR ($CDCl_3$), δ: 0.70 (9H, s), 1.20 (2H, t), 1.70 (2H, quint), 2.45 (3H, s), 4.00 (2H, t), 7.35 (2H, d), 7.79 (2H, d).

MS *m/z* 270 (M^+).

Scheme 2

3-(Trimethylsilyl)propyl 4-methylbenzenesulfonate (7)

Tosyl chloride (54 g, 0.28 mol) was added in small portions to a stirred, cooled (-5 °C) solution of compound **6** (25 g, 0.189 mol) and pyridine (31 g, 0.39 mol) in chloroform (200 ml). The mixture was stirred at 30 °C overnight. Lots of water was added, and the product was extracted into ether (x2). The combined ethereal extracts were washed successively with 10 % HCl (x2), water, saturated sodium hydrogen carbonate solution and water then dried ($MgSO_4$). The solvent was removed *in vacuo* to yield a colourless oil.

Yield = 54.3 g, (41 %).

^{1}H-NMR ($CDCl_3$), δ: 0.05 (9H, s), 0.50 (2H, t), 1.65 (2H, quint), 2.50 (3H, s), 4.00 (2H, t), 7.40 (2H, d), 7.83 (2H, d).

MS *m/z* 286 (M^+).

Scheme 3

3,3-Dimethylbutyl 4-(tert-butyl)benzenesulfonate (9)

Tosyl chloride (37.35 g, 0.196 mol) was added in small portions to a stirred, cooled (-5 °C) solution of compound **8** (20 g, 0.196 mol), triethylamine (30 g, 0.297 mol) and dimethylaminopyridine (2 g) in dichloromethane (200 ml). The mixture was stirred at 30 °C overnight. Lots of water was added, and the product was extracted into ether (x2). The combined ethereal extracts were washed successively with 10 %

HCl (x2), water, saturated sodium hydrogen carbonate solution and water then dried ($MgSO_4$). The solvent was removed *in vacuo* to yield a colourless oil.

Yield = 44 g, (88 %).

^{1}H-NMR ($CDCl_3$), δ: 0.90 (9H, s), 1.60 (2H, t), 2.60 (3H, s), 4.10 (2H, t), 7.40 (2H, d), 7.90 (2H, d).

MS *m/z* 256 (M^+).

Scheme 4

2-(Trimethylsilyl)ethyl 4-(tert-butyl)benzenesulfonate (11)

Several methods were used to try and synthesise this compound, but all were unsuccessful.

Method 1

Tosyl chloride (48 g, 0.252 mol) was added in small portions to a stirred, cooled (-5 °C) solution of compound **10** (25 g, 0.189 mol) and pyridine (31 g, 0.39 mol) in chloroform (200 ml). The mixture was stirred at 30 °C overnight. The next day a lot of water was added, and the product was extracted into ether (x2). The combined ethereal extracts were washed successively with 10 % HCl (x2), water, saturated sodium hydrogen carbonate solution and water then dried ($MgSO_4$). The solvent was removed *in vacuo* to yield a colourless oil (28 g).

(The reaction failed).

Method 2

This method is the same as method 1 but without chloroform.

Tosyl chloride (48 g, 0.252 mol) was added in small portions to a stirred, cooled (-5 °C) solution of compound **10** (25 g, 0.189 mol) in pyridine (50 ml) . The mixture was stirred at 30 °C overnight. The next day a lot of water was added, and the product was extracted into ether (x2). The combined ethereal extracts were washed

successively with 10 % HCl (x2), water, saturated sodium hydrogen carbonate solution and water then dried ($MgSO_4$). The solvent was removed *in vacuo* to yield a colourless oil (30 g).

(The reaction failed).

Method 3

Tosyl chloride (48 g, 0.252 mol) was added in small portions to a stirred, cooled (-5 $^{\circ}$C) solution of compound **10** (25 g, 0.189 mol), DMAP (2 g, 0.0164 mol) and triethylamine (32 g, 0.317 mol) in DCM (300 ml). The mixture was stirred at 30 $^{\circ}$C overnight. The next day a lot of water was added, and the product was extracted into ether (x2). The combined ethereal extracts were washed successively with 10 % HCl (x2), water, saturated sodium hydrogen carbonate solution and water then dried ($MgSO_4$). The solvent was removed *in vacuo* to yield a colourless oil (33 g).

(The reaction failed)

Method 4

Tosyl chloride TsCl (48 g, 0.252 mol) was added in small portions to a stirred, cooled (-5 $^{\circ}$C) solution of compound **10** (25 g, 0.189 mol), DMAP (2.1 g, 0.011 mol) and *n,n*-diisopropylethylamine (32 g, 0.317 mol) in DCM (300 ml). The mixture was stirred at 30 $^{\circ}$C overnight. The next day a lot of water was added, and the product was extracted into ether (x2). The combined ethereal extracts were washed successively with 10 % HCl (x2), water, saturated sodium hydrogen carbonate solution and water then dried ($MgSO_4$). The solvent was removed *in vacuo* to yield a colourless oil (25 g).

(The reaction failed).

Scheme 5

2,3-Difluorophenyl boronic acid (13)

n-Butyllithium solution (176 ml, 2.5 M, 0.44 mol) was added drop wise to a stirred, cooled (-78 °C) solution of compound **12** (60 g, 0.526 mol) in THF (anhydrous) (450 ml) under dry nitrogen. The reaction mixture was stirred at this temperature (-78 °C) for 1 hour. Trimethyl borate (91.09 g, 0.875 mol) was added as dropwise at -78 °C, and the reaction mixture was allowed to warm to room temperature overnight.10 % HCl (100 ml) was added and the mixture was stirred at room temperature for around 1 hour. The product was extracted into ether (x2), and the combined ethereal extracts were washed with brine and dried ($MgSO_4$). The solvent was removed *in vacuo* and the solid residue was stirred in hexane, filtered, and air dried under suction to yield a colourless powder.

Yield = 56.3 g, (81%).

^{1}H-NMR (D6-DMSO), δ: 6.98 (1H, dddd), 7.25 (1H, dddd), 7.32 (1H, dddd), 7.90 (2H, s).

MS *m/z* 158 (M^+).

2,3-Difluoro-4'-heptylbiphenyl (15)

Compound **13** (21 g, 0.148 mol), dissolved in DME (250 ml), was added to a stirred mixture of compound **14** (30 g, 0.118 mol), Na_2CO_3 (47 g, 0.443 mol), and $Pd(PPh_3)_4$ (1.4 g, 1.21 mmol) in water (200 ml) under nitrogen. The stirred mixture was heated under reflux overnight. TLC revealed a complete reaction and the mixture was poured into water. The product was extracted into ether (x2) and the combined ethereal extracts were washed with brine and dried ($MgSO_4$). The solvent was removed *in vacuo* and the crude product was purified by column chromatography (silica gel/ hexane) to yield a colourless oil.

Yield = 29.53 g, (87 %).

^{1}H-NMR ($CDCl_3$), δ: 0.87 (3H, t), 1.30 (8H, m), 1.62 (2H, quint), 2.62 (2H, t), 7.06 (2H, ddd), 7.15 (1H, ddd), 7.25 (2H, d), 7.44 (2H, d).

MS: *m/z* 288 (M^+).

2,3-Difluoro-4'-heptylbiphenyl-4-yl boronic acid (16)

n-Butyllithium solution (45 ml, 2.5 M, 0.113 mol) was added dropwise to a stirred, cooled (-78 °C) solution of the compound **15** (29.53 g, 0.103 mol) in anhydrous THF (400 ml) under dry nitrogen. The reaction mixture was stirred at (-78 °C) for almost 1 h. After that, trimethyl borate (16 g, 0.154 mol) was added dropwise at -78 °C, and the reaction mixture was allowed to warm to room temperature overnight. 10 % HCl (100 ml) was added and the mixture was stirred at room temperature for around 1 h. The product was extracted into ether (x2), and the combined ethereal extracts were washed with brine and dried ($MgSO_4$). The solvent was removed *in vacuo* and the solid residue was stirred in hexane, filtered, and air dried under suction to yield a colourless powder.

Yield = 11.56 g, (34 %).

^{1}H-NMR (D6-DMSO), δ: 0.82 (3H, t), 1.20 – 1.30 (8H, m), 1.56 (2H, quint), 2.58 (1H, t), 7.22 – 7.32 (3H, m), 7.38 (1H, ddd), 7.46 (2H, dd), 8.43 (2H, s).

1-Bromo-4-(4,4-dimethylpentyloxy)benzene (18)

A stirred mixture of compound **17** (28 g, 0.162 mol), compound **5** (40 g, 0.148 mol) and potassium carbonate (51 g, 0.37 mol) in butanone (250 ml) was heated under reflux overnight. The potassium carbonate was filtered off and the solvent was removed *in vacuo*. The product was purified by column chromatography (silica gel) with added mixture of hexane and DCM 1:1 to yield a colourless solid.

Yield = 30.36 g, (76 %).

^{1}H-NMR ($CDCl_3$), δ: 0.09 (9H, s), 1.50 (2H, t), 1.69 (2H, quint), 4.00 (2H, t), 6.80 (2H, d), 7.40 (2H, d).

MS *m/z* 270 (M^+), *m/z* 272 (M^+).

1-bromo-4-(3-trimethylsilylpropoxy)benzene (19)

A stirred mixture of compound **17** (25.6 g, 0.148 mol), compound **7** (35.28 g, 0.123 mol) and potassium carbonate (61.3 g, 0.444 mol) in butanone (250 ml) was heated under reflux overnight. The potassium carbonate was filtered off and the solvent was removed *in vacuo*. The product was purified by column chromotography (silica gel) with added mixture of hexane and DCM 1:1 to yield a colorless oil.

Yield = 17.51 g, (50 %).

^{1}H-NMR ($CDCl_3$), δ: 0.00 (9H, s), 0.55 (2H, t), 1.75 (2H, quint), 3.85 (2H, t), 6.74 (2H, d), 7.33 (2H, d).

MS *m/z* 286 (M^+), *m/z* 288 (M^+).

2',3'-Difluoro-4-heptyl-4''-(4,4-dimethylpentyloxy)-[1,1':4',1'']-terphenyl (20)

Compound **16** (1.90 g, 5.72 mmol), dissolved in DME (150 ml), was added to a stirred mixture of the compound **18** (1.30 g, 4.80 mmol), Na_2CO_3 (1.82 g, 0.017 mol), and $Pd(PPh_3)_4$ (0.18 g, 0.156 mmol) in water (50 ml) under nitrogen. The stirred mixture was heated under reflux overnight. TLC revealed a complete reaction and the mixture was poured into water. The product was extracted into ether (x2) and the combined ethereal extracts were washed with brine and dried ($MgSO_4$). The solvent was removed *in vacuo* and the crude product was purified by column chromatography (silica gel/ hexane) to yield a colourless solid. The product was recrystallised (ethanol) and dried (desiccators, P_2O_5) overnight to yield colourless crystals.

Yield = 1.17 g, (51 %).

^{1}H-NMR ($CDCl_3$), δ: 0.88 (3H, t), 0.91 (9H, s), 1.30 (10H, m), 1.65 (2H, quint), 1.80 (2H, quint), 2.66 (2H, t), 4.00 (2H, t), 6.99 (2H, d, J = 8.77 Hz), 7.22 (2H, d, J = 5.92 Hz), 7.28 (2H, d, J = 8.16 Hz), 7.52 (4H, ddd, J = 16.32 Hz, J = 8.36 Hz, J = 1.43 Hz).

^{13}C-NMR (100 MHz, $CDCl_3$), δ; 14.11, 22.66, 24.63, 29.10, 29.30, 30.10, 30.90, 31.40, 31.80, 35.70, 40.11, 68.90 (alkyl carbons, 12 required, 12 found); 114.50, 124.31 (dd), 124.50 (dd), 126.80, 128.65, 128.68, 129.10, 129.25, 129.98 (d, J = 3.07 Hz) 132, 143.04, 148.2 (2x) (dd), 159.11. (aromatic carbons, 14 required, 14 found).

Transition: ($^\circ$C) Cr 82 SmC 92 N 108 Iso.

MS: *m/z* 478 (M^+).

Elemental analysis: $C_{31}H_{40}F_2OSi$ requires C 80.30 %, H 8.42 %; found C 80.45 %, H 8.70 %.

HPLC: 99.40 %.

2',3'-Difluoro-4-heptyl-4''-(3-trimethylsilylpropoxy)-[1,1':4',1'']-terphenyl (21)

Compound **16** (1.80 g, 5.42 mmol), dissolved in DME (150 ml), was added to a stirred mixture of the compound **19** (1.30 g, 4.53 mmol), Na_2CO_3 (1.80 g, 0.017 mol), and $Pd(PPh_3)_4$ (0.1 g, $8.66x10^{-5}$ mol) in water (50 ml) under nitrogen. The stirred mixture was heated under reflux overnight. TLC revealed a complete reaction and the mixture was poured into water. The product was extracted into ether (x2) and the combined ethereal extracts were washed with brine and dried ($MgSO_4$). The solvent was removed *in vacuo* and the crude product was purified by column chromatography (silica gel/ hexane) to yield a colourless solid. The product was recrystallised (ethanol) and dried (desiccators, P_2O_5) overnight to yield colourless crystals.

Yield = 1.5 g, (67 %).

^{1}H-NMR ($CDCl_3$), δ: 0.00 (9H, s), 0.59 (2H, quint), 0.85 (3H,t), 1.28 (8H, m), 1.62 (2H, quint), 1.78 (2H, quint), 2.63 (2H, t), 3.94 (2H, t), 6.95 (2H, d, J = 8.77 Hz), 7.18 (2H, d, J = 5.92 Hz), 7.24 (2H, d, J = 8.16 Hz), 7.47 (4H, ddd, J = 16.32 Hz, J = 8.36 Hz, J = 1.43 Hz).

^{13}C-NMR (100 MHz, $CDCl_3$), δ: -1.73, 12.57, 14.10, 22.67, 23.84, 29.19, 29.33, 31.43, 31.81, 35.72, 70.76 (alkyl carbons, 11 requird, 11 found) ; 114.50, 124.31 (dd), 124.5 (dd), 126.8, 128.65, 128.68, 129.10, 129.25, 129.98 (d, J = 3.07 Hz) 132, 143.01, 148.20 (2x) (dd), 159.09. (aromatic carbons, 14 required, 14 found).

Transition: ($^\circ$C) Cr 81 SmC 90 N 94 Iso.

MS: *m/z* 494 (M^+).

Elemental analysis: $C_{31}H_{40}F_2OSi$ requires C 75.26 %, H 8.15 %; found C 75.42 %, H 8.32 %.

HPLC: 99.72 %.

Scheme 6

1,2-Difluoro-3-(4,4-dimethylpentyloxy)benzene (23)

A stirred mixture of compound **22** (20 g, 0.154 mol), compound **5** (34.34 g, 0.127 mol) and potassium carbonate (70 g, 0.507 mol) in butanone (250 ml) was heated under reflux overnight. The potassium carbonate was filtered off and the solvent was removed *in vacuo*. Then the product was purified by column chromatography (silica gel/ hexane / 10 % DCM) to yield a colourless oil.

Yield = 19.85 g, (69 %).

^{1}H-NMR ($CDCl_3$), δ: 0.90 (9H, s), 1.30 (2H, t), 1.80 (2H, quint), 4.00 (2H, t), 6.68-6.76 (2H, m), 6.95 (1H, dddd).

MS *m/z* 228 (M^+).

1,2-Difluoro-3-(3-trimethylsilylpropoxy)benzene (24)

A stirred mixture of compound **7** (54 g, 0.189 mol), potassium carbonate (89 g, 0.64 mol) and compound **22** (28 g, 0.215 mol) in butanone (250 ml) was heated under reflux overnight. The potassium carbonate was filtered off and the solvent was removed *in vacuo*. Then the crude product was purified by column chromatography (silica gel/ hexane/ 10% DCM) to yield a colourless oil.

Yield = 33 g, (72 %).

^{1}H-NMR ($CDCl_3$), δ: 0.07 (9H, s), 0.60 (2H, t), 1.83 (2H, quint), 4.00 (2H, t), 6.69-6.79 (2H, m), 6.95 (1H, dddd).

MS *m/z* 244 (M^+).

2,3-Difluoro-(4-((4,4-dimethylpentyl)oxy)phenyl)boronic acid (25)

n-Butyllithium solution (38 ml, 2.5 M, 0.095 mol) was added dropwise to a stirred, cooled (-78 °C) solution of compound **23** (19.6 g, 0.086 mol) in anhydrous THF (350 ml) under dry nitrogen. The reaction mixture was stirred at (-78 °C) for almost 1 h. After that, trimethyl borate (14 g, 0.135mol) was added dropwise at -78 °C, and the reaction mixture was allowed to warm to room temperature overnight. 10 % HCl (100 ml) was added and the mixture was stirred at room temperature for around 1 h. The product was extracted into ether (x2), and the combined ethereal extracts were washed with brine and dried ($MgSO_4$). The solvent was removed *in vacuo* and the solid residue was stirred in hexane, filtered, and air dried under suction to yield a colourless powder.

Yield = 12.33 g, (53 %).

^{1}H-NMR (D6-DMSO), δ: 0.80 (9H, s), 1.20 (2H, t), 1.60 (2H, quint), 3.97 (2H, t), 6.95 (1H, ddd), 7.30 (1H, ddd), 8.00 (2H, s).

2,3-Difluoro-4-(3-(trimethylsilyl)propoxy)phenyl boronic acid (26)

n-Butyllithium solution (60 ml, 0,15 mol) was added dropwise to a stirred, cooled (-78 °C) solution of compound **24** (32.87 g, 0.135 mol) in anhydrous THF (300 ml) under dry nitrogen. The reaction mixture was stirred at (-78 °C) for 1 h. After that, trimethyl borate (21 g, 0.02 mol) was added dropwise at -78 °C, and the reaction mixture was allowed to warm to room temperature overnight in the fume cupboard. 10 % HCl (100 ml) was added and the mixture was stirred at room temperature for around 1 h. The product was extracted into ether (x2), and the combined ethereal extracts were washed with brine and dried ($MgSO_4$). The solvent was removed *in vacuo* and the solid residue was stirred in hexane, filtered, and air dried under suction to yield a colourless powder.

Yield = 37.72 g, (97 %).

^{1}H-NMR (D6-DMSO), δ: 0.05 (9H, s), 0.60 (2H, t), 2.70 (2H, quint), 4.00 (2H, t), 6.90 (1H, ddd), 7.30 (1H, ddd), 8.17 (2H, s).

2,3-Difluoro-4''-heptyl-4-(4,4-dimethylpentyloxy)-{1,1':4',1'']-terphenyl (28)

Compound **25** (1.57g, 5.77 mmol), dissolved in DME (150 ml), was added to a stirred mixture of compound **27** (1.53 g, 4.62 mmol), Na_2CO_3 (1.85 g, 0.017 mol), and $Pd(PPh_3)_4$ (0.1 g, $8.66x10^{-5}$ mol) in water (50 ml) under nitrogen. The stirred mixture was heated under reflux overnight. TLC revealed a complete reaction and the mixture was poured into water. The product was extracted into ether (x2) and the combined ethereal extracts were washed with brine and dried ($MgSO_4$). The solvent was evaporated and the crude product was purified by column chromatography (silica gel/ hexane) to yield a colourless solid. The product was recrystallised (ethanol) and dried (desiccators, P_2O_5) overnight to yield a colourless crystal.

Yield: 1.13 g, (41 %).

^{1}H-NMR ($CDCl_3$), δ: 0.89 (3H, t), 0.94 (9H, s), 1.35 (10H, m), 1.65 (2H, quint), 1.83 (2H, m), 4.05 (2H, t), 6.81 (1H, ddd, J = 14.69 Hz, J = 8.98 Hz, J = 1.84 Hz), 7.14 (1H, ddd, J = 16.93 Hz, J = 8.77 Hz, J = 2.24 Hz), 7.27 (2H, d, J = 8.36 Hz), 7.56 (4H, m), 7.65 (2H, d, J = 8.57 Hz).

^{13}C-NMR (100 MHz, $CDCl_3$), δ: 14.10, 22.67, 24.60, 29.20, 29.30, 29.34, 30.17, 31.5, 31.82, 35.63, 39.90, 70.72 (alkyl carbons, 12 required, 12 found); 109.50, 122.50, 122.60, 123.40 (dd, J = 3.84 Hz, J = 3.84 Hz), 126.88, 127.06, 128.88, 129.02 (d, J = 3.07 Hz), 133.5, 137.84, 140.39, 142.35, 144.12 (dd, J = 714.13 Hz, J = 13.07 Hz), 146.58 (dd, J = 715.66 Hz, J = 13.068 Hz), (aromatic carbons, 14 required, 14 found).

Transition: ($^\circ$C) Cr 117 (G 101) SmC 146 Iso.

MS: *m/z* 478 (M^+).

Elemental analysis: $C_{31}H_{40}F_2OSi$ requires C 80.30 %, H 8.42 %; found C 80.45 %, H 8.61 %.

HPLC: 99.61 %.

2,3-Difluoro-4''-heptyl-4-(3-trimethylsilylpropoxy)-[1,1':4',1'']-terpheny1 (29)

Compound **26** (1.6 g, 5.56 mmol), dissolved in DME (150 ml), was added to a stirred mixture of compound **27** (1.5 g, 4.53 mmol) , Na_2 CO_3 (1.85 g, 0.017 mol), and $Pd(PPh_3)_4$ (0.1 g, $8.66x10^{-5}$ mol) in water (50 ml) under nitrogen. The stirred mixture was heated under reflux overnight. TLC revealed a complete reaction and the mixture was poured into water. The product was extracted into ether (x2) and the combined ethereal extracts were washed with brine and dried ($MgSO_4$). The solvent was evaporated and the crude product was purified by column chromatography (silica gel/ hexane) to yield a colourless solid. The product was recrystallised (ethanol) and dried (desiccators, P_2O_5) overnight to yield a colourless crystal.

Yield = 1.73 g, (63 %).

^{1}H-NMR ($CDCl_3$), δ: 0.01 (9H, s), 0.58 (2H, m), 0.85 (3H, t), 1.21-1.37 (8H, m), 1.62 (2H, quint) , 1.82 (2H, m), 2.61 (2H, t), 4.0 (2H, t), 6.77 (1H, ddd, J = 8.26 Hz, 8.26 Hz, 1.84 Hz), 7.10 (1H, ddd, J = 8.67 Hz, 8.67 Hz, 2.45 Hz), 7.23 (2H, d, J = 8.16 Hz), 7.51 (2H, d, J = 8.36 Hz), 7.53 (2H, dd, J = 7.96 Hz, J = 1.63 Hz), 7.62 (2H, d, J = 8.57 Hz).

^{13}C-NMR (100 MHz, $CDCl_3$), δ: 0.20, 16.90, 18.60, 28.30, 33.70, 33.80, 36.02, 36.34, 40.20, 77.00, 81.50 (alkyl carbons, 11 required, 11 found); 114.09, 127.11 (d, J = 11.53 Hz), 128.00 (dd, J = 4.61 Hz, J = 4.61 Hz), 131.41, 131.58, 133.41, 133.54 (d, J = 2.31 Hz), 138.07, 142.38, 144.92, 146.33 (dd, J = 247.14 Hz, J = 15.37 Hz), 146.88, 152.34 (dd, J = 8.07 Hz, J = 3.07 Hz), 153.45 (dd, J = 249.06 Hz, J = 10.76 Hz), (aromatic carbons, 14 required, 14 found).

Transition: (°C) Cr 111 SmC 140 Iso.

MS: *m/z* 494 (M^+).

Elemental analysis: $C_{31}H_{40}F_2OSi$ requires C 75.26 %, H 8.15 %; found C 75.54 %, H 8.26 %.

HPLC: 99.50 %.

Scheme 7

4-bromo-4'-(4,4-dimethylpentyloxy)-biphenyl (31)

A stirred mixture of compound **30** (15 g, 0.067 mol), compound **5** (19 g, 0.07 mol) and potassium carbonate (20 g, 0.14 mol) in butanone (250 ml) was heated under reflux overnight. The potassium carbonate was filtered off and the solvent was removed *in vacuo* from the isolated filtrate. Then the crude product was purified by column chromatography (silica gel/ hexane : DCM, 10:1).

Yield = 13 g, (76 %).

^{1}H-NMR ($CDCl_3$), δ: 0.92 (9H, s), 1.34 (2H, t), 1.77 (2H, quint), 3.96 (2H, t), 6.95 (2H, d), 7.39 (2H, d), 7.45 (2H, d), 7.52 (2H, d).

MS: *m/z* 346 (M^+), *m/z* 348 (M^+).

Scheme 17

4-bromo-4'-(3-trimethylsilylpropoxy)biphenyl (32)

A stirred mixture of compound **30** (61.5 g, 0.247 mol), compound **7** (70.75 g, 0.247 mol) and potassium carbonate (68 g, 0.49 mol) in butanone (250 ml) was heated under reflux overnight. The potassium carbonate was filtered off and the solvent was removed *in vacuo*. The crude product was purified by column chromatography (silica gel/ hexane) to yield a colourless solid.

Yield: 36.79 g, (41 %).

1H-NMR ($CDCl_3$), δ: 0.01 (9H, s), 0.58 (2H, t), 1.77 (2H, quint), 3.95 (2H, t), 6.92 (2H, d), 7.38 (2H, d), 7.44 (2H, d), 7.50 (2H, d).

MS: *m/z* 362 (M^+), *m/z* 364 (M^+).

1,2-Difluoro-3-heptylbenzene (34)

n-Butyllithium (100 ml, 2.5 M, 0.25 mol) was added carefully dropwise to a stirred, cooled (-78 °C) solution of compound **12** (35 g, 0.31 mol), in dry THF (400 ml) under dry nitrogen gas. This mixture was stirred 1 h (-78 °C), and heptanal (**33**) (32 g, 0.28 ml) was added dropwise at -78 °C. The stirred mixture was allowed to warm up to room temperature overnight. Aqueous ammonium chloride was added and the product was extracted into ether (x2). The combined extracts were washed with brine and dried ($MgSO_4$). The solvent was removed *in vacuo*. PTSA (5 g) was added to a stirred solution in toluene (150 ml) under reflux at room temperature overnight. The combined extracts where washed with aqueous sodium hydrogen carbonate and brine and dried ($MgSO_4$). The mixture was filtered. Pd/C (3 g) was added to the filtrate and the stirred mixture was hydrogenated for 1 day at room temperature. The Pd/C was filtered off, the solvent was removed *in vacuo* and the product was distillated to yield a colourless oil.

[bp 125 °C at 15 mm Hg].

Yield: 55.36 g, (84 %)

^{1}H-NMR ($CDCl_3$), δ: 0.87 (3H, t), 1.31 (8H, m), 1.58 (2H, quint), 2.6 (2H, t), 6.95 (3H, m).

MS: *m/z* 212 (M^+).

2,3-Difluoro-4-heptylphenyl boronic acid (35)

n-Butyllithium solution (72 ml, 2.5 M, 0.18 mol) was added dropwise to a stirred, cooled (-78 °C) solution of the compound **34** (35 g, 0.165 mol) in anhydrous THF (800 ml) under dry nitrogen. The reaction mixture was stirred at (-78 °C) for almost 1 h. Trimethyl borate (26 g, 0.25 mol) was added dropwise at -78 °C, and the reaction mixture was allowed to warm to room temperature overnight. 10 % HCl (100 ml) was added and the mixture was stirred at room temperature for around 1 h. The product was extracted into ether (x2), and the combined ethereal extracts were washed with brine and dried ($MgSO_4$). The solvent was removed *in vacuo* and the

solid residue was stirred in hexane, filtered, and air dried under suction to yield a colourless powder.

Yield: 19.32 g, (46 %).

^{1}H-NMR (D6-DMSO), δ: 0.85 (3H, t), 1.30 (8H, m), 1.5 (2H, t), 2.65 (2H, t), 7.01 (1H, ddd), 7.22 (1H, ddd), 8.30 (2H, s).

2,3-Difluoro-4-heptyl-4''-(4,4-dimethylpentyloxy)-[1,1':4',1'']-terphenyl (36)

Compound **35** (1.60 g, 0.25 mmol), dissolved in DME (100 ml), was added to a stirred mixture of the compound **31** (1.70 g, 4.9 mmol), Na_2CO_3 (1.6 g, 0.015 mol), and $Pd(PPh_3)_4$ (0.1 g, 0.086 mmol) in water (40 ml) under nitrogen. The stirred mixture was heated under reflux overnight. TLC revealed a complete reaction and the mixture was poured into water. The product was extracted into ether (x2) and the combined ethereal extracts were washed with brine and dried ($MgSO_4$). The solvent was removed *in vacuo* and the crude product was purified by column chromatography (silica gel/ hexane) to yield a colourless solid. The product was recrystallised (ethanol) and dried (desiccators, P_2O_5) overnight to yield colourless crystals.

Yield = 1.95 g, (83 %).

^{1}H-NMR ($CDCl_3$), δ: 0.90 (3H, t), 0.95 (9H, s), 1.36 (10H, m), 1.64 (2H, quint), 1.79 (2H, quint), 2.68 (2H, t), 3.98 (2H, t), 6.98 (2H, d, J = 8.80 Hz), 7.13 (1H, ddd, J = 16.93 Hz, J = 8.06 Hz, J = 1.65 Hz), 7.55 (2H, d, J = 8.61 Hz), 7.58 (2H, d, J = 8.89 Hz), 7.63 (2H, d, J = 8.61 Hz).

^{13}C-NMR (100 MHz, $CDCl_3$), δ: 14.09, 22.65, 24.68, 28.70, 29.08, 29.26, 29.33, 30.06, 30.17, 31.77, 40.14, 68.94 (alkyl carbons, 12 required, 12 found); 114.82, 124.13 (dd, J = 3.07 Hz, J = 3.07 Hz), 124.72 (dd, J = 4.61 Hz, J = 4.61 Hz) , 126.73, 128.06, 129.15, 130.78, 130.92, 132.81, 133.23, 140.35, 148.27 (dd, J = 247.91 Hz, J = 12.68 Hz), 149.40 (dd, J = 241.76 Hz, J = 9.60 Hz), 158.89, (aromatic carbons, 14 required, 14 found).

Transition: (°C) Cr 104 SmC 137 Iso.

MS: *m/z* 478 (M^+).

Elemental analysis: $C_{32}H_{40}F_2O$ requires C 80.3 %, H 8.42 %; found C 80.05 %, H 8.65 %.

HPLC: 100 %.

2,3-difluoro-4-heptyl-4''-(3-trimethylsilylpropoxy)-[1,1':4',1'']-terphenyl (37)

Compound **35** (1.41 g, 5.5 mmol), dissolved in DME (100 ml), was added to a stirred mixture of the compound **32** (1.65 g, 4.5 mmol), Na_2CO_3 (1.45 g, 0.014 mol), and $Pd(PPh_3)_4$ (0.10 g, 0.0865 mmol) in water (40 ml) under nitrogen. The stirred mixture was heated under reflux overnight. TLC revealed a complete reaction and the mixture was poured into water. The product was extracted into ether (x2) and the combined ethereal extracts were washed with brine and dried ($MgSO_4$). The solvent was removed *in vacuo* and the crude product was purified by column chromatography (silica gel/ hexane) to yield a colourless solid. The product was recrystallised (ethanol) and dried (desiccators, P_2O_5) overnight to yield colourless crystals.

Yield = 2.17 g, (98 %).

^{1}H-NMR ($CDCl_3$), δ: 0.00 (9H, s), 0.59 (2H, quint), 0.84 (3H, t), 1.26 (8H, m), 1.61 (2H, quint), 1.79 (2H, quint), 2.65 (2H, t), 3.90 (2H, t), 6.95 (2H, d, J = 8.80 Hz), 7.11 (1H, ddd, J = 15.12 Hz, J = 8.25 Hz, J = 1.83 Hz), 7.53 (2H, d, J = 8.80 Hz), 7.54 (2H, d, J = 8.06 Hz), 7.60 (2H, d, J = 8.61 Hz).

^{13}C-NMR (100 MHz, $CDCl_3$), δ: -1.73, 12.58, 14.09, 22.65, 23.87, 28.78, 29.08, 29.26, 30.06, 31.77, 70.78 (alkyl carbons, 11 required, 11 found); 114.82, 124.10 (dd, J = 3.07 Hz, J = 3.07 Hz), 124.77 (dd, J = 4.61 Hz, J = 4.61 Hz), 126.73, 128.07, 129.15 (d, J = 3.07 Hz), 130.09, 130.11, 132.80, 133.30, 140.05, 148.06 (dd, J = 244.06 Hz, J = 12.68 Hz), 149.30 (dd, J = 255.59 Hz, J= 12.68 Hz), 158.80, (aromatic carbons, 14 required, 14 found).

Transition: (°C) Cr 103 SmC 124 Iso.

MS: *m/z* 494 (M^+).

Elemental analysis: $C_{31}H_{40}F_2OSi$ requires C 75.26 %, H 8.15 %; found C 74.98 %, H 8.00 %.

HPLC: 100 %.

Scheme 8

1-Bromo-4-(3,3-dimethylbutoxy)benzene (38)

A stirred mixture of compound **17** (12 g, 0.069 mol), compound **9** (15 g, 0.0586 mol) and potassium carbonate (24 g, 0.17 mol) in butanone (200 ml) was heated under reflux overnight. The potassium carbonate was filtered off and the solvent was removed *in vacuo*. The product was purified by column chromatography with mixture of hexane and DCM 1:1 to yield a colourless solid.

Yield = 13.22 g, (75 %).

^{1}H-NMR ($CDCl_3$), δ: 0.98 (9H, s), 1.72 (2H, t), 3.98 (2H, t), 6.75 (2H, d), 7.35 (2H, d).

MS *m/z* 254 (M^+), *m/z* 256 (M^+).

2',3'-Difluoro-4-heptyl-4''-(3,3-dimethylbutoxy)-[1,1':4',1'']-terphenyl (39)

Compound **16** (1.90 g, 6.0 mmol), dissolved in DME (150 ml), was added to a stirred mixture of the compound **38** (1.21 g, 4.750 mmol), Na_2CO_3 (1.91 g, 0.018 mol), and $Pd(PPh_3)_4$ (0.18 g, 0.156 mmol) in water (50 ml) under nitrogen. The stirred mixture was heated under reflux overnight. TLC revealed a complete reaction and the mixture was poured into water. The product was extracted into ether (x2) and the combined ethereal extracts were washed with brine and dried ($MgSO_4$). The solvent was removed *in vacuo* and the crude product was purified by column chromatography (silica gel/ hexane) to yield a colourless solid. The product was recrystallised (ethanol) and dried (desiccators, P_2O_5) overnight to yield colourless crystals.

Yield: 1.36 g, (62 %).

^{1}H-NMR ($CDCl_3$), δ: 0.88 (3H, t), 1.00 (9H, s), 1.34 (8H, m), 1.66 (2H, t), 1. 76 (2H, t), 2.66 (2H, t), 4.10 (2H, t), 7.00 (2H, d, J = 8.98 Hz), 7.23 (2H, m), 7.28 (2H, d, J = 8.16 Hz), 7.53 (4H, ddd, J = 16.52 Hz, J = 8.57 Hz, J = 1.22 Hz).

^{13}C-NMR (100 MHz, $CDCl_3$), δ: 14.11, 22.66, 29.18, 29.33, 29.74, 31.10, 31.50, 32.10, 35.70, 42.32, 65.38 (alkyl carbons, 11 required, 11 found); 114.59, 124.33 (dd, J = 3.84 Hz, J = 3.84 Hz), 124.52 (dd, J= 3.84 Hz, J = 3.84 Hz), 126.80, 128.65, 128.68, 129.08 (d, J = 5.38 Hz), 129.2 (d, J = 5.38 Hz), 129.97 (d, J = 3.84 Hz), 131.98, 143.04, 148.35 (dd, J = 251.37 Hz, J = 11.00 Hz), 148.52 (dd, J = 250.98 Hz, J = 10.00 Hz), 159.00, (aromatic carbons, 14 required, 14 found).

Transition: ($^\circ$C) Cr 95 N 100 Iso.

MS: *m/z* 464 (M^+).

Elemental analysis: $C_{31}H_{40}F_2OSi$ requires C 80.14 %, H 8.24 %; found C 80.36 %, H 8.26 %.

HPLC: 99.2 %.

Scheme 9

1,2-difluoro-3-(3,3-dimethylbutoxy)benzene (40)

A stirred mixture of compound **22** (11.70 g, 0.09 mol), compound **9** (20 g, 0.078 mol) and potassium carbonate (37 g, 0.27 mol) in butanone (250 ml) was heated under reflux overnight. The potassium carbonate was filtered off and the solvent was removed *in vacuo*. The product was purified by column chromatography (silica gel/ hexane : DCM, 1:1) to yield a colourless oil.

Yield = 15.51 g, (96 %).

^{1}H-NMR ($CDCl_3$), δ: 1.00 (9H, s), 1.70 (2H, t), 4.10 (2H, t), 6.70 (2H, m), 6.90 (1H, m).

MS *m/z* 214 (M^+).

4-(3,3-dimethylbutoxy)-2,3-difluorophenylboronic acid (41)

n-Butyllithium solution (4.67 ml, 2.5 M, 0.073 mol) was added dropwise to a stirred, cooled (-78 °C) solution of compound **40** (15.51 g, 0.072 mol) in anhydrous THF (350 ml) under dry nitrogen. The reaction mixture was stirred at (-78 °C) for almost 1 h. Trimethyl borate (14 g, 0.135 mol) was added dropwise, and the reaction mixture was allowed to warm to room temperature overnight. 10 % HCl (100 ml) was added and the mixture was stirred at room temperature for around 1 h. The product was extracted into ether (x2), and the combined ethereal extracts were washed with brine and dried ($MgSO_4$). The solvent was removed *in vacuo* and the solid residue was stirred in hexane, filtered, and air dried under suction to yield a colourless powder.

Yield: 15 g, (78 %).

^{1}H-NMR (D6-DMSO), δ: 0.90 (9H, s), 1.60 (2H, t), 4.10 (2H, t), 7.00 (1H, t), 7.30 (1H, t), 8.10 (2H, s).

2,3-difluoro-4''-heptyl-4-(3,3-dimethylbutoxy)-[1,1':4',1'']-terphenyl (42)

Compound **41** (2.50 g, 9.69 mmol), dissolved in DME (150 ml), was added to a stirred mixture of the compound **27** (1.6 g, 4.83 mmol), Na_2CO_3 (2.5 g, 23.6 mmol), and $Pd(PPh_3)_4$ (0.18 g, 0.156 mmol) in water (50 ml) under nitrogen. The stirred mixture was heated under reflux overnight. TLC revealed a complete reaction and the mixture was poured into water. The product was extracted into ether (x2) and the combined ethereal extracts were washed with brine and dried ($MgSO_4$). The solvent was removed *in vacuo* and the crude product was purified by column chromatography (silica gel/ hexane) to yield a colourless solid. The product was recrystallised (ethanol) and dried (desiccators, P_2O_5) overnight to yield colourless crystals.

Yield = 1.65 g, (75 %).

^{1}H-NMR ($CDCl_3$), δ: 0.88 (3H, t), 1.01 (9H, s), 1.29 (8H, m), 1.65 (2H, quint), 1.80 (2H, t), 2.64 (2H, t), 4.14 (2H, t), 6.81 (1H, ddd, J = 16.32 Hz, J = 8.06 Hz, J = 1.84 Hz), 7.14 (1H, ddd, J = 16.93 Hz, J = 9.38 Hz, J = 2.24 Hz), 7.26 (2H, d, J = 8.16 Hz), 7.56 (4H, dd, J= 7.55 Hz, J = 7.55 Hz), 7.65 (2H, d, J = 8.36 Hz).

^{13}C-NMR (100 MHz, $CDCl_3$), δ: 14.10, 22.66, 29.19, 29.34, 29.69, 29.78, 31.50, 31.82, 35.62, 42.18, 67.19 (alkyl carbons, 11 required, 11 found); 109.34, 122.59 (d, J = 12.30 Hz), 123.45 (dd, J = 12.30 Hz, J = 4.61), 126.87, 127.06, 128.87, 129.00 (d, J = 3.07 Hz), 133.53, 137.87, 140.39, 141.00, 142.34, 144.88 (dd, J = 377.43 Hz, J = 16.14 Hz), 146.11 (dd, J = 311.71 Hz, J = 11.91 Hz), (aromatic carbons, 14 required, 14 found).

Transition: ($^\circ$C) Cr 106 SmC 121 SmA 126 N 129 Iso.

MS: *m/z* 464 (M^+).

Elemental analysis: $C_{31}H_{38}F_2O$ requires C 80.14 %, H 8.24 %; found C 79.99 %, H 8.44 %.

HPLC: 100 %.

Scheme 10

4-bromo-4'-(3,3-dimethylbutoxy)biphenyl (43)

A stirred mixture of compound **30** (21.4 g, 0.086 mol), compound **9** (20 g, 0.078 mol) and potassium carbonate (30 g, 0.22 mol) in butanone (250 ml) was heated under reflux overnight. The potassium carbonate was filtered off and the solvent was removed *in vacuo*. The product was purified by column chromatography (silica gel/ hexane : DCM, 1 : 1) to yield a colourless solid.

Yield: 18 g, (69 %).

^{1}H-NMR ($CDCl_3$), δ: 1.00 (9H, s), 1.74 (2H, t), 4.04 (2H, t), 6.95 (2H, d), 7.37 (2H, d), 7.45 (2H, d), 7.50 (2H, d).

MS *m/z* 333 (M^+).

2,3-Difluoro-4-heptyl-4''-(3,3-dimethylbutoxy)-[1,1':4',1'']-terphenyl (44)

Compound **35** (2.33 g, 4.80 mmol), dissolved in DME (150 ml), was added to a stirred mixture of the compound **43** (1.6 g, 5.86 mmol), Na_2CO_3 (1.5 g, 14.2 mmol), and $Pd(PPh_3)_4$ (0.18 g, 0.156 mmol) in water (50 ml) under nitrogen. The stirred mixture was heated under reflux overnight. TLC revealed a complete reaction and the mixture was poured into water. The product was extracted into ether (x2) and the combined ethereal extracts were washed with brine and dried ($MgSO_4$). The solvent was removed *in vacuo* and the crude product was purified by column chromatography (silica gel/ hexane) to yield a colourless solid. The product was recrystallised (ethanol) and dried (desiccators, P_2O_5) overnight to yield colourless crystals.

Yield = 1.7 g, (77 %).

^{1}H-NMR ($CDCl_3$), δ: 0.89 (3H, t), 1.01 (9H, s), 1.30 (8H, m), 1.65 (2H, quint), 1.75 (2H, t), 2.68 (2H, t), 4.06 (2H, t), 6.90 (3H, d, J = 8.57 Hz), 7.13 (1H, ddd, J = 15.10 Hz, J = 7.55 Hz, J = 1.63 Hz), 7.59 (6H, ddd, J = 27.85 Hz, J = 14.59 Hz, J = 8.46 Hz).

^{13}C-NMR (100 MHz, $CDCl_3$), δ: 14.09, 22.65, 28.78, 29.08, 29.26, 29.75, 29.81, 30.05, 31.77, 42.38, 65.39 (alkyl carbons, 11 required, 11 found); 114.80, 124.10 (dd, J = 3.07 Hz, J = 3.07 Hz), 124.72 (dd, J = 4.61 Hz, J = 4.61 Hz), 126.73, 128.05, 129.15 (d, J = 3.07 Hz), 130.78, 130.91, 132.78, 133.23, 140.34, 147.53 (dd, J = 151.82 Hz, J = 11.90 Hz), 149.96 (dd, J = 145.67 Hz, J = 12.68 Hz), 158.79, (aromatic carbons, 14 required, 14 found).

Transition: (°C) Cr 72 SmC 104 N 118 Iso.

MS: *m/z* 464 (M^+).

Elemental analysis: $C_{31}H_{38}F_2O$ requires C 80.14 %, H 8.24 %; found C 79.97 %, H 8.46 %.

HPLC: 100 %.

Scheme 11

1-Bromo-2,3-difluorobenzene (45)

n-Bromosuccinimide (NBS) (112 g, 0.63 mol) was added to stirred suspension of compound **13** (50 g, 0.32 mol) in acetonitrile (400 ml). The stirred mixture was heated under reflux overnight and then poured into water. The product was extracted into hexane (x2), and the combined organic extracts were washed with sodium metabisulfite and sodium hydrogen carbonate and dried ($MgSO_4$). The compound was filtrated and the solvent was evaporated and distilled at atmosphere pressure to yield a colourless oil.

[bp 158 °C at 760 mm Hg].

Yield = 31.24 g, (51 %).

^{1}H-NMR ($CDCl_3$), δ: 6.98 (1H, dddd), 7.13 (1H, dddd), 7.30 (1H, dddd).

MS *m/z* 192 (M^+), *m/z* 194 (M^+).

1,2-Difluoro-3-(3,3-dimethylbut-1-ynyl)benzene (50)

A solution of *n*-butyllithium (74.8 ml, 2.5 M in hexane, 0,187 mol) was added as dropwise to stirred, cooled (-5 °C or less than -5 °C) solution of compound **46** (15.35 g, 0.187 mol) in (200 ml) anhydrous THF under dry N_2. The mixture was stirred at -5 °C for 15 min and zinc chloride (31.8 g, 0.23 mol) was added, and then the mixture was stirred at room temperature for 1 h. A solution of compound **45** (30 g, 0.15 mol) in anhydrous THF (100 ml) was added followed by $Pd(PPh_3)_4$ tetrakis (triphenylphosphine) palladium(0) (8 g, 6.9 mmol), and the stirred mixture was heated under reflux overnight. The cooled mixture was poured into 10% hydrochloric acid and the product was extracted into ether (x2). The combined ethereal extracts were washed successively with water and then sodium hydrogen carbonate and dried ($MgSO_4$). The solvent was evaporated and the crude product was purified by column chromatography with added hexane to yield a colourless crystals.

Yield = 28 g, (93 %).

^{1}H-NMR ($CDCl_3$), δ: 1.33 (9H, s), 6.96 (1H, dddd), 7.05 (1H, dddd), 7.12 (1H, dddd).

MS *m/z* 194 (M^+).

1,2-Difluoro-3-trimethylsilylethynylbenzene (51)

A solution of *n*-butyllithium (78 ml, 2.5 M in hexane, 0,195 mol) was added as dropwise to stirred, cooled (-5 °C or less than -5 °C) solution of compound **47** (23 g, 0.235 mol) in (200 ml) anhydrous THF under dry N_2. The mixture was stirred at -5 °C for 15 min and zinc chloride (31.8 g, 0.234 mol) was added, and then the mixture was stirred at room temperature for 1 h. A solution of compound **45** (30 g, 0.15 mol) in anhydrous THF (100 ml) was added followed by $Pd(PPh_3)_4$ tetrakis (triphenylphosphine) palladium(0) (8 g, 6.9 mmol), and the stirred mixture was heated under reflux overnight. The cooled mixture was poured into 10% hydrochloric acid and the product was extracted into ether (x2). The combined ethereal extracts were washed successively with water and then sodium hydrogen

carbonate and dried ($MgSO_4$). The solvent was evaporated and the crude product was purified by column chromatography with added hexane to yield a colourless crystals.

Yield = 32.25 g, (32 %).

^{1}H-NMR ($CDCl_3$), δ: 0.25 (9H, s), 6.97 (1H, dddd), 7.10 (1H, dddd), 7.18 (1H, dddd).

MS *m/z* 210 (M^+).

1,2-Difluoro-3-(3,3-dimethylbutyl)benzene (52)

A mixture of compound **50** (27 g, 0.139 mol) and 10% palladium on carbon Pd/C (5 g) in ethanol (400 ml) was hydrogenated at 40 psi overnight. The catalyst was filtered off and the solvent was removed *in vacuo* and the product was distillated to yield a colourless oil.

[bp 80 °C at 15 mm Hg].

Yield = 21 g, (76 %).

^{1}H-NMR ($CDCl_3$), δ: 0.96 (9H, s), 1.48 (2H, t), 2.62 (2H, t), 6.89 – 6.97 (3H, m).

MS *m/z* 198 (M^+).

1,2-difluoro-3-trimethylsilylethylbenzene (53)

A mixture of compound **51** (32.25 g, 0.153 mol) and 10 % palladium on carbon Pd/C (3.5 g) in hexane (400 ml) was hydrogenated at 40 psi overnight. The catalyst was filtered off and the solvent was removed *in vacuo* and the product was distillated to yield a colourless oil.

[bp 80 °C at 15 mm Hg].

Yield = 16.96 g, (52%).

^{1}H-NMR ($CDCl_3$), δ: 0.00 (9H, s), 0.82 (2H, t), 2.63 (2H, t), 6.90 (3H, m).

MS *m/z* 214 (M^+).

1,2-Difluoro-4-(3,3-dimethylbutyl)phenyl boronic acid (54)

n-Butyllithium solution (40 ml, 2.5 M, 0.10 mol) was added dropwise to a stirred, cooled (-78 °C) solution of compound **52** (20 g, 0.10 mol) in anhydrous THF (250 ml) under dry nitrogen. The reaction mixture was stirred at -78 °C for 1 h. After that the trimethyl borate (20.78 g, 0.2 mol) was added as dropwise at -78 °C, and the reaction mixture was allowed to warm to room temperature overnight. 10 % HCl (100 ml) was added and the mixture was stirred at room temperature for around 1 h. The product was extracted into ether (x2), and the combined ethereal extracts were washed with brine and dried ($MgSO_4$). The solvent was evaporated and the solid residue was stirred in hexane, filtered, and air dried under suction to yield a colourless powder.

Yield = 15 g, (62 %).

^{1}H-NMR (D6-DMSO), δ: 0.81 (9H, s), 1.32 (2H, t), 2.41 (2H, quint), 6.95 (1H, ddd), 7.16 (1H, ddd), 8.19 (2H, s).

2,3-Difluoro-4-(2-trimethylsilylethyl)phenyl boronic acid (55)

n-Butyllithium solution (32 ml, 2.5 M, 0.080 mol) was added dropwise to a stirred, cooled (-78 °C) solution of compound **53** (16.96 g, 0.079 mol) in anhydrous THF (250 ml) under dry nitrogen. The reaction mixture was stirred at -78 °C for 1 h. After that the trimethyl borate (11 g, 10.6 mmol) was added as dropwise at -78 °C, and the reaction mixture was allowed to warm to room temperature overnight. 10 % HCl (100 ml) was added and the mixture was stirred at room temperature for around 1 h. The product was extracted into ether (x2), and the combined ethereal extracts were washed with brine and dried ($MgSO_4$). The solvent was evaporated and the solid residue was stirred in hexane, filtered, and air dried under suction to yield a colourless powder.

Yield = 11.33 g, (55 %).

^{1}H-NMR (D6-DMSO), δ: 0.00 (9H, s), 0.81 (2H, t), 2.63 (2H, quint), 5.47 (2H, s), 6.98 (1H, ddd), 7.22 (1H, ddd).

2,3-Difluoro-4-(2-trimethylsilylethyl)-4''-(3-trimethylsilylpropoxy)-[1,1':4',1'']-terphenyl (56)

Compound **55** (1.4g, 5.43 mmol), dissolved in DME (150 ml), was added to a stirred mixture of compound **32** (1.62g, 4.46 mmol), Na_2CO_3 (1.45 g, 0.014 mol), and $Pd(PPh_3)_4$ (0.1 g, 8.66 x 10^{-5} mol) in water (50 ml) under nitrogen. The stirred mixture was heated under reflux overnight. TLC revealed a complete reaction and the mixture was poured into water. The product was extracted into ether (x2) and the combined ethereal extracts were washed with brine and dried ($MgSO_4$). The solvent was removed *in vacuo* and the crude product was purified by column chromatography (silica gel/ hexane) to yield a colourless solid. The crude product was recrystallised (ethanol) and dried (desiccators, P_2O_5) overnight to yield colourless crystals.

Yield: 1.01 g, (46 %).

^{1}H-NMR ($CDCl_3$), δ: - 0.023 (9H, s), 0.005 (9H, s), 0.58 (2H, quint), 0.85 (2H, quint), 1.75 (2H, quint), 2.64 (2H, quint), 3.92 (2H, t), 6.92 (2H, d, J = 8.57 Hz), 6.97 (1H, dd, J = 15.71 Hz, J = 7.8 Hz), 7.00 (1H, dd, J = 14.48 Hz, J = 7.24 Hz), 7.55 (6H, ddd, J = 28.56 Hz, J = 17.54 Hz, J = 8.77 Hz).

^{13}C-NMR (100 MHz, $CDCl_3$), δ: -1.84, -1.73, 12.57, 17.33, 23.07, 23.86, 70.75 (alkyl carbons, 7 required, 7 found); 114.79, 123.93 (dd, J = 4.61 Hz, J = 3.84 Hz), 124.15 (dd, J = 3.07 Hz, J = 3.07 Hz), 126.7, 127.81 (d, J = 9.99 Hz), 128.00, 129.14 (d, J = 2.31 Hz), 132.76, 133.23, 133.34, 140.31, 147.98 (dd, J = 254.01 Hz, J = 15.37 Hz), 149.22 (dd, J = 247.14 Hz, J = 15.37 Hz), 150.19, (aromatic carbons, 14 required, 14 found).

Transition: (°C) Cr 139 Iso.

MS: *m/z* 496 (M^+).

Elemental analysis: $C_{29}H_{38}F_2OSi_2$ requires C 70.11 %, H 7.71 %; found C 70.06 %, H 7.91%.

HPLC: 100 %.

Scheme 12

4-(trans-4-Pentylcyclohexyl)phenyl trifluoromethanesulfonate (58)

Triflic anhydride (42 g, 0.149 mol), was added dropwise to a stirred cooled solution (0 °C) of the compound **57** (30 g, 0.12 mol) in dry pyridine (300 ml) under dry nitrogen. The mixture was stirred at room temperature overnight and poured into water. The product was extracted into ether (x2) and the combined ethereal extracts were washed successively with water, 10 % HCl (x2), brine, and dried ($MgSO_4$). The solvent was removed *in vacuo* to yield colourless solid.

Yield = 44.71 g, (99 %).

^{1}H-NMR ($CDCl_3$), δ: 0.85 (3H, t), 0.92 – 1.10 (2H, m), 1.11 – 1.48 (11H, m), 1.78 – 1.91 (4H, m), 2.48 (1H, m), 7.16 (2H, d), 7.26 (2H, d).

MS *m/z* 378 (M^+).

2,3-Difluoro-4-(4,4-dimethylpentyloxy)-4'-(trans-4-pentylcyclohexyl)biphenyl (59)

Compound **25** (1.8 g, 7.00 mmol), dissolved in DME (100 ml), was added to a stirred mixture of the compound **58** (2 g, 5.29 mmol), Na_2CO_3 (0.75 g, 7.08 mmol), LiCl (0.7 g, 0.0164 mol), and $Pd(PPh_3)_4$ (0.2 g, 0.172 mol) in water (40 ml) under nitrogen. The stirred mixture was heated under reflux overnight. TLC revealed a complete reaction and the mixture was poured into water. The product was extracted into ether (x2) and the combined ethereal extracts were washed with brine and dried ($MgSO_4$). The solvent was removed *in vacuo* and the crude product was purified by column chromatography (silica gel/ hexane) to yield a colourless solid. The product was recrystallised (ethanol) and dried (desiccators, P_2O_5) overnight to yield colourless crystals.

Yield = 1.70 g, (71 %).

^{1}H-NMR ($CDCl_3$), δ: 0.89 (3H, t), 0.92 (9H, s), 1.03 (2H, t), 1.30 (11H, m), 1.48 (2H, m), 1.85 (6H, m), 2.50 (1H, t), 4.02 (2H, t), 6.76 (1H, ddd, J = 16.32 Hz, J = 8.98 Hz, J = 1.63 Hz), 7.08 (1H, ddd, J = 16.93 Hz, J = 10.81 Hz, J = 2.24 Hz), 7.28 (2H, d, J = 8.36 Hz), 7.44 (2H, dd, J = 8.16 Hz, J = 1.43 Hz).

^{13}C-NMR (100 MHz, $CDCl_3$), δ: 14.12, 22.70, 24.60, 26.64, 29.30, 30.16, 32.21, 33.57, 34.28, 37.29, 37.37, 39.89, 44.33, 70.70 (alkyl carbons, 14 required, 14 found); 109.49, 122.90 (d, J = 10.76 Hz), 123.50 (dd, J = 3.84 Hz, J = 3.84 Hz), 127.02, 128.50 (d, J = 3.07 Hz), 132.36, 141.56 (dd, J = 246.75 Hz, J = 14.61 Hz), 147.39, 147.6 (m) 148.83 (dd, J = 249.44 Hz, J = 11.53 Hz), (aromatic carbons, 10 required, 10 found).

Transition: ($^\circ$C) Cr 79 SmA 129 Iso.

MS: *m/z* 456 (M^+)

Elemental analysis: $C_{30}H_{42}F_2O$ requires C 78.91 %, H 9.27 %; found C 78.93 %, H 9.51 %.

HPLC: 99.25 %.

2,3-Difluoro-4-(3-trimethylsilylpropoxy)-4'-(trans-4-pentylcyclohexyl)biphenyl (60)

Compound **26** (1.9 g, 6.60 mmol), dissolved in DME (100 ml), was added to a stirred mixture of the compound **58** (2 g, 5.29 mmol), Na_2CO_3 (0.75 g, 7.08 mmol) LiCl (0.7g, 0.0164 mol), and $Pd(PPh_3)_4$ (0.2 g, 0.172 mmol) in water (40 ml) under nitrogen. The stirred mixture was heated under reflux overnight. TLC revealed a complete reaction and the mixture was poured into water. The product was extracted into ether (x2) and the combined ethereal extracts were washed with brine and dried ($MgSO_4$). The solvent was removed *in vacuo* and the crude product was purified by column chromatography (silica gel/ hexane) to yield a colourless solid. The product was recrystallised (ethanol) and dried (desiccators, P_2O_5) overnight to yield colourless crystals.

Yield = 1.73 g, (69 %).

^{1}H-NMR ($CDCl_3$), δ: 0.0 (9H, s), 0.58 (2H, quint), 0.88 (3H, t), 1.05 (2H, t), 1.25 (9H, m), 1.45 (2H, m), 1.85 (6H, m), 2.45 (1H, t), 4.00 (2H, t), 6.74 (1H, dd, J = 16.52 Hz, J = 9.18 Hz), 7.05 (1H, ddd, J = 17.14 Hz, J = 8.57 Hz, J = 2.65 Hz), 7.25 (2H, d, J = 8.36 Hz), 7.40 (2H, dd, J = 8.16 Hz, J = 1.43 Hz).

^{13}C-NMR (100 MHz, $CDCl_3$), δ: -1.77, 12.36, 14.12, 22.70, 23.70, 26.60, 32.20, 33.57, 34.20, 37.20, 37.30, 44.30, 72.40 (alkyl carbons, 13 required, 13 found); 109.48, 122.90 (d, J = 10.76 Hz), 123.50 (dd, J = 4.61 Hz, J = 4.61 Hz), 127.02, 128.50 (d, J = 3.07 Hz), 132.36, 141.76 (dd, J = 247.14 Hz, J = 15.37 Hz), 147.38, 147.60 (m) 148.80 (dd, J = 247.52 Hz, J = 10.76 Hz), (aromatic carbons, 10 required, 10 found).

Transition: ($^\circ$C) Cr 73 SmA 125 Iso.

MS: *m/z* 472 (M^+).

Elemental analysis: $C_{29}H_{42}F_2OSi$ requires C 73.68 %, H 8.96 %; found C 73.74 %, H 9.14 %.

HPLC: 99. 1 %.

Scheme 13

4-(Benzyloxy)-4'-(trans-4-pentylcyclohexyl)-biphenyl (62)

Compound **61** (7 g, 0.031 mol), dissolved in DME (250 ml), was added to a stirred mixture of the compound **58** (9.2 g, 0.0243 mol) , Na_2CO_3 (3.4 g, 0.0321 mol), LiCl (3.2 g, 0.075 mol) and $Pd(PPh_3)_4$ (0.68 g, $5.9x10^{-5}$ mol) in water (100 ml) under nitrogen. The stirred mixture was heated under reflux overnight. TLC revealed a complete reaction and the mixture was poured into water. The product was extracted into ether (x2) and the combined ethereal extracts were washed with brine and dried ($MgSO_4$). The solvent was removed *in vacuo* and the crude product was purified by column chromatography (silica gel/ hexane/ 10% DCM) to yield a colourless solid.

Yield = 5.07 g, (51 %).

^{1}H-NMR ($CDCl_3$), δ: 0.89 (3H, t), 1.00 – 1.10 (2H, m), 1.18 – 1.38 (9H, m), 1.40 – 1.54 (2H, m), 1.82 – 1.95 (4H, m), 2.48 (1H, tt), 7.03 (2H, d), 7.24 (2H, d), 7.33 (1H, tt), 7.38 (2H, t), 7.42 – 7.52 (6H, m).

MS *m/z* 412 (M^+).

4-Hydroxy-4'-(trans-4-Pentylcyclohexyl)-biphenyl (63)

A mixture of compound **62** (5.07 g, 0.0123 mol) and 10 % palladium on carbon Pd/C (5 g) in THF (300 ml) was hydrogenated at 40 psi overnight. The catalyst was filtered off and the solvent was removed *in vacuo* to yield a colourless oil.

Yield = 3.6 g, (91 %).

^{1}H-NMR ($CDCl_3$), δ: 0.90 (3H, t), 1.00 – 1.10 (2H, m), 1.20 – 1.40 (11H, m), 1.40 – 1.50 (2H, m), 1.80 – 2.00 (4H, m), 2.51 (1H, tt), 4.75 (1H, s), 6.88 (2H, d), 7.25 (2H, d), 7.42 – 7.47 (4H, m).

MS *m/z* 322 (M^+).

4'-(trans-4-Pentylcyclohexyl)-biphenyl-4-yl trifluoromethanesulfonate (64)

Triflic anhydride (5 g, 0.1773 mol), was added dropwise to a stirred cooled solution (0 °C) of compound **63** (3.6 g, 0.0112 mol) in dry pyridine (50 ml) under dry nitrogen. The mixture was stirred at room temperature overnight and poured into water. The product was extracted into ether (x2) and the combined ethereal extracts were washed successively with water, 10% HCl (x2), brine, and dried ($MgSO_4$). The solvent was removed *in vacuo* to yield colourless solid.

Yield = 5 g, (98 %).

^{1}H-NMR ($CDCl_3$), δ: 0.90 (3H, t), 1.00 – 1.10 (2H, m), 1.20 – 1.40 (11H, m), 1.40 – 1.50 (2H, m), 1.80 – 2.00 (4H, m), 2.51 (1H, tt), 7.28 (2H, d), 7.32 (2H, d), 7.47 (2H, d), 7.63 (2H, d).

MS *m/z* 454 (M^+).

2,3-Difluoro-4-(4,4-dimethylpentyloxy)-4''-(trans-4-pentylcyclohexyl)-[1,1':4',1'']-terphenyl (65)

Compound **25** (1.35 g, 5.0 mmol), dissolved in DME (100 ml), was added to a stirred mixture of the compound **64** (1.95 g, 4.14 mmol), Na_2CO_3 (1.6 g, 1.51 mmol), LiCl (0.53 g, 0.0125 mol), and $Pd(PPh_3)_4$ (0.2 g, 0.172 mmol) in water (40 ml) under nitrogen. The stirred mixture was heated under reflux overnight. TLC revealed a complete reaction and the mixture was poured into water. The product was extracted into ether (x2) and the combined ethereal extracts were washed with brine and dried ($MgSO_4$). The solvent was removed *in vacuo* and the crude product was purified by column chromatography (silica gel/ hexane) to yield a colourless solid. The product was recrystallised (ethanol) and dried (desiccators, P_2O_5) overnight to yield colourless crystals.

Yield = 1.37 g, (68 %).

^{1}H-NMR ($CDCl_3$), δ: 0.89 (3H, t), 0.92 (9H, s), 1.30 (11H, m), 1.50 (2H, t), 1. 90 (6H, m), 2.56 (1H, t), 4.00 (2H, t), 6.83 (1H, dd, J = 16.32 Hz, J = 7.34 Hz), 7.15 (1H, dd, J = 16.9 Hz, J = 10.6 Hz), 7.30 (2H, d, J = 8.36 Hz), 7.56 (4H, d, J = 8.16 Hz), 7.66 (2H, d, J = 8.16 Hz).

^{13}C-NMR (100 MHz, CDCl3), δ: 14.12, 22.70, 24.59, 26.65, 29.30, 30.17, 32.21, 33.59, 34.30, 37.30, 37.38, 39.89, 44.30, 70.71, (alkyl carbons, 14 required, 14 found); 109.52, 122.80, 122.90, 123.46 (dd, J = 4.61 Hz, J = 3.85 Hz), 126.93, 127.08, 127.32, 129.00 (d, J = 3.07 Hz), 133.51, 138.05, 140.38, 144.50 (dd, J = 15.37 Hz, J = (m)), 146.57 (dd, J = 715.66 Hz, J = 13.50 Hz), 147.20 (aromatic carbons, 14 required, 14 found).

Transition: ($^\circ$C) Cr 138 SmC 169.7 SmA 270 Iso.

MS: *m/z* 532 (M^+).

Elemental analysis: $C_{36}H_{46}F_2O$ requires C 81.16 %, H 8.70 %; found C 81.21 %, H 8.97 %.

HPLC: 99.13 %.

2,3-difluoro-4-(3-trimethylsilylpropoxy)-4''(trans-4-pentylcyclohexyl)-[1,1':4',1''-terphenyl (66)

Compound **26** (1.4 g, 5.0 mmol), dissolved in DME (100 ml), was added to a stirred mixture of the compound **64** (1.9 g, 4.0 mmol), Na_2CO_3 (1.6 g, 1.51 mmol), LiCl (0.51 g, 0.012 mol), and $Pd(PPh_3)_4$ (0.2 g, 0.172 mmol) in water (40 ml) under nitrogen. The stirred mixture was heated under reflux overnight. TLC revealed a complete reaction and the mixture was poured into water. The product was extracted into ether (x2) and the combined ethereal extracts were washed with brine and dried ($MgSO_4$). The solvent was removed *in vacuo* and the crude product was purified by column chromatography (silica gel/ hexane) to yield a colourless solid. The product was recrystallised (ethanol) and dried (desiccators, P_2O_5) overnight to yield colourless crystals.

Yield = 1.53 g, (70 %).

^{1}H-NMR ($CDCl_3$), δ: 0.00 (9H, s), 0.55 (2H, quint), 0.85 (3H, t), 1.10 (2H, t), 1. 30 (9H, m), 1.85 (6H, m), 2.45 (1H, t), 4.00 (2H, t), 6.80 (1H, ddd, J = 18.16 Hz, J = 9.18 Hz, J = 1.84 Hz), 7.10 (1H, ddd, J = 16.93 Hz, J = 10.81 Hz, J = 2.24 Hz), 7.27 (2H, d, J = 8.36 Hz), 7.53 (4H, dd, J = 8.16 Hz, J = 1.84 Hz), 7.62 (2H, d, J = 8.16 Hz).

^{13}C-NMR (100 MHz, $CDCl_3$), δ: 2.76, 16.9, 18.66, 27.26, 28.31, 31.19, 36.70, 38.13, 38.86, 41.80, 41.90, 48.80, 77.00 (alkyl carbons, 13 required, 13 found); 114.10, 127.00, 127.20, 128.03 (dd, J = 3.85 Hz, J = 3.85 Hz), 131.47, 131.62, 131.85, 133.5 (d, J = 3.07 Hz), 138.06, 142.60, 144.92, 151.82, 153.5 (dd, J = 250.6 Hz, J = 12.68), 153.59 (dd, J = 250.6 Hz, J = 11.9 Hz), 159.13, (aromatic carbons, 14 required, 14 found).

Transition: ($^\circ$C) Cr 136 SmC 169.3 SmA 255 Iso.

MS: *m/z* 548 (M^+).

Elemental analysis: $C_{35}H_{46}F_2OSi$ requires C 76.60 %, H 8.45 %; found C 76.77 %, H 8.64 %.

HPLC: 99.93 %.

Scheme 14

2,3-difluoro-4'-(trans-4-pentylcyclohexyl)biphenyl (67)

Compound **13** (7.31 g, 0.0463 mol), dissolved in DME (250 ml), was added to a stirred mixture of the compound **58** (14 g, 0.037 mol), Na_2 CO_3 (14.7 g, 0.139 mol) LiCl (4.72 g, 0.111 mol), and $Pd(PPh_3)_4$ (1.5 g, 1.3 mmol) in water (150 ml) under nitrogen. The stirred mixture was heated under reflux overnight. TLC revealed a complete reaction and the mixture was poured into water. The product was extracted into ether (x2) and the combined ethereal extracts were washed with brine and dried ($MgSO_4$). The solvent was removed *in vacuo* and the crude product was purified by column chromatography (silica gel/ hexane) to yield a colourless solid. The product was recrystallised (ethanol) and dried (desiccators, P_2O_5) overnight to yield colourless crystals.

Yield = 12.44 g, (99 %).

^{1}H-NMR ($CDCl_3$), δ: 0.90 (3H, t), 1.05 (2H, t), 1.27 (9H, m), 1.46 (2H, t), 1.89 (4H, t), 2.50 (1H, t), 7.09 (2H, m), 7.15 (1H, m), 7.28 (2H, d), 7.58 (4H, m), 7.45 (2H, ddd).

MS: *m/z* 342 (M^+).

(2,3-difluoro-4'-(trans-4-pentylcyclohexyl)biphenyl-4-yl boronic acid (68)

n-Butyllithium solution (16 ml, 2.5 M, 0.04 mol) was added dropwise to a stirred, cooled (-78 °C) solution of compound **67** (12.44 g, 0.0361 mol) in dry THF (350 ml) under dry nitrogen. The reaction mixture was stirred at (-78 °C) for almost 1 h. Trimethyl borate (6 g, 0.058 mol) was added dropwise at -78 °C, and the reaction mixture was allowed to warm to room temperature overnight. 10 % HCl (100 ml) was added and the mixture was stirred at room temperature for around 1 h. The product was extracted into ether (x2), and the combined ethereal extracts were washed with brine and dried ($MgSO_4$). The solvent was removed *in vacuo* and the solid residue was stirred in hexane, filtered, and air dried under suction to yield a colourless powder.

Yield: 8.43 g, (61 %).

^{1}H-NMR (D6-DMSO), δ: 0.85 (2H, t), 1.20 (2H, t), 1.25 (10H, m), 1.44 (2H, q), 1.82 (4H, d), 7.27 (1H, t), 7.36 (3H, ddd), 7.47 (2H, d), 8.42 (2H, s).

2',3'-Difluoro-4-(dimethylpentyloxy)-4''-(trans-4-pentylcyclohexyl)-[1,1':4',1''-terphenyl(69)

Compound **68** (1.95 g, 5.1 mmol), dissolved in DME (100 ml), was added to a stirred mixture of the compound **18** (1.13 g, 4.2 mmol), Na_2CO_3 (1.6 g, 1.51 mol) and $Pd(PPh_3)_4$ (0.2 g, 0.172 mmol) in water (40 ml) under nitrogen. The stirred mixture was heated under reflux overnight. TLC revealed a complete reaction and the mixture was poured into water. The product was extracted into ether (x2) and the combined ethereal extracts were washed with brine and dried ($MgSO_4$). The solvent was removed *in vacuo* and the crude product was purified by column chromatography (silica gel/ hexane) to yield a colourless solid. The product was recrystallised (ethanol) and dried (desiccators, P_2O_5) overnight to yield colourless crystals.

Yield = 1.6 g, (72 %).

^{1}H-NMR ($CDCl_3$), δ: 0.89 (3H, t), 0.91 (9H, s), 1.03 (2H, t), 1.30 (11H, m), 1. 50 (2H, m), 1.80 (2H, quint), 1.91 (4H, t), 2.52 (1H, t), 4.00 (2H, t), 6.90 (2H, d, J = 8.57 Hz), 7.23 (2H, d, J = 6.53 Hz), 7.33 (2H, d, J = 8.36 Hz), 7.52 (4H, d, J = 8.57 Hz).

^{13}C-NMR (100 MHz, CDCl3), δ: 14.12, 22.72, 24.65, 26.65, 29.33, 30.17, 32.21, 33.57, 34.27, 37.30, 37.38, 40.14, 44.39, 68.92 (alkyl carbons, 14 required, 14 found); 114.59, 124.30 (dd, J = 3.07 Hz, J = 3.07 Hz), 124.50 (dd, J = 3.84 Hz, J = 3.84 Hz), 126.83, 127.11, 128.72 (d, J = 3.07 Hz), 129.12 (d, J = 6.92 Hz), 129.24 (d, J = 6.92 Hz), 129.9 (d, J = 3.07 Hz), 132.18, 147.92, 148.37 (dd, J = 250.6 Hz, J = 12.68), 148.54 (dd, J = 250.6 Hz, J = 11.9 Hz), 159.13, (aromatic carbons, 14 required, 14 found).

Transition: (°C) Cr 119 SmC 227 N 253 Iso.

MS: *m/z* 532 (M^+).

Elemental analysis: $C_{36}H_{46}F_2O$ requires C 81.46 %, H 8.70 %; found C 76.71 %, H 8.99 %.

HPLC: 99.89 %.

2',3'-Difluoro-4-(3-trimethylsilylpropoxy)-4''-(trans-4-pentylcyclohexyl-[1,1':4',1''-terphenyl (70)

Compound **68** (1.86 g, 5.0 mmol), dissolved in DME (100 ml), was added to a stirred mixture of the compound **19** (1.15 g, 4.0 mmol), Na_2CO_3 (1.6 g, 1.51 mmol) and $Pd(PPh_3)_4$ (0.2 g, 0.172 mmol) in water (40 ml) under nitrogen. The stirred mixture was heated under reflux overnight. TLC revealed a complete reaction and the mixture was poured into water. The product was extracted into ether (x2) and the combined ethereal extracts were washed with brine and dried by magnesium sulfate. The solvent was removed *in vacuo* and the crude product was purified by column chromatography (silica gel/ hexane) to yield a colourless solid. The product was recrystallised (ethanol) and dried (desiccators, P_2O_5) overnight to yield colourless crystals.

Yield = 1.41 g, (65 %).

^{1}H-NMR ($CDCl_3$), δ: 0.00 (9H, s), 0.58 (2H, quint), 0.87 (3H, t), 1.22 (2H, t), 1.25 (9H, m), 1.45 (2H, m), 1.83 (6H, m), 2.50 (1H, t), 3.99 (2H, t), 6.95 (2H, d, J = 8.77 Hz), 7.18 (2H, d, J = 6.53 Hz), 7.28 (2H, d, J = 8.36 Hz), 7.48 (4H, d, J = 8.36 Hz).

^{13}C-NMR (100 MHz, $CDCl_3$), δ: -1.73, 12.57, 14.12, 22.7, 23.85, 26.66, 32.21, 33.57, 34.27, 37.3, 37.38, 44.38, 70.75 (alkyl carbons, 13 required, 13 found); 114.59, 124.3 (dd, J = 3.84 Hz, J = 3.84 Hz), 124.5 (dd, J = 3.84 Hz, J = 3.84 Hz), 126.81, 127.11, 128.72 (d, J = 3.07 Hz), 129.13 (d, J = 7.69 Hz), 129.24 (d, J = 7.69 Hz), 129.9 (d, J = 3.07 Hz), 132.17, 147.92, 148.37 (dd, J = 250.98 Hz, J = 12.68),

148.54 (dd, J = 250.98 Hz, J = 11.9 Hz), 159.1, (aromatic carbons, 14 required, 14 found).

Transition: ($^{\circ}$C) Cr 94 SmC 223 N 235 Iso.

MS: *m/z* 548 (M^{+}).

Elemental analysis: $C_{35}H_{46}F_2OSi$ requires C 76.60 %, H 8.45 %; found C 76.71 %, H 8.67 %.

HPLC: 99.96 %.

Scheme 15

2,3-difluoro-4-(2-trimethylsilylethyl)-4''-(trans-4-pentylcyclohexyl)-[1,1':4',1'']-terphenyl (71)

Compound **55** (1.08 g, 4.2 mmol), dissolved in DME (100 ml), was added to a stirred mixture of the compound **64** (1.64 g, 3.5 mmol), Na_2CO_3 (1.33 g, 1.25 mol), LiCl (0.45 g, 10.6 mol) and $Pd(PPh_3)_4$ (0.2 g, 0.172 mol) in water (40 ml) under nitrogen. The stirred mixture was heated under reflux overnight. TLC revealed a complete reaction and the mixture was poured into water. The product was extracted into ether (x2) and the combined ethereal extracts were washed with brine and dried ($MgSO_4$). The solvent was removed *in vacuo* and the crude product was purified by column chromatography (silica gel/ hexane) to yield a colourless solid. The product was recrystallised (ethanol) and dried (desiccators, P_2O_5) overnight to yield colourless crystals.

Yield = 1.2 g, (66 %).

^{1}H-NMR (CDC_{l3}), δ: - 0.15 (1H, s), 0.00 (9H, s), 0.85 (5H, m), 1.00 (2H, m), 1. 25 (9H, m), 1.42 (2H, m), 1.85 (4H, t), 2.48 (1H,t), 2.64 (2H, quint), 6.97 (1H, dd, J = 14.28 Hz, J = 6.32 Hz), 7.09 (1H, dd, J = 14.28 Hz, J = 7.14 Hz), 7.25 (2H, d, J = 8.36 Hz), 7.502 (2H, d, J = 8.16 Hz), 7.54 (2H, d, J = 7.34 Hz), 7.60 (2H, d, J = 8.16).

^{13}C-NMR (100 MHz, $CDCl_3$), δ: -1.80, 14.12, 17.34, 22.72, 23.08, 26.65, 32.21, 33.59, 34.32, 37.31, 37.39, 44.30 (alkyl carbons, 12 required, 12 found); 123.95 (dd, J = 4.61 Hz, J = 4.61 Hz), 124.20 (dd, J = 3.07 Hz, J = 3.07 Hz), 127.00 (d, J = 10.76 Hz), 127.32, 127.80 (d, J = 9.22 Hz), 129.12 (d, J = 2.31 Hz), 133.30, 133.40, 133.50, 138.05, 140.63, 147.31, 147.90 (dd, J = 250.98 Hz, J = 15.50 Hz), 149.2 (dd, J = 247.52 Hz, J = 14.16 Hz), (aromatic carbons, 14 required, 14 found).

Transition: (°C) Cr 72 SmC 167.5 SmA 251 Iso.

MS: *m/z* 518 (M^+).

Elemental analysis: $C_{34}H_{44}F_2Si$ requires C 78.71 %, H 8.55 %; found C 78.99 %, H 8.74 %.

HPLC: 99.20 %.

Scheme 16

4-(tert-Butyl)-2',3'-difluoro-4''-heptyl-[1,1':4',1'']-terphenyl (73)

Compound **16** (2.15 g, 6.48 mmol), dissolved in DME (150 ml), was added to a stirred mixture of the compound **72** (1.15 g, 5.40 mmol), Na_2CO_3 (1.72 g, 0.016 mol), and $Pd(PPh_3)_4$ (0.18 g, 0.156 mmol) in water (50 ml) under nitrogen. The stirred mixture was heated under reflux overnight. TLC revealed a complete reaction and the mixture was poured into water. The product was extracted into ether (x2) and the combined ethereal extracts were washed with brine and dried ($MgSO_4$). The solvent was removed *in vacuo* and the crude product was purified by column chromatography (silica gel/ hexane) to yield a colourless solid. The product was recrystallised (ethanol) and dried (desiccators, P_2O_5) overnight to yield colourless crystals.

Yield = 1.58 g, (70 %).

Transition: (°C) Cr 56 Iso.

^{1}H-NMR ($CDCl_3$), δ: 0.88 (3H, t), 1.20 – 1.40 (17H, m), 1.68 (2H, quint), 2.65 (2H, t), 7.22 – 7.35 (5H, m), 7.45 – 7.60 (5H, m).

^{13}C-NMR (100 MHz, $CDCl_3$), δ: 14.11, 22.68, 29.20, 29.35, 31.28, 31.43, 31.82, 34.64, 35.73 (alkyl carbons, 9 requird, 9 found); 115.67 (d, J = 17.68 Hz), 123.9, 124.5, 125.21, 125.57, 128.52, 128.6 (m), 129.31, 129.45, 131.86 (d, J = 18.45 Hz), 143.08, 148.43 (dd, J = 250.60 Hz, J = 3.84 Hz), 148.58 (dd, J = 250.98 Hz, J = 4.22 Hz), (aromatic carbons, 14 required, 14 found).

MS: *m/z* 420 (M^+).

Elemental analysis: $C_{29}H_{34}F_2$ requires C 82.82 %, H 8.15 %; found C 81.03 %, H 8.36 %.

HPLC: 100 %.

Scheme 17

1-Bromo-4-octyloxybenzene (75)

A stirred mixture of compound **17** (20 g, 0.116mol), 1-bromooctane **74** (20 g, 0.104mol) and potassium carbonate (48 g, 0.35 mol) in butanone (250 ml) was heated under reflux overnight. The potassium carbonate is filtered off and the solvent was removed *in vacuo*. The product was purified by column chromatography (silica gel) with hexane to yield a colourless oil.

Yield = 29.53 g, (90 %).

^{1}H-NMR ($CDCl_3$), δ: 0.90 (3H, t), 1.45 (10H, m), 1.80 (2H, quint), 3.90 (2H, t), 6.80 (2H, d), 7.20 (2H, d).

MS: *m/z* 484 (M^+), *m/z* 486 (M^+).

2,3-Difluoro-4'-octyloxy-biphenyl (76)

Compound **13** (20 g, 0.127 mol), dissolved in DME (250 ml), was added to a stirred mixture of compound **75** (29.53 g, 0.104 mol), Na_2CO_3 (33 g, 0.311 mol), and $Pd(PPh_3)_4$ (2 g, 1.73 mmol) in water (200 ml) under nitrogen. The stirred mixture was heated under reflux overnight. TLC revealed a complete reaction and the mixture was poured into water. The product was extracted into ether (x2) and the combined ethereal extracts were washed with brine and dried ($MgSO_4$). The solvent was removed *in vacuo* and the crude product was purified by column chromatography (silica gel/ hexane) to yield a colourless solid.

Yield = 29.64 g, (90 %).

^{1}H-NMR ($CDCl_3$), δ: 0.89 (3H, t), 1.30 (8H, m), 1.50 (2H, quint), 1.80 (2H, quint), 4.00 (2H, t), 6.95 (2H, dd), 7.08 (2H, ddd), 7.22 (1H, ddd), 7.49 (2H, dd).

MS: *m/z* 318 (M^+)

(2,3-Difluoro-4'-(octyloxy)-[1,1'-biphenyl]-4-yl)boronic acid (77)

n-Butyllithium solution (20 ml, 2.5 M, 0.05 mol) was added dropwise to a stirred, cooled (-78 °C) solution of the compound **76** (15 g, 0.047 mol) in anhydrous THF (400 ml) under dry nitrogen. The reaction mixture was stirred at (-78 °C) for almost 1 h. Trimethyl borate (7.4 g, 0.071 mol) was added dropwise at -78 °C, and the reaction mixture was allowed to warm to room temperature overnight. 10 % HCl (100 ml) was added and the mixture was stirred at room temperature for around 1 h. The product was extracted into ether (x2), and the combined ethereal extracts were washed with brine and dried ($MgSO_4$). The solvent was removed *in vacuo* and the solid residue was stirred in hexane, filtered, and air dried under suction to yield a colourless powder.

Yield = 7.34 g, (43 %).

^{1}H-NMR (D6-DMSO), δ: 0.87 (3H, t), 1.20 – 1.35 (8H, m), 1.40 (2H, quint), 1.75 (2H, quint), 4.00 (2H, t), 7.05 (2H, d), 7.24 -7.42 (3H, m), 7.50 (2H, dd).

4-(tert-Butyl)-2',3'-difluoro-4''-octyloxy-[1,1':4',1'']-terphenyl (78)

Compound **77** (2.15 g, 5.94 mmol), dissolved in DME (150 ml), was added to a stirred mixture of the compound **72** (1.05 g, 4.93 mmol), Na_2CO_3 (1.9 g, 0.01 mol), and $Pd(PPh_3)_4$ (0.18 g, 0.156 m mol) in water (50 ml) under nitrogen. The stirred mixture was heated under reflux overnight. TLC revealed a complete reaction and the mixture was poured into water. The product was extracted into ether (x2) and the combined ethereal extracts were washed with brine and dried ($MgSO_4$). The solvent was removed *in vacuo* and the crude product was purified by column chromatography (silica gel/ hexane) to yield a colourless solid. The product was recrystallised (ethanol) and dried (desiccators, P_2O_5) overnight to yield colourless crystals, 0.93 g. Failed, found to be compound **77**.

Scheme 18

2',3'-Difluoro-4-heptyl-4'-hydroxybiphenyl (79)

Compound **35** (19.38 g, 0.076 mol), dissolved in DME (200 ml), was added to a stirred mixture of the compound **17** (9.82 g, 0.057 mol), KF (13.2 g, 0.23 mol), and $Pd(PPh_3)_4$ (1 g, $8.66x10^{-5}$ mol) under nitrogen. The stirred mixture was heated under reflux overnight. TLC revealed a complete reaction and the mixture was poured into water. The product was extracted into ether (x2) and the combined ethereal extracts were washed with brine and dried ($MgSO_4$). The solvent was removed *in vacuo* and the crude product was purified by column chromatography (silica gel/ hexane) to yield a colourless solid.

Yield = 13.13 g, (75 %).

^{1}H-NMR ($CDCl_3$), δ: 0.90 (3H, t), 1.50 (8H, m), 1.80 (2H, quint), 2.80 (2H, t), 4.95 (1H, s), 6.90 (2H, dd), 6.95 (1H, ddd), 7.05 (1H, ddd), 7.42 (2H, dd).

MS: *m/z* 306 (M^+).

2,3-Difluoro-4-heptylbiphenyl-4'-yl trifluoromethanesulfonate (80)

Triflic anhydride (15 g, 0.053 mol), was added dropwise to a stirred cooled solution (0 °C) of the compound **79** (13.13 g, 0.012 mol) in dry pyridine (100 ml) under dry nitrogen. The mixture was stirred at room temperature overnight and poured into water. The product was extracted into ether (x2) and the combined ethereal extracts were washed successively with water, 10 % HCl (x2), brine, and dried ($MgSO_4$). The solvent was removed *in vacuo* to yield colourless solid.

Yield = 18.8 g, (100 %).

^{1}H-NMR ($CDCl_3$), δ: 0.90 (3H, t), 1.50 (8H, m), 1.80 (2H, quint), 2.80 (2H, t), 7.02 (1H, ddd), 7.08 (1H, ddd), 7.35 (2H, d), 7.60 (2H, dd).

MS: *m/z* 438 (M^+).

4-tert-Butylphenyl boronic acid (81)

10 Drops of 1,2-dibromoethane was added to a stirred, mixture of Mg (6 g, 0.27 mol) in THF (120 ml) under dry nitrogen. The reaction mixture was stirred. After that the half amount of the compound **72** (25 g, 0.115 mol) was added to stirred in THF (400 ml) as dropwise and using the heat gun to heat the reaction. Then the another half of the compound **72** (25 g, 0.115 mol) was added also dropwise. Then , cooled (-78 °C) and trimethyl borate (43 g, 0.41 mol) was added as dropwise, and the reaction mixture was allowed to warm to room temperature overnight. 10 % HCl (100 ml) was added and the mixture was stirred at room temperature for around 1 h. The product was extracted into ether (x2), and the combined ethereal extracts were washed with brine and dried ($MgSO_4$). The solvent was removed *in vacuo* and the solid residue was stirred in hexane, filtered, and air dried under suction to yield a colourless powder.

Yield = 36.97 g, (90 %).

^{1}H-NMR (D6-DMSO), δ: 1.27 (9H, s), 7.34 (2H, d), 7.71 (2H, d), 7.95 (2H, s).

4''-(tert-Butyl)-2,3-difluoro-4-heptyl-[1,1':4',1'']-terphenyl (82)

Compound **81** (1.15 g, 6.46 mmol), dissolved in DME (150 ml), was added to a stirred mixture of the compound **80** (2.30 g, 5.25 mmol), LiCl (0.65 g, 0.015 mol), Na_2CO_3 (2.05 g, 0.02 mol), and $Pd(PPh_3)_4$ (0.18 g, 0.156 mmol) in water (50 ml) under nitrogen. The stirred mixture was heated under reflux overnight. TLC revealed a complete reaction and the mixture was poured into water. The product was extracted into ether (x2) and the combined ethereal extracts were washed with brine and dried ($MgSO_4$). The solvent was removed *in vacuo* and the crude product was purified by column chromatography (silica gel/ hexane) to yield a colourless solid. The product was recrystallised (ethanol) and dried (desiccators, P_2O_5) overnight to yield colourless crystal.

Yield = 1.84 g, (84 %).

^{1}H-NMR ($CDCl_3$), δ: 0.89 (3H, t), 1.29 (8H, m), 1.37 (9H, s), 1.63 (2H, quint), 2.69 (2H, t), 7.0 (1H, ddd, J = 14.69 Hz, J = 7.34 Hz, J = 1.225 Hz), 7.15 (1H, ddd, J = 14.99 Hz, J = 6.83 Hz, J = 1.735 Hz), 7.48 (2H, dd, J = 6.43 Hz, J = 1.94 Hz), 7.59 (4H, ddd, J = 14.28 Hz, J = 7.14 Hz, J = 1.835 Hz), 7.00 (2H, dd, J = 6.43 Hz, J = 1.94 Hz).

^{13}C-NMR (100 MHz, $CDCl_3$), δ: 14.09, 22.65, 28.7, 29.08, 29.26, 30.04, 31.30, 31.70, 34.55, (alkyl carbons, 9 required, 9 found); 124.13 (dd, J = 3.07 Hz, J = 3.07 Hz), 124.73 (dd, J = 4.61 Hz, J = 3.84 Hz), 125.78, 126.71, 127.07, 127.95 (d, J = 10.76 Hz), 129.15 (d, J = 3.07 Hz), 130.91 (d, J = 13.84 Hz), 133.64, 137.64, 140.52, 146.87 (dd, J = 150.67 Hz, J = 10.76 Hz), 149.50 (dd, J = 143.75 Hz, J = 10.76 Hz), 150.51, (aromatic carbons, 14 required, 14 found).

Transition: ($^\circ$C) Cr 90 Iso.

MS: *m/z* 420 (M^+).

Elemental analysis: $C_{29}H_{34}F_2$ requires C 82.82 %, H 8.15 %; found C 82.52 %, H 8.26 %.

HPLC: 100 %.

Scheme 19

1,2-Difluoro-3-octyloxybenzene (83)

A stirred mixture of compound **22** (30 g, 0.23 mol), compound **74** (39 g, 0.20 mol) and potassium carbonate (80 g, 0.58 mol) in butanone (250 ml) was heated under reflux overnight. The potassium carbonate was filtered off and the solvent was removed *in vacuo* from the isolated filtrate.

Yield = 44.98 g, (93 %).

^{1}H-NMR ($CDCl_3$), δ: 0.85 (3H, t), 1.50 (10H, m), 1.80 (2H, m), 4.00 (2H, t), 6.70 (2H, dddd), 6.95 (1H, dddd).

MS: *m/z* 242 (M^+).

2,3-Difluoro-4-octyloxyphenylboronic acid (84)

n-Butyllithium solution (40 ml, 2.5 M, 0.10 mol) was added dropwise to a stirred, cooled (-78 °C) solution of the compound **83** (22 g, 0.091 mol) in anhydrous THF (400 ml) under dry nitrogen. The reaction mixture was stirred at (-78 °C) for almost 1 h. Trimethyl borate (14.4 g, 0.14 mol) was added dropwise at -78 °C, and the reaction mixture was allowed to warm to room temperature overnight. 10 % HCl (100 ml) was added and the mixture was stirred at room temperature for around 1 h. The product was extracted into ether (x2), and the combined ethereal extracts were washed with brine and dried ($MgSO_4$). The solvent was removed *in vacuo* and the solid residue was stirred in hexane, filtered, and air dried under suction to yield a colourless powder.

Yield = 7.5 g, (29 %).

^{1}H-NMR (D6-DMSO), δ: 0.85 (2H, t), 1.36 (9H, m), 1.72 (1H, quint), 2.50 (3H, s), 4.10 (2H,t), 6.95 (1H, ddd), 7.30 (1H, ddd), 8.17 (2H, s).

2,3-Difluoro-4'-hydroxy-4-octyloxybiphenyl (85)

Compound **84** (7.50 g, 0.026 mol), dissolved in DME (200 ml), was added to a stirred mixture of compound **17** (3.63 g, 0.021 mol), KF (4.5 g, 0.078 mol), and $Pd(PPh_3)_4$ (1 g, $8.66x10^{-5}$ mol) under nitrogen. The stirred mixture was heated under reflux overnight. TLC revealed a complete reaction and the mixture was poured into water. The product was extracted into ether (x2) and the combined ethereal extracts were washed with brine and dried ($MgSO_4$). The solvent was removed *in vacuo* and the crude product was purified by column chromatography (silica gel/ hexane) to yield a colourless solid.

Yield = 3.91 g (56 %).

^{1}H-NMR ($CDCl_3$), δ: 0.89 (3H, t), 1.32 (8H, m), 1.80 (2H, q), 1.83 (2H, quint), 4.05 (2H, t), 4.77 (1H, s), 6.77 (1H, ddd), 6.88 (2H, dd) , 7.20 (1H, ddd), 7.38 (2H, dd).

MS: *m/z* 334 (M^+).

2,3-Difluoro-4-octyloxy-biphenyl-4'-yl trifluoromethanesulfonate (86)

Triflic anhydride (3.8 g, 0.023 mol), was added dropwise to a stirred cooled solution (0 °C) of the compound **85** (3.91 g, 0.012 mol) in dry pyridine (60 ml) under dry nitrogen. The mixture was stirred at room temperature overnight and poured into water. The product was extracted into ether (x2) and the combined ethereal extracts were washed successively with water, 10 % HCl (x2), brine, and dried ($MgSO_4$). The solvent was removed *in vacuo* to yield colourless solid.

Yield = 3.88 g, (69 %).

^{1}H-NMR ($CDCl_3$), δ: 0.90 (3H, t), 1.50 (10H, m), 1.84 (2H, quint), 4.06 (2H, t), 6.80 (1H, ddd), 7.2 (1H, ddd), 7.35 (2H, dd), 7.60 (2H, dd).

MS: *m/z* 466 (M^+).

4''-tert-Butyl-2,3-difluoro-4-octyloxy-[1,1':4',1'']-terphenyl (87)

Compound **81** (1.05 g, 5.9 mmol), dissolved in DME (150 ml), was added to a stirred mixture of the compound **86** (2.28 g, 4.89 mmol), LiCl (0.65 g, 0.015 mol), Na_2CO_3 (1.9 g, 0.018 mol), and $Pd(PPh_3)_4$ (0.18 g, 0.156 mmol) in water (50 ml) under nitrogen. The stirred mixture was heated under reflux overnight. TLC revealed a complete reaction and the mixture was poured into water. The product was extracted into ether (x2) and the combined ethereal extracts were washed with brine and dried ($MgSO_4$). The solvent was removed *in vacuo* and the crude product was purified by column chromatography (silica gel/ hexane) to yield a colourless solid. The product was recrystallised (ethanol) and dried (desiccators, P_2O_5) overnight to yield colourless crystals.

Yield = 1.3 g, (59 %).

^{1}H-NMR ($CDCl_3$), δ: 0.90 (3H, t), 1.30 (8H, m), 1.39 (9H, s), 1.49 (2H, quint), 1.85 (2H, quint), 4.09 (2H, t), 6.81 (1H, ddd, J = 16.32 Hz, J = 7.45 Hz, J = 1.84 Hz), 7.14 (1H, ddd, J = 16.93 Hz, J = 8.57 Hz, J = 2.24 Hz), 7.48 (2H, d, J = 8.36 Hz), 7.58 (4H, m), 7.62 (2H, d, J = 8.57 Hz).

^{13}C-NMR (100 MHz, $CDCl_3$), δ: 14.10, 22.60, 25.87, 29.20, 29.29, 31.34, 31.50, 31.79, 34.54, 69.85 (alkyl carbons, 10 required, 10 found); 110.00, 122.60, 122.64, 123.48 (dd, J = 3.84 Hz, J = 3.84 Hz), 125.77, 126.69, 127.09, 129.00, 133.56, 137.64, 140.25, 144.15 (dd, J = 735 Hz, J = (m)), 146.58 (dd, J = 715.28 Hz, J = 13 Hz), 150.19, (aromatic carbons, 14 required, 14 found).

Transition: ($^\circ$C) Cr 92 (SmC 76) Iso.

MS: *m/z* 450 (M^+).

Elemental analysis: $C_{31}H_{40}F_2OSi$ requires C 79.69 %, H 8.05 %; found C 80.25 %, H 8.30 %.

HPLC: 99.31 %.

Scheme 20

4-tert-butyl-4'-hydroxybiphenyl (88)

Compound **81** (26 g, 0.160 mol), dissolved in DME (250 ml), was added to a stirred mixture of the compound **17** (23 g, 0.133 mol) , KF (28 g, 0.483 mol), and $Pd(PPh_3)_4$ (1 g, $8.66x10^{-5}$ mol) under nitrogen. The stirred mixture was heated under reflux overnight. TLC revealed a complete reaction and the mixture was poured into water. The product was extracted into ether (x2) and the combined ethereal extracts were washed with brine and dried ($MgSO_4$). The solvent was removed *in vacuo* and the crude product was purified by column chromatography (silica gel/ hexane) to yield a colourless solid.

Yield = 29.92 g, (85 %).

^{1}H-NMR ($CDCl_3$), δ: 1.38 (9H, s), 4.98 (1H, s), 6.88 (2H, dd), 7.42 – 7.50 (6H, m).

MS: *m/z* 130 (M^+).

4'-tert-Butyl-biphenyl-4-yl trifluoromethanesulfonate (89)

Triflic anhydride (43 g, 0.152 mol), was added dropwise to a stirred cooled solution (0 °C) of the compound **88** (29.9 g, 0.132 mol) in dry pyridine (300 ml) under dry nitrogen. The mixture was stirred at room temperature overnight and poured into water. The product was extracted into ether (x2) and the combined ethereal extracts were washed successively with water, 10 % HCl (x2), brine, and dried ($MgSO_4$). The solvent was removed *in vacuo* to yield colourless solid.

Yield = 19.12 g, (41 %).

^{1}H-NMR ($CDCl_3$), δ: 1.30 (9H, s), 7.31 (2H, d), 7.49 (4H, s), 7.64 (2H, d).

MS: *m/z* 256 (M^+).

4'''-(tert-Butyl)-2',3'-difluoro-4-heptyl-[1,1':4',1'':4'',1''']-quaterphenyl (90)

Compound **16** (1.80 g, 5.40 mmol), dissolved in DME (100 ml), was added to a stirred mixture of the compound **89** (1.60 g, 4.5 mmol), Na_2CO_3 (1.6 g, 0.015 mol), and $Pd(PPh_3)_4$ (0.1 g, 0.086 mmol) in water (40 ml) under nitrogen. The stirred mixture was heated under reflux overnight. TLC revealed a complete reaction and the mixture was poured into water. The product was extracted into ether (x2) and the combined ethereal extracts were washed with brine and dried ($MgSO_4$). The solvent was removed *in vacuo* and the crude product was purified by column chromatography (silica gel/ hexane) to yield a colourless solid. The product was recrystallised (ethanol) and dried (desiccators, P_2O_5) overnight to yield colourless crystals.

Yield = 1.6 g, (72 %).

^{1}H-NMR ($CDCl_3$), δ: 0.90 (3H, t), 1.30 (8H, m), 1.40 (9H, s), 1.65 (2H, quint), 2.68 (2H, t), 7.30 (4H, dd, J = 7.75, Hz J = 2.24 Hz), 7.52 (4H, dd, J = 8.16, Hz J = 8.16 Hz), 7.60 (2H, d, J = 8.36 Hz), 7.68 (4H, dd, J = 16.32 Hz, J = 8.36 Hz).

^{13}C-NMR (100 MHz, $CDCl_3$), δ; 14.11, 22.67, 29.19, 29.34, 31.35, 31.43, 31.82, 34.57, 35.73 (alkyl carbons, 9 required, 9 found); 124.5 (dd), 124.65 (dd), 125.82, 126.74, 127.17, 128.69, 129.09, 129.19, 131.92, 133.15, 136.11, 137.57, 140.8, 143.17, 148.50 (2x) (dd), 150.61 (aromatic carbons, 18 required, 18 found).

Transition: ($^\circ$C) Cr 117 SmC 154 N 189 Iso.

MS: *m/z* 496 (M^+).

Elemental analysis: $C_{35}H_{38}F_2$ requires C 84.64 %, H 7.71 %; found C 84.52 %, H 7.86 %.

HPLC: 98.6 %.

Scheme 21

4'''-(tert-Butyl)-2',3'-difluoro-4-(octyloxy)-[1,1':4',1'':4'',1''']-quaterphenyl (91)

Compound **77** (1.85 g, 5.10 mmol), dissolved in DME (100 ml), was added to a stirred mixture of the compound **89** (1.55 g, 4.3 mmol), Na_2CO_3 (1.63 g, 0.0154 mol) LiCl (0.55 g, 0.013 mol), and $Pd(PPh_3)_4$ (0.2 g, 0.172 mmol) in water (40 ml) under nitrogen. The stirred mixture was heated under reflux overnight. TLC revealed a complete reaction and the mixture was poured into water. The product was extracted into ether (x2) and the combined ethereal extracts were washed with brine and dried ($MgSO_4$). The solvent was removed *in vacuo* and the crude product was purified by column chromatography (silica gel/ hexane) to yield a colourless solid. The product was recrystallised (ethanol) and dried (desiccators, P_2O_5) overnight to yield colourless crystals.

Yield = 1.52 g, (67 %).

^{1}H-NMR ($CDCl_3$), δ: 0.90 (3H, t), 1.39 (8H, m), 1.40 (9H, s), 1.52 (2H, quint), 1.80 (2H, quint), 4.10 (2H, t), 7.10 (2H, d, J = 8.77 Hz), 7.28 (2H, dd, J = 7.96 Hz, J = 7.95 Hz), 7.50 (2H, d, J = 8.36 Hz), 7.54 (2H, d, J = 8.77 Hz), 7.60 (2H, d, J = 8.36 Hz), 7.66 (2H, d, J = 8.77 Hz), 7.71 (2H, d, J = 8.36 Hz).

^{13}C-NMR (100 MHz, $CDCl_3$), δ; 14.11, 22.66, 26.04, 29.23, 29.35, 30.94, 31.33, 31.81, 34.56, 68.06 (alkyl carbons, 10 required, 10 found); 114.61, 124.44, 125.80, 126.73, 127.15, 128.70, 129.15 (d, J = 3.07), 129.50, 129.90 (d, J = 3.07 Hz), 131.30, 133.35, 135.10, 137.57, 140.75, 146.50 (2x) (dd), 150.58, 159.18 (aromatic carbons, 18 required, 18 found).

Transition: ($^\circ$C) Cr 126 SmC 187 N 208 Iso.

MS: *m/z* 526 (M^+).

Elemental analysis: $C_{36}H_{40}F_2O$ requires C 82.09 %, H 7.65 %; found C 81.83 %, H 7.78 %.

HPLC: 98.51 %.

3.5 References

1. K. M. Fergusson, PhD thesis, The Synthesis and Properties of Achiral and Chiral Bent-core Liquid Crystals, Hull University, 2008.
2. I. A. Radini, PhD thesis, The Synthesis and properties of Liquid Crystal with Bulky Terminal Groups for Bookshelf Geometry Ferroelectric Mixtures, Hull University, 2010.
3. G. Procter, J. Leonard and B. Lygo, *Advanced Practical Organic Chemistry*, Taylor & Francis, New York, 1998.
4. W. Still, M. Kahn and A. Mitra, *journal of Organic Chemistry*, 1978, **43**, 2923.
5. D. Coulson, *Inorganic Syntheses*, 1990, **28**, 107.
6. J. Haley, *Instrument details for thesis, papers, reports etc*, University of Hull. Hull, 2008.
7. H. E. Gottlieb, V. Kotlyar and A. Nudelman, *Journal of Organic Chemistry*, 1997, **62**, 7512.
8. D. D. Lacey, *Equipment*, University of Hull. Hull, 2008.

4- Experimental Discussion

This section discusses the strategy of synthesis both in term of the chosen methodology and specific techniques used to generate the final compounds shown below, see figure **4.1**.

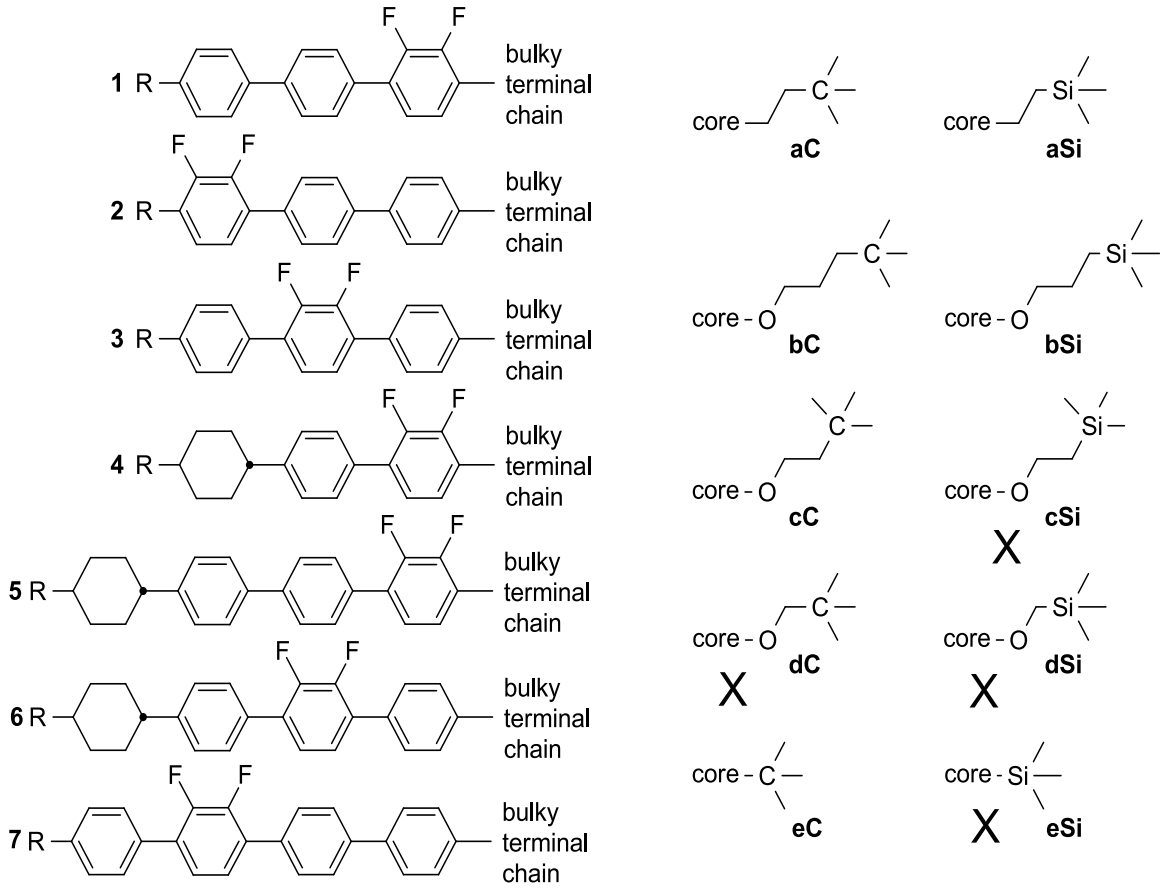

Figure 4.1. General structures of the compounds prepared.

In figure **4.1**, these compounds have been targeted to perform a particular function in LC mixtures for use in display devices. The aim is to remove layer shrinkage (zig-zag) to get a bookshelf alignment. The structural units in the material can tackle the layer shrinkage (zig-zag). These structural units can disrupt the intermolecular forces of attraction at the ends of the molecules. The study and research were about the effect of the bulky end group on mesophase and melting point of the final compounds and to consider how the final compounds affect the switching times of mixtures.

In general, the preparation of multi-aryl core compounds with many lateral fluoro substituents and two terminal chains cannot be achieved directly from the core unit.

The introduction of structural units into a phenyl ring is regularly attained utilizing electrophilic substitution reaction. The scope of units that can be presented is somewhat limited, however subsequent functional group interconversions can provide a vast group of substituents. The electrophonic substitutions in an aryl ring are controlled and rate- determined by exhibit substituents. Henceforth, as the quantity of substituents needed in an aryl ring is raised, the opportunity that a substituent will be controlled to an undesired position gets to be ever more prominent. Furthermore, steric obstacle will restrain the possibilities of a substituent being directed to a required position in the ring. In terphenyls and biphenyls, the range for electrophonic substitution is extremely limited because the positions in the bay areas of the core are sterically hindered by the ring structure itself, consequently in these positions substitution is extremely unlikely. The introduction of a terminal chain, for example, an alkoxy or alkyl chains into a terphenyl or a biphenyl core will activate positions in the terminal rings to more substitution.

On account of all these truths, alternative ways were needed for setting up the terphenyl materials with lateral fluoro substituents. The alternative ways include the starting synthesis of the individual ring units and the subsequent systematic connecting of these units to give the desired multi-aryl final product materials. Numerous strategies of producing carbon-carbon bonds between aryl units have been developed to a right standard of high result yields and operational simplicity to allow their widespread use in synthetic organic chemistry science.

The majority such methods utilize two aryl units, one having a substituent or leaving group and the second one aryl unit is an organometallic unit. The two aryl units can then be coupled together in the presence of a transition metal catalyst which has suitable ligands. Tetrakis(triphenylphosphine)palladium(0), $Pd(PPh_3)_4$ is one of the good and most useful catalysts. I, Br and Cl can be leaving groups as well as tosylate and triflate, these latter two are formed from phenols or enols which greatly enhance the range of the methodology. The arylboronic acids are the most successful organometallic units in the synthesis of liquid crystals because of boronic acids non-toxicity, lack of significant homocoupling, their ease of preparation especially at low temperature and compatibility with a wide range of other functional groups.

In 1981[1], Suzuki and co-workers developed the use of arylboronic acids in metal catalysed (cross-coupling) reactions. Suzuki and many other researchers[2-8] have developed the methodology to obtain an excellent result with a wide range of different substrates. In synthetic chemistry, especially in the LC area, the Suzuki reaction is very common due to common presence of biphenyl and terphenyl moieties within LC systems[9]. Generally, the palladium-catalysed reaction carried out in dimethoxyethane (DME), the substrate having the leaving group is added to a mixture of 2M aqueous sodium carbonate (Na_2CO_3) and dimethoxyethane (DME), under dry nitrogen gas. Then the palladium catalyst ($Pd(PPh_3)_4$) is added followed by 15-20% excess of the boronic acid.

In figure **4.2**, the mechanism of the Suzuki coupling catalytic cycle has been proposed[10-12] , but many variations have been reported. The oxidative addition of the aryl or vinyl halide (or triflate) is included as main steps in the cross-coupling reaction to pd(0), followed by transmetallation of an organic ligand from an organometallic to the resulting pd(II) intermediate.

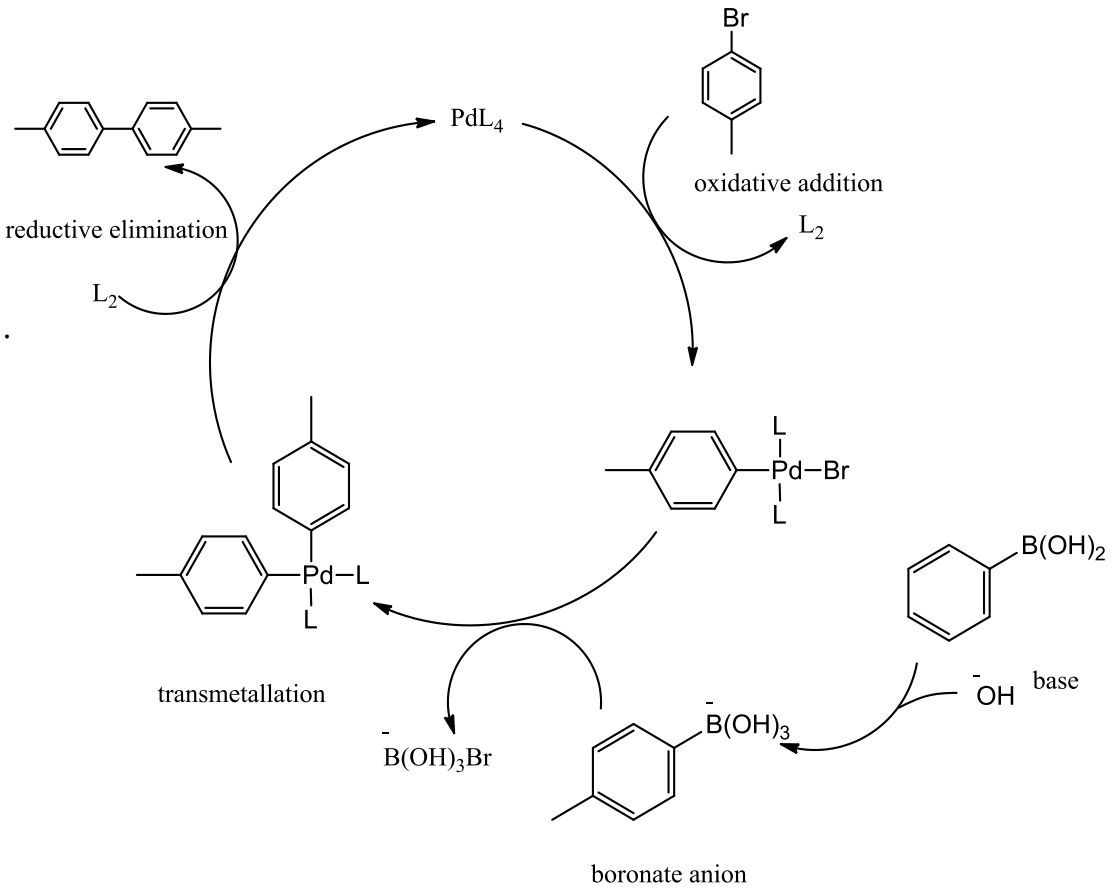

Figure 4.2. Proposed mechanism of the catalytic cycle for the palladium reaction (cross-coupling reaction).

Then, the disubstituted Pd(II) intermediate undergoes reductive, which provides the product by C bond formation and reproduces the catalytically active Pd(0) oxidation level. In determining the rates and equilibria of different steps the anions and ligands play a crucial role by controlling the detailed coordination environment at palladium[13].

Schemes **1** and **2** show the synthesis of compounds **5** and **7** which are needed to couple in different schemes later. The carboxylation reaction was used with compound **1** to get compound **2** (4,4-dimethylpent-2-ynoic acid) (yield = 90 %). The compound **2** was attempted with hydrogenolysis reaction to give alcohol compound **3** (4,4-dimethylpentanoic acid) (yield = 66 %). The compound **3** with lithium aluminium hydrate give compound **4** (4,4-dimethylpentan-1-ol) (yield = 79 %) which is tosylated to get compound **5** (4,4-dimethylpentyl 4-methylbe**nz**enesulfonate) (yield = 83 %). Scheme **2**, this scheme was facilitated by the condensation of the alcohol **6** and sulfonyl chloride to give a sulfonate ester **7** (yield = 41 %).

Scheme **3** shows the synthesis of compound **9**. This scheme was facilitated by the condensation of the alcohol (compound **8**) and sulfonyl chloride to give a sulfonate ester **9** (yield = 88 %).

Scheme **4** shows the four different ways to synthesis compound **11**, but they were failed.

Scheme **5** details the synthesis of the final compounds **20** and **21**. 1,2-Diflurorobenzene **12** has two equivalent proton ortho to a fluoro substituent which are acidic because of the electron-withdrawing effect of the adjacent fluoro substituent[14-16]. Metallation of 1,2-difluorobenzene with 1 mol equivalent of *n*-BuLi occurs at low temperature -78 $^{\circ}$C to give the mono-lithium derivative. The low temperatures (-78 $^{\circ}$C) are required in order to stabilise the ortho-fluoroaryllithium intermediates as at higher temperatures the ortho-fluoroaryllithium intermediates will decompose violently with elimination of lithium fluoride to produce the reactive benzyne species[17]. Adding the trimethyl borate slowly to mono-lithium derivative at -78 $^{\circ}$C and gradual warming to room temperature, gave the borate ester which was hydrolysed in situ with 10% hydrochloric acid to get the boronic acid **13** (yield = 81 %). Boronic acid **13** was coupled to compound **14** (palladium-catalyzed cross-coupling) to generate biphenyl **15** (yield = 87 %). Lithiation of the remaining acidic proton on the substituted ring allowed the conversion of compound **15** into corresponding boronic acids **16** (yield = 34 %). Following this, to form compounds **18** and **19**, the sulfonate compounds **5** and **7** are reacted with a 4-bromophenol **17** to form 1-bromo-4-((4,4-dimethylpentyl)oxy) benzene **18** (yield = 76 %) and (3-(4-

bromophenoxy)propyl)trimethylsilane **19** (yield = 50 %). Through the reaction, the potassium carbonate abstracts the phenolic proton (Williamson ether synthesis)[18] resulting in the formation of the corresponding phenolate anion which then attaches to alkyl bromide in a typical S_N2 reaction to produce the desired aryl-alkyl ether **18** and **19**. The compound **16** was then coupled (Suzuki cross-coupling reaction) to compounds **18** and **19** to give the final liquid crystal terphenyls **20** (yield = 51 %) and **21** (yield = 67 %).

Scheme **6** details the synthesis of the final compounds **28** and **29**. To form compounds **23** and **24**, the sulfonate ester compounds **5** and **7** are reacted with a 2,3-difluorophenol (alcohol difluorophenol) **22** in an S_N2 reaction to form compounds **23** (yield = 69 %) and **24** (yield = 72 %). To get the boronic acids **25** and **26**, a low temperature lithiation of the compounds **23** and **24** took place, followed by the addition of trimethyl borate to form the boronic ester, followed by addition of 10% HCl to hydrolyse the ester and form the compounds **25** (yield = 53 %) and **26** (yield = 97 %). Finally to get the final products, each of the boronic acids **25** and **26** is coupled to the heptyl biphenylbromide **27** using a Suzuki cross-coupling reaction, which gives the final products **28** (yield = 41 %) and **29** (yield = 63 %).

Scheme **7** details the synthesis of the final compounds **36** and **37**. The sulfonate ester compounds **5** and **7** are reacted with a biphenol bromide **30** to form compounds **31** (yield = 76 %) and **32** (yield = 41 %). This S_N2 reaction precedes by formation the biphenolate which then allows the nucleophilic attacks of the sulfonate esters **5** and **7**, forming the desired compounds **31** and **32**. The introduction of a terminal alkyl chain into a ring containing lateral fluror substituents (scheme 7) is more lengthy and involved than for an alkoxy terminal chain (scheme 19). The usual method of placing an alkyl chain into an aromatic unit involves a Friedel-Crafts acylation followed by a Wolff-Kishner reduction[12] of resulting ketone. However, in this case, the presence of the fluoro substituents directs the acylation into undesirable 4-position. Accordingly, in order to obtain the 1,2-difluoro-3-heptylbenzene **34** (yield = 84 %), a different route was required which would exploit the acidic proton of 1,2-difluorobenzene **12**. Generation of the mono-lithium salt of compound **12**, followed by addition of heptanal at low temperature – 78 °C and acidification with ammonium chloride

solution gave the benzylic alcohol **34a**. Dehydration of this alcohol **34a** was effected using phosphorus(V) oxide to yield the alkene **34b** which subsequently hydrogenated at room temperature over 10 % Pd/C to give a yield of 84 % from 1,2-difluoro-3-heptylbenzene **34**.

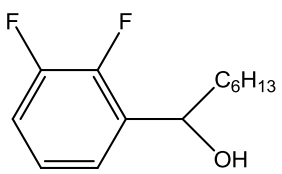

34a

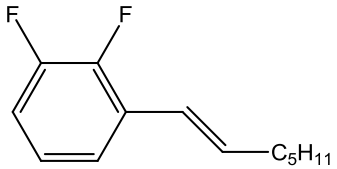

34b

Lithiation of the remaining acidic proton on the substituted ring allowed the conversion of compound **34** into the corresponding boronic acid **35** (yield = 46 %) using the procedures described for preparing compounds **25** and **26** (scheme **6**), to give a yield of 46 %. These compounds **31** and **32** are then coupled directly to a premade variation of an alkylic difluoroboronic acid **35** (Suzuki cross-coupling reaction) to forms the final products **36** (yield = 83 %) and **37** (yield = 98 %).

Scheme **8** details the synthesis of the final compound **39**. The sulfonate ester compound **9** was reacted with a 4-bromophenol **17** in an S_N2 reaction to form compound **38** (yield = 75 %). The compound **16** (boronic acid) was then coupled (Suzuki cross-coupling reaction) to compound **38** to give the final product terphenyls **39** (yield = 62 %).

Scheme **9** details the synthesis of the final compound **42**. The sulfonate ester compound **9** was reacted with a 2,3-difluorophenol **22** in an S_N2 reaction to form compound **40** (yield = 96 %). A low temperature lithiation of the compound **40** took place, followed by the addition of trimethyl borate to form the boronic ester, followed by addition of 10% HCl to hydrolyse the ester and form the boronic acid **41** (yield = 78 %). Finally to get the final products, the boronic acids **41** is coupled to the heptyl biphenylbromide **27** using a Suzuki cross-coupling reaction, which gives the final product **42** (yield = 75 %).

Scheme **10** details the synthesis of the final compound **44**. The sulfonate ester compound **9** is reacted with a biphenol bromide **30** to form compound **43** (yield = 69 %). This S_N2 reaction precedes by formation the biphenolate which then allows the nucleophilic attacks of the sulfonate ester **9**, forming the desired compound **43**. This compound **43** is then coupled directly to a premade variation of an alkylic difluoroboronic acid **35** (Suzuki cross-coupling reaction) to forms the final product **44** (yield = 77 %).

Scheme **11** details the synthesis of the final compound **56**. The compound **13**, a bromo substituent was introduced onto the aromatic ring 1,2-difluorobenzene from the brominolysis of boronic acid **13** to produce 1-bromo-2,3-difluorobenzene **45** (yield = 51 %). Kuivila and co-workers have studied the kinetics of brominolysis in aqueous acetic acid and found that bases catalyse the reaction[19], this observation and further kinetic studies of brominolysis of ten arylboronic acids[20] are consistent with a proposed mechanism involving the usual weakening effect of the C-B bond through formation of a boronate anion[21] , see figure **4.3**.

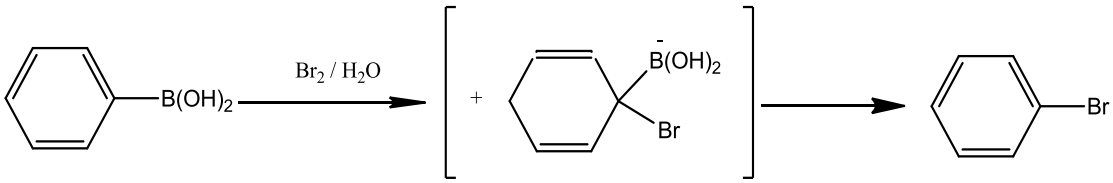

Figure 4.3. Mechanism of brominolysis of arylborinc acid.

The acidic proton of compounds **46** 4,4-dimethylpent-2-yne and **47** (trimethylsilyl)acetylene was removed by n-butyllithium at low temperature -78 °C, followed by treatment with zinc chloride to generate the unstable intermediate compounds **48** and **49**, which were coupled with compound **45** to provide compounds **50** (yield = 93 %) and **51** (yield = 32 %). Compound **45** was converted to the required phenyl alkynyls **50** and **51**. The hydrogenation of compounds **50** and **51** using palladium on charcoal deprotected the hydroxyl group in the same step as the reduction of the triple bond of the terminal alkynyl chain to result compounds **52** (yield = 76 %) and **53** (yield = 52 %). Lithiation of the remaining acidic proton on

the substituted ring allowed the conversion of compounds **52** and **53** into corresponding boronic acids **54** (yield = 62 %) and **55** (yield = 55 %). Then, the boronic acid **55** was coupled (Suzuki cross-coupling reaction) to alkoxy biphenyl **32** to give the final product terphenyl **56** (yield = 46 %).

Scheme **12** details the synthesis of the final compounds **59** and **60**. The triflate of compound **57** was synthesised by reaction with triflic anhydride in the presence of pyridine[22] to get compound **58** (yield = 99 %). Then, the compound **58** was coupled to boronic acids **25** and **26** to produce the final products **59** (yield = 71 %) and **60** (yield = 69 %). Scheme **12** details Suzuki cross-coupling reaction between boronic acid compounds **25** and **26** and the aryl triflate **58** to give compounds **59** and **60**. Lithium chloride (LiCl) is needed here. The need for LiCl can be understood by looking to the mechanism of this reaction which has been proposed[13] to be that shown below see figure **4.4**.

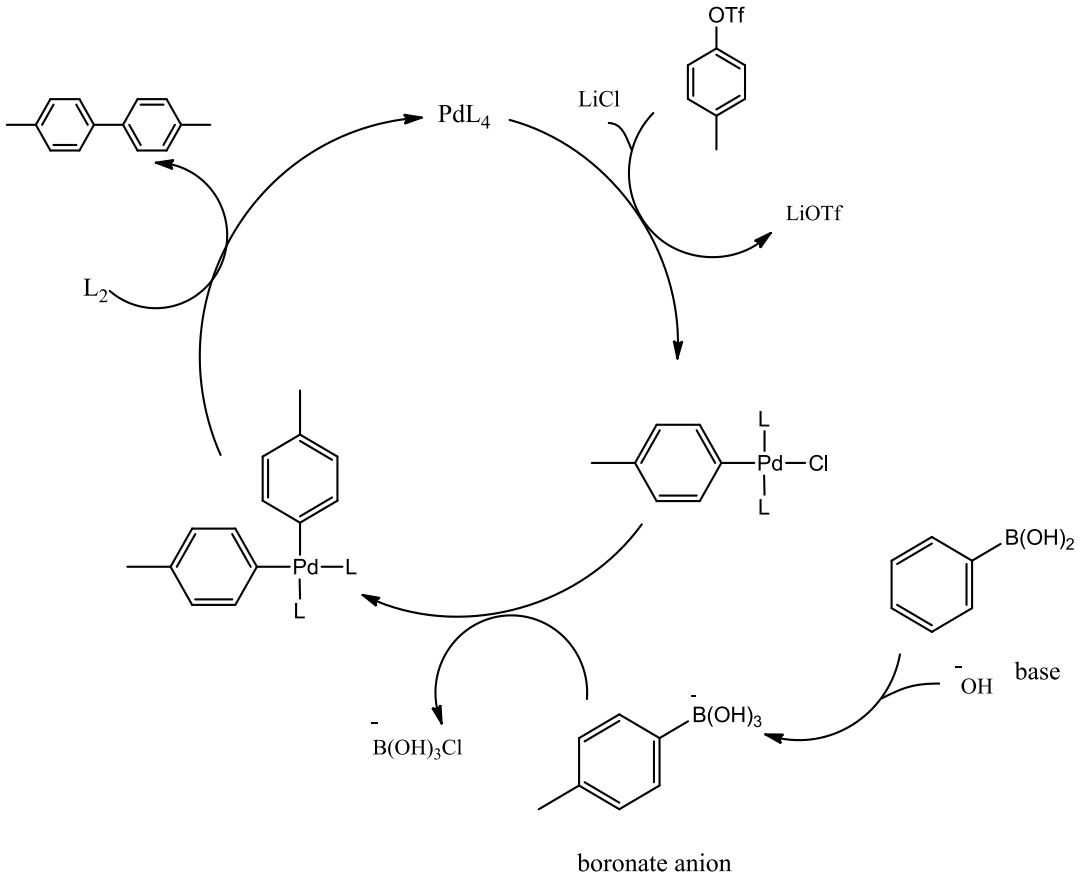

Figure 4.4. Proposed mechanism of the catalytic cycle for the palladium-catalyzed cross-coupling between a phenyl triflate and a boronic acid.

Scheme **13** details the synthesis of the final compounds **65** and **66**. This scheme details Suzuki cross-coupling reaction between boronic acid compound **61** and the aryl triflate **58** to produce compound **62** (yield = 51 %). Lithium chloride (LiCl) is needed here. The need for LiCl can be understood by looking to the mechanism of this reaction which has been proposed[13] to be that shown above see figure **4.4**. In the next step, hydrogenation using palladium on charocoal gave compound **63** (yield = 91 %). The triflate of the compound **63** was synthesised by reaction with triflic anhydride in the presence of pyridine[22] to produce compound **64** (yield = 98 %). Then, each of the boronic acids **25** and **26** was coupled (Suzuki cross-coupling reaction) to compound **64** to give the final products terphenyl **65** (yield = 68 %) and **66** (yield = 70 %). Lithium chloride (LiCl) is needed here.

Scheme **14** details the synthesis of the final compounds **69** and **70**. This scheme details Suzuki cross-coupling reaction between boronic acid compound **13** and the aryl triflate **58** to produce compound **67** (yield = 99 %). Lithium chloride (LiCl) is needed here. The need for LiCl can be understood by looking to the mechanism of this reaction which has been proposed[13] to be that shown in figure **4.4**. A low temperature lithiation of the compound **67** took place, followed by the addition of trimethyl borate to form the boronic ester, followed by addition of 10% HCl to hydrolyse the ester and form the boronic acid **68** (yield = 61 %). Finally to get the final products, the boronic acids **68** is coupled (Suzuki cross-coupling reaction) to each of compounds **18** and **19** using a Suzuki cross-coupling reaction, which gives the final products **69** (yield = 72 %) and **70** (yield = 65 %). Lithium chloride (LiCl) is needed here.

Scheme **15** details the synthesis of the final compound **71**. This scheme details Suzuki cross-coupling reaction between boronic acid compound **55** and the aryl triflate **64** to produce compound **71** (yield = 66 %). Lithium chloride (LiCl) is needed here, see figure **4.4**.

Scheme **16** details the synthesis of the final compound **73**. This scheme details Suzuki cross-coupling reaction between boronic acid compound **16** and the 1-bromo-4-(tert-butyl)benzene **72** to produce compound **73** (yield = 70 %).

Scheme **17** details the synthesis of the final compound **78**. 4-Bromophenol **17** was *O*-alkylated with 1-bromooctane **74** to produce compound **75** (yield = 90 %). Compound **75** is very common intermediate in the synthesis of liquid crystals. Followed by a Suzuki cross-coupling reaction between the resulting boronic acid **13** with the 1-Bromo-4-(octyloxy)benzene **75** to give the biphenyls **76** (yield = 90 %). Lithiation of the remaining acidic proton on the substituted ring allowed the conversion of compound **76** into corresponding boronic acid **77** (yield = 43 %) as described previously. Followed by a palladium-catalysed cross-coupling reaction between compound **72** and the boronic acid **77** to produce the final compound **78**. But, this reaction was failed, found to be compound **77**.

Scheme **18** details the synthesis of the final compound **82**. The boronic acid **35** is coupled to compound **17** using a Suzuki cross-coupling reaction, which gives the biphenyls **79** (yield = 75 %). The advantages of 4-bromophenol **17** is that having a bromo site *para* to the hydroxyl group, the bromo site can couple to another benzene ring, and the hydroxyl group can be converted to a triflate group to undergo another coupling reaction to a different benzene ring group. The triflate of compound **79** was synthesised by reaction with triflic anhydride in the presence of pyridine[22] to get compound **80** (yield = 100 %). To generates the boronic acid **81** (yield = 81 %) from the bromo-compound **72** (second way), it would be possible to try two ways. First way is a Grignard reaction using magnesium and second way is a lithiation using *n*-butylitium which was been used many times in this research. On other hand, treating compound **72** with *n*-BuLi requires low temperature -78 $^{\circ}$C to prevent addition of a butyl chain of the lithiated site, and therefore it was decided that a Grignard reaction should be employed to prevent problems with solubility at the lower temperature. Although, Grignard reactions themselves can sometimes be problematic with regard to initiating the reaction, and possible dimerisation during homocoupling, a good yield of the boronic acid **81** was obtained[6]. Then, the compound **80** was coupled (Suzuki cross-coupling reaction) to boronic acid **81** to produce the final products **82** (yield = 84 %).

Scheme **19** details the preparation of the final liquid crystal compound **87**. The preparation starts with an *O*-alkylation of difluorophenol **22** with1-bromooctane **74**,

using potassium carbonate in butanone to produce the 1,2-difluoro-3-octyloxybenzene **83** (yield = 93 %) in order to eventually generate the boronic acid **84** (yield = 29 %). The treatment of compound **83** with *n*-BuLi generated the aryllithium intermediate *via* hydrogen-metal interconversion, which upon quenching with trimethyl borate yielded the boronic acid **84**. The reaction was carried out at a low temperature -78 °C to avoid benzene formation by loss of LiF. Compound **84** is a common intermediate in the synthesis of liquid crystals. Then, the compound **17** was coupled (Suzuki cross-coupling reaction) to boronic acid **84** to produce the compound **85** (yield = 56 %). The triflate of compound **85** was synthesised by reaction with triflic anhydride in the presence of pyridine to get compound **86** (yield = 69 %). The trifluoroterphenyl compound **87** (final compound) was collected in yield of 59 % after the coupling reaction between the triflate **86** and the boronic acid **81**.

Scheme **20** details the synthesis of the final compound **90**. Scheme **20** illustrates the boronic acid **81** with the commercially available phenol **17** to produce the biphenyl **88** (yield = 85 %). The points of 4-bromophenol **17** is that having a bromo site *para* to the hydroxyl group, the bromo site can couple to another benzene ring. The triflate of the hydroxybiphenyl **88** was synthesised by reaction with trifluoromethanesulfonic anhydride in the presence of pyridine to get compound **89** (yield = 41 %). Then, the compound **89** was coupled (Suzuki cross-coupling reaction) to boronic acid **16** to produce the final products **90** (yield = 72 %).

Scheme **21** details the synthesis of the final compound **91**. The compound **89** was coupled (Suzuki cross-coupling reaction) to boronic acid **77** to produce the final products **91** (yield = 67 %).

4.2 References

1. N. Miyaura, T. Yanagi and A. Suzuki, *Synthetic Communications*, 1981, **11**, 513.
2. M. Hird, G. W. Gray and K. J. Toyne, *Molecular Crystals and Liquid Crystals*, 1991, **206**, 187.
3. G. Gray, M. Hird, D. Lacey and K. Toyne, *Journal of the Chemical Society-Perkin Transactions 2*, 1989, **12**, 2041.
4. G. Gray, M. Hird, D. Lacey and K. Toyne, *Molecular Crystals and Liquid Crystals*, 1989, **172**, 165.
5. R. B. Miller and S. Dugar, *Organometallics*, 1984, **3**, 1261.
6. K. M. Fergusson, PhD thesis, The Synthesis and Properties of Achiral and Chiral Bent-core Liquid Crystals, Hull University, 2008.
7. R. B. Miller and S. Dugar, *Organometallics*, 1984, **3**, 1261-1263.
8. I. A. Radini, PhD thesis, The Synthesis and properties of Liquid Crystal with Bulky Terminal Groups for Bookshelf Geometry Ferroelectric Mixtures, Hull University, 2010.
9. P. J. Collings and M. Hird, *Introduction to liquid crystals chemistry and physics*, Taylor & Francis, 1997.
10. W. J. Scoot and J. K. Stille, *Journal of the American Chemical Society*, 1986, **108**, 3033.
11. G. Cosquer, Liquid Crystal with Novel Terminal Chains as Ferroelectric Hosts' PhD Thesis, University of Hull, UK, 2000.
12. F. A. Carey, *Advanced Organic Chemistry / Francis A. Carey and Richard J. Sundberg*, 4 edn., Plenum Press, New York, 2000.
13. P. Stang, M. Kowalski, M. Schiavelli and D. Longford, *Journal of the American Chemical Society*, 1989, **111**, 3347.
14. B. J. Wakefield, *Organolithium methods*, London : Academic Press, 1988.
15. L. Barsky, H. W. Gschwend, J. McKenna and H. Rodriguez, *Journal of Organic Chemistry*, 1976, **41**, 3651.
16. J. Fitt and H. Gschwend, *Journal of Organic Chemistry*, 1976, **41**, 4029.
17. J. Eisch, *The Chemistry of Organometallic compounds*, 1 edn., The Macmillan company, New York, 1967.

18. G. Solomons and C. Fryhle, *Organic chemistry*, John Wiley & Sons, new York, 2004.
19. H. Kuivila and E. Easterbrook, *Journal of the American Chemical Society*, 1951, **73**, 4629.
20. H. Kuivila and A. Hendrickson, *Journal of the American Chemical Society*, 1952, **74**, 5068.
21. D. Hall, *Boronic Acids: Preparation, Applications in Organic Synthesis and Medicine*, Wiley-VCH Verlag GmbH & Co. KGaA, Weinheim, 2005.
22. C. Beard, K. Baum and V. Grakausk, *Journal of Organic Chemistry*, 1973, **38**, 3673.

5- Results and Discussions

One of the best ways of production appropriate ferroelectric LC mixtures is to use achiral host materials doped with a good chiral material to provide the important reduced symmetry properties to the mixture. This part of this research focuses on the mesomorphic studies of novel materials (*ortho*-difluoroterphenyl compounds) prepared in this thesis. The *ortho*-difluoroterphenyl compounds are excellent host materials for ferroelectric mixtures[1]. Many novel *ortho*-difluoroterphenyl compounds, two analogous novel *ortho*-difluoroquarterphenyl compounds two cyclohexylbiphenyl compounds and cyclohexylterphenyl compounds have been synthesised to show the effect on melting points, mesophase morphologies and transition temperatures.

The effect on the overall mesophase morphology especially in the production of tilted smectic phases (such as SmC phase) is one of the most important implications of lateral fluoro substitution[2-5].

The two lateral fluoro substitute into terphenyl core generate the 2,3- and 2',3'-difluoroterphenyl compounds[1, 6] which are an improvement as ferroelectric host materials. There are two reasons to use difluoro rather than monofluoro. The first reason is the second fluoro substituent does not give a raise in the molecular breadth since the two fluoro substituents are naturally fixed on one side of the molecule[7], therefore, the overall LC phases are not considerably reduced, as a result LC phase transition temperatures are upheld. Secondly, (physical properties) the viscosity tends to be comparatively low in order to the minimized molecular breadth, and the large lateral dipole produced by additive combination of the two fluoro substituents which tends to be the tilted phase (SmC phase)[8]. `

The terphenyl materials have terminal chains with a short bulky end unit (tert-butyl, 3-trimethylsilylpropoxy, 4,4-dimethylpentyloxy or 2-trimethylsilylethyl) and either heptyl or octyloxy on the other side of the core. The discussion will focus on the effect of replacing one of the terminal chains with a short bulky end unit on the transition temperatures, melting points and mesophase morphology of the materials. These discussions will also cover lateral fluoro substituents in different rings of the core.

5.1 Difluoroterphenyl Compounds (with three benzene rings)

All the difluoroterphenyls compounds, which have been prepared, have two lateral fluoro substituents and two terminal chains. One side of the terminal chain contains alkoxy or alkyl and on the other side of the core has a bulky unit (tert-butyl, 3-trimethylsilylpropoxy, 4,4-dimethylpentyloxy, 3,3-dimethylbutoxy, or 2-trimethylsilylethyl), see figure **5.1**.

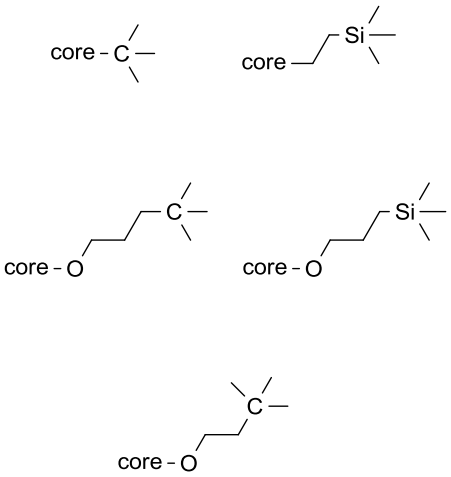

Figure 5.1. A selection of bulky end groups employed in the novel difluoroterphenyl compounds.

The difluoroterphenyl compounds were needed to get sensibly low melting points (mp) and sensibly high SmC phase stabilities combined with a low viscosity. These compounds are used as ferroelectric host materials and additives to ferroelectric mixtures.

There are two combinations of *ortho*-difluoroterphenyls compounds, the first one where the two fluoro substituents are at an outer ring such as compounds **28**, **29** and **42**, and second way where the occupy an inner-core (position in the centre ring) such as compounds **20**, **21** and **39**.

Thirteenth novel *ortho*-difluoroterphenyls compounds have been prepared. Melting points, transition temperatures and mesophase morphology of these novel *ortho*-difluoroterphenyl compounds were compared with the known novel compounds with conventional terminal chains. In tables **2**, **3** and **4**, melting points, transition temperatures and mesophase morphologies of the novel *ortho*-difluoroterphenyls compounds are presented and also some of the known analogues are shown. Compounds **A1**, **A2**, **A3**, **A4**, **A5** and **A6**[9-13] are known analogues and have been selected as parent systems for the thirteen novel *ortho*-difluoroterphenyl compounds.

There is a difference between the structures of novel *ortho*-difluoroterphenyls compounds and their novel *ortho*-difluoroterphenyls analogues (compounds **A1**, **A2**, **A3**, **A4**, **A5** and **A6**). The novel *ortho*-difluoroterphenyl compounds have the bulky group in two sides of the terminal chains (tert-Butyl, 3-trimethylsilylpropoxy, 4,4-dimethylpentyloxy or 2-trimethylsilylethyl) however, the parent systems has a longer unbranched group. It can be possible to evaluate the effect on mesophase morphology and transition temperatures of the short bulky terminal group.

The effect of the bulky end-groups is to eliminate the SmA phase and N phase because of its steric hindrance minimizes the stabilities of mesophase. It suppresses the SmA and N phases more than the SmC phase. In general, the branch terminal chain effect is to reason a disruption in the molecular which usually decreases the mesophase stability and melting points (especially smectic phase)[14]. Due to the bulky end-groups, the SmC phase results from the molecular phase separation. The strong lateral dipole of the *ortho*-difluoroterphenyl causes the strong tendency to molecular tilting especially when there is an alkoxy terminal chain. The molecules will be assisted by the bulky end-group[15].

In this work, these bulky end-groups (tert-butyl, 3-trimethylsilylpropoxy, 4,4-dimethylpentyloxy or 2-trimethylsilylethyl) contain carbon and silicon in the terminal chain. To compare carbon atom (C) with silicon atom (Si) in the terminal chain:

- Carbon is a smaller atom than silicon.
- Carbon has higher melting points than silicon.
- Carbon has higher transition temperatures than silicon[12, 13].

The novel compounds, which contain a terminal alkoxy chain, have higher transition temperatures and higher melting points than novel compounds with terminal alkyl chain[12]. This is due to oxygen with aromatic core. This oxygen extends the length of the rigid core and enhances polarisability anisotropy[14]. Moreover, the alkoxy terminal chain is more linear than the alkyl chain. The bond angle at the ring to CH_2 to alkyl chain is smaller than the angle for the ring to oxygen to alkyl chain.

Next discussion, the thirteen novel *ortho*-difluoroterphenyl compounds will be classified to three groups according to the positions of the fluoro substituents. Table **5.1** displays the first group with fluoro substituents in the end ring. The second group is shown in table **5.2** with fluoro substituents in the other end ring. The third group is that with fluoro substituents in the centre ring, see table **5.3**. However, each table also has known parent compound for comparison.

5.1.1 Transition Temperatures (°C) for 2,3 difluoroterphenyls (compounds 28, 29 and 42)

In table **5.1**, the mesomorphism of the three novel *ortho*-difluoroterphenyl compounds (compounds **28**, **29** and **42**) with the fluoro substituents in the end ring that also possesses the bulky terminal unit is displayed. Additionally, table **5.1** shows the known analogous (compound **A1**) for comparison. The known analogue (compound **A1**) is different in having a smaller unbranched group. The compound (compounds **28**, **29** and **42**) will be compared with its known analogue to see the effect of introducing the bulky terminal unit into the *ortho*-difluoroterphenyl. Moreover, the difference in the melting points and transition temperatures will be compared between the Si series and C series. Outer-ring, the arrangement of *ortho*-difluoro substituents gives two important structural features to dominate mesogenicity. The first important structural feature, the interannular twist happens and a common unsubstituted biphenyl region stays. This leads to an enhanced

polarisability which enhances transition temperatures. The second important structural feature, the fluoro substituent at the outer-ring position tends to fill space with polar unit, making possible the side to side intermolecular forces of attractions, and therefore upholding the stability of smectic phase[5, 8, 16].

Table 5.1. The transition temperatures of those compounds with the fluoro substituents in the end ring having the bulky terminal unit and known compounds for comparison.

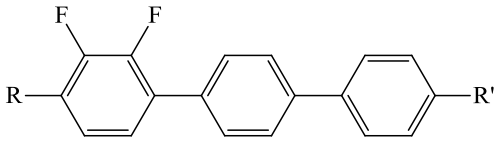

compound			Transition temperatures (°C)							
No.	R	R'	Cryst		SmC		SmA		N		Iso
28	$(CH_3)_3C(CH_2)_3O$	C_7H_{15}	●	117	●	146	___	___	___	___	●
29	$(CH_3)_3Si(CH_2)_3O$	C_7H_{15}	●	111	●	140	___	___	___	___	●
42	$(CH_3)_3C(CH_2)_2O$	C_7H_{15}	●	106	●	121	●	126	●	129	●
A1	$C_8H_{17}O$	C_7H_{15}	●	89	●	148	●	151	●	154	●

Compound **28** has crystal G (G 101).

Table **5.1** shows the alkoxy-alkyl compounds (compounds **28**, **29**, **42** and **A1**). Both compound **28** and compound **29** have a smectic C phase (SmC), but compound **28** also exhibits crystal G (G 101°C). The melting point and clearing point (transition temperatures) of compound **28** (with C series) are higher than compound **29** because of the silicon atom. The silicon atom is larger than carbon atom and confers lower temperatures throughout. The materials from the carbon series have higher melting points and transition temperatures than silicon-based material.

The compound **28** displays crystal G (G 101°C) and smectic C (SmC) phase. However, compound **42** shows smectic C, smectic A and nematic phases (SmC – SmA – N). The compound **28** illustrates high transition temperatures compared with compound **42**, this is due to odd-even effect, see figure **5.2**.

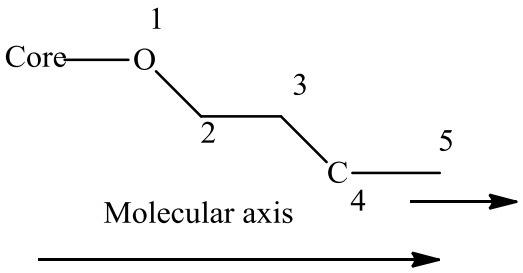

The bulky end group with an odd number of atoms in the chain gives lower melting and clearing points, see compound **42**.

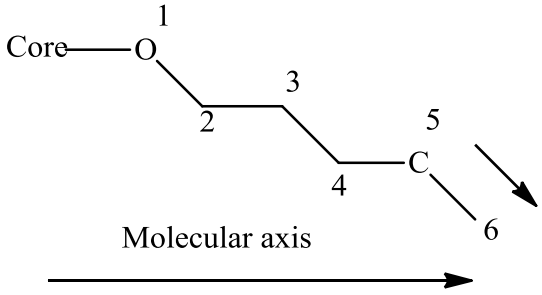

The bulky end group with an even number of atoms in the chain gives higher melting and clearing points, see compound **28**.

Figure 5.2. Representation of the odd-even effect for compounds 28 and 42.

The compound **A1** is a known compound and does not have a bulky group but has an unbranched group. It is the highest degree of smectic C stability (148 °C) compared to compounds **28**, **29** and **42**. Smectic C, smectic A and nematic phase are shown in compound **A1**, see figure **5.3**.

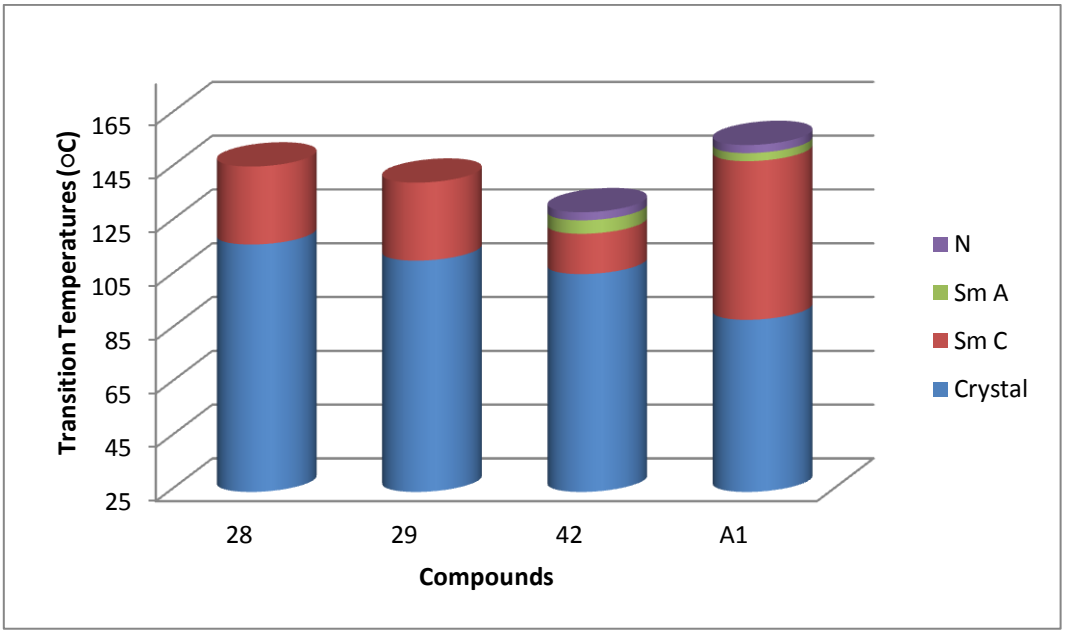

Figure 5.3. The transition temperatures for compounds 28, 29, 42 and A1.

Compounds **42** and **A1** display a narrow smectic A and nematic phase above the smectic C phase. Those compounds having a large difference in R possess the broadest smectic A phase ranges. The increased smectic C phase stability of compound **A1** is a result of the ether oxygen either *ortho* to the difluoro-substituents, or at the other end of the molecule. Also, the ether oxygen has the effect of raising the dipole and the dipole could be seen in one of two ways. Firstly, the existence of an additional electronegative element near the difluoro-substituents merely adds to the accumulative dipole. The second one takes into account the mesomeric effect, see figure **5.4**.

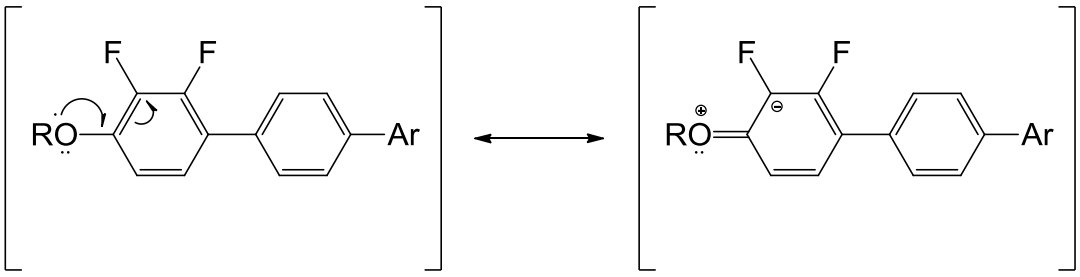

Figure 5.4. The mesomeric effect of the ether oxygen.

In addition, the ether oxygen will have the effect of increasing the degree of polarisability within the core, therefore enhancing the stability of smectic phase.

There are some examples of liquid crystal phases. Figure **5.5** and figure **5.6** show the Schlieren textures of the smectic C liquid crystal phase of compounds **28** and **29**.

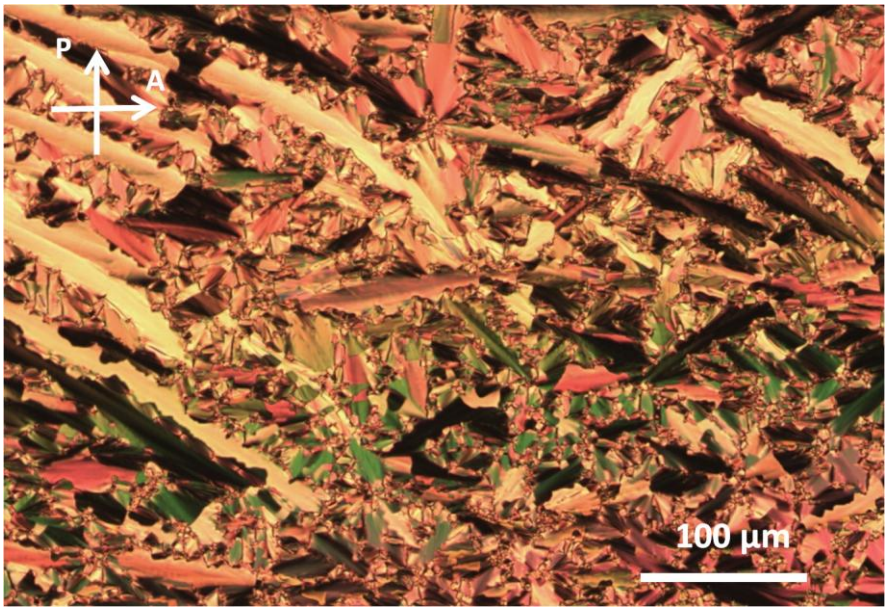

Figure 5.5. The SmC phase of compound 28 at 145 °C (Focal Conic texture).

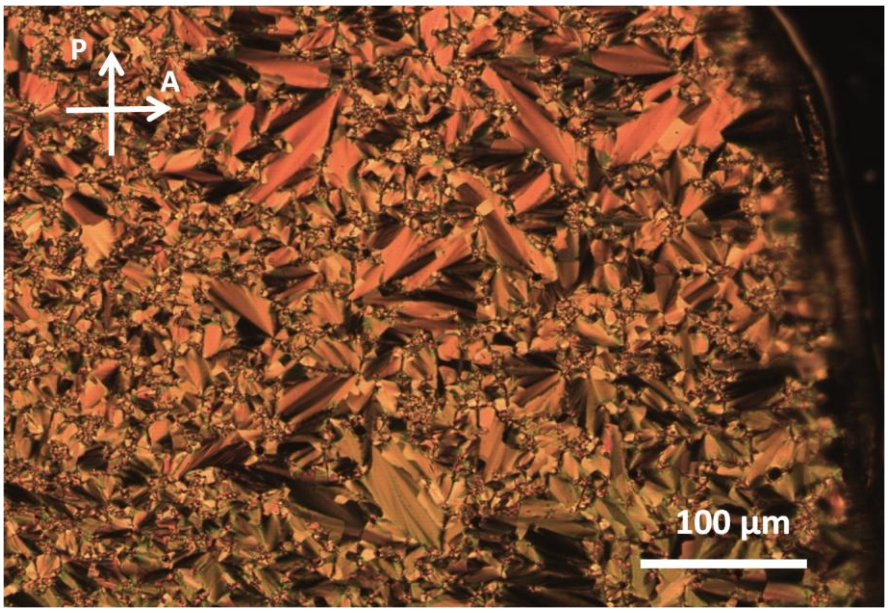

Figure 5.6. The SmC phase of compound 29 at 135 °C (Focal Conic texture).

5.1.2 Transition Temperatures (°C) for 2,3-difluoroterphenyls (compounds 36, 37, 44, 56, 82 and 87)

Table 5.2. The transition temperatures of those compounds with the fluoro substituents in the end ring having the bulky terminal unit and known compounds for comparison.

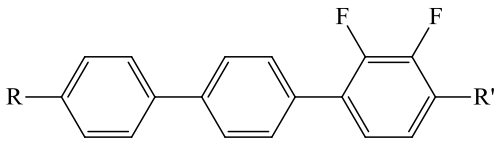

compound			Transition temperatures (°C)								
No.	R	R'	Cryst		SmC		SmA		N		Is
36	$(CH_3)_3C(CH_2)_3O$	C_7H_{15}	●	104	●	137	___	___	___	___	●
37	$(CH_3)_3Si(CH_2)_3O$	C_7H_{15}	●	103	●	124	___	___	___	___	●
44	$(CH_3)_3C(CH_2)_2O$	C_7H_{15}	●	72	●	104	___	___	●	118	●
56	$(CH_3)_3Si(CH_2)_3O$	$(CH_2)_2Si(CH_3)_3$	●	139	___	___	___	___	___	___	●
82	$(CH_3)_3C$	C_7H_{15}	●	90	___	___	___	___	___	___	●
87	$(CH_3)_3C$	OC_8H_{17}	●	90	●	(76)	___	___	___	___	●
A2	$(CH_3)_3Si(CH_2)_3O$	C_9H_{19}	●	80	●	113	___	___	___	___	●
A3	$(CH_3)_3C(CH_2)_2$	C_7H_{15}	●	71	●	101	___	___	___	___	●
A4	$(CH_3)_3C(CH_2)_2$	OC_8H_{17}	●	81	●	131	___	___	___	___	●
A5	$C_6H_{13}O$	C_5H_{11}	●	102	●	157	●	167	●	172	●

Table **5.2** illustrates novel compounds (compounds **36**, **37**, **44**, **56**, **82** and **87**) with the two fluoro substituents in the end ring with the conventional unbranched chain. Compounds **A2**, **A3**, **A4** and **A5** are known compounds for comparison.

By comparing the novel compound (**36**) with the novel compound (**37**); it could be to evaluate the effect on mesophase morphology, melting points and transition temperatures of the smaller size of carbon (C) in comparison with silicon (Si). The compound **37** with silicon has lower transition temperatures than the compound **36**

with carbon, because of the smaller size of carbon in comparison with silicon. Compound **37** has a lower melting point and a much lower clearing point than compound **36** (1.0 and 13.0 °C respectively).

Compounds **37**, **56** and **A2** are alkoxy-alkyl compounds. Compounds **37** and **A2** display the smectic C phase however; compound **56** does not illustrate any liquid crystal phase. Those compounds have a difference in R'. Compound **A2** has a much lower melting point and lower clearing point than compound **37** (23.0 and 11.0 °C respectively).

Compound **A5** (with linear terminal chain) has SmC, SmA and N phase but compound **36** (with bulky group) only gives SmC phase. Comparing the alkoxy-alkyl compound (**44**) to its dialkyl analogue compound (**A3**), the melting and clearing points of compound **44** are higher than the melting and clearing points of compound **A3**. The arrangement of dipole moments in compound **44** is tilt inducing. The strong lateral dipole of the *ortho* difluorophenyl unit is complemented by ether oxygen at the other side of the molecule to produce a high stability of the smectic C phase. In table **3**, the smectic C and nematic phases are displayed by compound **44** but compound **A3** shows smectic C phase only.

Figure **5.7** gives a good illustration of the difference between dialkyl compounds (*e.g.*, compounds **82** and **A3**) and alkyl-alkoxy compounds (*e.g.*, compounds **87** and **A4**). The biphenyl section can be said to confer relatively good over smectic character to those compounds **87**, **A3** and **A4**. However, compounds **87** and **A4** have the alkoxy-2,3- difluorophenyl unit which confers good SmC character, therefore no SmA is shown in this material; compounds **82** and **A3** however, have an alkyl – substituted 2,3- difluorophenyl unit which is not good for the tilted SmC phase. The effect of an alkoxy terminal chain on transition temperatures is made clearer when the alkyl-alkoxy compounds are compared with dialkyl compounds. When the difluoro unit is part of an alkoxy substituted end ring, melting points are higher than the compounds which do not have an alkoxy substituted end ring.

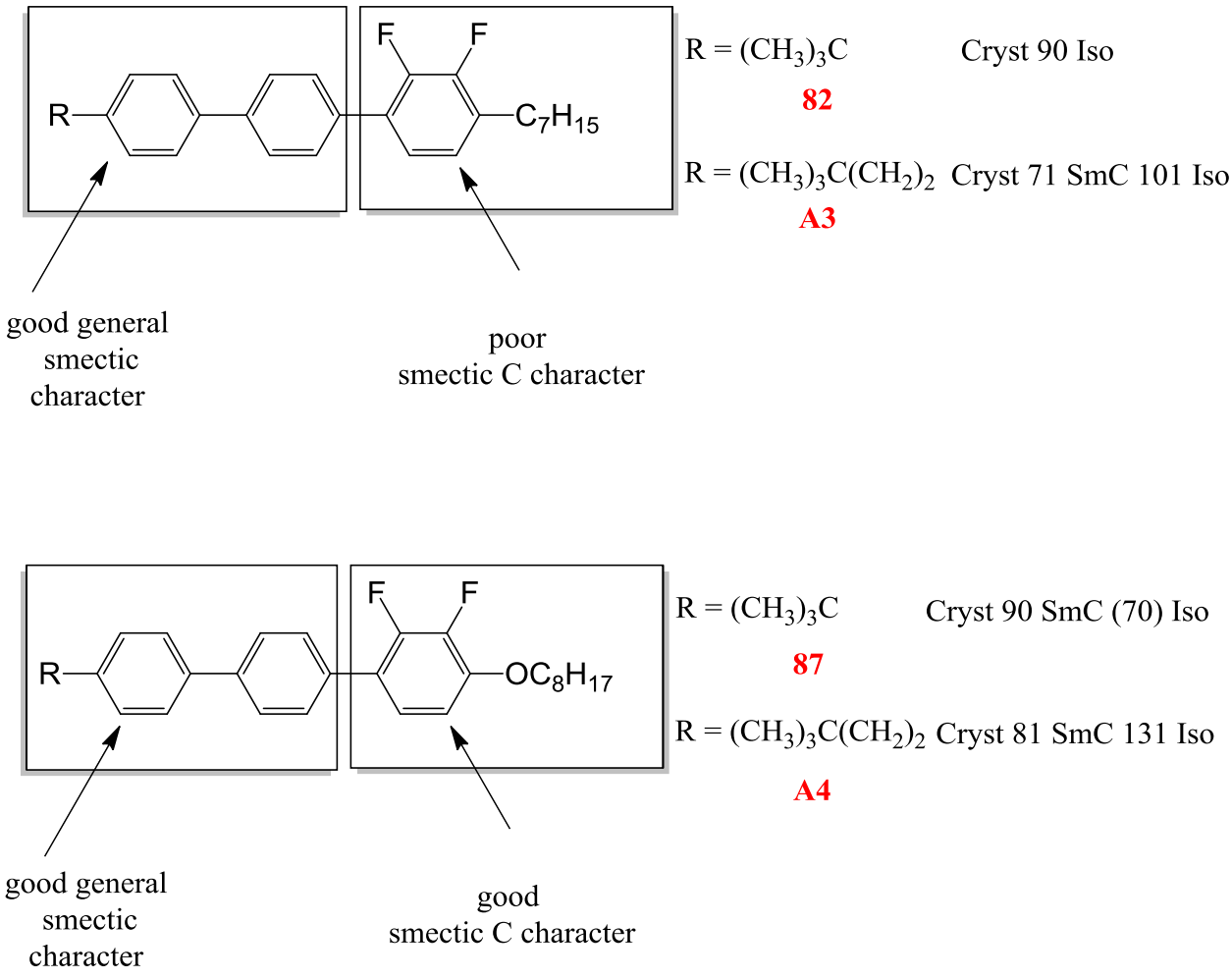

Figure 5.7. The effect of the terminal chains on the relative smectic C stabilities.

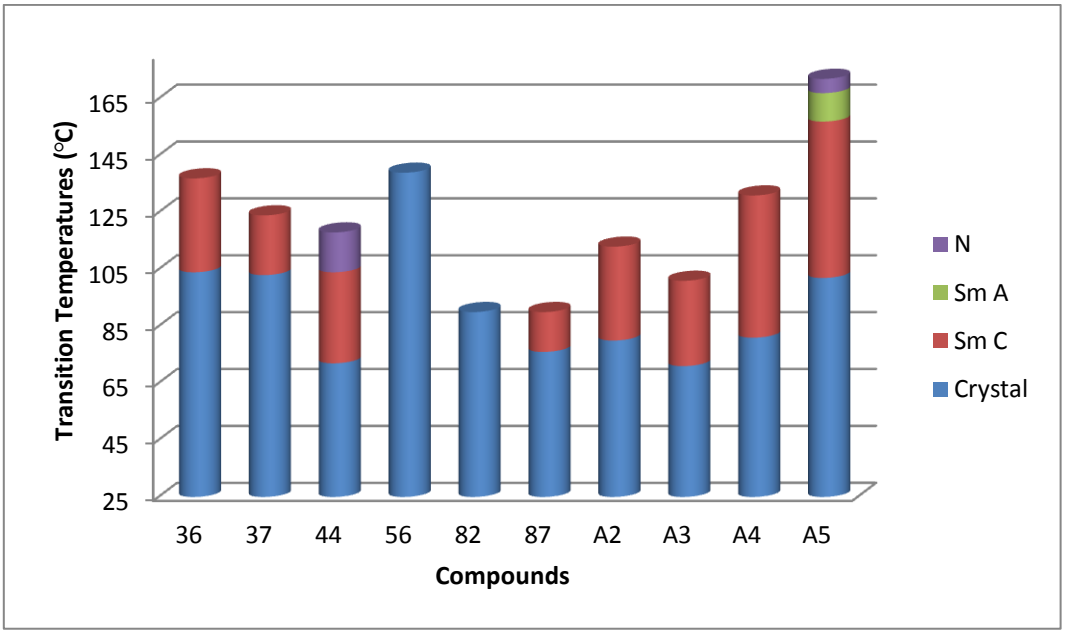

Figure 5.8. The transition temperatures for compounds 36, 37, 44, 56, 82, 87, A2, A3, A4 and A5.

There are some examples of liquid crystal phases. Figures **5.9**, **5.10** and **5.11** show the Schlieren textures of the smectic C liquid crystal phase of compounds **37**, **44** and **87**.

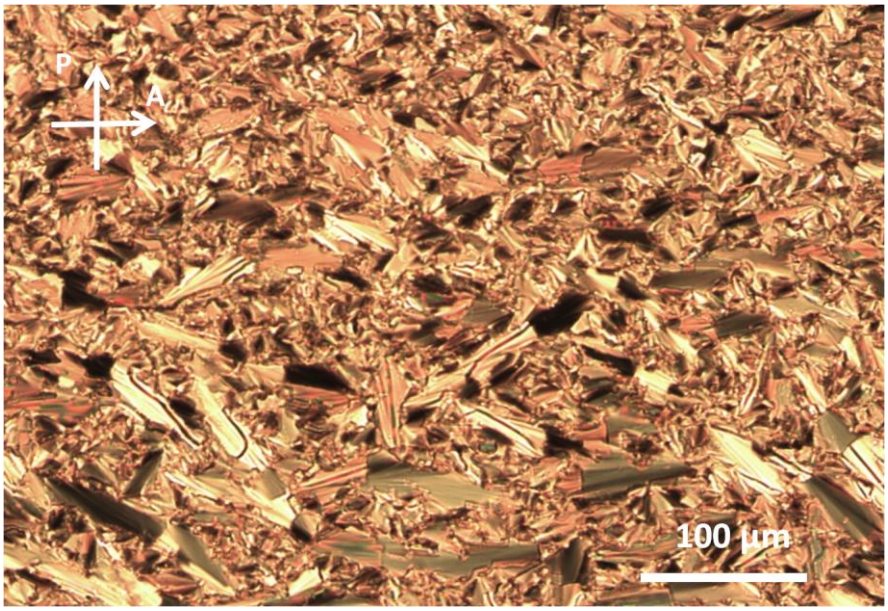

Figure 5.9. The SmC phase of compound 37 at 115 °C (Focal Conic texture).

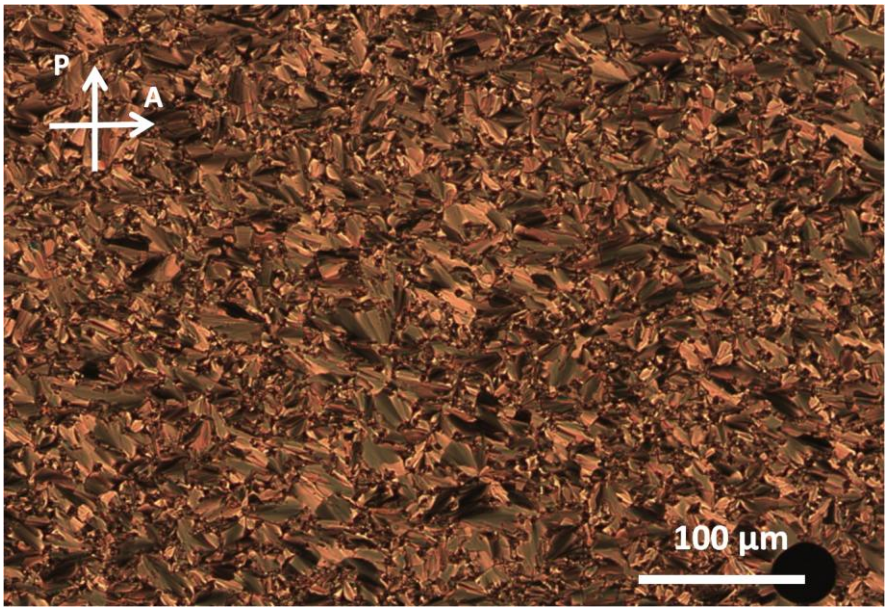

Figure 5.10. The SmC phase of compound 44 at 80 °C (Focal Conic texture).

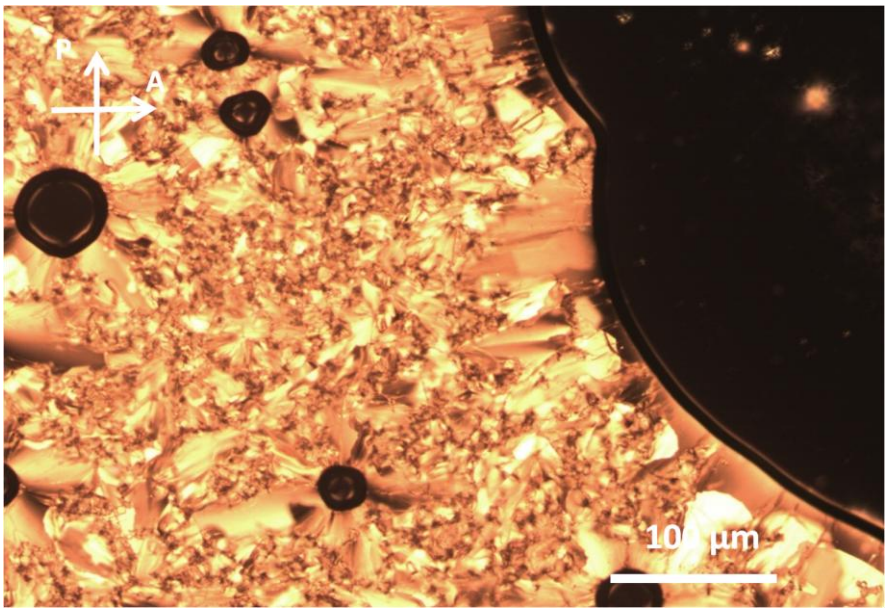

Figure 5.11. The SmC phase of compound 87 at (76) °C (Focal Conic texture).

5.1.3 Transition Temperatures (°C) for 2,3-difluoroterphenyls (compounds 20, 21, 39 and 73)

Table **5.3** displays these compounds (**20**, **21**, **39**, **73**, **A6** and **A7**) with the two fluoro substituents in the centre ring. These compounds in table **5.3** with the lateral fluoro substituents in the 'inner-core' (centre ring) position have a completely different transition temperatures and mesomorphism to the comparable compounds with the lateral fluoro substituents in the 'outer-edge' (end ring) location. The compounds with fluoro substituent at the end ring position have higher smectic phase stability, and less tendency toward nematic phase, than compounds with the fluorines in the inner-ring.

Compounds with the fluoro substituent at the end ring location twist about one interannular bond and a normal biphenyl region remains, on the other hand, lateral fluoro substituents in the inner-ring cause two interannular twisting, which effectively provides separate, non- coplanar, phenyl units which reduces polarizability, and therefore the stability LC phase is reduced, especially stability of smectic phase[7, 16, 17]. On the other hand, even with two interannular twisting, the strong, centrally positioned dipole is more conducive towards the tilted smectic C phase. Therefore, any imbalance in the molecular structure, such as that created by the use of two unequal terminal chains, promotes the production of a SmC phase.

Table 5.3. The transition temperatures of those compounds with the fluoro substituents in the centre ring having the bulky terminal unit and known compounds for comparison.

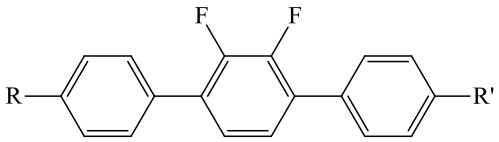

	compound		Transition temperatures (°C)								
No.	R	R'	Cryst		SmC		SmA		N		Iso
20	$(CH_3)_3C(CH_2)_3O$	C_7H_{15}	●	82	●	92	___	___	●	108	●
21	$(CH_3)_3Si(CH_2)_3O$	C_7H_{15}	●	81	●	90	___	___	●	94	●
39	$(CH_3)_3C(CH_2)_2O$	C_7H_{15}	●	95	___	___	___	___	●	100	●
73	$(CH_3)_3C$	C_7H_{15}	●	56	___	___	___	___	___	___	●
A6	$(CH_3)_3C(CH_2)_2$	C_7H_{15}	●	60	●	76	___	___	●	77.7	●
A7	$(CH_3)_3Si(CH_2)_2$	C_7H_{15}	●	58.9	●	61.7	___	___	___	___	●
A8	$C_6H_{13}O$	C_5H_{11}	●	54	●	67	___	___	●	149	●

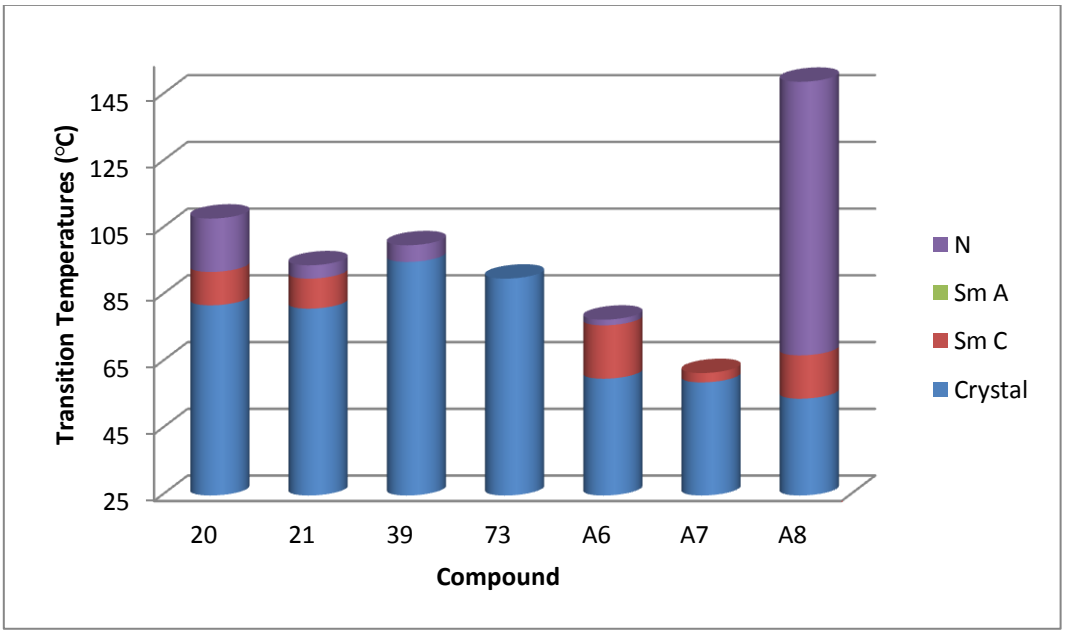

Figure 5.12. The transition temperatures for compounds 20, 21, 39, 73, A6, A7 and A8.

The raise in breadth being in the centre of the molecule tends to disrupt the stability of smectic phase by significantly more than the stability of N phase. The same reasoning also tends to give low melting points for compounds with this position of lateral fluoro-substituents.

It is a good to see the mesophase morphology, transition temperature and melting points of the final compounds (**20**, **21**, **39**, **A6**, **A7** and **A8**) displayed in table **5.3**. These compounds in table **5.3** (inner-ring) have a low melting points and transition temperatures than those compounds in the tables **5.1** and **5.2** (outer-ring).

As known, lateral fluoro substitution has a detrimental effect on the stabilities of the LC phase, especially the stabilities of smectic phase. On the other hand, it is the relative positioning of the lateral fluoro substituents on the molecular core that is of fundamental importance to mesomorphic behaviour[1, 5, 7]. Addition of lateral fluoro substituents in centre ring locations has a more drastic effect on the stabilities of mesophase thermal because of the resultant interannular twisting of the core than fluorination on the outer ring of the core.

Comparing the centre ring fluoro-substituted compound **20** (table **5.3**) to its outer ring analogues (compounds **28** and **36**, tables **2** and **3**) illustrates the effect of including the fluoro substituents in the centre ring (inner-core) rather than outer ring (outer-edge), compound **20** has a lower stability of SmC phase (92.0 °C) compared to compound **28** (146.0 °C) and compound **36** (137.0 °C). The reduced stability of SmC phase of compound **20** lets the nematic phase to be produced to high temperature (108.0 °C). This effect of lateral fluoro substituents in centre ring and outer ring locations on the stability of SmC phase is displayed in figure **5.13** for compounds **20**, **28** and **36**.

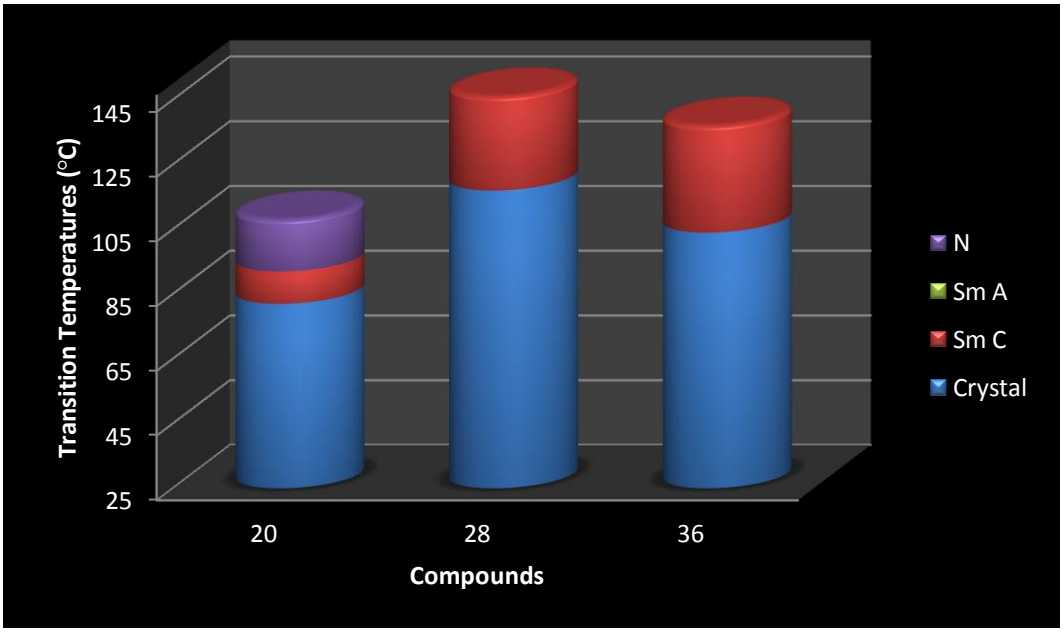

Figure 5.13. Effect on transition temperatures of relative positioning of the lateral fluoro substituents on the molecular core (*e.g.*, compounds 20, 28 and 36).

In figure **5.14**, comparing the centre ring fluoro-substitueted compound **21** (table **5.3**) to its outer ring analogues (compounds **29** and **37**, tables **5.1** and **5.2**) illustrates the effect of including the fluoro substituents in the centre ring (inner-core) rather than outer ring (outer-edge), compound **21** has a lower stability of SmC phase (90.0 °C) compared to compound **29** (140.0 °C) and compound **37** (124.0 °C). The reduced stability of SmC phase of compound **21** lets the nematic phase to be produced to high temperature (94.0 °C). This effect of lateral fluoro substituents in centre ring and outer ring locations on the stability of SmC phase is displayed in figure **5.14** for compounds **21**, **29** and **37**.

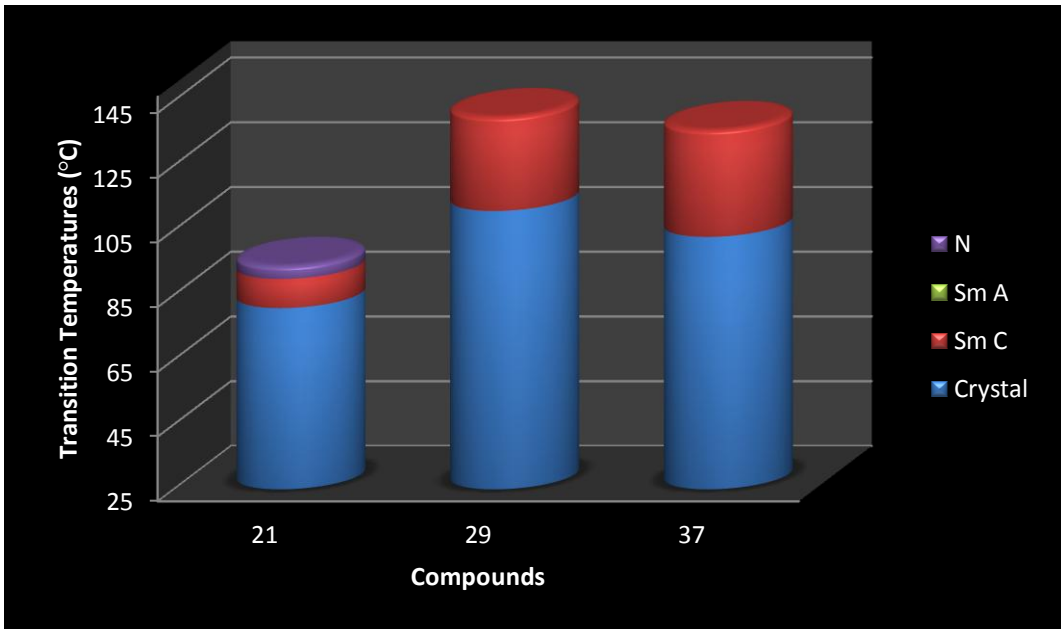

Figure 5.14. Effect on transition temperatures of relative positioning of the lateral fluoro substituents on the molecular core (*e.g.*, compounds 21, 29 and 37).

Compound **20** in table **5.3** has higher transition temperatures and melting point than compound **21** due to compound **20** has carbon atom and compound **21** has silicon atom. As known, carbon is smaller atom than silicon so the liquid crystals have a higher melting points and transition temperatures. Comparing the compound **20** to compound **A6** illustrates the difference of the mesophase morphology, melting points and transition temperatures. Compound **A6** has a lower melting point and transition temperatures than compound **20** due to compound **20** contain a terminal alkoxy chain which have higher transition temperatures and higher melting points than novel compounds with terminal alkyl chain such as compound **A6**. Also, compound **20** has longer terminal chain than compound **A6**. The comparison between compound **21** and compound **A7** (with C series) are the same as comparison between compound **20** and compound **A6** (with Si series). The final compound **73** did not show any liquid crystal phase. Nematic phase is only exhibited in compound **39** compared to compound **42** and **44**.

Compound **A8** has a lower melting point than compound **20**. Both compounds **A8** and **20** have smectic C and nematic phases.

Comparing the centre ring fluoro-substitueted compound **73** (table **4**) to its outer ring analogues (compound **82**, tables **2**) illustrates the effect of including the fluoro substituents in the centre ring (inner-core) rather than outer ring (outer-edge), compound **73** has a lower melting point (56.0 °C) compared to compound **82** (90.0 °C).

There are some examples of liquid crystal phases; Figures **5.15**, **5.16** and **5.17** show the Schlieren textures of the nematic liquid crystal phase of compounds **20** and **39** and the Focal Conic texture of the smectic C liquid crystal phase of compounds **21**.

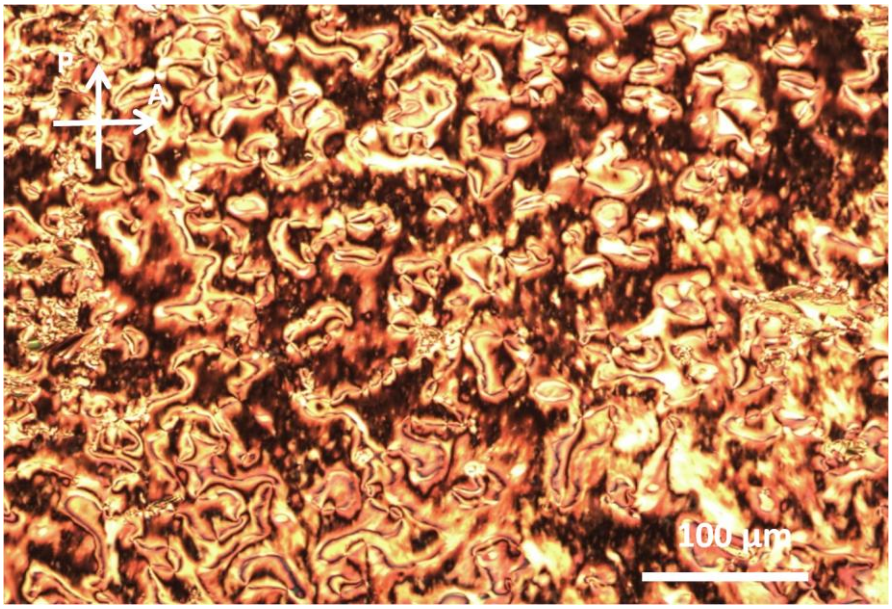

Figure 5.15. The nematic phase of compound 20 at 86 °C (Schlieren texture).

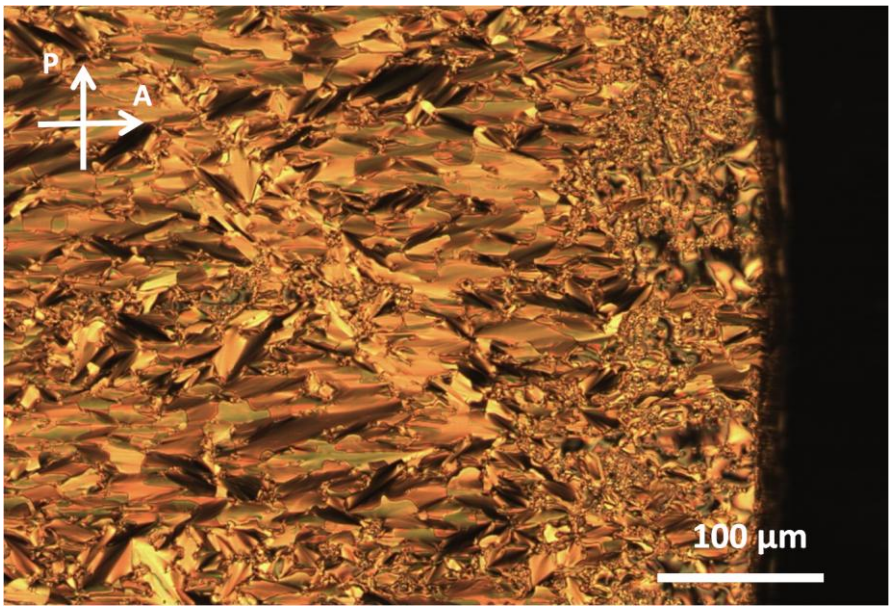

Figure 5.16. The SmC phase of compound 21 at 88 °C (Focal Conic texture).

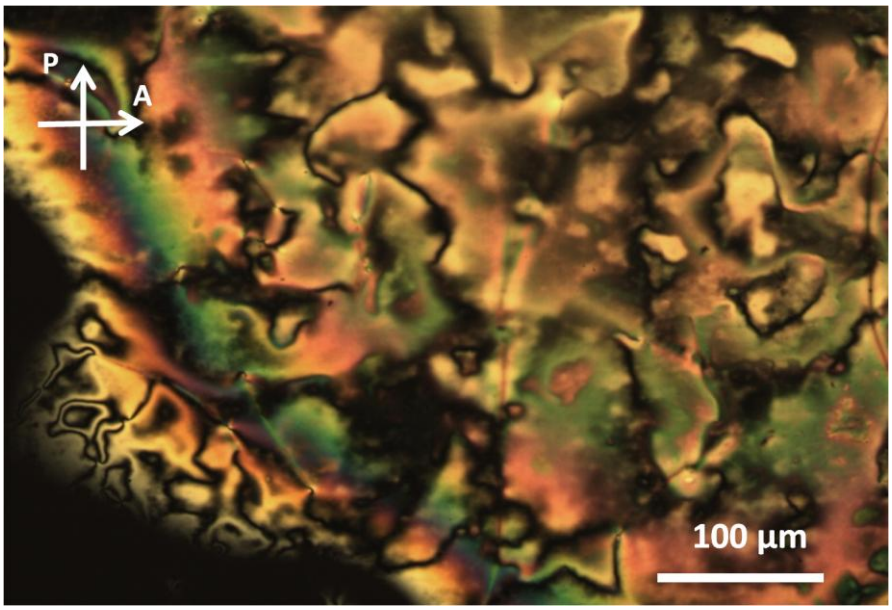

Figure 5.17. The nematic phase of compound 39 at 96 °C (Schlieren texture).

5.2 Cyclohexylbiphenyl Compounds (with the *ortho* difluorophenyl unit)

Table **5.4** illustrates the transition temperatures of novel compounds **59** and **60** with known compounds (**B1** and **B2**)[18] for comparison. The melting point and transition temperatures of compound **59** are higher than compound **60** due to compound **59** possesses terminal butyl unit and compound **60** possesses trimethylsilyl unit. Compound **B1** is a dialkyl and was thus not expected to display smectic C phase (although the dialkyl *ortho*-difluoroterphenyls do have high stabilities of the smectic C phase up to 120 °C)[1]. The technique in which the ring moieties pack tends to promote SmA phase formation (see figure **5.18**) and the lateral dipoles are not suitably placed in compound **B1** to disrupt the orthogonal molecular packing. On the other hand, compound **B1** is interesting due to its wide SmA range and its melting point.

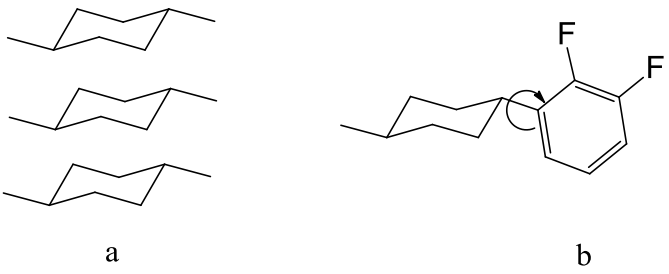

Figure 5.18. (a) Packing of cyclohexane rings promoting the smectic A phase. (b) Packing disrupted by the lateral fluoro-substituents.

The two novel alkoxy compounds (**59** and **60**) both introduce only the smectic A phase. The melting points of these compounds are high compared with compound **B2** (known compound). The lateral dipole of the ether oxygen in the terminal chain of compound **B2** combines with the strong lateral dipole from the *ortho*-difluoro unit to allow molecular tilting at a low temperature. Moreover, compound **B2** exhibits smectic C, smectic A and nematic phases but, compounds **59** and **60** exhibit just the

smectic A phase. Figure **5.20** shows the smectic A phase of compound **59** (Focal conic textures).

Table 5.4. The transition temperatures of those compounds with the fluoro substituents in the outer ring having the bulky terminal unit and known compounds for comparison.

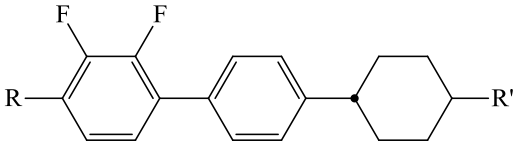

compound			Transition temperatures (°C)								
No.	R	R'	Cryst		SmC		SmA		N		Iso
59	$(CH_3)_3C(CH_2)_3O$	C_5H_{11}	●	79	___	___	●	129	___	___	●
60	$(CH_3)_3Si(CH_2)_3O$	C_5H_{11}	●	73	___	___	●	125	___	___	●
B1	C_5H_{11}	C_5H_{11}	●	33	___	___	●	97	●	123	●
B2	$C_8H_{17}O$	C_5H_{11}	●	54	●	57	●	126	●	142	●

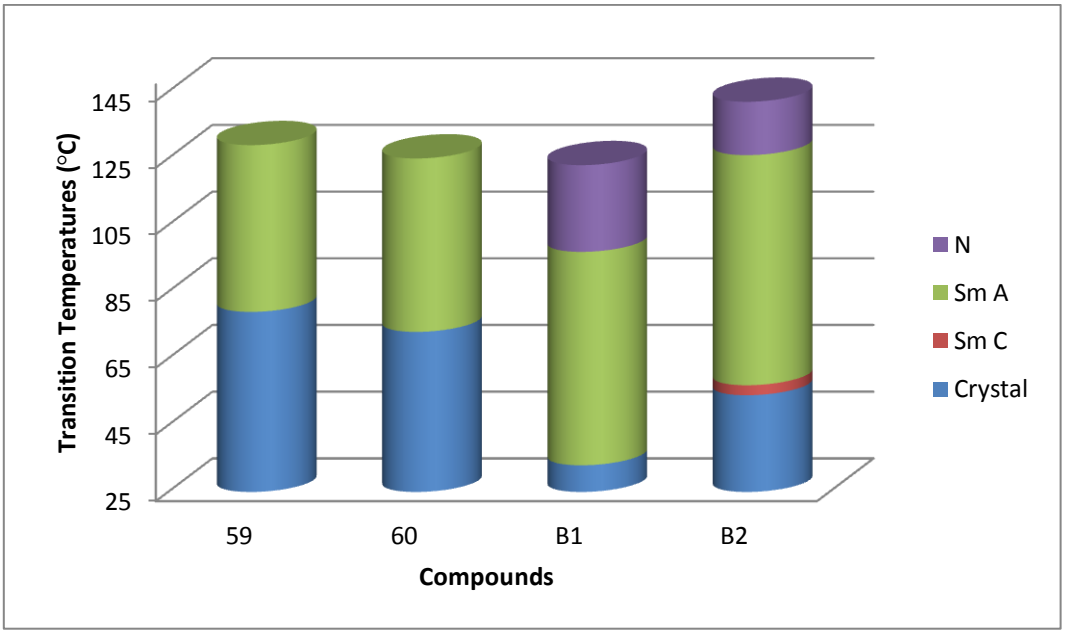

Figure 5.19. The transition temperatures for compounds 59, 60, B1 and B2.

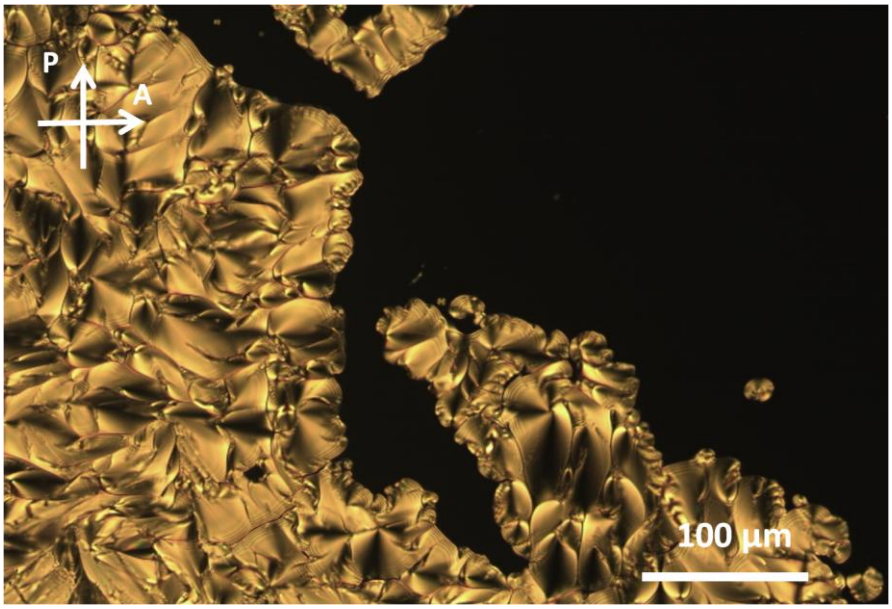

Figure 5.20. The SmA phase of compound 59 at 99 °C (Focal conic and homeotropic texture).

5.3 Cyclohexylterphenyl Compounds (with the *ortho* difluorophenyl unit)

Table 5.5. The transition temperatures of those compounds with the fluoro substituents in the outer ring having the bulky terminal unit and known compounds for comparison.

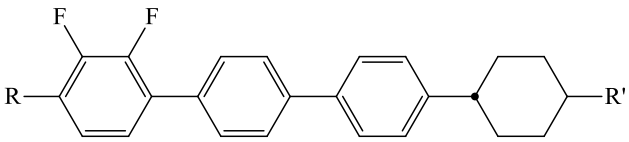

compound			Transition temperatures (°C)								
No.	R	R'	Crst		SmC		SmA		N		Iso
65	$(CH_3)_3C(CH_2)_3O$	C_5H_{11}	●	138	●	169.7	●	270	___	___	●
66	$(CH_3)_3Si(CH_2)_3O$	C_5H_{11}	●	136	●	169.3	●	255	___	___	●
71	$(CH_3)_3Si(CH_2)_2$	C_5H_{11}	●	72	●	167.5	●	251	___	___	●

Table **5.5** illustrates the transition temperatures of novel compounds **65**, **66** and **71**. The melting point and transition temperatures of compound **65** are higher than compound **66** due to compound **65** possessing terminal butyl unit and compound **66** possessing trimethylsilyl unit. Compound **66** has higher melting point and transition temperatures than compound **71** because compound **66** contains long terminal chain and oxygen. All the compounds **65**, **66** and **71** have smectic C and smectic A as shown in table **5.5**.

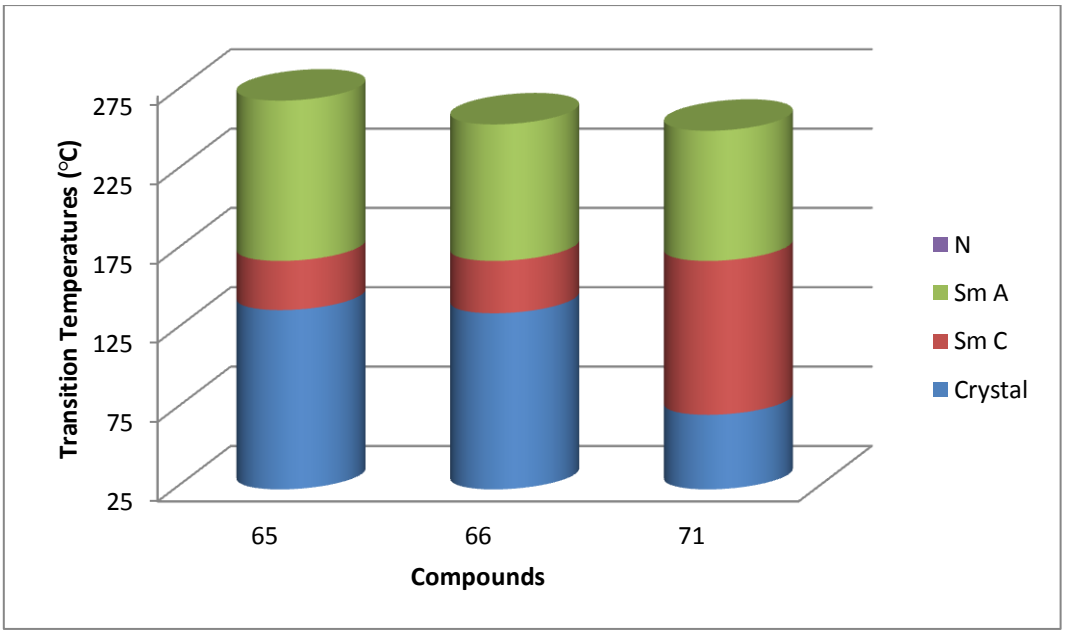

Figure 5.21. The transition temperatures for compounds 65, 66 and 71.

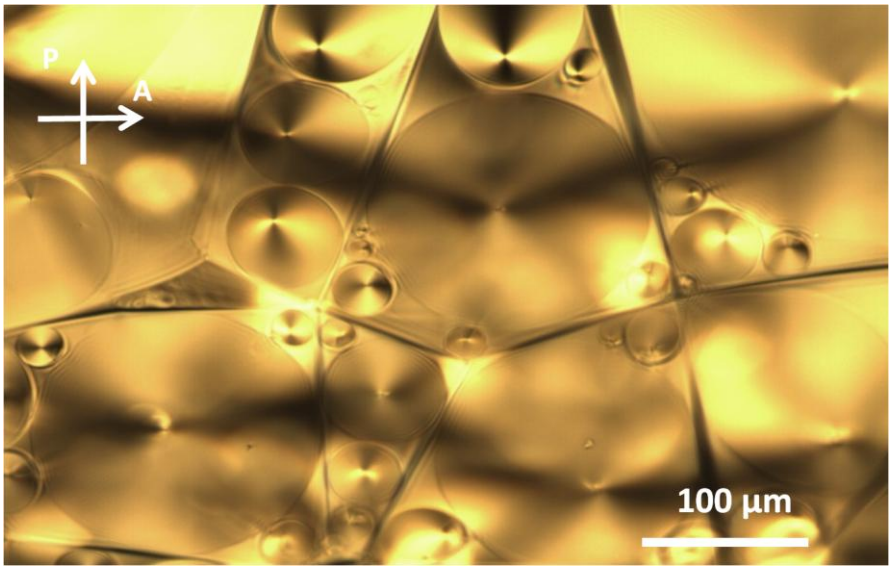

Figure 5.22. The SmA phase of compound 65 at 250 °C (Polyganal texture).

Table 5.6. The transition temperatures of those compounds with the fluoro substituents in the inner ring having the bulky terminal unit and known compounds for comparison.

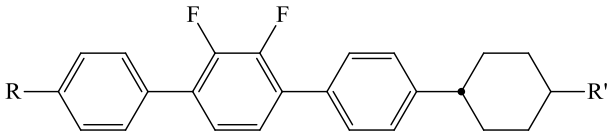

compound			Transition temperatures (°C)								
No.	R	R'	Cryst		SmC		SmA		N		Iso
69	$(CH_3)_3C(CH_2)_3O$	C_5H_{11}	●	119	●	227	___	___	●	253	●
70	$(CH_3)_3Si(CH_2)_3O$	C_5H_{11}	●	94	●	223	___	___	●	235	●

In table **5.6**, the novel compounds **69** and **70** illustrate smectic C and nematic phases. The melting point and transition temperatures of compound **70** are lower than compound **69** because of compound **69** has terminal butyl unit and compound **70** has trimethylsilyl. As known, carbon is smaller atom than silicon so the liquid crystals have a higher melting points and transition temperatures.

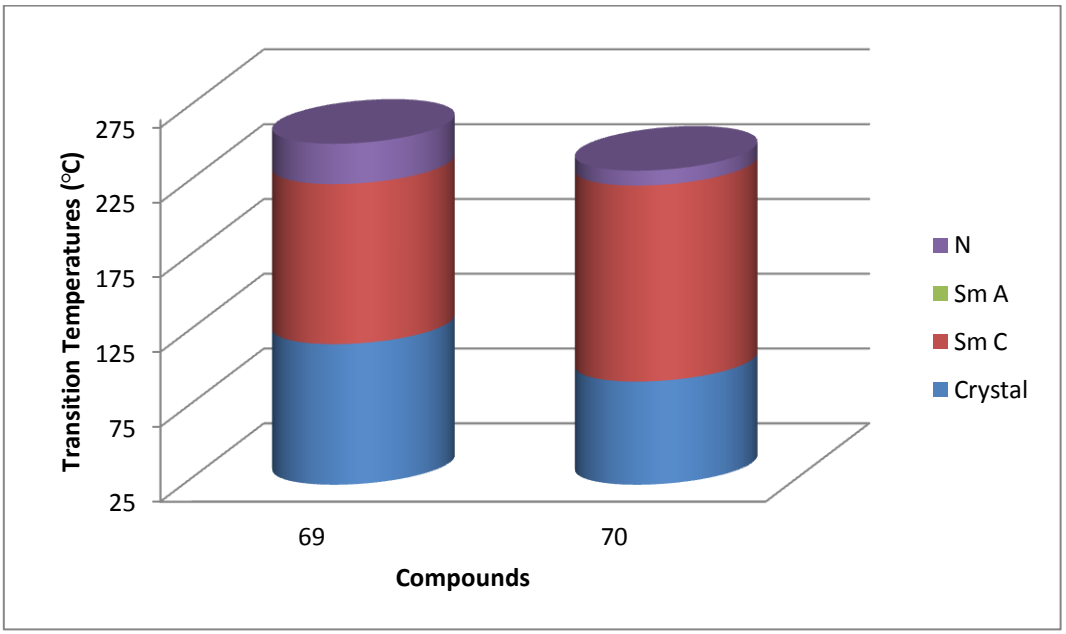

Figure 5.23. The transition temperatures for compounds 69 and 70.

5.4 Difluoroquarterphenyl Compounds

Table **5.7** illustrates the novel liquid crystal compounds (**90** and **91**) and the known compound **D1**. Compound **90** has a melting point (117 °C) lower than compound **91** (126 °C) because compound **91** has an alkoxy terminal chain. The novel compound **91**, which contains a terminal alkoxy chain, has higher transition temperatures and higher melting points than the novel compound **90** with terminal alkyl chain[12]. This is due to oxygen attached to the aromatic core. This oxygen extends the length of the rigid core and enhances anisotropy polarisability [14]. Moreover, the alkoxy terminal chain is more linear than the alkyl chain. The bond angle at the ring to CH_2 to alkyl chain is smaller than the angle for the ring to oxygen to alkyl chain. Both compound **90** and compound **91** exhibit smectic C and nematic phases. The smectic C stability in compound **91** is higher than SmC stability in compound **90**.

Table 5.7. The transition temperatures of those compounds with the fluoro substituents in the inner ring having the bulky terminal unit and known compounds for comparison.

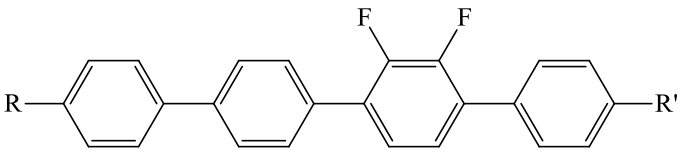

compound			Transition temperatures (°C)								
No.	R	R’	Cryst		SmC		SmA		N		Iso
90	$(CH_3)_3C$	C_7H_{15}	●	117	●	154	___	___	●	189	●
91	$(CH_3)_3C$	OC_8H_{17}	●	126	●	187	___	___	●	208	●
D1	C_5H_{11}	C_7H_{15}	●	86	●	193	●	220	●	275	●

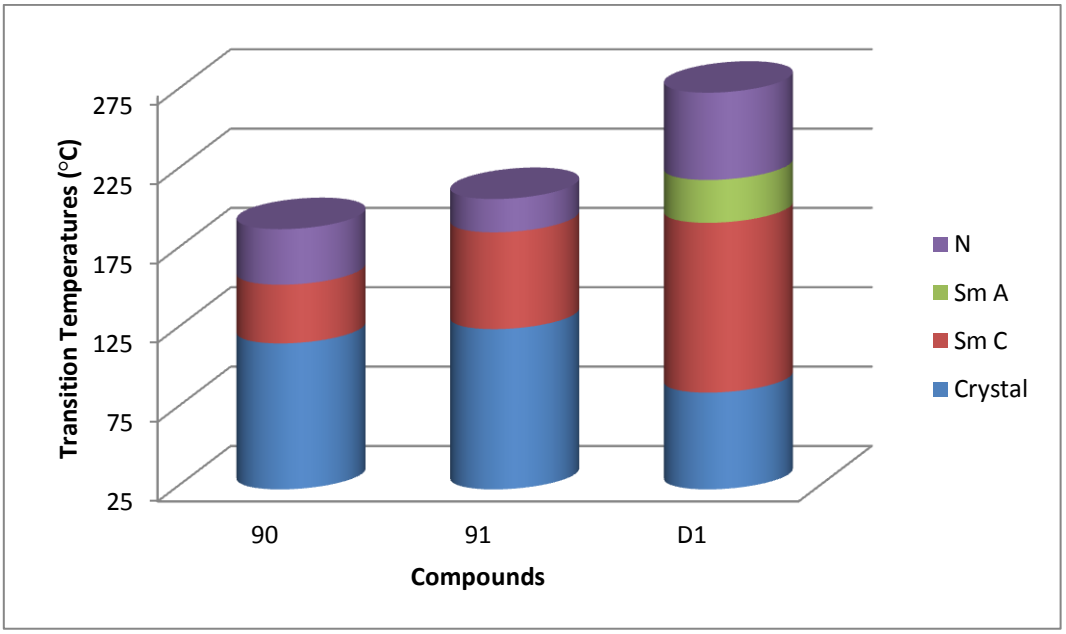

Figure 5.24. The transition temperatures for compounds 90, 91 and D1.

The compound **90** with the short bulky group has higher melting point and transition temperatures than the analogous compound **D1**. Compound **D1** possesses smectic C, smectic A and nematic phases, however compound **90** exhibits smectic C and nematic phases. The highest smectic C phase stability is 193 °C (compound **D1**).

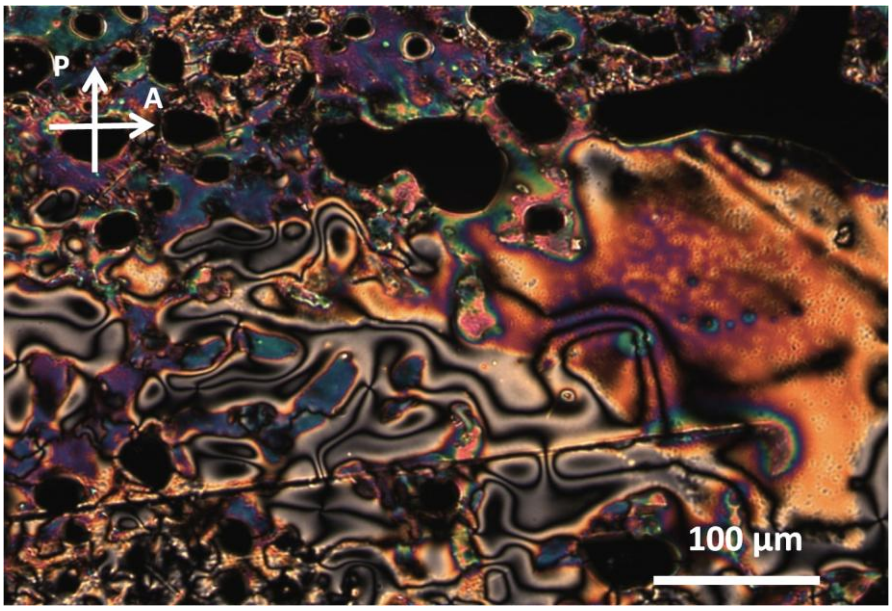

Figure 5.25. The nematic phase of compound 90 at 188 °C (Schlieren texture).

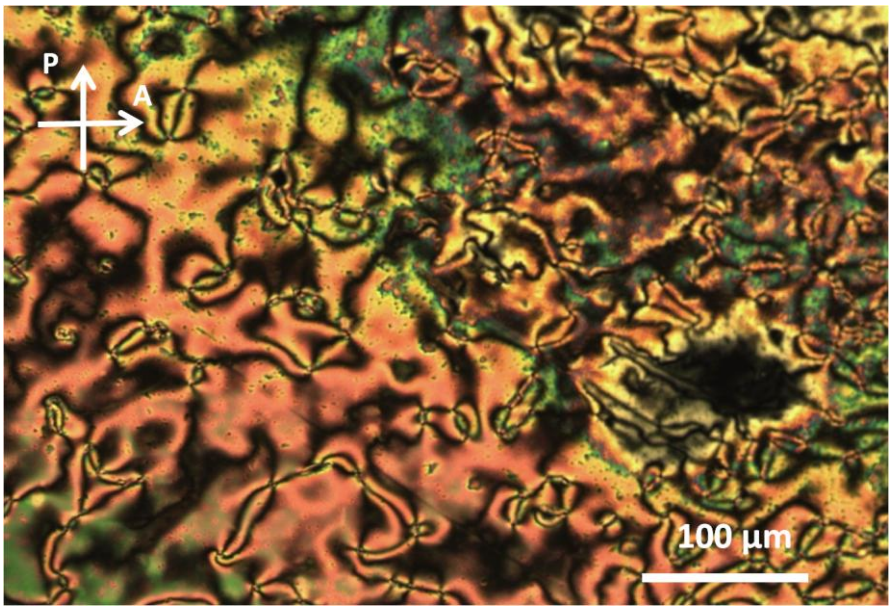

Figure 5.26. The nematic phase of compound 91 at 203 °C (Schlieren texture).

5.5 Mixture Studies on Compounds having a Bulky end group

Assessments of the miscibility of compounds with bulky end groups were carried out. Compounds **20**, **36**, **39**, **42**, **44**, **59**, **73** and **87** were mixed with a host material. The host material chosen for the mixture work was **KCHM211** (see table **5.8**), which is composed of compounds of comparable core structures to the novel molecules being assessed. Each of these compounds (**20**, **36**, **39**, **42**, **44**, **59**, **73** and **87**) was mixed with **KCHM211** in different percentages (such as 10 %, 20 %, 30 %, 40 %, 50 %, 60 %, 70 %, 80 %, 90 % and 100 %) as shown in figures **5.27** to **5.35**. These mixtures were to be used later with chiral compound **BE8OF2N** to generate ferroelectric mixtures for further evaluation.

Table 5.8. Transition temperatures (°C) for mixtures of compound KCHM211.

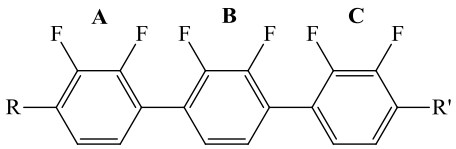

Compound			Transition temperatures										
No	R	R'	Cr		SmI		SmC		SmA		N		I
A	C_5H_{11}	C_7H_{15}	●	36.5	-	-	●	(24)	-	-	●	111	●
B	C_5H_{11}	C_7H_{15}	●	65.5	●	74.5	●	118.5	●	135	●	137	●
C	C_5H_{11}	C_7H_{15}	●	56	-	-	●	105.5	●	131	●	136	●
Mix	A:B:C	2:1:1	●	15	-	-	●	91.5	●	99.5	●	124	●

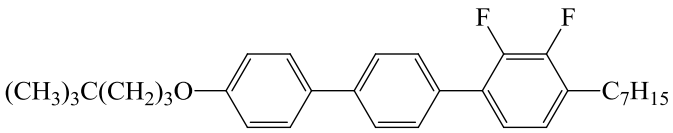

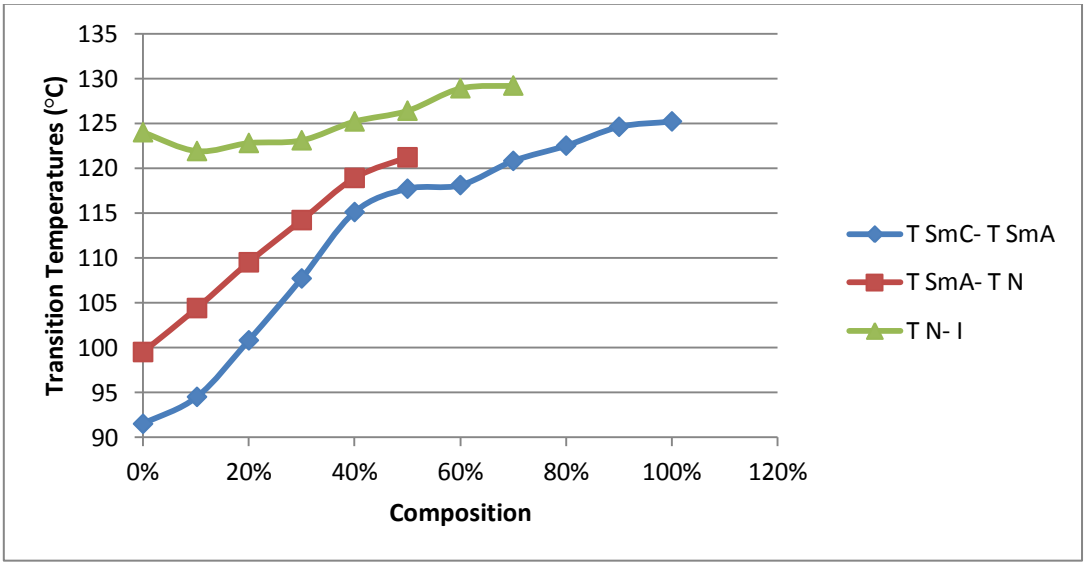

Figure 5.27. Transition temperatures (°C) for mixtures of compound 36 and KCHM211 in different percentage (miscibility of compound 36 with KCHM211).

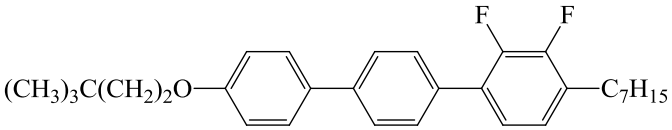

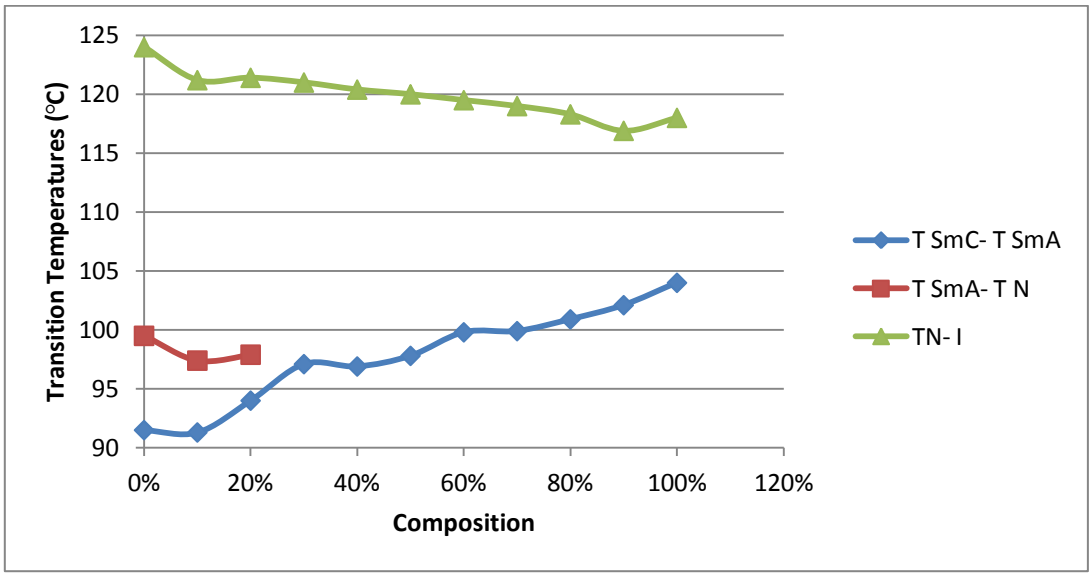

Figure 5.28. Transition temperatures (°C) for mixtures of compound 44 and KCHM211 in different percentage (miscibility of compound 44 with KCHM211).

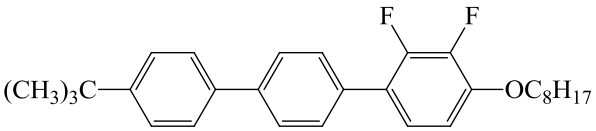

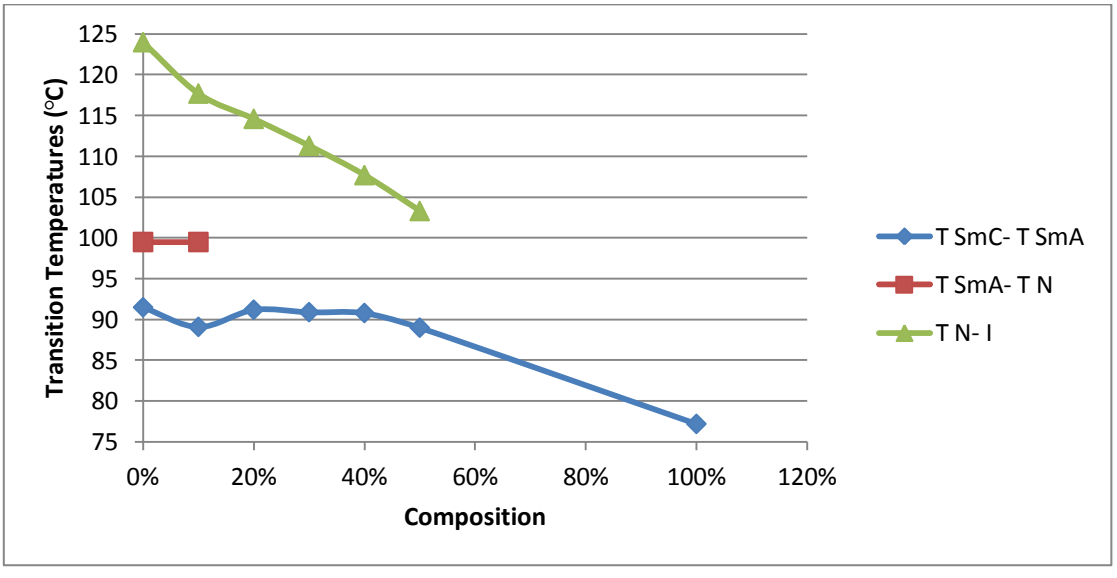

Figure 5.29. Transition temperatures (°C) for mixtures of compound 87 and KCHM211 in different percentage (miscibility of compound 87 with KCHM211).

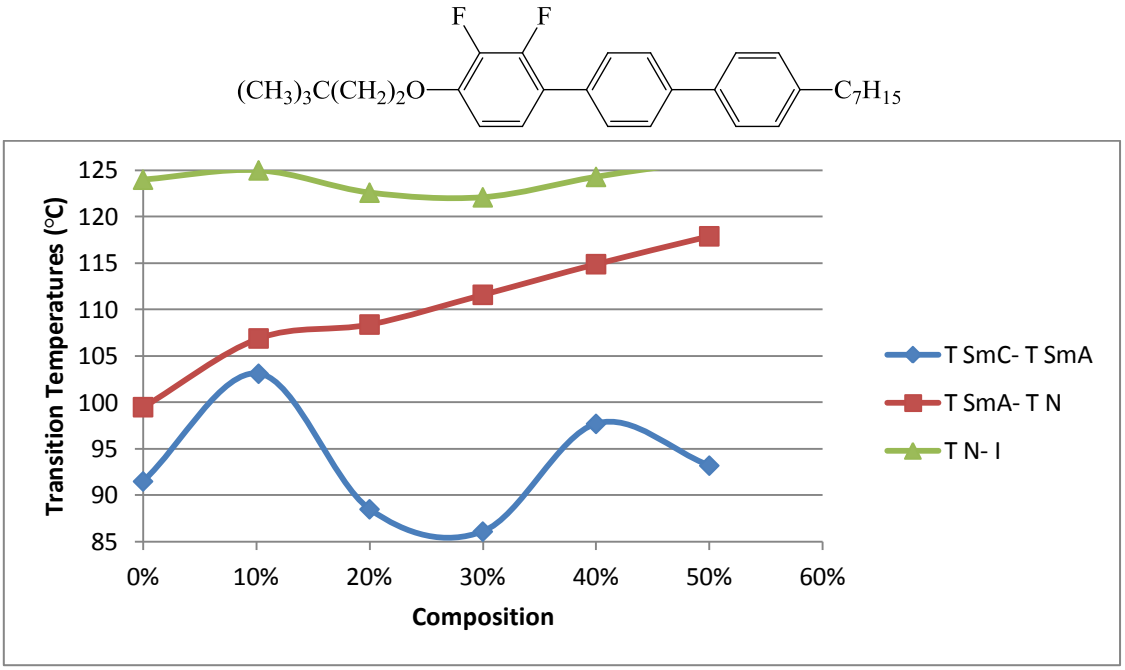

Figure 5.30. Transition temperatures (°C) for mixtures of compound 42 and KCHM211 in different percentage (miscibility of compound 42 with KCHM211).

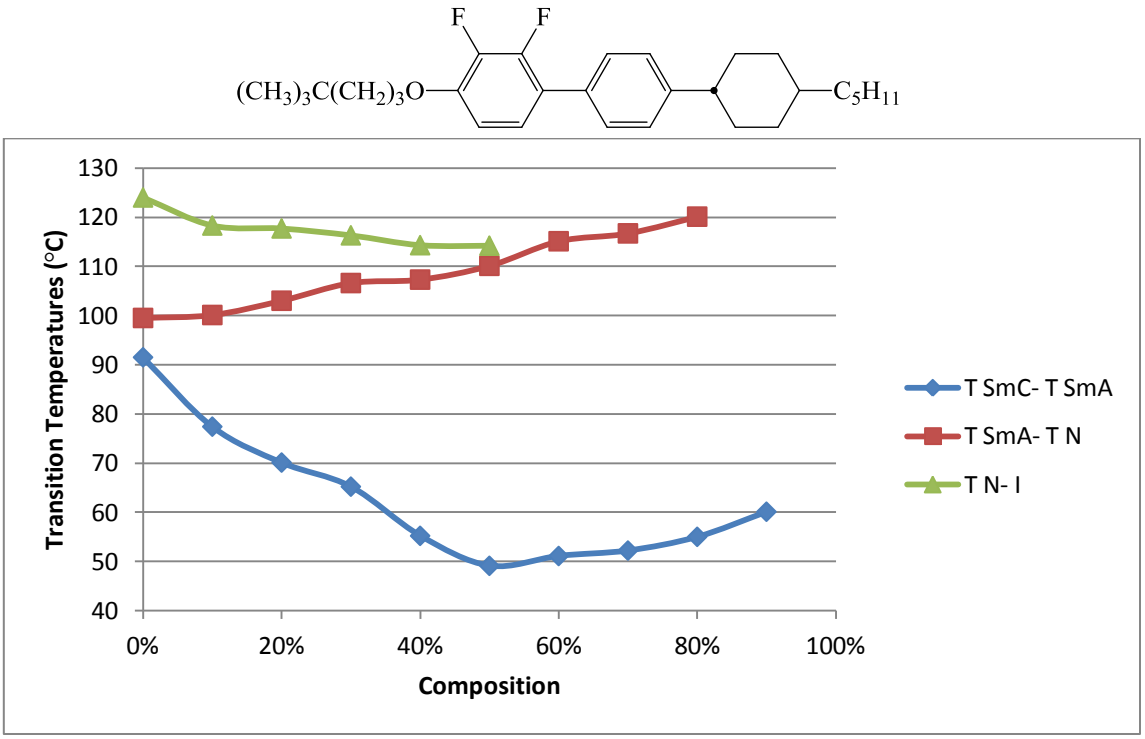

Figure 5.31. Transition temperatures (°C) for mixtures of compound 59 and KCHM211 in different percentage (miscibility of compound 59 with KCHM211).

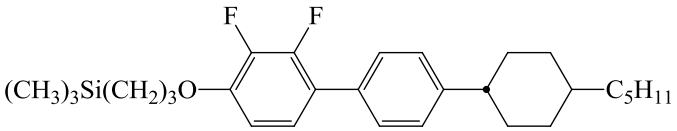

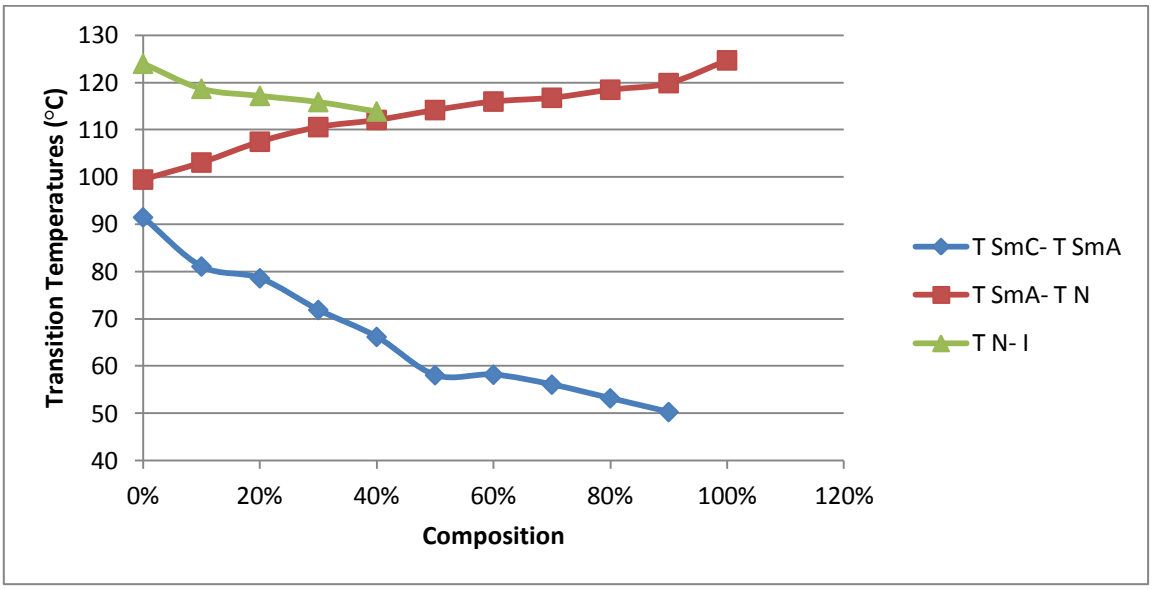

Figure 5.32. Transition temperatures (°C) for mixtures of compound 60 and KCHM211 in different percentage (miscibility of compound 60 with KCHM211).

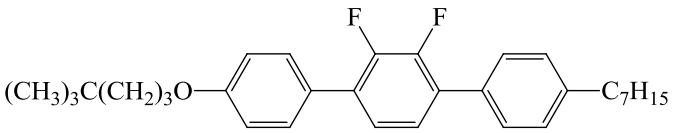

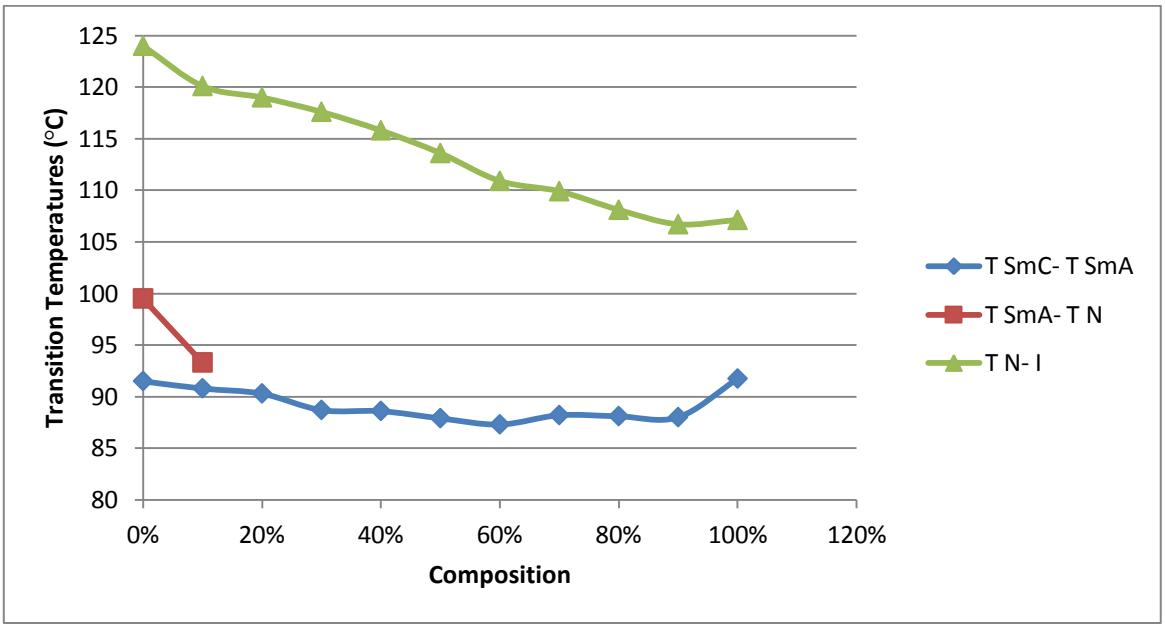

Figure 5.33. Transition temperatures (°C) for mixtures of compound 20 and KCHM211 in different percentage (miscibility of compound 20 with KCHM211).

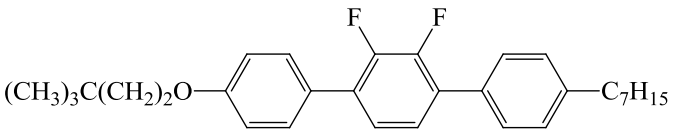

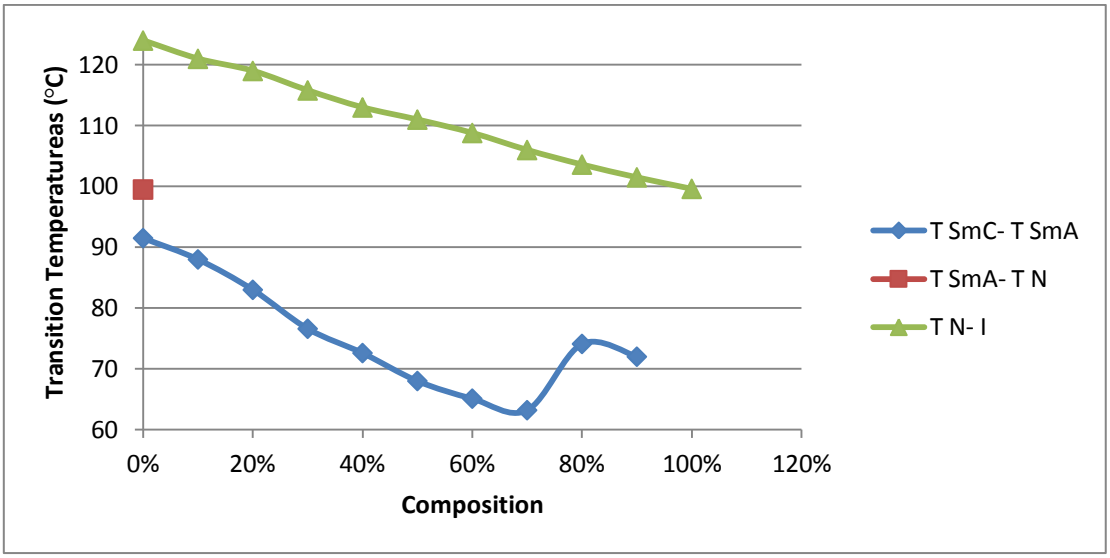

Figure 5.34. Transition temperatures (°C) for mixtures of compound 39 and KCHM211 in different percentage (miscibility of compound 39 with KCHM211).

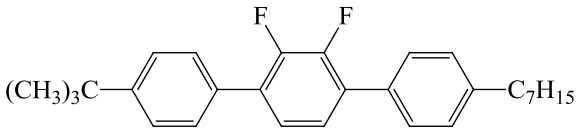

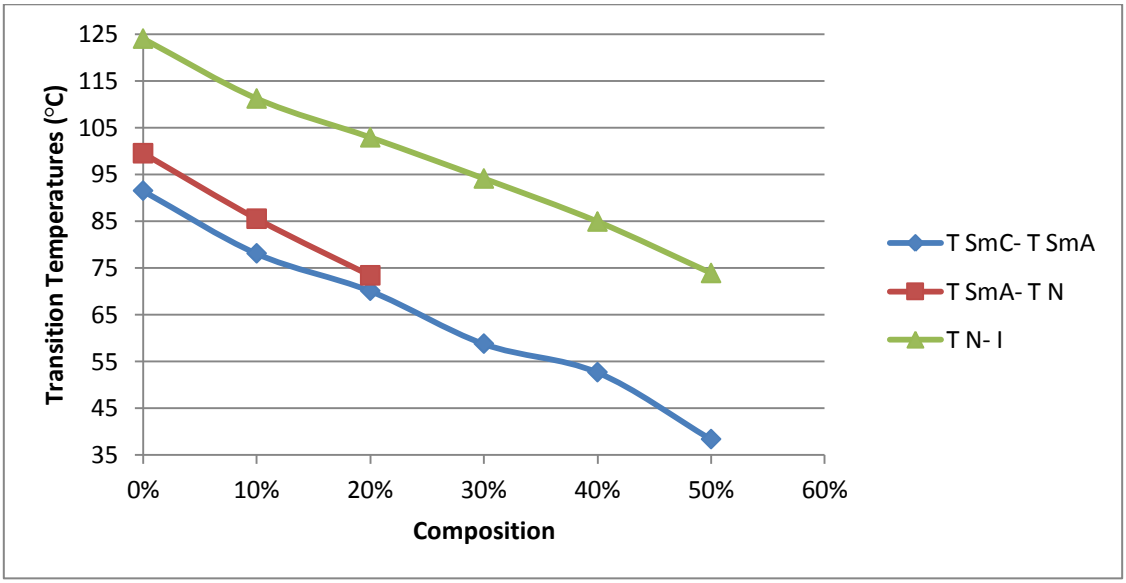

Figure 5.35. Transition temperatures (°C) for mixtures of compound 73 and KCHM211 in different percentage (miscibility of compound 73 with KCHM211).

5.5.1 Discussion of Achiral Miscibility Studies

Table **5.8** shows the transition temperatures of the three materials constituting KCHM211, the composition and the transition temperatures of this well-known ferroelectric host mixture. Several novel compounds with bulky end groups were selected for miscibility studies on the basis of their mesomorphism. Compound **36** has a similar core structure to the materials of the host mixture, however, the mesomorphism is somewhat different with only a smectic C phase being exhibited to 137 °C (see Table **5.2**). This difference in mesomorphism is wholly attributed to the bulky nature of the terminal chain, which is causing molecular segregation and hence conferring a strong smectic tendency, and because of the strong lateral dipole the tilted smectic C phase is exhibited. On adding compound **36** to the KCHM211 (Figure **5.27**) the nematic phase stability is largely unaffected, but does increase in value slightly, despite compound **36** not exhibiting the nematic phase, which is masked by the very high smectic tendency. The smectic phases (SmA and SmC) are both enhanced in phase stability very markedly, proving the influence of the bulky terminal chain on molecular segregation and hence generating high smectic phase stability. The SmC phase stability, aided by the lateral polarity from the combination of ether oxygen and the two lateral fluoro substituents, continues to rise sharply to 136 °C, which is the value for 100% compound **36**. However, the SmA phase stability stalls at around 80% composition because of the very strong tendency towards the SmC phase.

Figure **5.28** shows the influence of compound **44**, which has a mesomorphism (°C) of Cryst 72 SmC 104 N 118 Iso (see Table **5.2**), on the KCHM211 host mixture. The nematic phase stability of KCHM211 reduces in a normal manner towards 118 °C as 100% compound **44** is approached. However, because the smectic C phase is so well supported by the high lateral dipole of compound **44** the SmA phase stability is eliminated from mixtures of just 20% of compound **44**, with the SmC phase stability rising gradually towards 104 °C.

Figure **5.29** shows a rather different scenario to figure **5.28** as compound **87** has a rather low SmC phase stability because of the bulky group being directly attached to the core. Hence compound **87** is very destructive to the mesomorphism of the

KCHM211. However, it is interesting to see the nematic phase stability falling very steeply for the first 50% of compound **87**, and even more significantly the SmA phase disappearing beyond 10%. Yet it is surprising to see the SmC phase stability being upheld until beyond the 50% of compound **87**, which must be attributed to the high lateral polarity of the two fluoro substituents in combination with the adjacent ether oxygen.

Figure **5.30** involves compound **42**, which is analogous in structure to compound **44** shown in Figure 5.28, except for the location of the two lateral fluoro substituents. Compound **42** has a mesomorphism (°C) of Cryst 106 SmC 121 SmA 126 N 129 Iso (see Table 5.1), which is significantly higher than that of compound **44**. The effect of compound **42** on the mesomorphism of KCHM211 is quite normal for the nematic and SmA phase stability, and both rise gradually towards that for 100% compound **42**. However, the SmC phase stability behaves in a most unusual manner with an initial increase, then a marked, steep fall, followed by another rise and fall, and does not look like ever reaching the 121 °C of 100% compound **42**. There appears to be a rather marked incompatibility of the SmC phase exhibited by KCHM211 and that of compound **42**.

The use of a cyclohexane-containing material such as compound **59** in ferroelectric mixtures is most advantageous in terms of the low birefringence required for ideal device performance. With a mesomorphism (°C) of Cryst 79 SmA 129 Iso (see Table **5.4**), compound **59** does not actually exhibit the desired SmC phase, but provided it is not too destructive in host materials then it could still be used advantageously. As can be seen in Figure **5.31**, compound **59** is indeed a very good promoter of a smectic A phase, largely expected because of the cyclohexane ring and the bulky end group. The nematic phase stability tails off slightly, but is quickly subsumed by the steeply rising SmA phase stability, hence the nematic and SmA phase stability is being affected in the expected manner. As might be feared from a compound with such a strong tendency for a SmA phase, the SmC phase stability of the host material is decimated by the addition of compound **59**. However, the fall does stop at around 50% composition and the SmC phase stability recovers somewhat and begins to rise towards the melting point area of compound **59**.

The silyl analogue of compound **59** (compound **60**) is also very strongly SmA in its mesomorphism (°C) of Cryst 73 SmA 125 Iso (see Table **5.4**), rather surprisingly so given the larger size of the silicon compared with a carbon. As can be seen in Figure **5.32**, the influence of compound **60** on the mesomorphism of the host material is very similar to that seen for compound **59**, except that the SmC phase stability fails to pick up.

Hence the cyclohexane compounds with the bulky end groups would not be considered suitable for ferroelectric mixtures, which is disappointing given the need for lower birefringence in such commercial mixtures.

Difluoroterphenyls with the two fluoro substituents in the centre ring are not renowned for their support of smectic phases, however, the nature of the bulky end group in promoting phase separation leads to relatively high smectic phase stability, which when combined with the high lateral dipole manifests as the tilted SmC phase in compounds such as **20** and **39**. Such a location of the two fluoro substituents, as in compounds **20** and **39** away from the edge of the core confers a relatively low viscosity, so the inclusion of such compounds in ferroelectric mixtures would be most advantageous in terms of short switching times.

Compound **20** shows a very high SmC phase stability considering the nature of the core, with a mesomorphism (°C) of Cryst 82 SmC 92 N 108 Iso. When added to the ferroelectric host material, compound **20** shows an ideal behaviour with the nematic phase stability reducing quite rapidly, the SmA phase falling very steeply, and the SmC phase stability upholding very well across the phase diagram (Figure **5.33**). Hence, compound **20** in the host material was chosen to be carried forward for evaluation in ferroelectric mixtures (see Figures **5.39** and **5.40**).

Compound **39** has a bulky end group that gives a non-linear angle from the core and hence would be expected to have a lower mesomorphism (°C) of Cryst 95 N 100 Iso (see Table **5.3**), and a reduced smectic tendency. The addition of compound **39** to the host mixture (Figure **5.34**) results in an immediate destruction of the SmA phase stability, but the nematic phase stability behaves normally. The SmC phase stability is also markedly depressed but does remain prevalent, and rather strangely shows an

upturn towards 100% composition, rather like the behaviour seen for compound **42** (see Figure **5.30**), which has the same non-linear bulky end group.

Compound **73** has the bulky end group as close as is possible to the core, and it is this location that might be expected to cause the most influence on the phase separation of molecules so as to eliminate layer shrinkage on cooling to the smectic C phase. However, this structural architecture is also expected to result in a very low mesophase stability, and this is reflected in the lack of mesomorphism Cryst 56 Iso (°C) for compound **73** (see Table **5.3**). Nevertheless the behaviour of compound **73** in mixtures with the host material needed to be evaluated (see Figure **5.35**). Interestingly, the phase stability of the nematic, SmA and SmC phases is all equally affected in a destructive manner, and so only mixtures to 50% were evaluated.

5.6 Electro-Optical Studies of Bulky end Groups in a Standard Mixture

5.6.1 Experimental Techniques

Many of the novel compounds prepared were mixed with standard ferroelectric mixture (KCHM211) and a chiral dopant to determine the magnitude of their tilt angle and spontaneous polarisation (Ps) as a temperature function. The tilt angle and spontaneous polarisation (Ps) measurements were carried out in 5 μm cells filled by capillary action as shown below. The cells used were coated with an antiparallel-rubbed polyimide alignment layer.

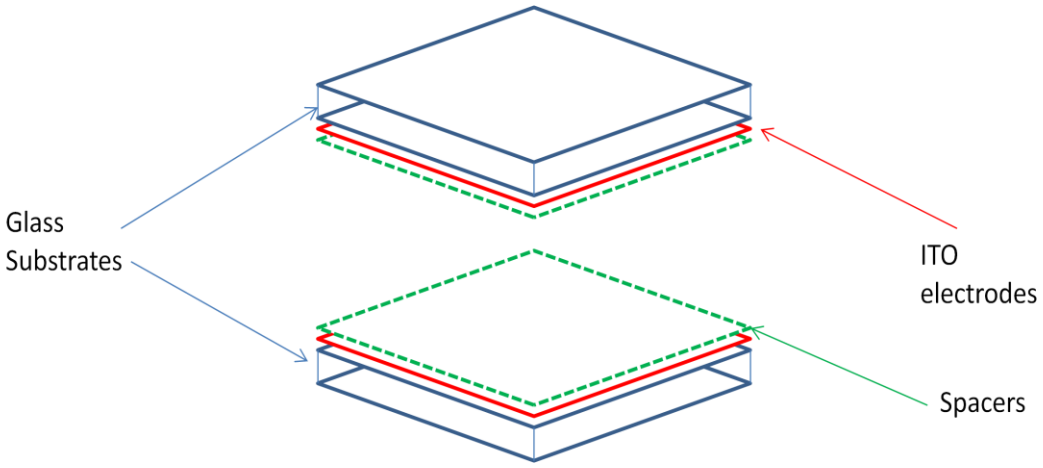

Figure 5.36. An exploded view of a cell used for electro-optical studies.

Figure **5.36** illustrates an exploded view of a typical cell which includes three parts (glass substrates, ITO electrodes and spacers). The way used to fill the cell was to allow the material to flow into the cell at a temperature around 10 °C above the clearing point and then leave it to cool. Two wires were attached on top and bottom of the cell (using indium metal) to provide a connection to the electrodes for the application of an electric field. Directly, the cell was placed in the heating stage (THM600) on an optical microscopy (Zeiss microscope). The heating stage was controlled by the temperature controller (Linkam TP61).

The liquid crystal sample was aligned homogeneously. It was cooled from isotropic liquid into the chiral smectic C (SmC*) via the chiral nematic (N*) and chiral smectic A (SmA*) phases as shown below:

(cooling) Iso ⟶ N* ⟶ SmA* ⟶ SmC*

The best way to get optimum alignment in the cells was as follows;

Frequency = 200 Hz.

Voltage = ± 10 V (2 V μm^{-1} for the 5 μm cells).

Cooling rate = 0.2 $^{\circ}C\ min^{-1}$.

The desired cooling sequences (N – SmA – SmC) to get good homogeneous alignment was not present the majority of the novel compounds prepared. Therefore, a standard host mixture was used to give the desired cooling sequence and the novel ferroelectric host compounds were added in the proportion as illustrated below. The **KCHM211** mixture (see table **9**) is composed of the following compounds (% by weight):

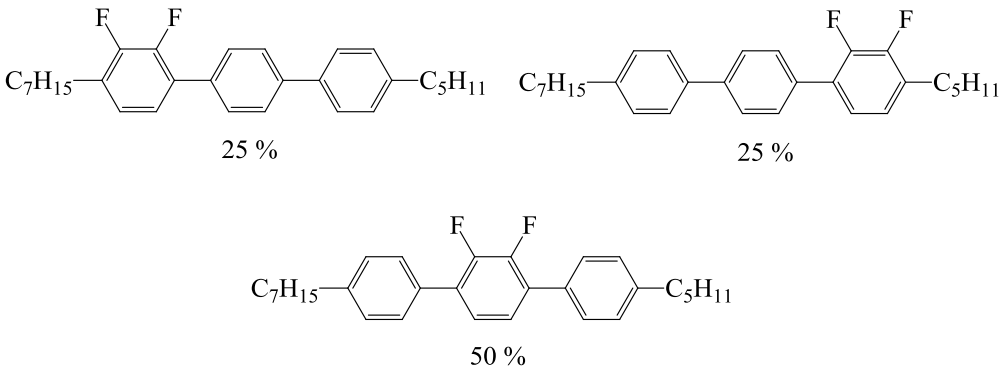

Figure 5.37. The percentage (% by weight) of the compounds in KCHM211 mixture.

The novel compounds was mixed with the **KCHM211** mixture (see figures **5.27** to **5.35**) then doped with chiral dopant (**BE8OF2N** dopant) as shown in figure **5.38**. The materials selected for this study were compounds **20**, **36**, **39**, **42**, **44**, **59**, **60** and **87**.

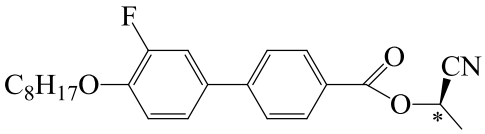

Figure 5.38. chiral dopant (BE8OF2N dopant).

5.6.2 Procedure for Measuring Ps Values

The cell was placed in the heating stage on a Zeiss microscope and connected to the electronic wave generator. An AC driving voltage was applied using a triangular waveform therefore that when the electrical field started to increase in the cell, at a certain area the dipoles would align with the field and aligned sample would switch. By using the computer programme the spontaneous polarisation (Ps) was calculated automatically.

The spontaneous polarisation (Ps) value was measured by the application of an AC driving voltage using a triangular waveform to an aligned chiral smectic C (SmC*). Also, this method is known as current reversal.

The spontaneous polarisation (Ps) reported in nC cm^{-2}. The good field applied across the cell ±50 V at a frequency (20 Hz), which was possible to observe the sample switching.

The spontaneous polarisation (Ps) values for all the samples increased when the temperature decreased.

5.6.3 Tilt Angle Measurements

The measurements of the tilt angles of aligned sample were measured by applying a driving voltage using a square waveform across the cell ±50 and lower frequency (10 mHz is typically) to determine the extinction point. The sample was rotated through the minimum angle in order when the switching had occurred to get optical extinction again. This measurement provided the cone angle. The tilt angle is θ.

5.6.4 Tilt Angle and Ps Measurements for compounds 20mix1*, 20mix2*, 36mix1*, 36mix2*, 39mix1*, 42mix1*, 44mix1*, 59mix1*, 60mix1* and 87mix1*.

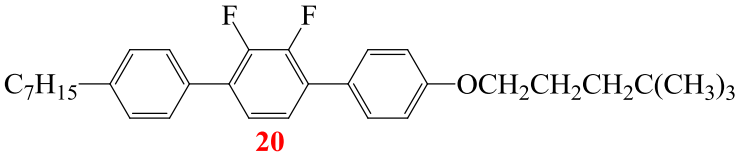

20

The compound **20mix1** is 20 % of the novel compound **20** with 80 % of **KCHM211** mixture, see figure **5.33** (% by weight).

The chiral compound **20mix1** (**20mix1***) is 93 % of (**20mix1**) with 7 % of chiral dopant (**BE8OF2N**).

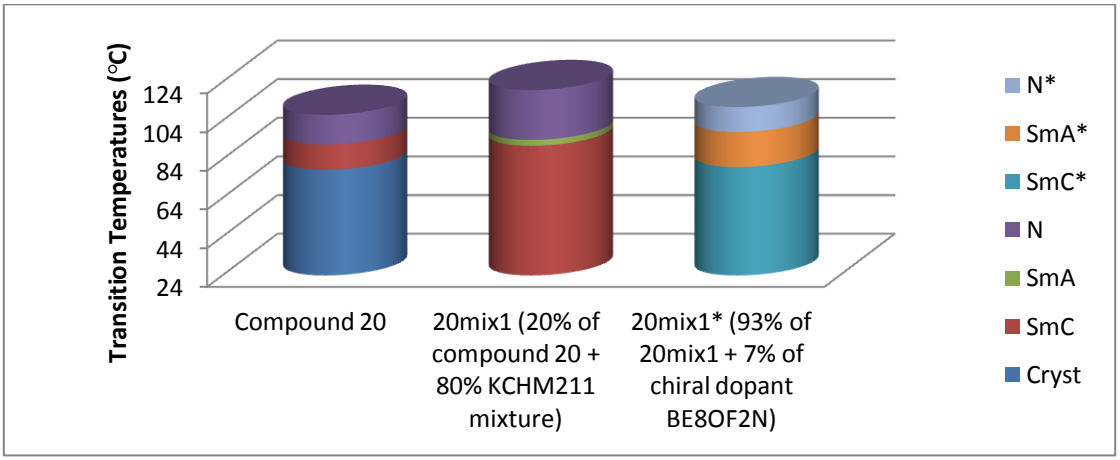

Figure 5.39. The difference of transition temperatures between compound 20, 20mix1 and 20mix1*.

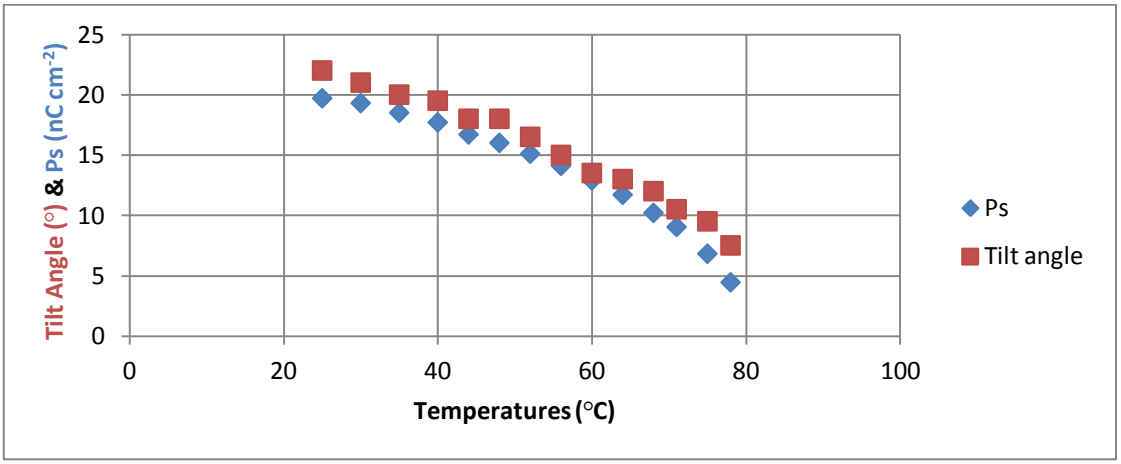

Figure 5.40. The Ps and tilt angle *vs* temperatures of compound 20mix1*.

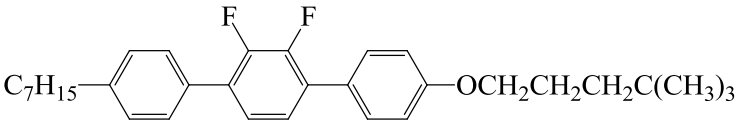

20

The compound **20mix2** is 40 % of the novel compound **20** with 60 % of **KCHM211** mixture, see figure **5.33** (% by weight).

The chiral compound **20mix2** (**20mix2***) is 93 % of (**20mix2**) with 7 % of chiral dopant (**BE8OF2N**).°

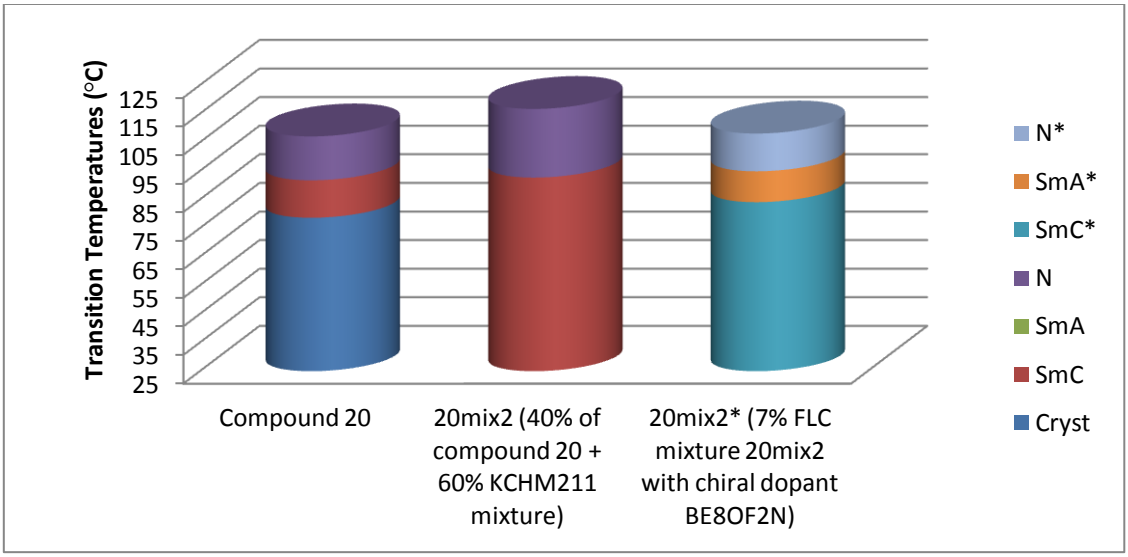

Figure 5.41. The difference of transition temperatures between compound 20, 20mix2 and 20mix2*.

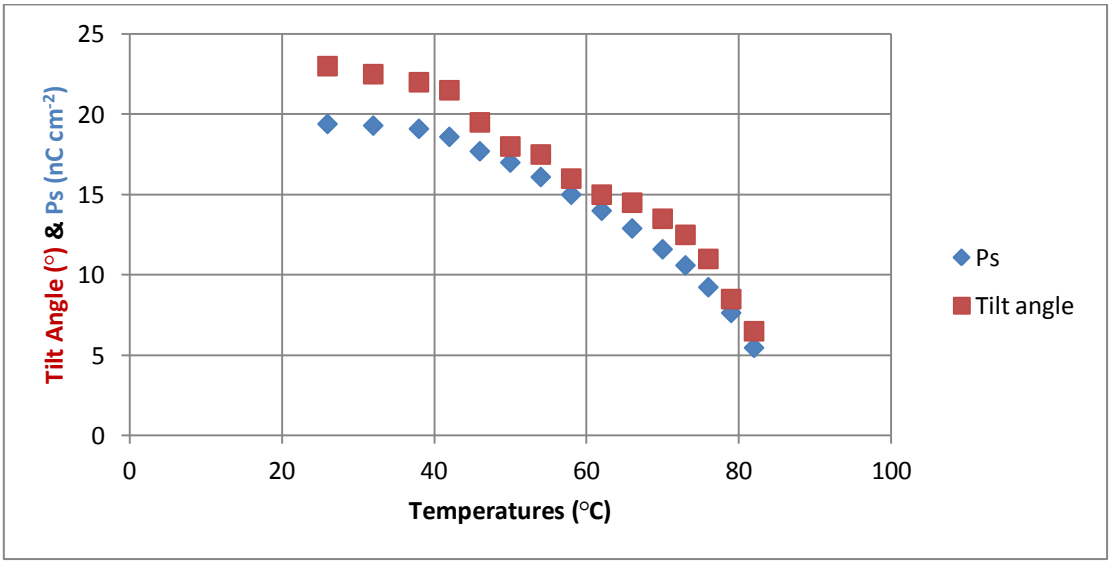

Figure 5.42. The Ps and tilt angle *vs* temperatures of compound 20mix2*.

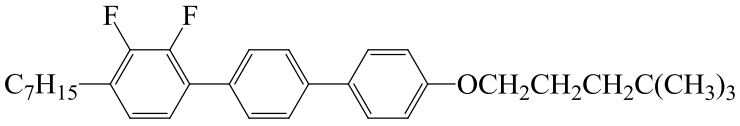

36

The compound **36mix1** is 20 % of the novel compound **36** with 80 % of **KCHM211** mixture, see figure **5.27** (% by weight).

The chiral compound **36mix1** (**36mix1***) is 93 % of (**36mix1**) with 7 % of chiral dopant (**BE8OF2N**).

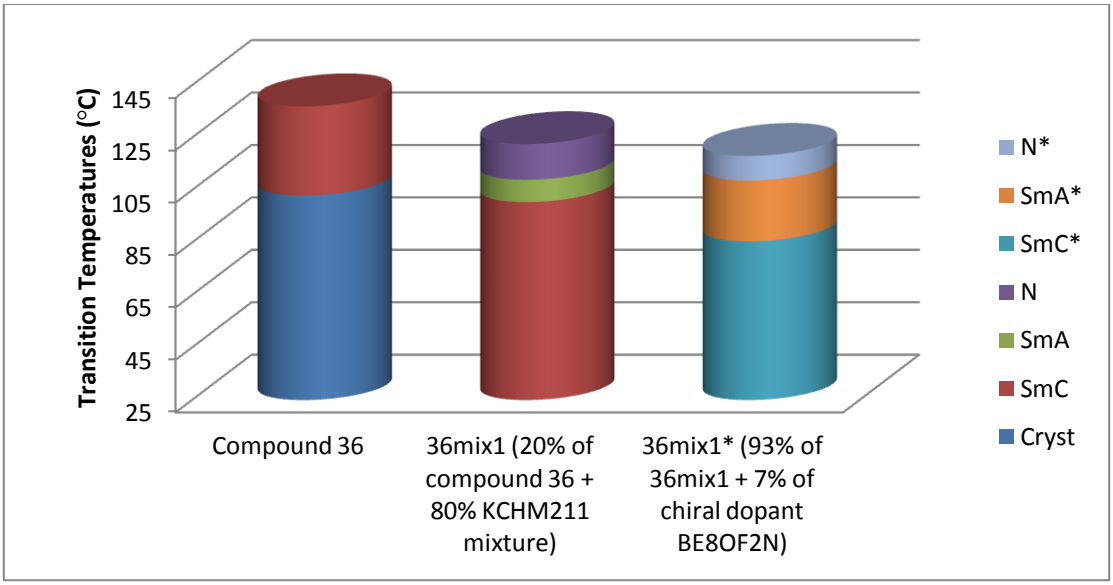

Figure 5.43. The difference of transition temperatures between compound 36, 36mix1 and 36mix1*.

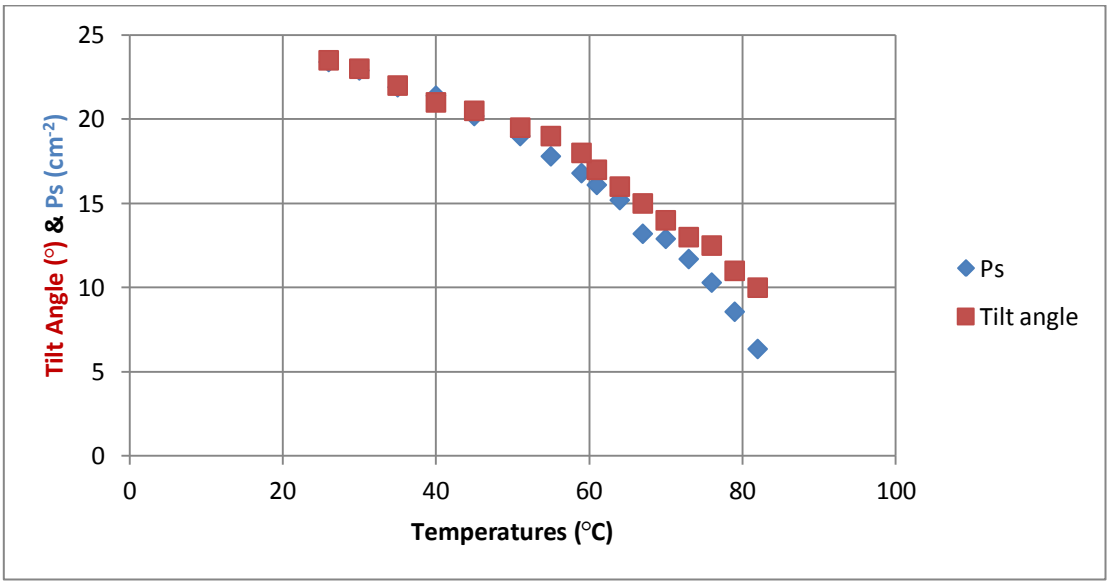

Figure 5.44. The Ps and tilt angle *vs* temperatures of compound 36mix1*.

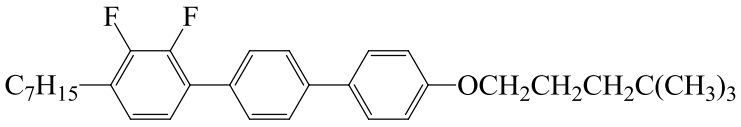

36

The compound **36mix2** is 40 % of the novel compound **36** with 60 % of **KCHM211** mixture, see figure **5.27** (% by weight).

The chiral compound **36mix2** (**36mix2***) is 93 % of (**36mix2**) with 7 % of chiral dopant (**BE8OF2N**).

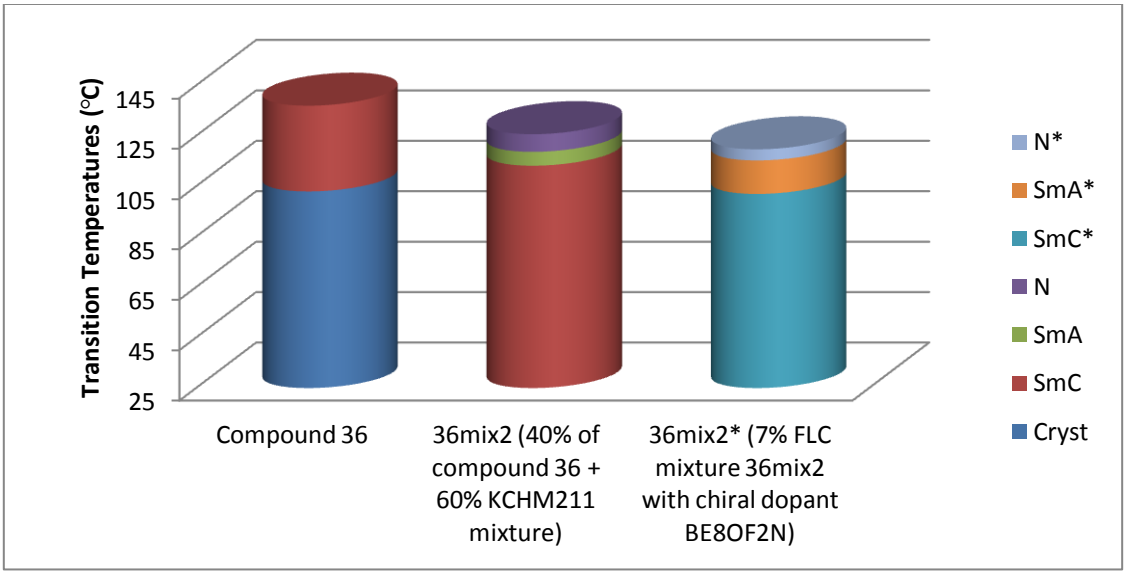

Figure 5.45. The difference of transition temperatures between compound 36, 36mix2 and 36mix2*.

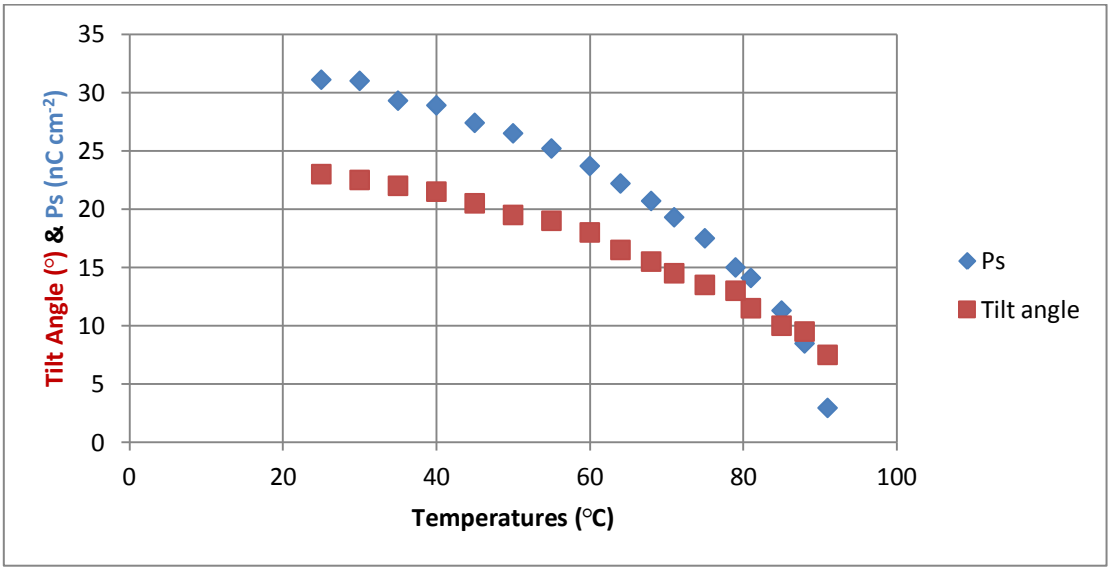

Figure 5.46. The Ps and tilt angle *vs* temperatures of compound 36mix2*.

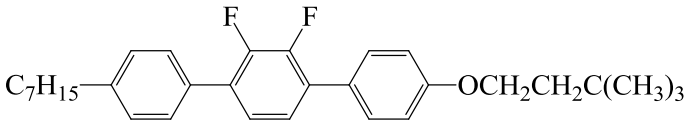

39

The compound **39mix1** is 20 % of the novel compound **39** with 80 % of **KCHM211** mixture, see figure **5.34** (% by weight).

The chiral compound **39mix1** (**39mix1***) is 93 % of (**39mix1**) with 7 % of chiral dopant (**BE8OF2N**).

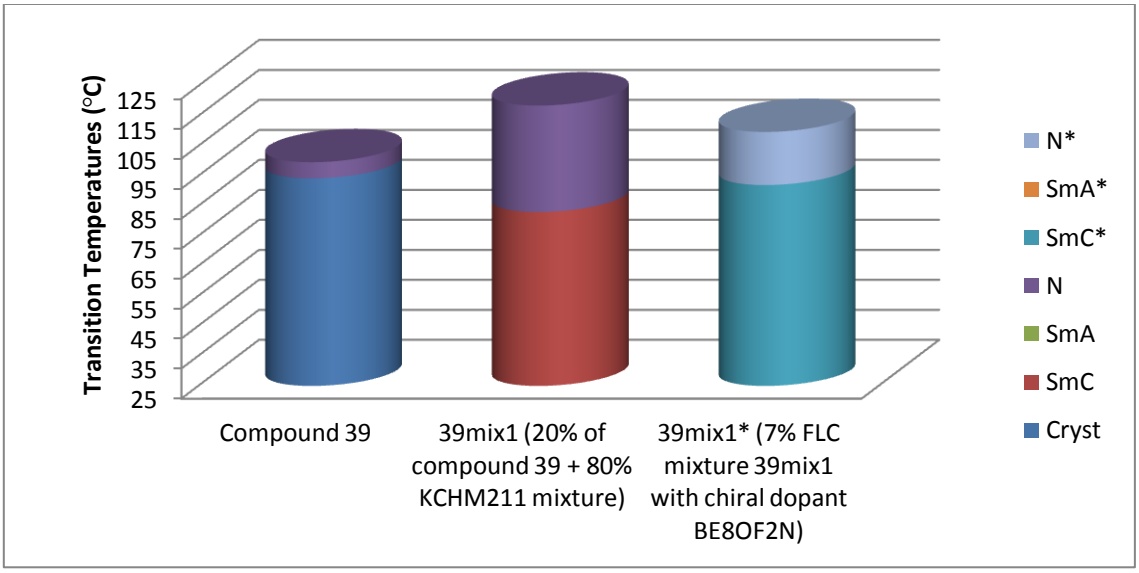

Figure 5.47. The difference of transition temperatures between compound 39, 39mix1 and 39mix1*.

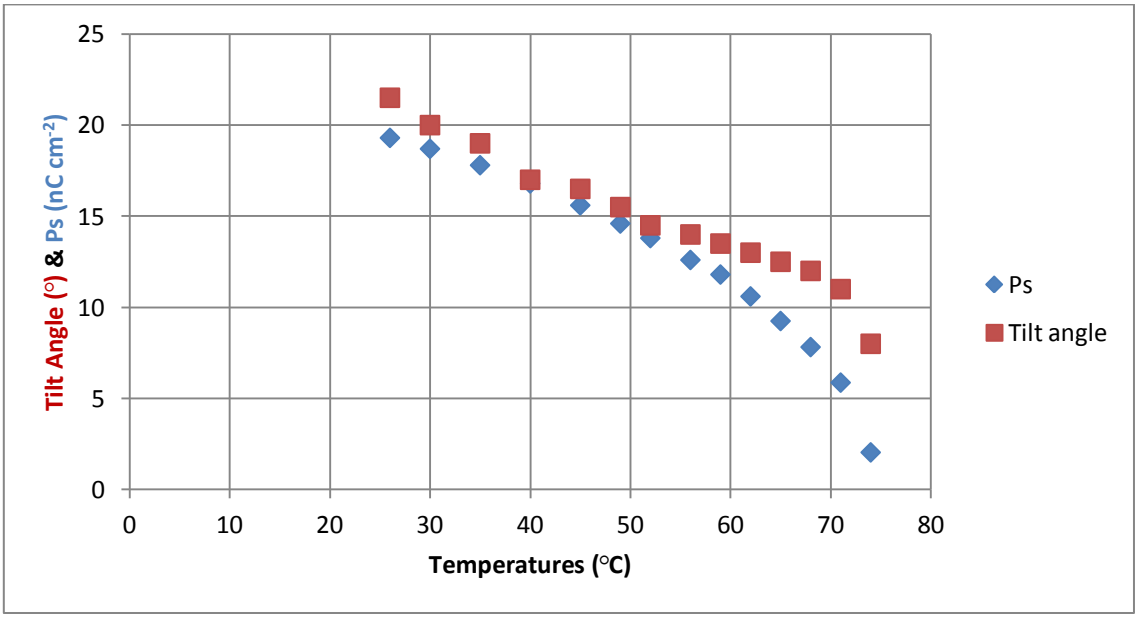

Figure 5.48. The Ps and tilt angle *vs* temperatures of compound 39mix1*.

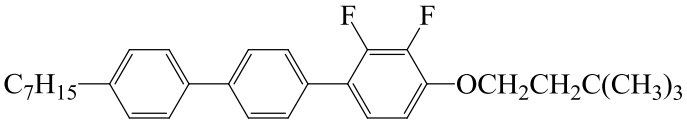

42

The compound **42mix1** is 20 % of the novel compound **42** with 80 % of **KCHM211** mixture, see figure **5.30** (% by weight).

The chiral compound **42mix1** (**42mix1***) is 93 % of (**42mix1**) with 7 % chiral dopant (**BE8OF2N**).

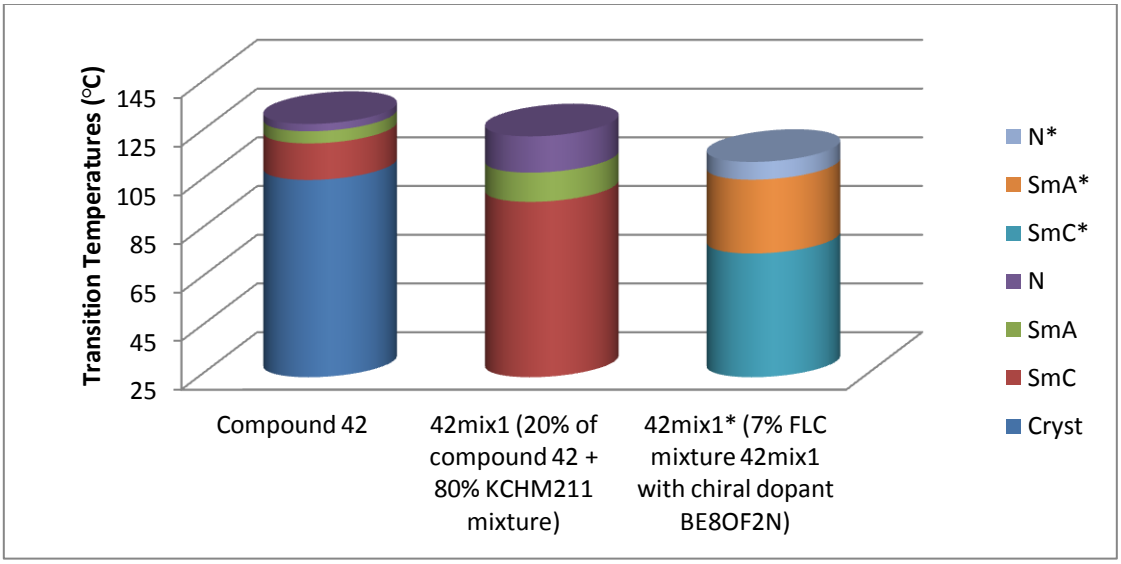

Figure 5.49. The difference of transition temperatures between compound 42, 42mix1 and 42mix1*.

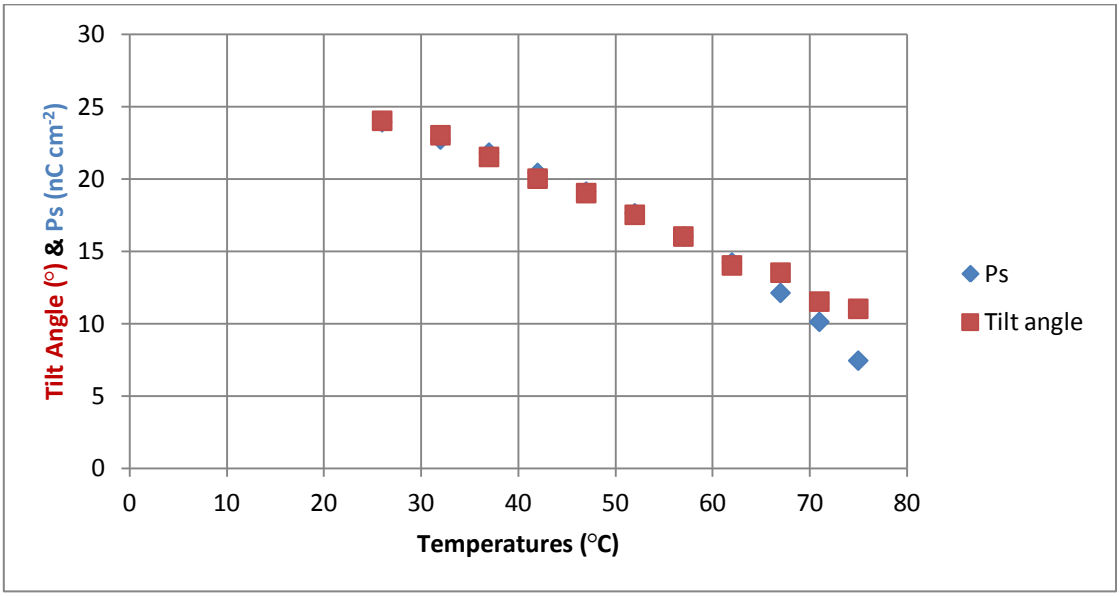

Figure 5.50. The Ps and tilt angle *vs* temperatures of compound 42mix1*.

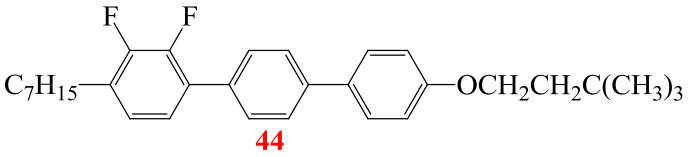

44

The compound **44mix1** is 20 % of the novel compound **44** with 80 % of **KCHM211** mixture, see figure **5.28** (% by weight).

The chiral compound **44mix1** (**44mix1***) is 93 % of (**44mix1**) with 7 % of chiral dopant (**BE8OF2N**).

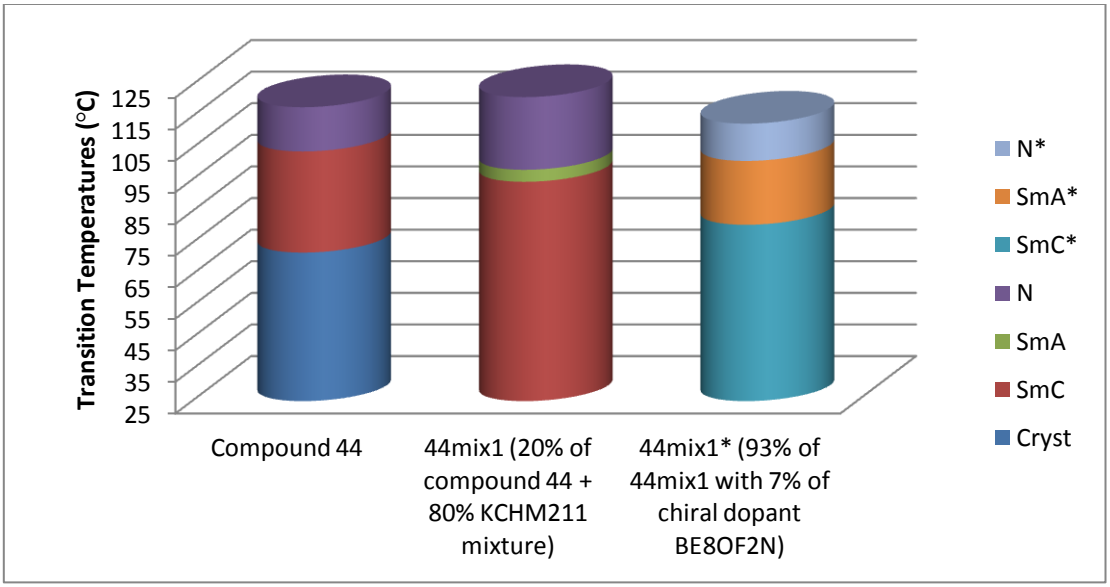

Figure 5.51. The difference of transition temperatures between compound 44, 44mix1 and 44mix1*.

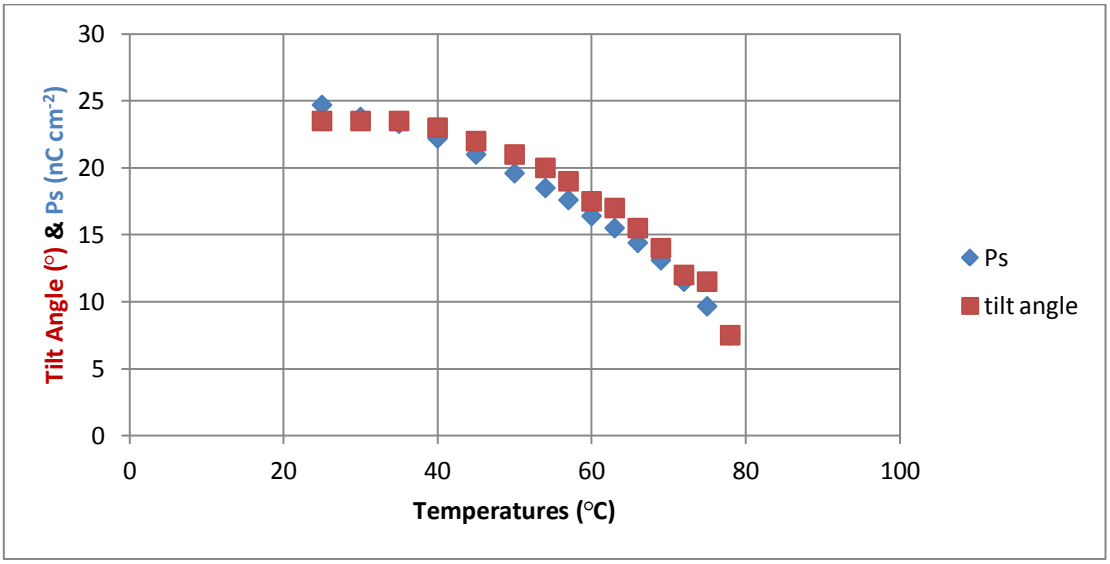

Figure 5.52. The Ps and tilt angle *vs* temperatures of compound 44mix1*.

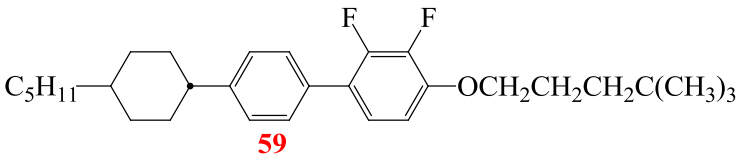

59

The compound **59mix1** is 20 % of the novel compound **59** with 80 % of **KCHM211** mixture, see figure **5.31** (% by weight).

The chiral compound **59mix1** (**59mix1***) is 93 % of (**59mix1**) with 7 % of chiral dopant (**BE8OF2N**).

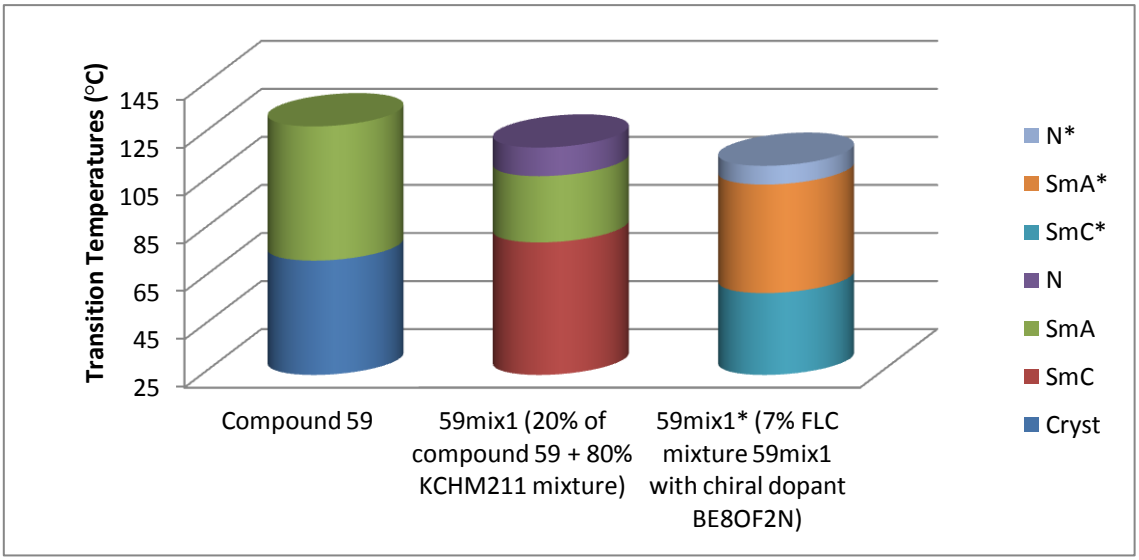

Figure 5.53. The difference of transition temperatures between compound 59, 59mix1 and 59mix1*.

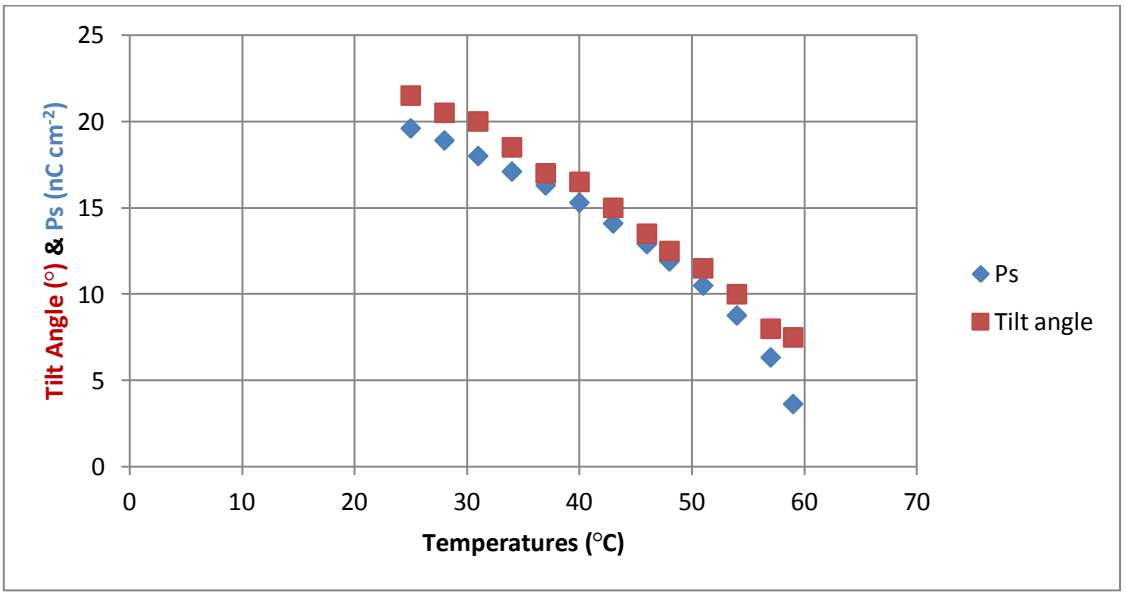

Figure 5.54. The Ps and tilt angle *vs* temperatures of compound 59mix1*.

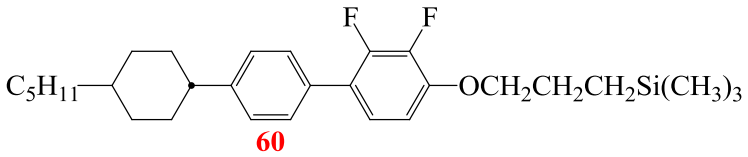

60

The compound **60mix1** is 20 % of the novel compound **60** with 80 % of **KCHM211** mixture, see figure **5.32** (% by weight).

The chiral compound **60mix1** (**60mix1***) is 93 % of (**60mix1**) with 7 % of chiral dopant (**BE8OF2N**).

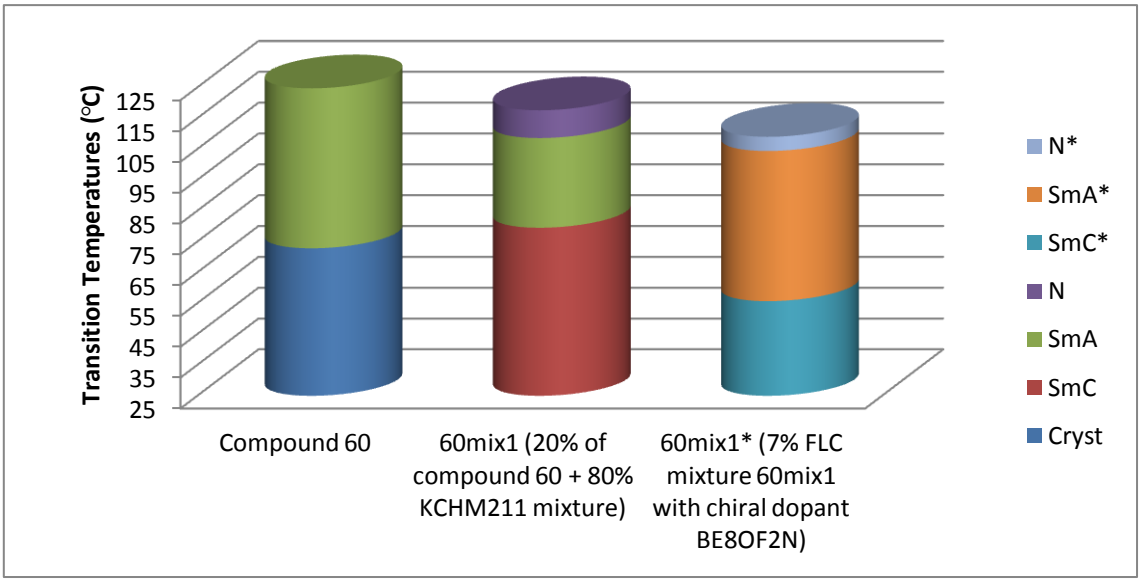

Figure 5.55. The difference of transition temperatures between compound 60, 60mix1 and 60mix1*.

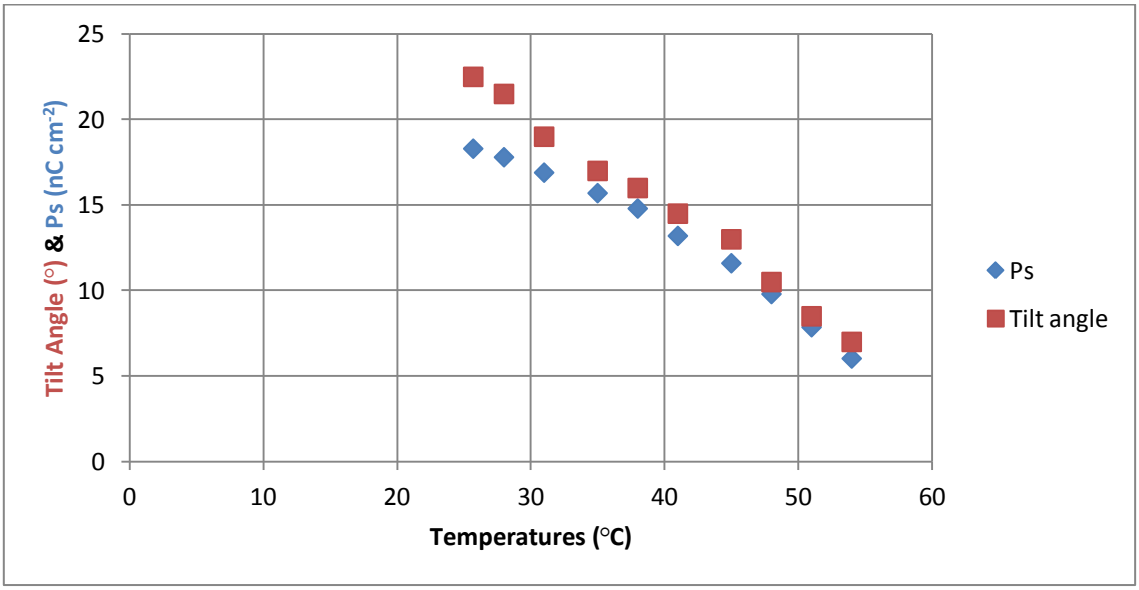

Figure 5.56. The Ps and tilt angle *vs* temperatures of compound 60mix1*.

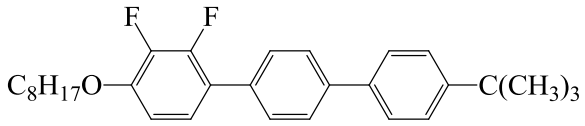

87

The compound **87mix1** is 10 % of the novel compound **87** with 90 % of **KCHM211** mixture, see figure **5.29** (% by weight).

The chiral compound **87mix1** (**87mix1***) is 93 % of (**87mix1**) with 7 % of chiral dopant (**BE8OF2N**).

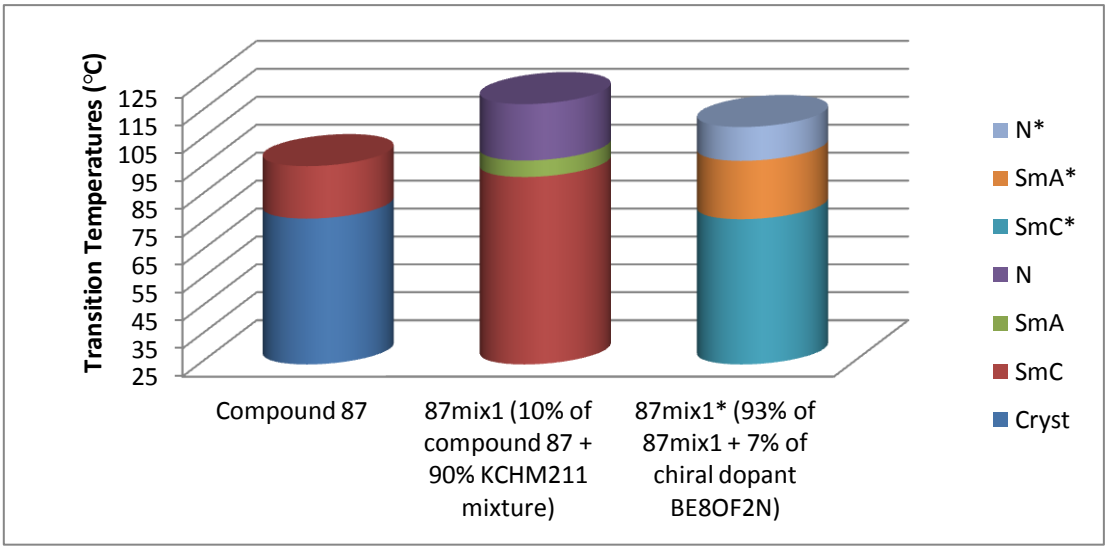

Figure 5.57. The difference of transition temperatures between compound 87, 87mix1 and 87mix1*.

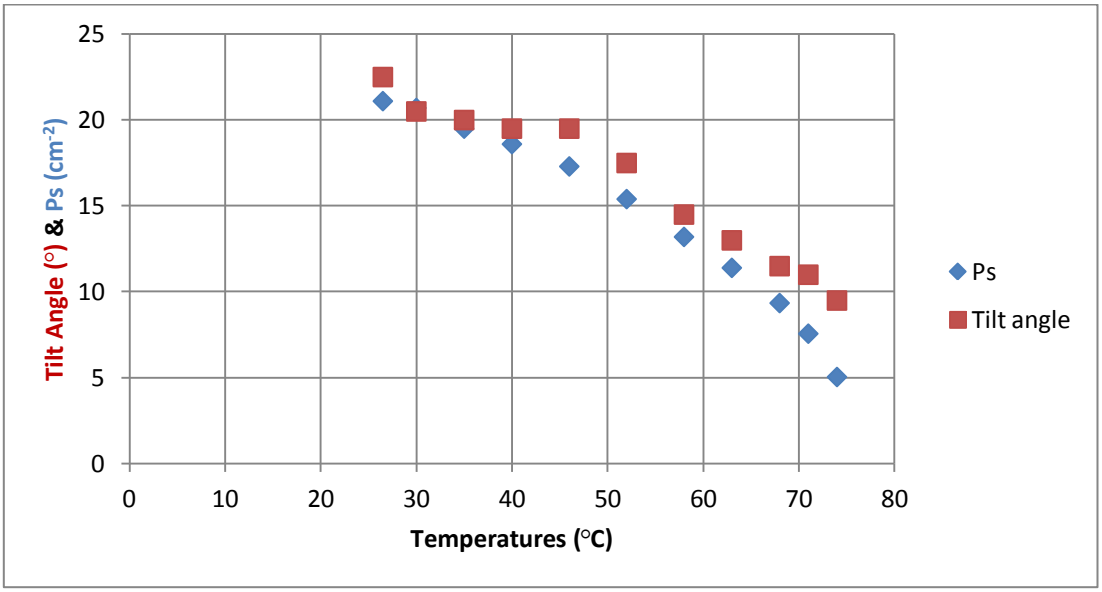

Figure 5.58. The Ps and tilt angle *vs* temperatures of compound 87mix1*.

5.6.5 Discussion of Properties of Ferroelectric Mixtures

Following the evaluation of several of the novel compounds as mixtures with a known ferroelectric host material (**KCHM211**), the next step involved selecting some of those mixtures and adding a chiral dopant (7%) to formulate ferroelectric mixtures for evaluation for mesomorphism, tilt angle and spontaneous polarization. Such investigations of ferroelectric properties are rather preliminary and further investigations in respect of alignment and switching times in test devices will need to be carried out.

Figures **5.39** and **5.40** show the results of an 80:20 mixture of KCHM211 and compound **20** that was then doped with 7% of the chiral dopant (**BE8OF2N**). The 80:20 composition was selected as having a sufficient quantity of compound **20** to make a potential difference to the layer shrinkage on cooling from the SmA phase to the tilted SmC phase, yet retaining the tried and tested properties of **KCHM211**, such as a good SmC phase temperature range and a relatively low viscosity. As is typical of using **BE8OF2N** as the chiral dopant, the SmA phase stability is promoted, and the SmC phase stability is depressed, however, not significantly so with just 7% added. As is typical, the tilt angle and hence the spontaneous polarization increase in a second order manner on cooling the ferroelectric mixture into the SmC phase, topping out at around 23° and 20 nC cm^{-2} respectively. The values for the host mixture alone are 22° and 16 nC cm^{-2} respectively, which shows that the addition of compound **20** at the 20% level makes no difference to the fundamental properties of the ferroelectric mixture, and so this is an excellent result. However, it remains to be seen if there is any influence on the alignment properties in terms of the desired defect-free bookshelf configuration.

The results of a similar mixture involving 40% of compound **20** are illustrated in Figures **5.41** and **5.42**. As can be seen, the much greater quantity of compound **20** has had no influence on the fundamental ferroelectric properties, which is somewhat expected given the virtually identical SmC phase stability to the original host material (92 °C). Again this is an excellent result, and so even if a greater quantity of compound **20** is required to provide the desired defect-free bookshelf alignment then there would not be any detrimental effects on ferroelectric properties.

Compounds with the two lateral fluoro substituents in the outer ring have greater mesophase stability than those with the substituents in the centre ring, and so compound **36** has a much greater SmC phase stability (137 °C) than compound **20** (92 °C). Hence the results of using a ferroelectric mixture with 20% of compound **20** illustrated in Figures **5.43** and **5.44** show a slightly higher tilt angle and spontaneous polarization due to the results being recorded further into the SmC phase. Of course this aspect is further reinforced by the results illustrated in Figures **5.45** and **5.46**, which show the analogous results with a higher proportion (40%) of compound **20**, where the tilt angle and spontaneous polarization reach 24° and 32 nC cm^{-2} respectively.

The results shown in Figures **5.47** and **5.48** illustrate the influence of 20% of compound **39** on tilt angle and spontaneous polarization. Compound **39** does not exhibit a SmC phase, and the initial mixture studies (see Figure **5.34**) showed the destructive nature of the SmC phase stability. Hence it is rather surprising that the SmC phase stability is greater on adding the chiral dopant (**BE8OF2N**) and that no SmA phase is induced, because in all previous studies this dopant causes a reduction in the SmC phase stability and often the induction of an SmA phase where it is not present in the original achiral mixture. Despite this issue, the tilt angle and spontaneous polarization behaviour in response to reduced temperature are, as expected where no SmA phase is present, rather more second order in nature, and reach similar values to those of the mixture without any compound **39**.

Isomeric compounds **42** and **44** both have the two lateral fluoro substituents in an outer ring, and both have relatively high SmC phase stability of 121 °C and 104 °C respectively. The results for compounds **42** and **44** as 20% mixtures in terms of tilt angle and spontaneous polarization are illustrated in Figures **5.49** and **5.50** and Figures **5.51** and **5.52** respectively. Both of these mixtures show analogous behaviour to those described previously and are in line with what would be expected from compounds that have higher Sm C phase stability than the parent host mixture, with tilt angle and spontaneous polarization rising gradually on cooling and topping out at around 25° and 25 nC cm^{-2} respectively.

The cyclohexane compounds proved far too destructive of SmC phase stability to be of any practical use in ferroelectric mixtures (see Figures **5.31** and **5.32**), nevertheless and evaluation was made of these two compounds (**59** and **60**) in ferroelectric mixtures in 20% composition (see Figures **5.53** and **5.54** and Figures **5.55** and **5.56** respectively). As expected given the nature of the chiral dopant (**BE8OF2N**), the ferroelectric mixtures involving both compounds (**59** and **60**) showed a rather low SmC phase stability and a very wide SmA phase temperature range, but the tilt angle and spontaneous polarization behaviour on cooling the SmC phase is similar to the other compounds evaluated.

Finally, compound **87** (non-mesogenic) was evaluated as a ferroelectric mixture, and a composition of just 10% was chosen because of the destructive nature to mesomorphism (see Figure **5.35**). The mesomorphism of the ferroelectric mixture containing 10% of compound **87** shows a most acceptable SmC* phase stability, and the tilt angle and spontaneous polarization behave in the expected manner with values levelling out at around 23° and 21 nC cm^{-2} respectively.

5.7 References

1. G. Gray, M. Hird, D. Lacey and K. Toyne, *Journal of the Chemical Society-Perkin Transactions 2*, 1989, **12**, 2041.
2. L. Chan, G. Gray and D. Lacey, *Molecular Crystals and Liquid Crystals*, 1985, **123**, 185.
3. L. K. M. Chan, Hull University, 1987.
4. L. Chan, G. Gray, D. Lacey and K. Toyne, *Molecular Crystals and Liquid Crystals*, 1988, **158**, 209.
5. G. W. Gray, M. Hird and K. J. Toyne, *Molecular Crystals and Liquid Crystals*, 1991, **195**, 221.
6. G. W. Gray, M. Hird, D. Lacey and K. J. Toyne, *Molecular Crystals and Liquid Crystals*, 1990, **191**, 1.
7. G. Gray, M. Hird and K. Toyne, *Molecular Crystals and Liquid Crystals*, 1991, **204**, 43.
8. M. Hird, *Chemical Society Reviews*, 2007, **36**, 2070.
9. J. W. Goodby, K. J. Tooyne, M. Hird, P. Styring, R. A. Lewis, A. Beer, C. C. Dong, M. E. Glendenning, J. C. Jones, K. P. Lymer, A. J. Slaney, V. Minter and L. K. Chan, *Liquid Crystal Materials* 2000, **3955**, 6.
10. N. Gough, PhD thesis, Smectic C Materials for Ferroelectric Applications, Hull University, 1999.
11. G. Cosquer, Liquid Crystal with Novel Terminal Chains as Ferroelectric Hosts' PhD Thesis, University of Hull, UK, 2000.
12. I. Radini and M. Hird, *Liquid Crystals*, 2009, **36**, 1417.
13. I. A. Radini, PhD thesis, The Synthesis and properties of Liquid Crystal with Bulky Terminal Groups for Bookshelf Geometry Ferroelectric Mixtures, Hull University, 2010.
14. P. J. Collings and M. Hird, *Introduction to liquid crystals chemistry and physics*, Taylor & Francis, 1997.
15. P. J. Collings, *Liquid Crystals, 1 edn., Princeton Universty Press, Princton, New Jersey, USA* 1990.
16. M. E. Glendenning, J. W. Goodby, M. Hird and K. J. Toyne, *Journal of the Chemical Society-Perkin Transactions 2*, 1999, 481.

17. M. Glenenning, J. W. Goodby, M. Hird and K. J. Toyne, *Journal of the Chemical Society-Perkin Transactions 2*, 2000, 27.
18. M. Hird, K. J. Toyne, A. J. Slaney and J. W. Goodby, *Mater. Chem.*, 1995, **5**, 423-430.

6- Conclusion

A range of novel compounds with a bulky terminal chain have been synthesised and prepared which incorporate two fluoro substituents in different positions within terphenyl and quarterphenyl core. These compounds with bulky group (silicon or carbon), and with terminal chain (alkoxy or alkyl chain) were synthesised to see how the bulky terminal groups influence the mesophase morphology of the final compounds. The novel compounds were compared with the known analogues to see a comprehensive investigation of melting point, transition temperatures and mesophase morphology. From the results obtained, the following observation can be made:

- The stability of smectic phase (especially SmC) is upheld by more than the stability of N phase, and in some cases the stability of SmC phase is higher than comparable analogues with conventional unbranched terminal chains.
- The surprisingly high stability of SmC phase comes from a phase separation effect because of the incompatibility of the conventional unbranched terminal chain and spherical bulky group.
- The N phase is suppressed by the bulky end group.
- Generally, the dialkyl materials have lower melting points and mesophase transition temperatures than the alkyl-alkoxy materials[1, 2].
- Since silicon has a larger atom than carbon, more disruption of the intermolecular forces of attraction confers lower transition temperatures and lower melting points on the silicon series when compared with carbon series in the final compounds.
- Gray *et al*[1]. have shown that compounds with two fluorines in the end ring (outer-edge) have higher transition temperatures and melting points, with greater smectic tendencies compared to the compounds with two fluorines in the centre ring (inner-core). Compounds with two fluorines in the centre ring (inner-core) tend to be more N in character.
- Some of the final compounds mixed with **KCHM211** mixtures and doped with chiral dopant (**BE8OF2N** dopant) to be chiral compound and measure the tilt angle and spontaneous polarisation (Ps).

6.1 References

1. G. Gray, M. Hird, D. Lacey and K. Toyne, *Journal of the Chemical Society-Perkin Transactions 2*, 1989, **12**, 2041.
2. M. Hird, *Chemical Society Reviews*, 2007, **36**, 2070.